Mathematical and Numerical Analysis of Elastoplastic Material with Multi-Surface Stress-Strain Relation

Dissertation

Zur Erlangung des akademischen Grades
Doktor der Naturwissenschaften
(Dr. rer. nat.)
der Technischen Fakultät
der Christian-Albrechts-Universität zu Kiel

Jan Valdman

Kiel
2001

Referent/in: Prof. Dr. Carsten Carstensen

Korreferenten: Prof. Dr. Martin Brokate, Prof. Dr. Ulrich Langer

Tag der mündlichen Prüfung: 25. 2. 2002

Zum Druck genehmigt: Kiel, 25. 2. 2002

Acknowledgments

It is my pleasure to express my thanks to my supervisors *Professor Dr. C. Carstensen* (Vienna University of Technology) and *Professor Dr. M. Brokate* (Munich University of Technology) for suggesting this topic to me, for many valuable discussions, and for their supervision during my stays in Kiel and Munich.

This work was supported by *Deutsche Forschungsgemeinschaft* through a three-year scholarship in the *Graduiertenkolleg 357-Effiziente Algorithmen und Mehrskalenmethoden* at the *Christian-Albrechts-Universität zu Kiel*.

I wish to thank all of my colleagues at the *Lehrstuhl für Wissenschaftliches Rechnen* and *Dr. G. Grammel* for scientific advice. I am grateful to *Dr. J. Alberty* and *R. Klose* for constructive discussions on plasticity and *PD Dr. A. Prohl* and *S. Bartels* for their useful advice concerning numerical analysis.

I am indebted to *Dr. J. Alberty, Dr. S. Bartels, Dr. J. Fiala* (Prague), *Dr. A. Kharytonov, PD Dr. A. Prohl* for carefully reading the earlier drafts of this thesis and helpful criticism as well as to *Dipl. Ing. J. Žán* (Pilsen) for his typesetting tips.

Kiel, December 2001

J. Valdman

Summary

The aim of this thesis is the mathematical and numerical analysis of a multi-yield (surface) model in elastoplasticity. The presented Prandtl-Ishlinskii model of play type generalizes the linear kinematic hardening model and leads to a more realistic description of the elastoplastic transition of a material during a deformation process. The unknowns in the quasi-static formulation are displacement and (several) plastic strains which satisfy a time-dependent variational inequality. As for the linear kinematic hardening model, the variational inequality consists of a bounded and elliptic bilinear form, a linear functional, and a positive homogeneous, Lipschitz continuous functional; hence existence and uniqueness of a weak solution is then concluded from a general theory.

Our time and space discretization consists of the implicit Euler method and the lowest order finite element method. For any one-time step discrete problem, the vector of plastic strains (considered on one element) depends on the (unknown) displacement only. In contrast to the linear kinematic hardening model, the dependence can not be stated explicitly, but has to be calculated by an iterative algorithm. An a priori error estimate is established and shows linear convergence with respect to time and space under the assumption of sufficient regularity of the solution.

A MATLAB solver, which includes the nested iteration technique combined with an (ZZ-) adaptive mesh-refinement strategy and the Newton-Raphson method, is employed for solving the two-yield material model. Various numerical experiments support our theoretical results and give more insight to complex dynamics in elastoplasticity problems.

Zusammenfassung

Das Ziel dieser Arbeit ist die mathematische und numerische Analyse eines Multiflächen-Modells in der Elastoplastizität. Das vorgestellte, so genannte ”play type” Modell von Prandt-Ishlinskii verallgemeinert das Modell der linearen kinematischen Verfestigung und führt zu einer realistischeren Beschreibung der elastoplastischen Verformung des Materials. Die Unbekannten in der quasistatischen Formulierung sind die Verschiebung und (mehrere) plastische Verzerrungen, die als Lösung einer zeitabhängigen Variationsungleichung auftreten. Wie im Problem der linearen kinematischen Verfestigung beinhaltet die Variationsungleichung eine beschränkte, elliptische Bilinearform, ein lineares Funktional sowie ein positiv-homogenes, Lipschitz-stetiges Funktional, so daß Standardaussagen der Variationsrechnung die Existenz und Eindeutigkeit einer schwachen Lösung garantieren.

Die Diskretisierung in Zeit und Raum erfolgt durch ein implizites Euler-Verfahren und eine Finite Elemente Methode niedrigster Ordnung. In jedem Zeitschritt des diskreten Problems hängt der zu einem Element assoziierte Vektor der plastischen Verzerrungen nur von den Verschiebungen ab. Im Gegensatz zum Modell der linearen kinematischen Verfestigung lässt sich diese Abhängigkeit nicht in einer geschlossenen Formel darstellen und muß daher iterativ bestimmt werden. Eine a-priori Analyse zeigt lineare Konvergenz in Zeit und Raum unter hinreichenden Regularitätvoraussetzungen.

Ein MATLAB Programm, welches ”nested iteration” Techniken mit adaptiven Netzverfeinerungsalgorithmen kombiniert und ein Newton-Raphson Verfahren verwendet, wird zur

Lösung des ”two-yield” Problems herangezogen. Zahlreiche numerische Experimente belegen die theoretischen Resultate dieser Arbeit und führen zu einem besseren Verständnis des Materialmodells.

Contents

Chapter 1

Introduction

Elastoplastic material behavior is often exploited in many engineering problems for calculation of permanent deformation of structures, stability in the structural and solid mechanics, metal forming operations and other processes beyond elasticity. Mathematical and numerical aspects of problems in elastoplasticity date back to works of Duvaut and Lions [DL76], Hlaváček et al. [HHNL88], Johnson et al. [EEHJ95, Joh76], Han and Reddy [HR95, HR99], Simo and Hughes [SH98], Korneev and Langer [KL84], amongst others.

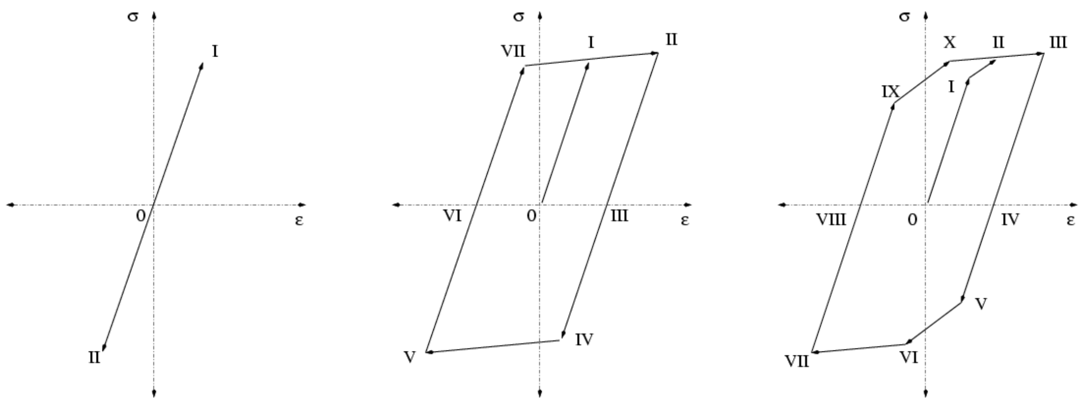

Figure 1.1: Examples of stress-strain relations in material science: linear elasticity (left), linear kinematic hardening (middle), and two-yield model (right) in elastoplasticity.

The theory of elastoplasticity models the behavior of every point in the deformed continuum in terms of the stress and strain tensors, σ and ε. A linear stress-strain relation, which describes reversible processes, e.g., a small homogeneous (relative) elongation ε of a beam with a density of force σ, is depicted in Figure 1.1 (left). If the force σ is withdrawn, the elongation goes back to zero as in the beginning of the deformation (point 0). A typical ductile material (Figure 1.1, middle) behaves elastically as long as the strains are small. For stresses beyond a yield limit (point I), the material reacts irreversible and the plastic strain p appears. That is, after the force is withdrawn, the material stays deformed (point III). The stress-strain relation follows a hysteresis curve, which consists of three parallel lines $0 - I, II - IV, V - VII$ and two parallel lines $IV - V, VII - II$. The *two-yield* model (Figure 1.1, right) generalizes the stress-strain relation of the *linear kinematic hardening* model introducing the third set of parallel lines

$I-II, V-VII, IX-X$, which is modeled by splitting the plastic strain p additionally into two internal plastic strains p_1, p_2, i.e., $p = p_1 + p_2$. The mathematical and numerical analysis of the two-yield model or more generally of a *multi-yield model* generalizes the situation for the linear kinematic hardening problem and is the main interest of this thesis.

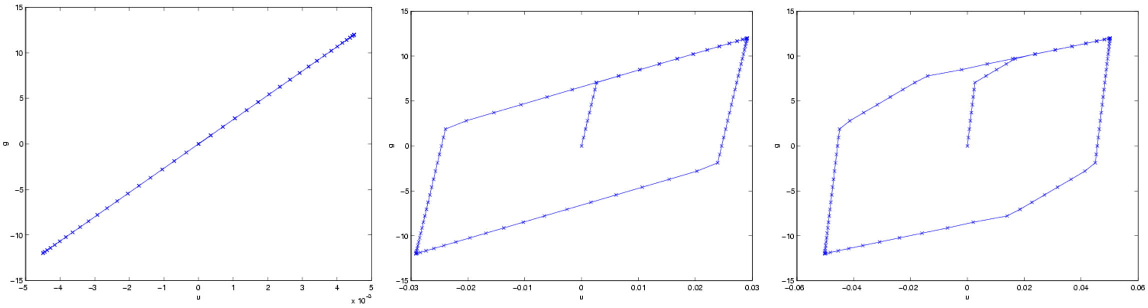

Figure 1.2: Loading-deformation relation calculated for the problem of beam with 1D effects: linear elasticity (left), linear kinematic hardening (middle) and two-yield model (right) in elasto-plasticity.

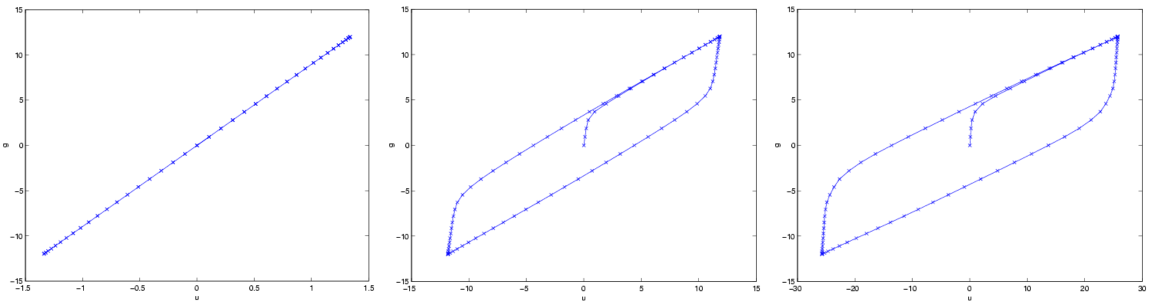

Figure 1.3: Loading-deformation relation calculated for the Cook's membrane problem: linear elasticity (left), linear kinematic hardening (middle), and two-yield model (right) in elastoplasticity.

The construction of multi-yield models as well as more complicated hardening models in terms of *rheological models* has already been studied in works of Brokate, Krejčí, Visintin, Sprekels and others [Bro87, Bro98, BK98a, BK98b, BS96, Kre96, Vis94]. We consider here a multi-yield model that operates with M plastic strains $p_1, \ldots, p_M$ and an additive decomposition of the strain ε,

$$\varepsilon = e + p_1 + \cdots + p_M.$$

The presented multi-yield model is *Prandtl-Ishlinskii model of play type* [Kre96]. We show that a weak formulation of this model can be written as a *variational inequality* on a Hilbert space $\mathcal{H}$, The variational inequality consists of a bilinear form $a(\cdot,\cdot)$, a linear functional $\ell(\cdot)$ and a nonlinear functional $\psi(\cdot)$ and has the following form: Seek $w(t) \in \mathcal{H}$, such that, for all $z \in \mathcal{H}$ and almost all times $t \in [0,T]$,

$$0 \leq a(w(t), z - \dot{w}(t)) + \psi(z) - \psi(\dot{w}(t)) - \langle \ell(t), z - \dot{w}(t) \rangle. \tag{1.1}$$

Variational inequalities such as (1.1) arise in many problem, such as the obstacle or contact problems or the non-differentiable problems with constraints. For their mathematical analysis we refer to Glowinskii et al. [GLR81]. As for the linear kinematic hardening model [HR99] we prove that terms $a(\cdot,\cdot), \ell(\cdot), \psi(\cdot)$ in (1.1) satisfy sufficient assumptions to guarantee *existence* and *uniqueness* of a weak solution $w(t) \in \mathcal{H}$.

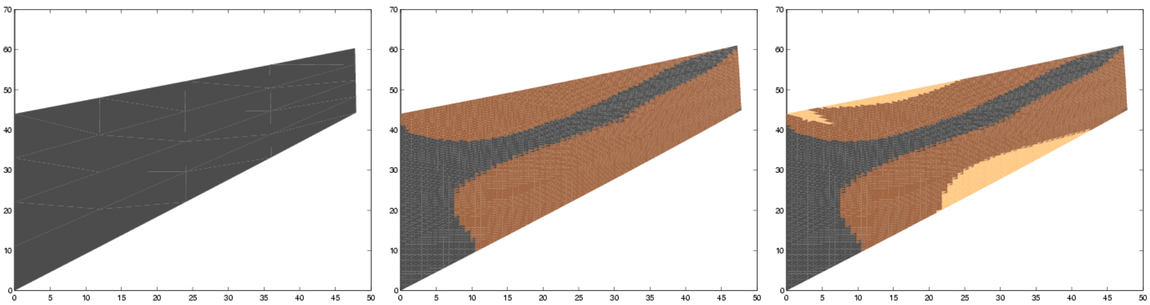

Figure 1.4: Elastoplastic zones of the Cook's membrane problem for purely elastic model (left), single-yield (middle) and two-yield (right) models. Black color shows elastic zones ($P_1 = P_2 = 0$), darker and lighter gray color zones in the first ($P_1 \neq 0, P_2 = 0$) and second plastic phase ($P_2 \neq 0$).

The time dependent variational inequality (1.1) is discretized at each time step by the *implicit Euler* scheme, using *finite element method* [HR99, Alb01, ACZ99, Sut97]. This approach leads to the minimization problem for a discrete approximation of $W^1 = (U^1, P_1^1, \ldots, P_M^1)$ of the exact solution at the first discrete time $w(t_1) = (u, p_1, \ldots, p_M)(t_1)$. If we denote by $W^0 = (U^0, P_1^0, \ldots, P_M^0)$ the discrete approximation of $w(0) = (u, p_1, \ldots, p_M)(0)$, then the incremental variable $X = (U, P_1, \ldots, P_M) = W^1 - W^0$ minimizes a functional

$$f(X) = \frac{1}{2}a(X,X) + \psi(X) - L(X), \tag{1.2}$$

over all X in a finite dimensional subspace S of $\mathcal{H}$. The minimization problem (1.2) with the *convex* but *non smooth* functional ψ is solved by the Newton-Raphson method [Neč83] and the nested iteration method in a multilevel framework.

For a space discretization we use *piecewise affine* functions to approximate the displacement U and *piecewise constant* functions to approximate the plastic strains $P_1, \ldots, P_M$ on the same regular triangulation $\mathcal{T}$. Similarly as in the linear kinematic hardening case [AC00], the vector of incremental plastic strains $P = (P_1, \ldots, P_M)^T$ depends on every element T of the triangulation $\mathcal{T}$ on the displacement U only, i.e., it is the minimizer of a functional

$$g(Q) = \frac{1}{2}(\hat{\mathbb{C}} + \hat{\mathbb{H}})Q : Q - \hat{A} : Q + ||Q||_{\sigma^y}, \quad Q = (Q_1, \ldots, Q_M)^T, \tag{1.3}$$

over all deviatoric symmetric $d \times d$ matrices $Q_1, \ldots, Q_M$ ($d = 2, 3$). The resulting matrix operator $\hat{\mathbb{C}} + \hat{\mathbb{H}}$ is not diagonalizable and hence it is not possible to separate the minimization of (1.3) into M subproblems. In the two-yield case, $M = 2$, an analytical calculation of minimizing (1.3) infers that $\xi_2 = ||P_2||$ is a root of a 8-th degree polynomial. Therefore, the minimizer of a functional (1.3) can not be expressed exactly as for the single-yield model [AC00], but has to be

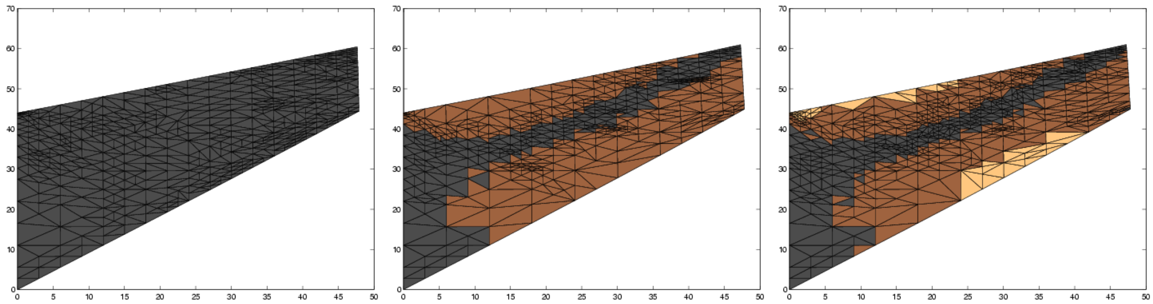

Figure 1.5: Adaptive refinements of Cook's membrane problem for purely elastic model (left), single-yield (middle), and two-yield (right) models. The black color shows elastic zones ($P_1 = P_2 = 0$), darker and lighter gray color zones in the first ($P_1 \neq 0, P_2 = 0$), and second plastic phase ($P_2 \neq 0$).

approximated by an iterative algorithm. The iterative algorithm belongs to the class of *alternating direction algorithms* and converges to the minimizer (P_1, P_2) with the convergence rate $1/2$.

By application of the arguments of the proof for the linear kinematic hardening model [AC00], we show linear convergence in time and space for the implicit Euler scheme and the lowest order finite element method under the assumption of sufficient regularity of the solution.

Numerical experiments for the calculation of *two-yield plasticity* problems support the theoretical results and give more insight to complex dynamics of elastoplasticity problems. We observe two-yield plastic effects that arise in addition to single-yield effects, like different hysteresis curves and the time evolution of elastoplastic zones. Figures 1.2 and 1.3 show the loading-displacement relation (measured at one material point) for elastic, single-yield and two-yield material models. For the material under the cyclic uniaxial tension (Figure 1.2), the hysteresis relation is in agreement with the theoretically analyzed stress-strain relation. The typical hysteresis curve (Figure 1.3) is not sharp, but it is smoothened through two-dimensional deformation effects and the non-homogeneous elastoplastic material behavior.

The developed MATLAB solver involves a nested iteration technique with *adaptive* mesh-refinements and an adaptive time-stepping. The following properties have been observed in the numerical experiments:

1. *Adaptive* mesh-refinement strategy is superior to *uniform* mesh-refinement strategy.
2. The nested iteration technique performs efficiently (i.e, the direct calculation requires more time). One Newton step in the nested iteration technique is usually sufficient; more steps only increase computational costs without large improvements with respect to accuracy.
3. Computations based on the two-yield material model require longer CPU time than computations where the single-yield material or the elastic material models are used.
4. Adaptive time-stepping (controlled by the number of Newton steps in the previous time step) is inefficient.

The conclusions from this thesis are the following points: Generalization of the mathematical and numerical analysis for the linear kinematic hardening model to the multi-yield model is indeed feasible and seems to lead to more realistic numerical simulations. The numerical discretization leads to the similar structure of the discrete problem; however the explicit relation between plastic strains and displacement can not be stated analytically and therefore the practical calculation of a multi-yield plasticity problem is more expensive. The convergence of inner-outer multilevel oriented algorithms has been observed, and elements of a priori and a posteriori error control are established. Adaptive mesh-refinement is applicable and advantageous; in contrast, the construction of adaptive time-stepping requires more sophisticated approach and deserves further future research.

The thesis is organized as follows. The boundary value problem of linear elasticity which leads to the Navier-Lamé equations (Problem 2.1), is described in Chapter 2. This becomes a part of the more complex elastoplastic material response laws as explained below. Chapter 2 also provides basic tools like Korn's inequality and the Lax-Milgram Lemma and closes with outlooks for nonlinear elasticity.

Chapter 3 introduces three rheological elements, the elastic, rigid-plastic and kinematic element. Elementary results from convex analysis are recalled which yield equivalent formulations of rheological laws for the rigid-plastic element (Lemma 3.3 on page 17). A combination of the three rheological elements results in the linear kinematic hardening single-yield (surface) model in elastoplasticity. The weak time-evolution formulation of the boundary value problem of elastoplasticity (Problem 3.1 on page 22) is derived in the form of an abstract variational inequality.

Chapter 4 concerns the composition of more rigid-plastic elements, leading to the multi-yield (surface) elastoplastic model, namely the Prandtl-Ishlinskii model of the play type. The weak formulation of the boundary value problem of multi-yield elastoplasticity (Problem 4.1) on page 31) is also discussed here.

Chapter 5 is devoted to the mathematical analysis of the boundary value problem of multi-yield plasticity (Problem 4.1). Theorem 5.2 (on page 41) is a special case of a general theory [HR99] and establishes existence and uniqueness of weak solutions. Its application is based on the verification of the assumptions on the terms in the variational inequality (1.1): boundedness and ellipticity of the bilinear form $a(\cdot, \cdot)$ (Propositions 5.1, 5.2 on pages 35, 38) and the Lipschitz-continuity of the nonlinear functional $\psi(\cdot)$ (Proposition 5.3 on page 40).

The discretization of the boundary value problem of multi-yield plasticity (Problem 4.1) is described in Chapter 6. For the two-yield material model, the relation between plastic strains and displacement can not be calculated explicitly (as in case of the single-yield material model [AC00]). Algorithm 2 (on page 60) establishes the elementwise computation of discrete plastic stresses and Proposition 6.1 (on page 62) states its global convergence.

Chapter 7 studies convergence of the fully-discrete method. Proposition 7.1 (on page 65) establishes a priori error estimates and the linear convergence in time and space by assuming sufficient regularity of the solution. Proposition 7.2 (on page 71) formulates an a posteriori error estimate for a one time-step problem and clarifies the residual error estimator which allows adaptive mesh-refinement strategy.

The numerical algorithms of Chapter 8 include a nested iteration technique combined with adaptive mesh-refinement and adaptive time-stepping.

Chapter 9 reports on the calculations of two-yield plasticity in MATLAB and presents hysteresis curves for single and two-yield material, evolutions of elastoplastic zones within the deformed continuum and experimental convergence rates.

Conclusions and some open questions are summarized in Chapter 10. Finally, the Appendix contains notation and MAPLE and MATLAB programs.

Chapter 2

Mathematical models in elasticity

This chapter introduces a mathematical model of linear elasticity and explains related concepts. This is part of more involved elastoplastic stress-strain relations of the following chapters. A model of nonlinear elasticity, whose studies leads to *non-convex analysis* and are beyond the range of this thesis, is also mentioned.

2.1 Model of linear elasticity

The elastic body is assumed to occupy a bounded domain $\Omega \subset \mathbb{R}^d$, with a *Lipschitz* boundary $\Gamma = \partial\Omega$. The boundary Γ is split into a *Dirichlet* boundary Γ_D, a closed subset of Γ with a positive surface measure, and the remaining (relatively open and possibly empty) *Neumann* part $\Gamma_N := \Gamma \setminus \Gamma_D$. Applied volume and surface forces cause internal stresses within the body. This is modeled by a symmetric second order *Cauchy stress* tensor $\sigma : \Omega \to \mathbb{R}^{d\times d}_{sym}$. An equilibrium between external and internal forces in the *quasi-static* case is expressed by the equation of *equilibrium of forces*

$$\operatorname{div}\sigma + f = 0 \quad \text{for all } x \in \Omega, \tag{2.1}$$

where $f : \Omega \to \mathbb{R}^d$ denotes volumes forces (i.e., a gravity force) and $\operatorname{div}\sigma$ the divergence defined by $(\operatorname{div}\sigma)_j := \sum_{k=1}^{d} \frac{\partial \sigma_{jk}}{\partial x_k}$ for all $j = 1, \dots, d$. Every material point of the body moves with respect to its position in a reference configuration Ω by a *displacement* $u : \Omega \to \mathbb{R}^d$. The deformation of the body is characterized for very small deformations through the linearized *Green strain tensor*

$$\varepsilon(u) = \frac{1}{2}(\nabla u + (\nabla u)^T).$$

In linear elasticity theory we assume a linear relation between the stress σ and the deformation ε, i.e.,

$$\sigma = \mathbb{C}\varepsilon. \tag{2.2}$$

The linear operator $\mathbb{C} : \mathbb{R}^{d\times d} \to \mathbb{R}^{d\times d}$ denotes a symmetric, positive definite elastic tensor. For isotropic materials it holds that

$$\mathbb{C}\varepsilon = 2\mu\varepsilon + \lambda(\operatorname{tr}\varepsilon)\mathbb{I}, \tag{2.3}$$

where the (positive) coefficients μ and λ are called *Lamé* coefficients. Here $\mathbb{I}$ denotes the second order identity tensor (an identity matrix) and $\operatorname{tr} : \mathbb{R}^{d\times d} \to \mathbb{R}$ defines the *trace* of a matrix,

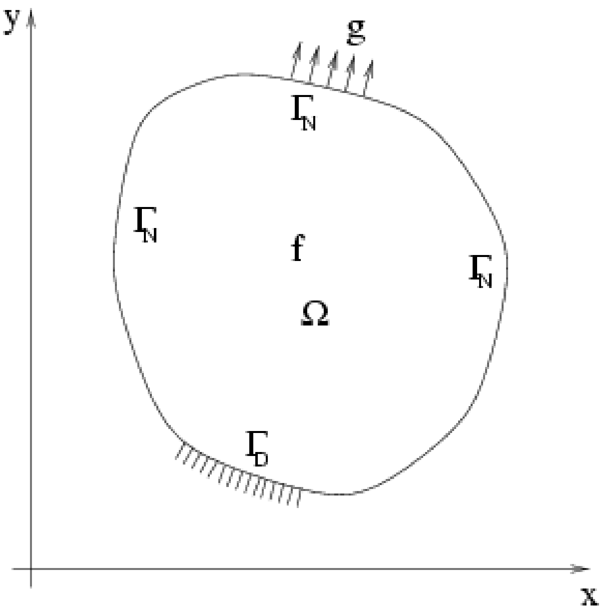

Figure 2.1: Material under deformation.

$\operatorname{tr}\varepsilon := \sum_{j=1}^{d} \varepsilon_{jj}$, for $\varepsilon \in \mathbb{R}^{d\times d}$. We pose essential and static boundary conditions, namely

$$u = 0 \quad \text{on } \Gamma_D \qquad \text{and} \qquad \sigma \cdot n = g \quad \text{on } \Gamma_N,$$

where g is a given applied surface force and n denotes the outer normal to the boundary Γ_N. Substitution of (2.2) into (2.1) leads to the linear boundary value problem of quasi-static elasticity in the space

$$H^1_D(\Omega) = \{v \in H^1(\Omega)^d | v = 0 \text{ on } \Gamma_D\}.$$

Problem 2.1 (Linear BVP of quasi-static elasticity). *For given $f \in L^2(\Omega)^d$ and $g \in L^2(\Gamma_N)^d$, find $u \in H^1_D(\Omega)$ that satisfies*

$$\begin{aligned} \operatorname{div} \mathbb{C}\varepsilon(u) + f &= 0 \quad \textit{in } \Omega, \\ u &= 0 \quad \textit{on } \Gamma_D, \\ \mathbb{C}\varepsilon(u) \cdot n &= g \quad \textit{on } \Gamma_N. \end{aligned} \tag{2.4}$$

We multiply (2.4) by an arbitrary $v \in H^1_D(\Omega)$, apply *Green's theorem* from vector analysis and derive the weak formulation of the equation of equilibrium of forces

$$\int_\Omega \sigma : \varepsilon(v)\,\mathrm{d}x = \int_\Omega f \cdot v\,\mathrm{d}x + \int_{\Gamma_N} g \cdot v\,\mathrm{d}x \quad \text{for all } v \in H^1_D(\Omega). \tag{2.5}$$

Here : denotes a scalar product of matrices, and it is defined as $a : b := \sum_{i,j=1}^{d} a_{ij} b_{ij}$.

Definition 2.1 (Weak formulation of BVP). For given $f \in L^2(\Omega)^d$ and $g \in L^2(\Gamma_N)^d$, find $u \in H^1_D(\Omega)$ that satisfies

$$a(u, v) = b(v) \quad \text{for all } v \in H^1_D(\Omega), \tag{2.6}$$

where the bilinear form $a(\cdot,\cdot)$ and the linear functional $b(\cdot)$ are defined by

$$a(u,v) := \int_\Omega \varepsilon(u) : \mathbb{C}\varepsilon(v)\,\mathrm{d}x, \tag{2.7}$$

$$b(u) := \int_\Omega f \cdot u\,\mathrm{d}x + \int_{\Gamma_N} g \cdot u\,\mathrm{d}s. \tag{2.8}$$

Before we state existence and uniqueness of the weak solution of Problem 2.1 we recall *Korn's first inequality* that is of central importance in linear continuum mechanics, cf. [Val88] for a proof of the subsequent lemma.

Lemma 2.1 (Korn's first inequality). *Let $\Omega \subset \mathbb{R}^d$ be a nonempty, open, bounded, and connected domain in $\mathbb{R}^d$ with a Lipschitz boundary Γ that consists of a Dirichlet part Γ_D of a positive surface measure. Then there exists a constant $c > 0$ that depends only on Ω such that*

$$||u||_{H^1(\Omega)} \leq c \int_\Omega ||\varepsilon(u)||^2\,dx \quad \textit{for all } u \in H^1_D(\Omega). \tag{2.9}$$

With the help of Korn's first inequality we can prove that the bilinear form $a(\cdot,\cdot)$ is elliptic in $H^1_D(\Omega)$ and the linear BVP of quasi-static elasticity has a unique solution in $H^1_D(\Omega)$, owing to the *Lax-Milgram lemma*.

Theorem 2.1 (Lax-Milgram). *Let V be a Hilbert space, $a : V \times V \to \mathbb{R}$ a bilinear form that is continuous and V-elliptic, and $b : V \to \mathbb{R}$ a bounded linear functional. Then the problem*

$$a(u,v) = b(v) \quad \textit{for all } v \in V \tag{2.10}$$

has a unique solution $u \in V$, and for some constant $c > 0$ independent of b,

$$||u|| \leq c||b||. \tag{2.11}$$

Remark 2.1. The above assumptions,

$$f \in L^2(\Omega)^d \quad \text{and} \quad g \in L^2(\Gamma_N)^d$$

can be weakened. For instance in three dimensions, i.e., $d = 3$, the assumptions

$$f \in L^{6/5}(\Omega)^3 \quad \text{and} \quad g \in L^{4/3}(\Gamma_N)^3$$

already guarantee a uniqueness of solutions $u \in H^1_D$, see [Cia94].

If we are provided a sufficient regularity of $\partial\Omega$ and f, one can prove even a higher regularity of the solution u [Cia94].

Theorem 2.2. *Let $\Omega \subset \mathbb{R}^3$ be a domain with boundary Γ of class $\mathcal{C}^2$, let $f \in L^p(\Omega)^3, p \geq \frac{6}{5}$, and let $\Gamma = \Gamma_D$. Then the solution $u \in H^1_D(\Omega)$ of Problem 2.1 is in the space $W^{2,p}(\Omega)^3$ and satisfies*

$$\text{div } \mathbb{C}\varepsilon(u) + f = 0 \quad \textit{in } \Omega.$$

Let $m \geq 1$ be a non-negative integer. Suppose the boundary Ω is of class $\mathcal{C}^{m+2}$ and $f \in W^{m,p}(\Omega)^3$. The the solution $u \in H^1_D$ of Problem 2.1 belongs to $W^{m+2,p}(\Omega)^3$.

Proof. [Cia94]. □

Remark 2.2. The previous theorem can be extended to problems with nonzero Neumann boundary Γ_N. The closures of Γ_D and Γ_N must not intersect, i.e., dist$(\Gamma_N, \Gamma_D) > 0$, and here $g \in W^{m-1/p,p}\ (\Gamma_N)^3$.

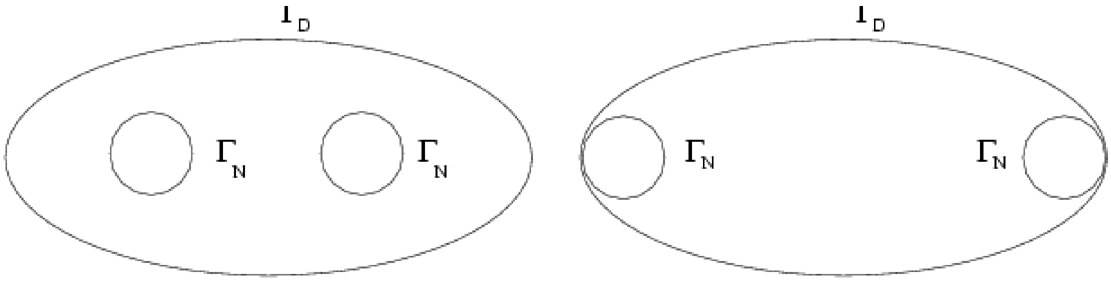

Figure 2.2: Examples of domains with a positive (left) and zero (right) distance of Dirichlet and Neumann boundaries.

2.2 Model of nonlinear elasticity

Problem 2.1 can be seen as a linearized version of nonlinear elasticity with *large deformations*. Then the (nonlinear) Green strain tensor is of the form

$$\varepsilon(u) = \frac{1}{2}(\nabla u + (\nabla u)^T + (\nabla u)^T \nabla u). \tag{2.12}$$

For a description of the internal stresses, the *second Piola-Kirchhof strees tensor* $S : \Omega \to \mathbb{R}^{d\times d}_{sym}$ is connected with $\varepsilon(u)$ through (a relation defined with the help of a given function $\mathbb{C}$)

$$S = \mathbb{C}\varepsilon(u). \tag{2.13}$$

An equilibrium of internal and external forces is expressed as

$$\text{div}\,\Big((1 + \nabla u)S\Big) + f = 0 \quad \text{in } \Omega. \tag{2.14}$$

The term $(1 + \nabla u) := F$ is the *deformation gradient*, essential, and static boundary conditions read

$$u = 0 \quad \text{on } \Gamma_D \qquad \text{and} \qquad (1 + \nabla u)S \cdot n = g \quad \text{on } \Gamma_N.$$

The equilibrium equation (2.14) can be stated for a purely Dirichlet problem (i.e., $\Gamma_D = \partial\Omega, \Gamma_N = 0$) by an operator equation

$$A(u) = f, \tag{2.15}$$

with an operator $A : V \to Y$ defined by

$$A(u) = -\text{div}\,\Big((1 + \nabla u)\mathbb{C}(\frac{1}{2}(\nabla u + (\nabla u)^T + (\nabla u)^T \nabla u))\Big). \tag{2.16}$$

For a special choice

$$V = \{v \in W^{2,p}(\Omega)^d : v|_{\Gamma_D} = 0\} \quad \text{and} \quad Y = L^p(\Omega),$$

A is a continuous mapping between spaces V and Y (for appropriate smoothness and growth conditions imposed on $\mathbb{C}$). It can be noticed, that $u = 0$ satisfies the equation (2.15) for zero external forces $f = 0$. With the help of *implicit function theorem* [Cia83], one can prove local existence of solutions of the equation (2.15) for sufficiently small f.

Theorem 2.3 (Local existence theorem in nonlinear elasticity). *Let $\Omega \subset \mathbb{R}^d$ be a bounded Lipschitz domain with boundary Γ_D of class $\mathcal{C}^2$. Let the mapping $\mathbb{C}$ of class $\mathcal{C}^1(\mathbb{R}^{d\times d}_{sym} \times \mathbb{R}^{d\times d}_{sym})$ satisfy*

$$\mathbb{C}(\varepsilon) = \lambda \mathrm{tr}\,(\varepsilon) + 2\mu\varepsilon + O(|\varepsilon|^2)$$

for $\lambda, \mu > 0$. (Here $O(|\varepsilon|^2)$ denotes the Landau-symbol such that $\limsup_{\varepsilon\to 0} O(|\varepsilon|^2)/|\varepsilon|^2 < \infty$.) Then there exists for every $p > d$ a neighborhood V of 0 in $X := W^{1,p}_0(\Omega)^d \cap W^{2,p}(\Omega)^d$ (with respect for the norm in $W^{2,p}(\Omega)$) and a neighborhood U of 0 in $L^p(\Omega)^d$, such that for all $f \in U$ there exist unique $u \in Y$ that solves

$$-\mathrm{div}\left((1+\nabla u)\mathbb{C}(\frac{1}{2}(\nabla u + (\nabla u)^T + (\nabla u)^T\nabla u))\right) = f.$$

The defined mapping $A^{-1} : f \to u, U \to V$ is Fréchet-differentiable.

Proof. See [Cia83]. □

For a more detailed discussion on nonlinear elasticity and the global existence technique, which is based on the polyconvex energy densities due to J.M. Ball, we refer to [Cia83, Val88, Car00b].

Chapter 3

Single-Yield Plasticity

This chapter introduces the classical concepts in small strain elastoplasticity with hardening. The main focus is the linear kinematic hardening model, which belongs to the category of single-yield models.

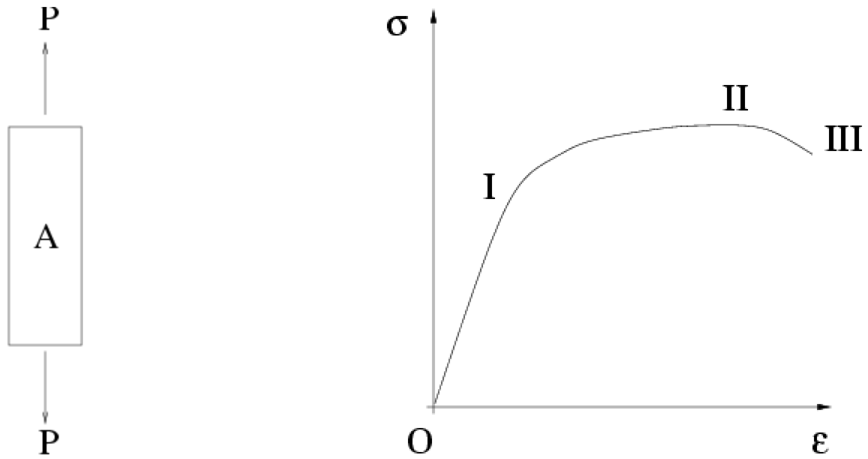

Figure 3.1: The tensile test: an increasing stress $\sigma = P/A$ is applied to the specimen (left), the resulting stress-strain relation (right).

The simplest mechanical test to visualize a nonlinear material behavior is the tensile test: an increasing tensile load is applied to a specimen and resulting changes in lengths are monitored. A typical stress-strain relation is displayed in Figure 3.1. At the beginning of the test the material extends elastically in the region $O - I$, the strain ε is directly proportional to the stress σ and the specimen returns to its original length on the removal of the stress. Beyond the elastic limit (point I) the applied stress produces plastic deformations so that a permanent extension remains after the removal of the applied load. The ratio σ/ε continues to decrease with elongation due to work *hardening* until the *ultimate tensile stress* is reached. At this point a neck begins to develop somewhere along the length of the specimen and further plastic deformation is localized within the neck. After necking (point II) has begun the nominal stress decreases until the material fractures at the point of minimum cross-sectional area within the neck. In this thesis we discuss models with a stress-strain relation in the $O - II$ region: we omit *softening* effects in the $II - III$ region.

3.1 Rheological elements

The behavior of an elastoplastic material is described by a combination of the following rheological elements: the linear, the rigid-plastic and the kinematic element [Kre96]. Every element is characterized by its (internal) stress and strain tensors. We denote the stress by σ and the strain by ε for the simplicity of notation. For combinations of more elements, we distinguish (internal) strains and stresses by introducing different indices, for instance σ^p, σ^e or different letters, for instance e, p.

3.1.1 The linear elastic element

The linear elastic element is a rheological element with a linear stress-strain relation, which is used in mechanics to characterize elastic material. The second order stress tensor σ is given by an action of the elastic tensor $\mathbb{C}$ on the second order strain tensor ε

$$\sigma = \mathbb{C}\varepsilon. \tag{3.1}$$

For *isotropic materials*, the action of $\mathbb{C}$ is given as in the linear elasticity by (2.3).

3.1.2 The rigid-plastic element

We define a stress space as the space of symmetric tensors $\mathbb{R}^{d\times d}_{sym}$. The basic concept in plasticity is the *yield surface* which is defined as the boundary ∂Z of a convex closed set $Z \subset \mathbb{R}^{d\times d}_{sym}$. The material remains rigid as long as $\sigma \in \operatorname{int} Z$ (the *interior* of Z). In this work we assume the *von-Mises* yield condition, which specifies Z for some $\sigma^y > 0$ as

$$Z = \{\sigma \in \mathbb{R}^{d\times d}_{sym} : ||\operatorname{dev}\sigma||_F \leq \sigma^y\}, \tag{3.2}$$

where $||\cdot||_F$ denotes the Frobenius matrix norm $||a||_F^2 = a : a = \sum_{i,j=1}^d a_{ij}^2$. Since the Frobenius norm is the only matrix norm being used, we omit the letter F and write $||\cdot||$ only. The matrix operator dev is the deviator defined by $\operatorname{dev}\sigma := \sigma - \frac{1}{d}(\operatorname{tr}\sigma)\mathbb{I}$, where tr denotes the trace of a matrix, $\operatorname{tr}\sigma := \sum_{i=1}^d \sigma_{ii}$.

Remark 3.1 (Tresca yield condition). The *Tresca* yield condition is an example of another yield condition:

$$Z = \{\sigma \in \mathbb{R}^{d\times d}_{sym} : \xi_1 + \cdots + \xi_d \leq \sigma^y\}, \tag{3.3}$$

where $\xi_1, \ldots, \xi_d$ are the eigenvalues of σ.

No deformation occurs, i.e., $\dot{\varepsilon} = 0$ as long as $\sigma \in \operatorname{int} Z$, The symbol $\dot{\varepsilon}$ denotes the time derivative of ε. The material behaves plastic if σ reaches the boundary ∂Z of Z. Plasticity is governed by following physical principles:

$$\begin{aligned} &\sigma \in Z, \\ &\langle \dot{\varepsilon}, q - \sigma \rangle \leq 0 \qquad \text{for all } q \in Z. \end{aligned} \tag{3.4}$$

In this expression brackets denote a scalar product, $\langle a, b\rangle := a : b$. The volume change is neglected during the plastic deformation. Therefore the *incompressibility condition* of the plastic strain reads

$$\mathrm{tr}\,\dot{\varepsilon} = 0. \tag{3.5}$$

We introduce some elementary results from *convex analysis* that are important in the following. It is convenient to work in the set of extended real numbers, $\mathbb{R}_\infty := \mathbb{R}\cup\{\infty\}, \mathbb{R}_{-\infty} := \mathbb{R}\cup\{-\infty\}, \mathbb{R}_{\pm\infty} := \mathbb{R}\cup\{-\infty,\infty\}$ with operations, i.e. $x+\infty := \infty, -\infty-\infty := -\infty, 0\cdot\infty := 0$ and so on. An expression $\infty - \infty$ is not allowed. In all definitions X is a Banach space.

Definition 3.1 (convex set, convex functional). A subset $Y \subseteq X$ is *convex*, if

$$\forall x, y \in Y, \lambda \in \langle 0, 1\rangle : \lambda x + (1-\lambda)y \in Y.$$

A functional $f : X \to \mathbb{R}_{+\infty}$ is a convex functional, if

$$\forall x, y \in Y, \lambda \in \langle 0, 1\rangle : f(\lambda x + (1-\lambda)y) \leq \lambda f(x) + (1-\lambda)f(y).$$

Definition 3.2 (normal cone, indicator function, conjugate function). Let $Y \subset X$ be a convex set, $x \in Y$. Then

$$N_Y(x) = \{x^* \in X^* : \langle x^*, y - x\rangle \leq 0 \qquad \text{for all } y \in Y\} \tag{3.6}$$

defines the *normal cone* to a convex set Y at point x. For any set $S \subset X$, the *indicator function* I_S of S is defined by

$$I_S(x) = \begin{cases} 0 & \text{if } x \in S, \\ +\infty & \text{if } x \notin S. \end{cases} \tag{3.7}$$

For a function $f : X \to [-\infty, \infty]$ we define the *conjugate function* $f^* : X^* \to [-\infty, \infty]$ by

$$f^*(x^*) = \sup_{x\in X}(\langle x^*, x\rangle - f(x)). \tag{3.8}$$

Definition 3.3 (subdifferential). Let f be a convex function on X. For any $x \in X$ the *subdifferential* $\partial f(x)$ of x is the possibly empty subset of X^* defined by

$$\partial f(x) = \{x^* \in X^* : \langle x^*, y - x\rangle \leq f(y) - f(x) \quad \forall y \in X\}. \tag{3.9}$$

Definition 3.4 (lower semicontinuity). A function $f : X \to [-\infty, +\infty]$ is called *lower semicontinuous* if

$$\{x_n\}_{n\in\mathbb{N}} \to x \Rightarrow \lim\inf_{n\to\infty} f(x_n) \geq f(x).$$

Definition 3.5 (proper function). A function $f : X \to [-\infty, +\infty]$ is called *proper* if there exists a point $x \in X$ such that $f(x) < \infty$.

By using the definition of the normal cone the inequality in (3.4) can be expressed as

$$\dot{\varepsilon} \in N_Z(\sigma). \tag{3.10}$$

Is it possible to invert (3.10), precisely to express σ in terms of $\dot{\varepsilon}$? In convex analysis it is proved that normal cone to the convex set Z at x is the subdifferential of the indicator function I_Z of Z at x,

$$\partial I_Z(x) = N_Z(x) \quad \text{for all } x \in Z.$$

Lemma 3.1. *Let X be a Banach space, $f : X \to [-\infty, \infty]$ be a proper, convex, lower semi-continuous function. Then*

$$x^* \in \partial f(x) \Leftrightarrow x \in \partial f^*(x^*). \tag{3.11}$$

Proof. See [Kos91]. □

We apply Lemma 3.1 to the inclusion (3.10) and obtain

$$\dot{\varepsilon} \in \partial I_Z(\sigma) \Leftrightarrow \sigma \in \partial I_Z^*(\dot{\varepsilon}). \tag{3.12}$$

We define a *dissipation function* $\mathcal{D}(x)$ by $\mathcal{D}(x) := I_Z^*(x)$. It means, that the indication and dissipation functions are *conjugate* functions of each other. The following result characterizes the form of the dissipation function for the von-Mises type yield function:

Lemma 3.2. *For $Z = \{\sigma \in \mathbb{R}^{d\times d}_{sym} : ||\text{dev}\,\sigma|| \leq \sigma^y\}$, the dissipation function $\mathcal{D}(x) = I_Z^*(x)$ satisfies*

$$\mathcal{D}(x) = \begin{cases} \sigma^y ||x|| & \textit{if}\ \text{tr}\, x = 0, \\ +\infty & \textit{otherwise}. \end{cases} \tag{3.13}$$

Proof. By the definition, the conjugate function to $I_Z^*(x)$ is given as

$$I_Z^*(x) = \sup_{y \in \mathbb{R}^{d\times d}_{sym}} (\langle x, y\rangle - I_Z(y)).$$

Since the indicator function $I_Z(.)$ only attains values 0 or $+\infty$ it is sufficient to find a supremum over the subset $\{y \in \mathbb{R}^{d\times d}_{sym} : ||\text{dev}\, y|| \leq \sigma^y\}$,

$$I_Z^*(x) = \sup_{y \in \mathbb{R}^{d\times d}_{sym}} (\langle x, y\rangle - I_Z(y)) = \sup_{y \in \mathbb{R}^{d\times d}_{sym} : ||\text{dev}\, y|| \leq \sigma^y} \langle x, y\rangle. \tag{3.14}$$

One of the following cases may occur:
(i) $\text{tr}\, x = 0$. We decompose y as $y = \text{dev}\, y + \frac{1}{d}(\text{tr}\, y)\mathbb{I}$ and get

$$\langle x, y\rangle = \langle x, \text{dev}\, y\rangle + \langle x, \frac{1}{d}(\text{tr}\, y)\mathbb{I}\rangle = \langle x, \text{dev}\, y\rangle + \frac{1}{d}\text{tr}\, x\ \ \text{tr}\, y.$$

Since $\text{tr}\, x = 0$ we have $\langle x, y\rangle = \langle x, \text{dev}\, y\rangle$ and

$$I_Z^*(x) = \sup_{y \in \mathbb{R}^{d\times d}_{sym} : ||\text{dev}\, y|| \leq \sigma^y} \langle x, y\rangle = \sup_{y \in \mathbb{R}^{d\times d}_{sym} : ||\text{dev}\, y|| \leq \sigma^y} \langle x, \text{dev}\, y\rangle. \tag{3.15}$$

We apply *Cauchy-Schwarz inequality* $\langle x, \text{dev}\, y\rangle \leq ||x|| \cdot ||\text{dev}\, y||$ and bound (3.15) as

$$I_Z^*(x) \leq \sigma^y ||x||.$$

The substitution of $y = \frac{x}{||x||}\sigma^y$ into (3.15) yields

$$I_Z^*(x) \geq \sigma^y ||x|| \tag{3.16}$$

and the comparison of (3.15) with (3.16) deduces

$$I_Z^*(x) = \sigma^y ||x||. \tag{3.17}$$

(ii) $\mathrm{tr}\, x \neq 0$. For all $x \in \mathbb{R}^{d\times d}_{sym}$, arbitrary $\alpha \in \mathbb{R}$ and the choice $y = \alpha\mathbb{I}$ we conclude from (3.14) that

$$I_Z^*(x) \geq \alpha(\mathrm{tr}\, x). \tag{3.18}$$

After the substitution $\alpha = \mathrm{sign}(\mathrm{tr}\, x)n$ the inequality (3.18) necessary implies $I_Z^*(x) = +\infty$. □

Lemma 3.2 and the definition of the subdiferential of the dissipation function $\mathcal{D}$ result in

Lemma 3.3. *For every $\dot\varepsilon, \sigma \in \mathbb{R}^{d\times d}_{sym}, Z = \{\sigma \in \mathbb{R}^{d\times d}_{sym} : ||\mathrm{dev}\,\sigma|| \leq \sigma^y\}$, the following statements (a),(b),(c),(d) are pairwise equivalent:*

$$\begin{aligned}
&\textit{(a) } \langle\dot\varepsilon, q-\sigma\rangle \leq 0 \quad \textit{for all } q \in Z.\\
&\textit{(b) } \dot\varepsilon \in N_Z(\sigma).\\
&\textit{(c) } \sigma \in \partial\mathcal{D}(\dot\varepsilon), \ \ \textit{where } \mathcal{D}(x) = \begin{cases} \sigma^y||x|| & \textit{if } \mathrm{tr}\, x = 0,\\ +\infty & \textit{otherwise}. \end{cases}\\
&\textit{(d) } \sigma : (q-\dot\varepsilon) \leq \mathcal{D}(q) - \mathcal{D}(\dot\varepsilon) \quad \textit{for all } q \in \mathbb{R}^{d\times d}_{sym}.
\end{aligned} \tag{3.19}$$

The satisfaction of the incompressibility condition (3.5) leads to another simplified equivalent statement with trace-free arguments.

Lemma 3.4. *Let the assumptions of Lemma 3.3 be satisfied and furthermore let $\mathrm{tr}\,\dot\varepsilon = 0$. Then the statement*

$$\textit{(e) } \sigma : (q-\dot\varepsilon) \leq \mathcal{D}(q) - \mathcal{D}(\dot\varepsilon) \quad \textit{for all } q \in \mathrm{dev}\,\mathbb{R}^{d\times d}_{sym} := \{q \in \mathbb{R}^{d\times d}_{sym} : \mathrm{tr}\, q = 0\}. \tag{3.20}$$

is equivalent to the statements (a),(b),(c),(d) in Lemma 3.3.

Proof. It is sufficient to prove the equivalence of statements (d) and (e). The implication $(d) \Rightarrow (e)$ follows from the inclusion $\mathrm{dev}\,\mathbb{R}^{d\times d}_{sym} \subseteq \mathbb{R}^{d\times d}_{sym}$. The implication $(e) \Rightarrow (d)$ can be proved by contradiction. □

Remark 3.2 (Trace-free arguments). Lemma 3.4 states that under the condition $\mathrm{tr}\,\dot\varepsilon = 0$ is is sufficient to consider only trace-free arguments $q \in \mathrm{dev}\,\mathbb{R}^{d\times d}_{sym}$ and the dissipation function in the form

$$\mathcal{D}(x) = \sigma^y||x||$$

in the statement (d) of Lemma 3.3.

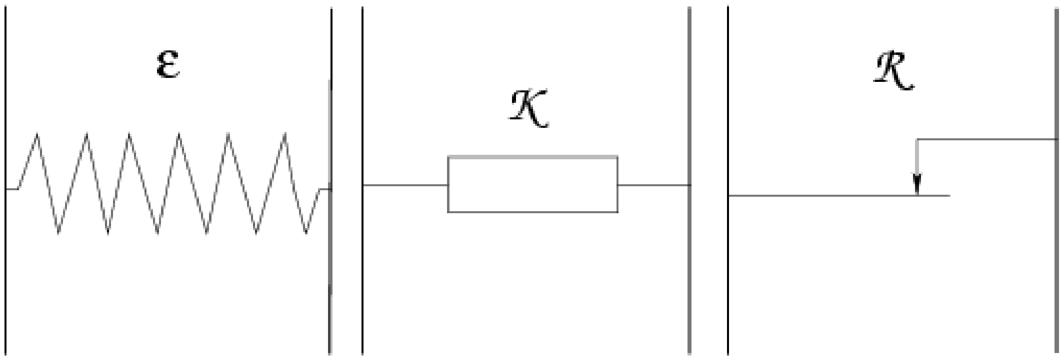

Figure 3.2: The elastic, kinematic and rigid-plastic element.

3.1.3 The kinematic element

We assume only the linear kinematic element, i.e. the element driven by the linear relation

$$\sigma = \mathbb{H}\varepsilon, \tag{3.21}$$

where $\mathbb{H}$ is a positive definite matrix. Typically $\mathbb{H} = h\mathbb{I}$, where $h > 0$ is a hardening coefficient and $\mathbb{I}$ represents the identical matrix.

Remark 3.3. The linear kinematic hardening element represents the simplest hardening element. There exists a variety of rheological elements describing nonlinear kinematic hardening, such as the Armstrong-Frederick model, the Bover's model, the model of Mróz and others [Bro98].

3.2 Composition of rheological elements

A large variety of models for the behavior of materials can be obtained by the composition of rheological elements. Let G_1, G_2 be two rheological elements and ε_i, σ_i let then be their strains and stresses, respectively, corresponding to the element $G_i, i = 1, 2$. More generally, a potential energy of each element is taken into consideration in [Kre96], however the stress and strain characteristics are sufficient for our purpose here.

The total strain ε and stress σ are defined by the following relations (the sign $|$ means the parallel combination of elements and $-$ is used for the serial combination)

G_1, G_2 parallel
$\varepsilon = \varepsilon_1 = \varepsilon_2$
$\sigma = \sigma_1 + \sigma_2$

G_1, G_2 serial
$\varepsilon = \varepsilon_1 + \varepsilon_2$
$\sigma = \sigma_1 = \sigma_2$

Now we explore constitutive relations for the simplest possible combination of the rheological elements, namely $\varepsilon|R$ and $\varepsilon - R$. Let the linear elastic element be described by internal stress σ^e, internal strain e and let the rigid-plastic element be described by internal stress σ^p and internal strain p. Composed rheological rules then yield

ε, R parallel
$\varepsilon = e = p$
$\sigma = \sigma^e + \sigma^p$
$\sigma^e = \mathbb{C}\varepsilon$
$\sigma^p \in Z$
$\langle \dot{\varepsilon}, q - \sigma^p \rangle \leq 0$ for all $q \in Z$

ε, R serial
$\varepsilon = e + p$
$\sigma = \sigma^e = \sigma^p$
$\sigma = \mathbb{C}e$
$\sigma^p \in Z$
$\langle \dot{p}, q - \sigma \rangle \leq 0$ for all $q \in Z$

3.3 Kinematic hardening model

There is a very important model combining the linear elastic, the rigid-plastic and the kinematic elements in the way $\varepsilon - (K/R)$. The rheological rules yield

$$\boxed{\begin{aligned} &\varepsilon = e + p \\ &\sigma = \sigma^e + \sigma^p \\ &\sigma^e = \mathbb{H}p \\ &\sigma = \mathbb{C}e \\ &\sigma^p \in Z \\ &\langle \dot{p}, q - \sigma^p \rangle \leq 0 \quad \text{for all } q \in Z. \end{aligned} \qquad (3.22)}$$

We call this rheological model a *kinematic hardening* model. Since the consider kinematic element is linear, we speak of *linear kinematic hardening model*. This model consists of one rigid-plastic element only and therefore can be classified as a *single-yield* model.

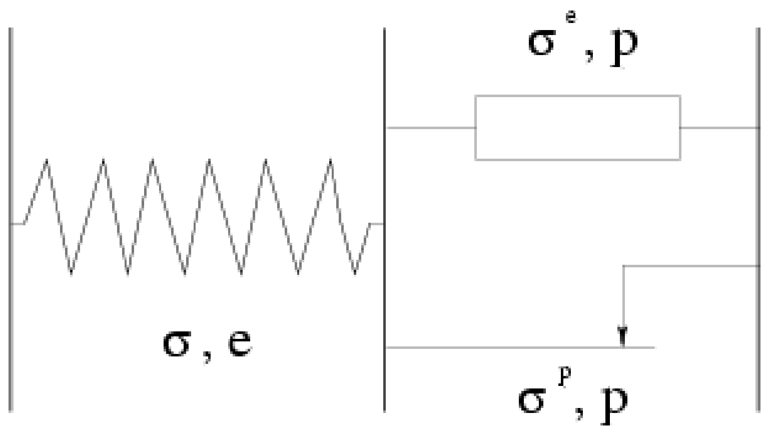

Figure 3.3: Kinematic hardening model.

Theorem 3.1. *Let $\mathcal{H}$ be a real separable Hilbert space endowed with a scalar product $\langle .,. \rangle_{\mathcal{H}}$. Let $Z \subset \mathcal{H}$ be a convex closed set, $0 \in Z$ and let $x^0 \in Z$ be a given element. Then for every function $u \in W^{1,1}(0,T;\mathcal{H})$ there exists a unique $x \in W^{1,1}(0,T;\mathcal{H})$ satisfying the variational inequality*

$$\langle \dot{u}(t) - \dot{x}(t), \tilde{x} - x(t) \rangle_{\mathcal{H}} \geq 0 \quad \textit{for almost every } \tilde{x} \in Z \qquad (3.23)$$

and the initial condition

$$x(0) = x^0. \qquad (3.24)$$

Proof. See [Kre96]. □

Remarks 3.1. (i) The solution of (3.23) is expressed by *stop* and *play* operators $\mathcal{S}, \mathcal{P} : Z \times W^{1,1}(0,T;\mathcal{H}) \to W^{1,1}(0,T;\mathcal{H})$ that are defined as

$$\mathcal{S}(x^0, u) := x, \quad \mathcal{P}(x^0, u) := u - \mathcal{S}(x^0, u). \tag{3.25}$$

(ii) The stop and play operators represent hysteresis operators with many interesting properties such as the rate independence, the semigroup property and causality [Kre96, BS96].

The important question is the $\sigma - \varepsilon$ relation. More precisely, we may ask: If σ is given as the function of time t, $\sigma = \sigma(t)$, is it possible to determine $\varepsilon = \varepsilon(t)$ from (3.22)? The answer to this question is positive [Kre96], namely we can rewrite $\langle \dot{p}, q - \sigma^p \rangle$ in the kinematic hardening case as

$$\langle \dot{p}, q - \sigma^p \rangle = \left\langle \mathbb{H}^{-1} \dot{\sigma}^e, q - \sigma^p \right\rangle = \langle \dot{\sigma} - \dot{\sigma}^p, q - \sigma^p \rangle_{\mathbb{H}^{-1}}$$

and therefore with the help of Theorem 3.1 we have

$$\varepsilon(t) = \mathbb{C}^{-1}\sigma(t) + \mathbb{H}^{-1}\sigma^e(t) = \mathbb{C}^{-1}\sigma(t) + \mathbb{H}^{-1}\mathcal{P}_{\mathbb{H}^{-1}}(\sigma_0^p, \sigma)(t), \tag{3.26}$$

where $\sigma_0^p = \sigma^p(t = 0)$ and the play operator $\mathcal{P}_{\mathbb{H}^{-1}}(.,.)$ is the solution operator to the problem with the scalar product $\langle x, y \rangle_{\mathbb{H}^{-1}} = \langle \mathbb{H}^{-1}x, y \rangle$. Figures 3.4 and 3.5 illustrate an example of the one-dimensional play operator and the stress-strain relation for the case of the prescribed cyclic stress $\sigma = A\sin(t)$ with an amplitude A, an initial zero plastic stress $\sigma_0^p = 0$, and a yield set $Z = [-\sigma^y, \sigma^y]$. Note that for $\sigma(t)$ growing from 0 to A (for $t \in (0, \pi/2)$),

$$\mathcal{P}(0, \sigma) = \begin{cases} 0 & \text{if } \sigma \leq \sigma^y, \\ \sigma - \sigma^y & \text{if } \sigma > \sigma^y. \end{cases} \tag{3.27}$$

3.4 Boundary value problem

Rheological models describe the mechanical behavior of the material at one point. Let a situation at every point of our continuum be described by a system (3.22). According to Lemma 3.4 we replace the inequality

$$\langle \dot{p}, q - \sigma^p \rangle \leq 0 \quad \text{for all } q \in Z$$

in (3.22) by its equivalent form

$$\sigma^p : (q - p) \leq \mathcal{D}(q) - \mathcal{D}(\dot{p}) \quad \text{for all } q \in \operatorname{dev} \mathbb{R}^{d\times d}_{sym} \tag{3.28}$$

and integrate this over Ω to show

$$\int_\Omega \sigma^p : (q - \dot{p})\,\mathrm{d}x \leq \int_\Omega \mathcal{D}(q)\,\mathrm{d}x - \int_\Omega \mathcal{D}(\dot{p})\,\mathrm{d}x \quad \text{for all } q \in \operatorname{dev} L^2(\Omega)^{d\times d}_{sym}. \tag{3.29}$$

Now we can subtract the equilibrium equation

$$\int_\Omega \sigma : \varepsilon(v - \dot{u})\,\mathrm{d}x = \int_\Omega f \cdot (v - \dot{u})\,\mathrm{d}x + \int_{\Gamma_N} g \cdot (v - \dot{u})\,\mathrm{d}x \tag{3.30}$$

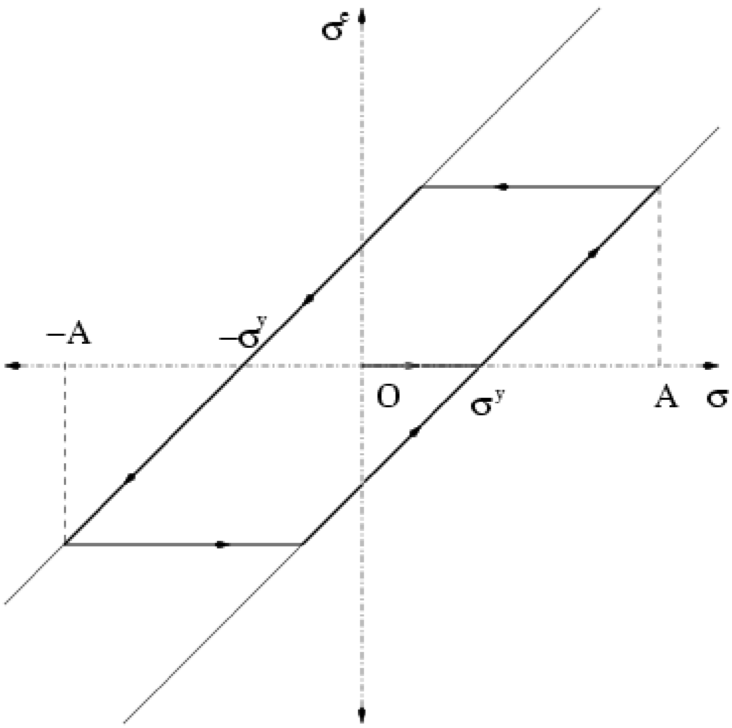

Figure 3.4: The play operator $\sigma^e = P(0, \sigma)$ in case of the cyclic stress $\sigma = A\sin(t)$.

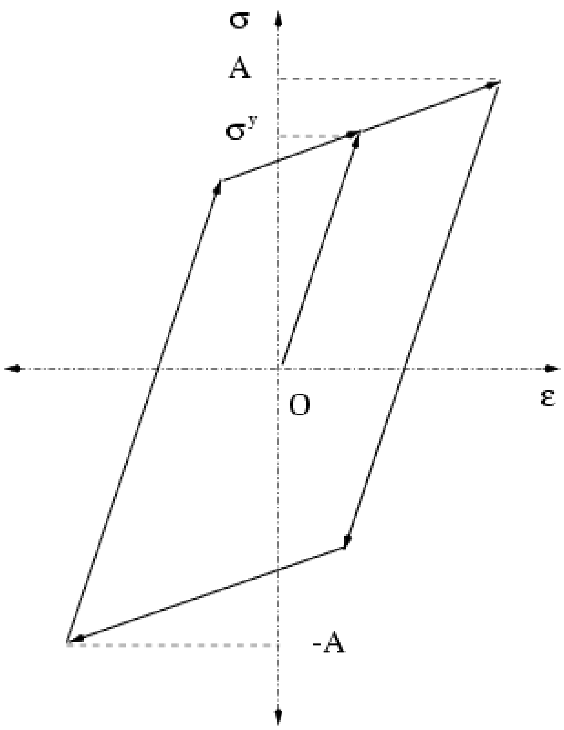

Figure 3.5: Stress-strain relation in case of linear kinematic hardening model and the cyclic stress $\sigma = A\sin(t)$.

from the inequality (3.29) and obtain

$$\begin{aligned}
&\int_\Omega \sigma : (\varepsilon(v) - q))\,\mathrm{d}x - \int_\Omega \sigma : (\varepsilon(\dot u) - \dot p)\,\mathrm{d}x + \int_\Omega \sigma^e : (q - \dot p)\,\mathrm{d}x \\
&+ \int_\Omega \mathcal{D}(q)\,\mathrm{d}x - \int_\Omega \mathcal{D}(\dot p)\,\mathrm{d}x - \int_\Omega f \cdot (v - \dot u)\,\mathrm{d}x - \int_{\Gamma_N} g \cdot (v - \dot u)\,\mathrm{d}x \geq 0, \\
&\quad \text{for all } v \in H^1_D(\Omega), q \in \text{dev}\, L^2(\Omega)^{d\times d}_{sym}.
\end{aligned} \tag{3.31}$$

Since $\sigma = \mathbb{C}(\varepsilon(u) - p)$ and $\sigma^e = \mathbb{H}p$ we denote

$$w = (u, p) \quad \text{and} \quad z = (v, q)$$

and rewrite (3.31) as a variational inequality

$$\langle \ell(t), z - \dot w(t)\rangle \leq a(w(t), z - \dot w(t)) + \psi(z) - \psi(\dot w(t)) \quad \text{for all } z \in \mathcal{H}. \tag{3.32}$$

Here

$$\mathcal{H} = H^1_D(\Omega) \times \text{dev}\, L^2(\Omega)^{d\times d}_{sym}$$

and the bilinear form $a(\cdot,\cdot)$, the linear functional $\ell(\cdot)$ and the nonlinear functional $\psi(\cdot)$ in (3.32) have the form:

$$\begin{aligned}
&a : \mathcal{H} \times \mathcal{H} \to \mathbb{R}, \quad a(w, z) = \int_\Omega \mathbb{C}(\varepsilon(u) - p) : (\varepsilon(v) - q)\,\mathrm{d}x + \int_\Omega \mathbb{H}p : q\,\mathrm{d}x, \\
&\ell(t) : \mathcal{H} \to \mathbb{R}, \quad \langle \ell(t), z\rangle = \int_\Omega f(t) \cdot v\,\mathrm{d}x + \int_{\Gamma_N} g(t) \cdot v\,\mathrm{d}x, \\
&\psi : \mathcal{H} \to \mathbb{R}, \quad \psi(z) = \int_\Omega \mathcal{D}(q)\,\mathrm{d}x.
\end{aligned} \tag{3.33}$$

Now we can formulate a boundary value problem of quasi-static elastoplasticity.

Problem 3.1 (BVP of quasi-static elastoplasticity). *For given $\ell \in H^1(0, T; \mathcal{H}^*), \ell(0) = 0$ find $w = (u, p) : [0, T] \to \mathcal{H}, w(0) = 0$, such that for almost $t \in (0, T)$*

$$\langle \ell(t), z - \dot w(t)\rangle \leq a(w(t), z - \dot w(t)) + \psi(z) - \psi(\dot w(t)) \quad \textit{for all } z \in \mathcal{H}. \tag{3.34}$$

3.5 Analogies

So far we have described a behavior at one point of our elastoplastic body by a system of equalities and inequalities directly derived from rheological laws. Such approach is used, e.g., in works of Brokate, Krejčí, Visintin [Bro97, Kre96, Vis94]. There exists another approach, based on a theory of *internal variables*, used in works of Carstensen et al [ACZ99], Han and Reddy [HR99], Simo and Hughes [SH98] and others. We mention some very basic information from the theory of internal variables and show that a linear kinematic hardening model described by (3.33) is a special case of a more general model.

In the contents of small strain elastoplasticity, the total strain $\varepsilon(u)$ is split additively into two contributions

$$\varepsilon(u) = \mathbb{C}^{-1}\sigma + p. \tag{3.35}$$

The *Prandtl-Reuß law* in a stress formulation, requires *generalized stresses* $(\sigma, \chi) \in \mathbb{R}^{d\times d}_{sym} \times \mathbb{R}^m$ to be *admissible*, i.e.,

$$\varphi(\sigma, \chi) < \infty \qquad \text{a.e. in } \Omega, \tag{3.36}$$

for some functional φ which is convex and non-negative but may be $+\infty$ such

$$(\dot{p}, \dot{\xi}) \in \partial\varphi(\sigma, \chi). \tag{3.37}$$

Due to the convex analysis, we equivalently reformulate (3.37) with the help of a dual functional φ^* as

$$(\sigma, \chi) \in \partial\varphi^*(\dot{p}, \dot{\xi}). \tag{3.38}$$

In the case of *combined kinematic and isotropic* hardening with the von-Mises yield function a (generalized) stress (σ, χ) is admissible if $\chi = (\alpha, \beta) \in \mathbb{R} \times \mathbb{R}^{d\times d}_{sym} \equiv \mathbb{R}^m, m = 1 + d(d+1)/2$, with $\alpha \geq 0$ and

$$\Phi(\sigma, \alpha, \beta) := ||\text{dev}\, \sigma - \text{dev}\, \beta|| - \sigma^y(1 + H\alpha) \leq 0. \tag{3.39}$$

Here, $\sigma^y > 0$ is the yield stress and $H \geq 0$ is the hardening modulus related to the isotropic hardening. The characteristic functional of the admissible stresses φ in (3.36) is for $(\sigma, \alpha, \beta) \in \mathbb{R}^{d\times d}_{sym} \times \mathbb{R} \times \mathbb{R}^{d\times d}_{sym}$

$$\varphi(\sigma, \alpha, \beta) = \begin{cases} 0 & \text{if} \quad \alpha \geq 0 \wedge \Phi(\sigma, \alpha, \beta) \leq 0, \\ +\infty & \text{otherwise} \end{cases} \tag{3.40}$$

and the corresponding dual functional $\varphi^* : \mathbb{R}^{d\times d}_{sym} \times \mathbb{R} \times \mathbb{R}^{d\times d}_{sym} \to \mathbb{R} \cup \{+\infty\}$ is

$$\varphi^*(p, a, b) = \begin{cases} \sigma^y||p|| & \text{if } \operatorname{tr} p = 0 \wedge p = -b \wedge a + \sigma^y H||p|| \leq 0, \\ +\infty & \text{otherwise.} \end{cases} \tag{3.41}$$

Variables $\xi = (a, b)$ and $\chi = (\alpha, \beta)$ are connected in the relation

$$\xi = -\mathbb{H}^{-1}\chi, \tag{3.42}$$

where $\mathbb{H} := \text{diag}(\mathbb{H}_1, \mathbb{H}_2)$ represents a hardening matrix that consists of an isotropic hardening matrix $\mathbb{H}_1 \in \mathbb{R}$ and a kinematic hardening matrix $\mathbb{H}_2 \in \mathbb{R}^{d\times d}_{sym}$. Further it was shown [HR99] that $w = (u, p, \xi)$ satisfies the variational inequality (3.32) holding for all $w = (v, q, \eta)$ with terms

$$\begin{aligned} &a : \mathcal{H} \times \mathcal{H} \to \mathbb{R}, \quad a(w, z) = \int_\Omega \mathbb{C}(\varepsilon(u) - p) : (\varepsilon(v) - q)\, \mathrm{d}x + \int_\Omega \xi * \mathbb{H}\, \eta\, \mathrm{d}x \\ &\ell(t) : \mathcal{H} \to \mathbb{R}, \quad \langle \ell(t), z\rangle = \int_\Omega f(t) \cdot v\, \mathrm{d}x + \int_{\Gamma_N} g(t) \cdot v\, \mathrm{d}x, \\ &\psi : \mathcal{H} \to \mathbb{R}, \psi(z) = \int_\Omega \varphi^*(q, \eta)\, \mathrm{d}x. \end{aligned} \tag{3.43}$$

The star $*$ denotes the scalar product defined as $\xi * \chi := a \cdot \alpha + b : \beta$ for all $\xi = (a, b), \chi = (\alpha, \beta), a, \alpha \in \mathbb{R}, b, \beta \in \mathbb{R}^{d\times d}_{sym}$. There are discussed special cases, in dependence on the choice of values of $\mathbb{H}_1, \mathbb{H}_2, H$ schematically displayed as

	$\mathbb{H}_1$	$\mathbb{H}_2$	H
Isotropic hardening	$\mathbb{H}_1 > 0$	0	$H > 0$
Kinematic hardening	0	$\mathbb{H}_2 > 0$	0
Perfect plasticity	0	0	0

In particular, for the case of kinematic hardening $\mathbb{H}_1 = 0, \mathbb{H}_2 > 0, H = 0$ implies (3.42) that the internal variable ξ at $w = (u, p, \xi)$ can be omitted and it can be further shown that $w = (u, p)$ solves a variational inequality (3.32) with terms (3.33), where $\mathbb{H} = \mathbb{H}_1$.

Chapter 4

Multi-Yield Plasticity

This chapter discusses the concept of multi-yield plasticity models as a natural generalization of the single-yield plasticity model, which was introduced in the previous chapter.

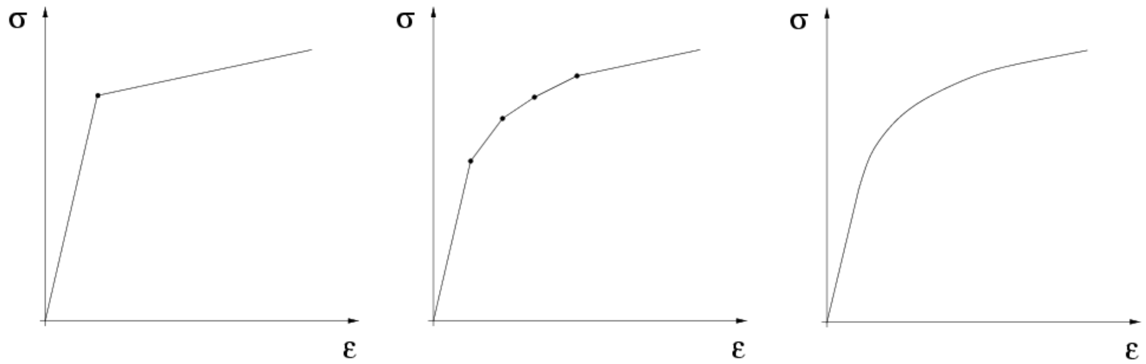

Figure 4.1: Stress-strain relation in case of single-yield (left), multi-yield (middle) and realistic model (right).

The model of linear kinematic hardening consists of only one rigid-plastic element and belongs therefore to the category of *single yield* models. As it has already been seen, such a model does not provide a satisfactory description of a real material behavior. The real relation $\varepsilon - \sigma$ is smooth. For this reason we introduce *multi-yield models*, schematically shown in Figure 4.1. Compared with a single yield model (left) the generalization with the multi-yield model (right) to more plastic phases makes the relation $\varepsilon - \sigma$ smoother and more realistic.

4.1 Prandtl-Ishlinskii model of play type

The following model is the typical representative of a multi-yield model. We call the *Prandtl-Ishlinskii model of play type* the rheological element defined by the formula $\varepsilon | \sum_{r \in I} (K_r - R_r)$, where the sign $\sum$ denotes the combination of elements in series, I denotes a measure space, with a finite nonnegative measure μ on I. We are basically concerned with two cases depending on the structure of the index set I:

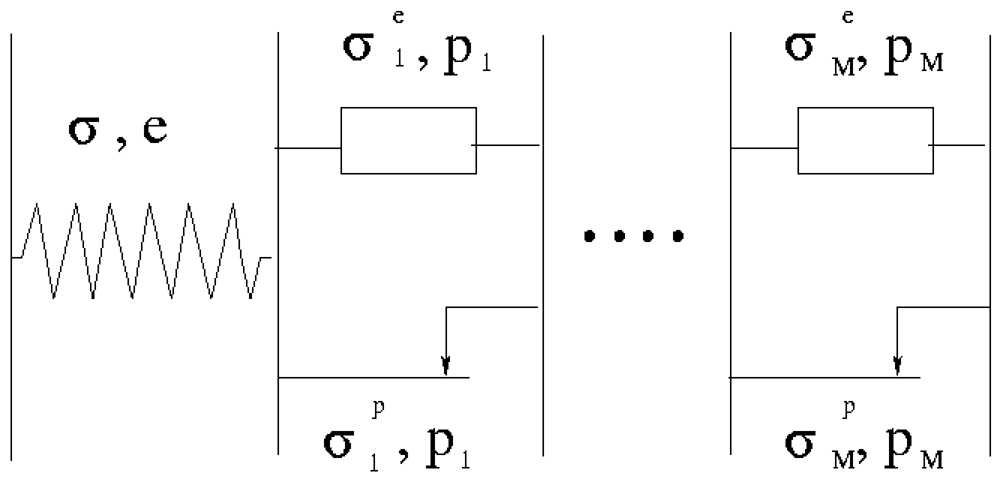

Figure 4.2: Prandtl-Ishlinskii model of play type.

1. I is a finite set, say $I = \{1, \ldots, M\}, M \in \mathbb{N}$, and furthermore μ is chosen to be a *counting measure*. Then we speak of *standard Prandtl-Ishlinskii model of play type* with M rigid-plastic elements. Alternatively we use the term the *multi-yield model*, or *M-yield model* in order to emphasize M rigid-plastic elements in the model structure.

2. I is a measurable set with a finite measure μ. Then we speak of *measure Prandtl-Ishlinskii model of play type*.

Remark 4.1. If $I = \{1\}$ then the standard Prandtl-Ishlinskii model of play type is reduced to the linear kinematic hardening model. Sometimes in the following we use the term *single-yield model*.

Rheological rules yield in the standard case $I = \{1, \ldots, M\}$:

$$\boxed{\begin{aligned}
&\varepsilon = e + p,\\
&p = \sum_{r=1}^{M} p_r,\\
&\sigma = \sigma_r^e + \sigma_r^p \quad \text{for all } r = 1, \ldots, M,\\
&\sigma_r^p \in Z_r,\\
&\langle \dot{p}_r, q_r - \sigma_r^p \rangle \le 0 \quad \text{for all } q_r \in Z_r, r = 1, \ldots, M,\\
&\sigma = \mathbb{C}e,\\
&\sigma_r^e = \mathbb{H}_r p_r, \quad r = 1, \ldots, M.
\end{aligned}} \tag{4.1}$$

In the measure case, we have the same system of equalities and variational inequalities. The only difference is that $p = \sum_{r=1}^{M} p_r$ in (4.1) is generalized as

$$p = \int_I p_r \, \mathrm{d}\mu(r)$$

and the condition $r \in \{1,\ldots,M\}$ is replaced by $r \in I$. Similarly as in linear kinematic hardening case (3.26) we can express the $\varepsilon - \sigma$ relation by using a play operator as

$$\varepsilon = \mathbb{C}^{-1}\sigma + \int_I \mathbb{H}_r^{-1}\mathcal{P}_{\mathbb{H}_r^{-1}}(\sigma_{0r}^p, \sigma)\,\mathrm{d}\mu(r), \tag{4.2}$$

where $\mathcal{P}_r, r \in I$ is a solution operator of the variational inequality

$$\langle \dot{u}(t) - \dot{x}(t), x(t) - \tilde{x}\rangle_{\mathbb{H}_r^{-1}} \geq 0 \quad \text{for almost every } \tilde{x} \in Z_r. \tag{4.3}$$

Example 4.1 (One-dimensional measure Prandtl-Ishlinskii model of play type). Let us consider the one-dimensional case, i.e., $\mathbb{C}, \mathbb{H}_r \in \mathbb{R}, r \in I$. Then (4.2) reads

$$\varepsilon = \mathbb{C}^{-1}\sigma + \int_I \mathbb{H}_r^{-1}\mathcal{P}_{\mathbb{H}_r^{-1}}(\sigma_{0r}^p, \sigma)\,\mathrm{d}\mu(r). \tag{4.4}$$

In the case of the interval index set $I = \langle \alpha, \beta\rangle, \alpha > 0$ with $Z_r = \langle -r, r\rangle, \sigma_{0r}^p = 0$ for all $r \in I$, for all $r \in I, \sigma(t) \nearrow \infty,\ \ \sigma(0) = 0$ we further have:

$$\varepsilon = \begin{cases} \mathbb{C}^{-1}\sigma & \text{if } \sigma \in (0, \alpha\rangle \\ \mathbb{C}^{-1}\sigma + \int_\alpha^\sigma \mathbb{H}_r^{-1}(\sigma - r)\,\mathrm{d}\mu(r) & \text{if } \sigma \in (\alpha, \beta) \\ \mathbb{C}^{-1}\sigma + \int_\alpha^\beta \mathbb{H}_r^{-1}(\sigma - r)\,\mathrm{d}\mu(r) & \text{if } \sigma \in \langle \beta, \infty). \end{cases} \tag{4.5}$$

Concavity of the curve $\varepsilon - \sigma$ (convexity of the curve $\sigma - \varepsilon$) is than guaranteed by the condition

$$\mathbb{H}_r > 0 \quad \text{for all } r \in I \tag{4.6}$$

and the monotonicity of both curves is ensured due to the condition

$$\mathbb{C}^{-1} + \int_I \mathbb{H}_r^{-1}\,\mathrm{d}\mu(r) \leq \infty. \tag{4.7}$$

Example 4.2 (One-dimensional two-yield Prandtl-Ishlinskii model of play type). This model represents the simplest multi-yield model and its modeling will be treated in the forthcoming sections. We assume two rigid-plastic elements with yield sets

$$Z_1 = [-\sigma_1^y, \sigma_1^y] \quad \text{and} \quad Z_2 = [-\sigma_2^y, \sigma_2^y]$$

with $0 < \sigma_1^y \leq \sigma_2^y$. The stress-strain relation reads

$$\varepsilon = \mathbb{C}^{-1}\sigma + \mathbb{H}_1^{-1}\mathcal{P}_{\mathbb{H}_1^{-1}}(\sigma_{01}^p, \sigma) + \mathbb{H}_2^{-1}\mathcal{P}_{\mathbb{H}_2^{-1}}(\sigma_{02}^p, \sigma). \tag{4.8}$$

An example of the linear combination of two play operators is displayed in Figures 4.4 and 4.3 for a prescribed cyclic stress $\sigma = A\sin(t), A > \sigma_2^y$ and initial zero plastic stresses $\sigma_{01}^p = \sigma_{02}^p = 0$. In the time interval $t = (0, \pi/2)$ there is $\sigma - \epsilon$ relation described by a piecewise affine increasing function that consist of three affine parts (Figure 4.4). The values of angles α, β_1, β_2 between one of three lines and σ axis (Figure 4.5) are derived from relations

$$\begin{aligned} \tan\alpha &= \mathbb{C}^{-1}, \\ \tan\beta_1 &= \mathbb{C}^{-1} + \mathbb{H}_1^{-1}, \\ \tan\beta_2 &= \mathbb{C}^{-1} + \mathbb{H}_1^{-1} + \mathbb{H}_2^{-1}. \end{aligned} \tag{4.9}$$

Conditions $\mathbb{C}, \mathbb{H}_1, \mathbb{H}_2 > 0$ ensure the concavity of the $\epsilon - \sigma$ curve and also its monotonicity with a relation $\alpha < \beta_1 < \beta_2 < \pi/2$.

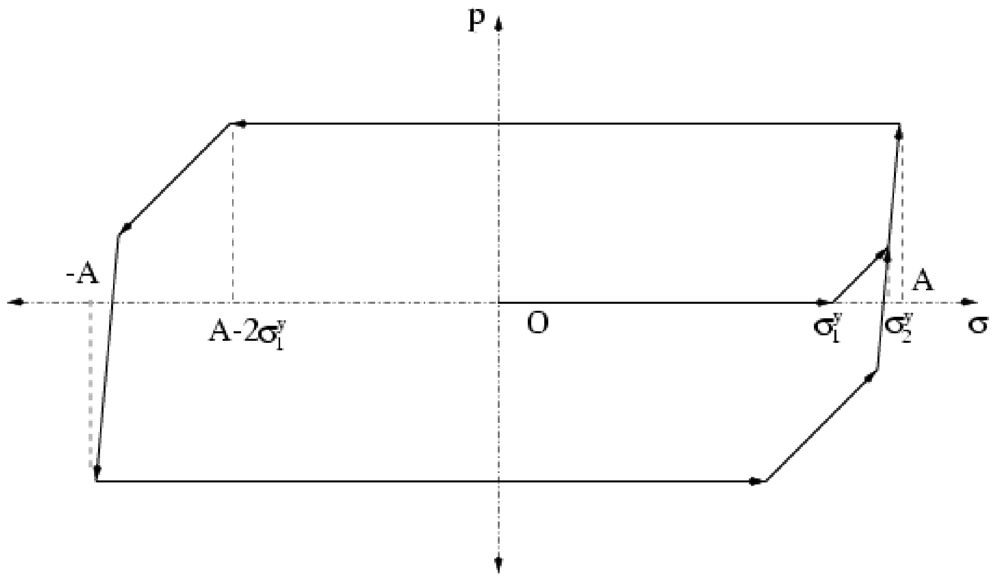

Figure 4.3: Linear combination of two play operators in case of cyclic stress $\sigma = A\sin(t)$.

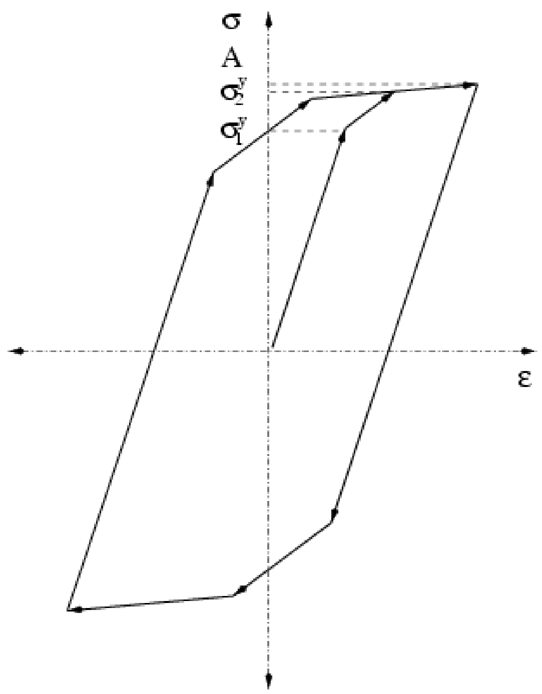

Figure 4.4: Stress-strain relation in case of two-yield model and cyclic stress $\sigma = A\sin(t)$.

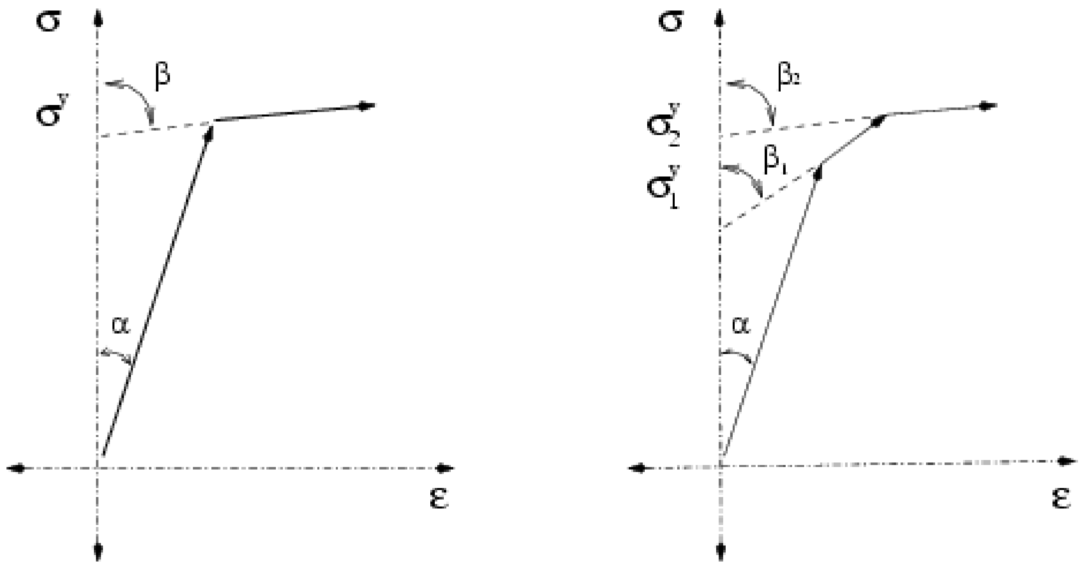

Figure 4.5: Stress-strain relation described by angles α, β for single-yield model (left) and by angles α, β_1, β_2 for two-yield model (right).

Remark 4.2 (Generation of multi-yield model from single-yield model). Let us assume a single-yield model specified by material parameters: $\mathbb{C}, \mathbb{H}, \sigma^y > 0$. To this single-yield model we can construct corresponding two-yield model specified by parameters $\mathbb{C}, \mathbb{H}_1, \mathbb{H}_2, \sigma_2^y \geq \sigma_1^y > 0$ with similar stress-strain relation. If we require that

- the elastic tensor $\mathbb{C}$ is the same for both single-yield and two-yield models,
- the angles β and β_2 are equal, i.e., $\beta = \beta_2$,
- the value of σ^y is between σ_1^y and σ_2^y, i.e., $0 < \sigma_1^y < \sigma^y < \sigma_2^y < \infty$,

than both models are identical for $\sigma \in (0, \sigma_1^y) \cup (\sigma_2^y, \infty)$, cf. Figure 4.5. The equality $\beta = \beta_2$ yields the condition on $\mathbb{H}_1, \mathbb{H}_2$,

$$\mathbb{H} = \mathbb{H}_1^{-1} + \mathbb{H}_2^{-1}. \tag{4.10}$$

Possible choice of $\mathbb{H}_1$ and $\mathbb{H}_2$ is for instance

$$\mathbb{H}_1 = \mathbb{H}_2 = 2\mathbb{H}. \tag{4.11}$$

The technique of the generalization of the single-yield model can easily be extended to the multi-yield model and it reads for the M-yield model

$$\mathbb{H}_1 = \cdots = \mathbb{H}_M = M\mathbb{H}. \tag{4.12}$$

4.2 The boundary value problem

Similarly as for the linear kinematic hardening model we can derive a variational inequality (3.32) with more general terms. As a rheological model we take the standard Prandtl-Ishlinskii model of play type with two rigid-plastic elements, i.e., $M = 2$. According to Lemma 3.4, we replace two inequalities in (4.1)

$$\begin{aligned} \langle \dot{p}_1, q_1 - \sigma_1^p \rangle &\le 0 \quad \text{for all } q_1 \in Z_1, \\ \langle \dot{p}_2, q_2 - \sigma_2^p \rangle &\le 0 \quad \text{for all } q_2 \in Z_2, \end{aligned} \tag{4.13}$$

by their equivalent forms

$$\begin{aligned} \sigma_1^p : (q_1 - p_1) &\le \mathcal{D}_1(q_1) - \mathcal{D}_1(\dot{p}_1) \quad \text{for all } q_1 \in \operatorname{dev} \mathbb{R}^{d\times d}_{sym}, \\ \sigma_2^p : (q_2 - p_2) &\le \mathcal{D}_2(q_2) - \mathcal{D}_2(\dot{p}_2) \quad \text{for all } q_2 \in \operatorname{dev} \mathbb{R}^{d\times d}_{sym}. \end{aligned} \tag{4.14}$$

The integration of (4.14) over Ω gives

$$\begin{aligned} \int_\Omega \sigma_1^p : (q_1 - \dot{p}_1)\,\mathrm{d}x &\le \int_\Omega \mathcal{D}_1(q_1)\,\mathrm{d}x - \int_\Omega \mathcal{D}_1(\dot{p}_1)\,\mathrm{d}x \quad \text{for all } q_1 \in \operatorname{dev} L^2(\Omega)^{d\times d}_{sym}, \\ \int_\Omega \sigma_2^p : (q_2 - \dot{p}_2)\,\mathrm{d}x &\le \int_\Omega \mathcal{D}_2(q_2)\,\mathrm{d}x - \int_\Omega \mathcal{D}_2(\dot{p}_2)\,\mathrm{d}x \quad \text{for all } q_2 \in \operatorname{dev} L^2(\Omega)^{d\times d}_{sym}. \end{aligned} \tag{4.15}$$

We subtract the equilibrium equation (3.30) from both inequalities (4.15) and obtain

$$\begin{aligned} &\int_\Omega \sigma : (\varepsilon(v) - q_1 - q_2))\,\mathrm{d}x - \int_\Omega \sigma : (\varepsilon(\dot{u}) - \dot{p}_1 - \dot{p}_2)\,\mathrm{d}x + \int_\Omega \sigma_1^e : (q_1 - \dot{p}_1)\,\mathrm{d}x, \\ &+ \int_\Omega \sigma_2^e : (q_2 - \dot{p}_2)\,\mathrm{d}x + \int_\Omega (\mathcal{D}_1(q_1) + \mathcal{D}_2(q_2))\,\mathrm{d}x - \int_\Omega (\mathcal{D}_1(\dot{p}_1) + \mathcal{D}_2(\dot{p}_2))\,\mathrm{d}x - \\ &\int_\Omega f \cdot (v - \dot{u})\,\mathrm{d}x - \int_{\Gamma_N} g \cdot (v - \dot{u})\,\mathrm{d}x \ge 0 \quad \text{for all } v \in H^1_D(\Omega), q_1, q_2 \in \operatorname{dev} L^2(\Omega)^{d\times d}_{sym}. \end{aligned} \tag{4.16}$$

Since $\sigma = \mathbb{C}(\varepsilon(u) - p_1 - p_2), \sigma_1^e = \mathbb{H}_1 p_1$ and $\sigma_2^e = \mathbb{H}_2 p_2$ we can rewrite (4.16) as a variational inequality (3.32) for

$$w = (u, p_1, p_2) \quad \text{and} \quad z = (v, q_1, q_2)$$

in a space

$$\mathcal{H} = H^1_D(\Omega) \times \operatorname{dev} L^2(\Omega)^{d\times d}_{sym} \times \operatorname{dev} L^2(\Omega)^{d\times d}_{sym},$$

where a bilinear form $a(.,.)$, a linear functional $\ell(.)$ and a nonlinear functional $\psi(.)$ have the form

$$\begin{aligned} a : \mathcal{H} \times \mathcal{H} \to \mathbb{R}, \quad a(w, z) &= \int_\Omega \mathbb{C}(\varepsilon(u) - p_1 - p_2) : (\varepsilon(v) - q_1 - q_2)\,\mathrm{d}x \\ &\quad + \int_\Omega \mathbb{H}_1 p_1 : q_1\,\mathrm{d}x + \int_\Omega \mathbb{H}_2 p_2 : q_2\,\mathrm{d}x, \\ \ell(t) : \mathcal{H} \to \mathbb{R}, \quad \langle \ell(t), z \rangle &= \int_\Omega f(t) \cdot v\,\mathrm{d}x + \int_{\Gamma_N} g(t) \cdot v\,\mathrm{d}x, \\ \psi : \mathcal{H} \to \mathbb{R}, \quad \psi(z) &= \int_\Omega (\mathcal{D}_1(q_1) + \mathcal{D}_2(q_2))\,\mathrm{d}x. \end{aligned} \tag{4.17}$$

The generalization to the standard Prandtl-Ishlinskii model of play type with M rigid-plastic elements yields obviously again the variational inequality (3.32) for

$$w = (u, p_1, \dots, p_M) \quad \text{and} \quad z = (v, q_1, \dots, q_M),$$

in a space

$$\mathcal{H} = H^1_D(\Omega) \times \underbrace{\operatorname{dev} L^2(\Omega)^{d\times d}_{sym} \times \dots \times \operatorname{dev} L^2(\Omega)^{d\times d}_{sym}}_{M \text{ times}},$$

where a bilinear form $a(\cdot,\cdot)$, a linear functional $\ell(\cdot)$ and a nonlinear functional $\psi(\cdot)$ have the form

$$\begin{aligned}
a : \mathcal{H}\times\mathcal{H} \to \mathbb{R}, \quad a(w,z) &= \int_\Omega \Big(\mathbb{C}(\varepsilon(u) - \sum_{i=1}^M p_i)\Big) : \Big(\varepsilon(v) - \sum_{i=1}^M q_i\Big)\,\mathrm{d}x \\
&\quad + \sum_{i=1}^M \int_\Omega \mathbb{H}_i p_i : q_i \,\mathrm{d}x, \\
\ell(t) : \mathcal{H} \to \mathbb{R}, \quad \langle \ell(t), z\rangle &= \int_\Omega f(t)\cdot v\,\mathrm{d}x + \int_{\Gamma_N} g(t)\cdot v\,\mathrm{d}x, \\
\psi : \mathcal{H} \to \mathbb{R}, \quad \psi(z) &= \int_\Omega \sum_{i=1}^M \mathcal{D}_i(q_i)\,\mathrm{d}x.
\end{aligned} \tag{4.18}$$

Problem 4.1 (BVP of quasi-static multi-yield elastoplasticity). *For given $l \in H^1(0,T;\mathcal{H}^*), \ell(0) = 0$ find $w = (u, p_1, \dots, p_M) : [0,T] \to \mathcal{H}, w(0) = 0$, such that for almost all $t \in (0,T)$*

$$\langle \ell(t), z - \dot w(t)\rangle \le a(w(t), z - \dot w(t)) + \psi(z) - \psi(\dot w(t)) \quad \textit{for all } z \in \mathcal{H}. \tag{4.19}$$

Similarly, for the measure Prandtl-Ishlinskii model of play type one analogically obtains the variational inequality (3.32) for

$$w = (u, p_r) \quad \text{and} \quad z = (v, q_r), \quad r \in I$$

in a space

$$\mathcal{H} = \{(v, q_r), r \in I : v \in H^1_D(\Omega), q_r \in \operatorname{dev} L^2(\Omega)^{d\times d}_{sym}\}, \tag{4.20}$$

where a bilinear form $a(\cdot,\cdot)$, a linear functional $\ell(\cdot)$ and a nonlinear functional $\psi(\cdot)$ have the form

$$\begin{aligned}
a : \mathcal{H}\times\mathcal{H} \to \mathbb{R}, \quad a(w,z) &= \int_\Omega \Big(\mathbb{C}(\varepsilon(u) - \int_I p_r\,\mathrm{d}\mu(r)\Big) : \Big(\varepsilon(v) - \int_I q_r \mu(r)\Big)\,\mathrm{d}x \\
&\quad + \int_\Omega \int_I \mathbb{H}_r p_r : q_r \,\mathrm{d}\mu(r)\,\mathrm{d}x, \\
\ell(t) : \mathcal{H} \to \mathbb{R}, \quad \langle \ell(t), z\rangle &= \int_\Omega f(t)\cdot v\,\mathrm{d}x + \int_{\Gamma_N} g(t)\cdot v\,\mathrm{d}x, \\
\psi : \mathcal{H} \to \mathbb{R}, \quad \psi(z) &= \int_\Omega \int_I \mathcal{D}_r(q_r)\,\mathrm{d}\mu(r)\,\mathrm{d}x.
\end{aligned} \tag{4.21}$$

The boundary value problem of quasi-static multi-yield elastoplasticity in the measure case reads:

Problem 4.2 (BVP of quasi-static multi-yield elastoplasticity, measure case). *For given* $l \in H^1(0, T; \mathcal{H}^*), \ell(0) = 0$ *find* $w = (u, p_r), r \in I : [0, T] \to \mathcal{H}, w(0) = 0$*, such that for almost all* $t \in (0, T)$

$$\langle \ell(t), z - \dot{w}(t) \rangle \leq a(w(t), z - \dot{w}(t)) + \psi(z) - \psi(\dot{w}(t)) \quad \textit{for all } z \in \mathcal{H}. \tag{4.22}$$

Chapter 5

Mathematical Analysis

This chapter is focused on the analysis of boundary value problems of quasi-static multi-yield elastoplasticity. First, the standard problem (Problem 4.1) is considered, and second the obtained results are generalized for the measure problem (Problem 4.2). We show that the variational inequality (3.32) has a unique solution by checking the validity of assumptions of a more general theorem [HR99].

In the standard case, we search for a solution $w = (u, p_1, \ldots, p_M) \in \mathcal{H}$ of the variational inequality (3.32). The Hilbert space $\mathcal{H}$ is defined as the Cartesian product of Hilbert spaces V, Q_0

$$\mathcal{H} = V \times \underbrace{Q_0 \times \cdots \times Q_0}_{M \text{ times}},$$

where

$$V := H^1_D(\Omega) \quad \text{and} \quad Q_0 := \{q : q \in \operatorname{dev} \mathbb{R}^{d\times d}_{sym}, q_{ij} \in \operatorname{dev} L^2(\Omega)\}.$$

A scalar product $(\cdot,\cdot)_{\mathcal{H}}$ and an induced norm $||\cdot||_{\mathcal{H}}$ in the space $\mathcal{H}$ are

$$\begin{aligned} (w, z)_{\mathcal{H}} &:= (u, v)_V + (p_1, q_1)_{Q_0} + \cdots + (p_M, q_M)_{Q_0}, \\ ||w||^2_{\mathcal{H}} &:= (u, u)^2_V + (p_1, p_1)^2_{Q_0} + \cdots + (p_M, p_M)^2_{Q_0}, \\ ||z||^2_{\mathcal{H}} &:= (v, v)^2_V + (q_1, q_1)^2_{Q_0} + \cdots + (q_M, q_M)^2_{Q_0}. \end{aligned}$$

In the forthcoming sections we prove that

- The bilinear form

  $$a(w, z) = \int_\Omega \Big(\mathbb{C}(\varepsilon(u) - \sum_{i=1}^M p_i)\Big) : \Big(\varepsilon(v) - \sum_{i=1}^M q_i\Big)\,\mathrm{d}x + \sum_{i=1}^M \int_\Omega \mathbb{H}_i p_i : q_i \,\mathrm{d}x$$

  is bounded and elliptic in the space $\mathcal{H}$.

- The functional

  $$\psi(z) = \int_\Omega \sum_{i=1}^M \mathcal{D}_i(q_i)\,\mathrm{d}x$$

  is nonnegative and positive homogeneous in the space $\mathcal{H}$.

5.1 Boundedness of $a(w, z)$

By the definition of boundedness, it is to prove

$$|a(w,z)| \leq c_b ||w||_{\mathcal{H}} ||z||_{\mathcal{H}}, \tag{5.1}$$

where $c_b > 0$. For simplicity of notation, only the case $M = 2$ is analyzed. An extension to the case $M > 2$ follows automatically. By the triangle inequality,

$$|a(w,z)| \leq \Big| \int_\Omega \mathbb{C}(\varepsilon(u) - p_1 - p_2) : (\varepsilon(v) - q_1 - q_2) \, \mathrm{d}x \Big| + \Big| \int_\Omega (\mathbb{H}_1 p_1 : q_1 + \mathbb{H}_2 p_2 : q_2) \, \mathrm{d}x \Big|. \tag{5.2}$$

The first term in the inequality (5.2) can be bounded by Cauchy-Schwartz inequality for the scalar product $(a, b) = a : b$, and the multiplicativity of the Euclidean norm $|| \cdot ||$,

$$\begin{aligned} \Big| \int_\Omega \mathbb{C}(\varepsilon(u) - p_1 - p_2) : (\varepsilon(v) - q_1 - q_2) \, \mathrm{d}x \Big| &\leq \int_\Omega \Big| \mathbb{C}(\varepsilon(u) - p_1 - p_2) : (\varepsilon(v) - q_1 - q_2) \Big| \, \mathrm{d}x \\ &\leq ||\mathbb{C}|| \Big(\int_\Omega ||\varepsilon(u) - p_1 - p_2||^2 \, \mathrm{d}x \Big)^{\frac{1}{2}} \Big(\int_\Omega ||\varepsilon(v) - q_1 - q_2||^2 \, \mathrm{d}x \Big)^{\frac{1}{2}}. \end{aligned}$$

By using the inequality $|a + b + c|^2 \leq 3(|a|^2 + |b|^2 + |c|^2)$ for all $a, b, c \in \mathbb{R}$, we obtain

$$\begin{aligned} \int_\Omega ||\varepsilon(u) - p_1 - p_2||^2 \, \mathrm{d}x &\leq \int_\Omega \sum_i \sum_j \Big(\varepsilon_{ij}(u) - p_{1_{ij}} - p_{2_{ij}} \Big)^2 \, \mathrm{d}x \\ &\leq 3 \int_\Omega \sum_i \sum_j \Big((\varepsilon_{ij}(u))^2 + (p_{1_{ij}})^2 + (p_{2_{ij}})^2 \Big) \, \mathrm{d}x \\ &\leq 3 \int_\Omega \Big(||\varepsilon(u)||^2 + ||p_1||^2 + ||p_2||^2 \Big) \, \mathrm{d}x. \end{aligned} \tag{5.3}$$

Since $\varepsilon(u) : \varepsilon(u) = \sum_{i,j} \frac{1}{2}(u_{i,j} + u_{j,i})^2 \leq \sum_{i,j} u_{i,j}^2$, it holds consequently $\int_\Omega ||\varepsilon(u)||^2 \, \mathrm{d}x \leq ||u||^2_{H^1_D(\Omega)^d}$, which further implies

$$\int_\Omega \Big(||\varepsilon(u)||^2 + ||p_1||^2 + ||p_2||^2 \Big) \, \mathrm{d}x \leq ||u||^2_{H^1_D(\Omega)^d} + \int_\Omega \Big(||p_1||^2 + ||p_2||^2 \Big) \, \mathrm{d}x = ||w||^2_{\mathcal{H}}.$$

Putting estimates (5.3) and (5.3) together, one obtains

$$\int_\Omega ||\varepsilon(u) - p_1 - p_2||^2 \, \mathrm{d}x \leq 3 ||w||^2_{\mathcal{H}} \tag{5.4}$$

and for the same reason

$$\int_\Omega ||\varepsilon(v) - q_1 - q_2||^2 \, \mathrm{d}x \leq 3 ||z||^2_{\mathcal{H}}. \tag{5.5}$$

The second term in (5.2) is bounded as

$$
\begin{aligned}
&\Big|\int_\Omega (\mathbb{H}_1 p_1 : q_1 + \mathbb{H}_2 p_1 : q_1)\,\mathrm{d}x\Big| \leq \int_\Omega \Big|\mathbb{H}_1 p_1 : q_1 + \mathbb{H}_2 p_2 : q_2\Big|\,\mathrm{d}x \\
&\leq \int_\Omega \Big(||\mathbb{H}_1 p_1||\cdot||q_1|| + ||\mathbb{H}_2 p_2||\cdot||q_2||\Big)\,\mathrm{d}x \\
&\leq \max\{||\mathbb{H}_1||, ||\mathbb{H}_2||\} \int_\Omega \Big(||p_1||\cdot||q_1|| + ||p_2||\cdot||q_2||\Big)\,\mathrm{d}x \\
&\leq \max\{||\mathbb{H}_1||, ||\mathbb{H}_2||\} \int_\Omega \Big(||p_1||^2 + ||p_2||^2\Big)^{1/2}\Big(||q_1||^2 + ||q_2||^2\Big)^{1/2}\,\mathrm{d}x \\
&\leq \max\{||\mathbb{H}_1||, ||\mathbb{H}_2||\}\Big(\int_\Omega \Big((||p_1||^2 + ||p_2||^2)\,\mathrm{d}x\Big)^{1/2}\Big(\int_\Omega (||q_1||^2 + ||q_2||^2)\,\mathrm{d}x\Big)^{1/2} \\
&\leq \max\{||\mathbb{H}_1||, ||\mathbb{H}_2||\}\, ||w||_{\mathcal{H}}||z||_{\mathcal{H}}
\end{aligned}
\tag{5.6}
$$

Combining the estimates (5.4), (5.5) and (5.6), we conclude the following proposition for $M = 2$.

Proposition 5.1 (Boundedness of the bilinear form $a(\cdot,\cdot)$). *A bilinear form $a(\cdot,\cdot)$ is bounded in the space $\mathcal{H}$,*

$$
|a(w,z)| \leq \Big((M+1)||\mathbb{C}|| + \max_{i=1,\ldots,M} ||\mathbb{H}_i||\Big)||w||_{\mathcal{H}}||z||_{\mathcal{H}}. \tag{5.7}
$$

Proof. The proof is a direct modification of the aforementioned situation for $M = 2$. □

5.2 $\mathcal{H}$-ellipticity of $a(w, z)$

We aim to prove the existence of a constant $c_e > 0$, so that

$$
a(w,w) \geq c_e||w||^2_{\mathcal{H}} \qquad \text{for all } w \in \mathcal{H}.
$$

Under the natural assumptions of symmetry of elastic and hardening tensors

$$
\begin{aligned}
&\xi : \mathbb{C}\lambda = \mathbb{C}\xi : \lambda \quad \text{for all } \xi, \lambda \in \mathbb{R}^d, \\
&\xi : \mathbb{H}_i\lambda = \mathbb{H}_i\xi : \lambda \quad \text{for all } \xi, \lambda \in \mathbb{R}^d, i = 1, \ldots, M
\end{aligned}
\tag{5.8}
$$

and their positive definiteness

$$
\begin{aligned}
&\mathbb{C}\xi : \xi \geq c||\xi||^2 \quad \text{for all } \xi \in \mathbb{R}^d, \\
&\mathbb{H}_i\xi : \xi \geq h_i||\xi||^2 \quad \text{for all } \xi \in \mathbb{R}^d, i = 1, \ldots, M
\end{aligned}
\tag{5.9}
$$

we can bound the integrand in the scalar product $a(w, w)$ as

$$
\begin{aligned}
&\mathbb{C}(\varepsilon(u) - p_1 - \cdots - p_M) : (\varepsilon(u) - p_1 - \cdots - p_M) + \mathbb{H}_1 p_1 : p_1 + \cdots + \mathbb{H}_M p_M : p_M \\
&\geq c||\varepsilon(u) - p_1 - \cdots - p_M||^2 + h_1||p_1||^2 + \cdots + h_M||p_M||^2 \\
&\geq \min\{c, h_1, \ldots, h_M\}\Big(||\varepsilon(u) - p_1 - \cdots - p_M||^2 + ||p_1||^2 + \cdots + ||p_M||^2\Big).
\end{aligned}
\tag{5.10}
$$

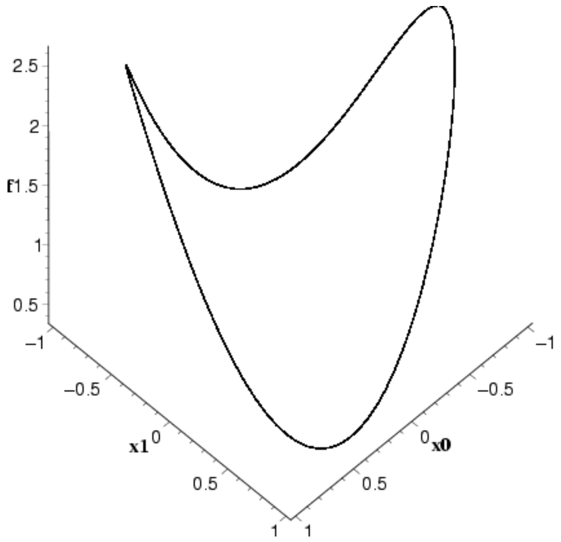

Figure 5.1: Continuous function $f(x)$ on the torus ($x_0^2 + x_1^2 = 1$) in Lemma 5.2 for $M = 1$. Its minimum is 0.3819.

Lemma 5.1. *Let $D \in \mathbb{R}^{N\times N}$ be a diagonal matrix $D =$ diag $(d_1, \ldots, d_N), d_j \neq 0$ for $j = 1, \ldots, N$, let $a \in \mathbb{R}^N$. Then there holds*

$$\textit{det}\,(D + a \otimes a) = (\prod_{j=1}^{N} d_j)(1 + \sum_{j=1}^{N} a_j^2/d_j). \tag{5.11}$$

Proof. The proof consists in constructing similar matrices to $(D + a \otimes a)$ by equivalent operations, that do not change the determinant. Firstly, the last column $\begin{pmatrix} -a \\ 1 \end{pmatrix}$ of the matrix $\begin{pmatrix} D & -a \\ a^T & 1 \end{pmatrix}$ is multiplied with $-a_j$ and added it to the $j-$th column for $j = 1, \ldots, N$, and we obtain

$$\begin{pmatrix} D + a \otimes a & -a \\ 0 & 1 \end{pmatrix}.$$

Secondly, the j-th row of the matrix matrix $\begin{pmatrix} D & -a \\ a^T & 1 \end{pmatrix}$ is multiplied with $-a_j/d_i$ and added to the last one for $j = 1, \ldots, N$, and we obtain

$$\begin{pmatrix} D & -a \\ 0 & 1 + \sum_{j=1}^{N} a_j^2/d_j \end{pmatrix}.$$

Thus, the following formula is derived

$$\det(D + a \otimes a) = \det \begin{pmatrix} D + a \otimes a & -a \\ 0 & 1 \end{pmatrix} = \det \begin{pmatrix} D & -a \\ a^T & 1 \end{pmatrix} = \det \begin{pmatrix} D & -a \\ 0 & 1 + \sum_{j=1}^{N} a_j^2/d_j \end{pmatrix}.$$

Since D is a diagonal matrix with det $(D) = \prod_{j=1}^N d_j$, we have

$$\det \begin{pmatrix} D & -a \\ 0 & 1+\sum_{j=1}^N a_j^2/d_j \end{pmatrix} = (\prod_{j=1}^N d_j)(1+\sum_{j=1}^N a_j^2/d_j),$$

which concludes the proof. □

Lemma 5.2. *There exists $k = k(M) > 0$ such that, for all $x_0, x_1, \dots, x_M \in \mathbb{R}$,*

$$\Big(x_0 - \sum_{i=1}^M x_i\Big)^2 + \sum_{i=1}^M x_i^2 \geq k \sum_{i=0}^M x_i^2. \tag{5.12}$$

Proof. Let us denote $f(x) = (x_0 - \sum_{i=1}^M x_i)^2 + \sum_{i=1}^M x_i^2$, where $x = (x_0, \cdots, x_M) \in \mathbb{R}^{M+1}$. It is easy to check that f is homogeneous of degree 2, $f(rx) = r^2 f(x)$ for all $r \in \mathbb{R}$. Thus

$$\inf_{x\in\mathbb{R}^{M+1}, x\neq 0} \frac{f(x)}{||x||^2} = \min_{x\in\mathbb{R}^{M+1}, ||x||^2=1} f(x) \geq k. \tag{5.13}$$

Since $f(x)$ is a continuous function on the compact set $\{x \in \mathbb{R}^{M+1} : ||x||^2 = 1\}$, there exists $\bar{x} \in \mathbb{R}^{M+1}$ such that $f(\bar{x}) = \min_{x\in\mathbb{R}^{M+1}} \frac{f(x)}{||x||^2} = k$. Additionally, since $f(x) > 0$ for all $x \in \mathbb{R}^{M+1}$ satisfying $||x||^2 = 1$, there holds $k > 0$. □

Remarks 5.1. (i) Lemma 5.2 holds also for matrices $x_0, x_1, \dots, x_M \in \mathbb{R}^{d\times d}$ when $(\cdot)^2$ is replaced $||\cdot||^2 = \sum_{i,j=1}^d (\cdot)_{ij}^2$, i.e.,

$$\Big|\Big|x_0 - \sum_{i=1}^M x_i\Big|\Big|^2 + \sum_{i=1}^M ||x_i||^2 \geq k \sum_{i=0}^M ||x_i||^2. \tag{5.14}$$

(ii) According to Lemma 5.2, the value k depends on M only. In order to calculate k as a function of M explicitly, we rewrite

$$\Big(x_0 - \sum_{i=1}^M x_i\Big)^2 + \sum_{i=1}^M x_i^2 = x^T A x, \quad x = (x_0, \dots, x_M) \in \mathbb{R}^{M+1}$$

with the matrix

$$A = (1, -1, \dots, -1) \otimes (1, -1, \dots, -1) + \operatorname{diag}(0, 1, \dots, 1).$$

Then (5.13) is reformulated as

$$k \leq \frac{x^T A x}{x^T x}.$$

That means that the maximal k is the smallest eigenvalue of matrix A. All eigenvalues λ of matrix A satisfy the condition

$$\det(A - \lambda I) = \det(\operatorname{diag}(-\lambda, 1-\lambda, \dots, 1-\lambda) + (1, -1, \dots, -1) \otimes (1, -1, \dots, -1)) = 0.$$

The application of Lemma 5.1 with $D = \text{diag}\,(-\lambda, 1-\lambda, \ldots, 1-\lambda)$ and $a = (1, -1, \ldots, -1)$ deduces under the assumptions $\lambda \neq 0, 1$,

$$-\lambda(1-\lambda)^M(1 + \frac{1}{-\lambda} + \frac{M}{1-\lambda}) = 0,$$

with the solution $\lambda_{1,2} = 1 + \frac{M}{2} \pm \frac{1}{2}\sqrt{4M + M^2}$. Since k is the smaller value of λ_1 and λ_2, we finally have

$$k(M) = 1 + \frac{M}{2} - \frac{1}{2}\sqrt{4M + M^2}. \tag{5.15}$$

Table 5.1 displays some values of k and Mk. Meaning of the value Mk will be given in Remark 5.1. Note that $k(M) \searrow 0$ as $M \to \infty$ and $Mk \to 1$ as $M \to \infty$.

M	k	Mk
1	0.3819	0.3819
2	0.2679	0.5358
3	0.2087	0.6261
4	0.1715	0.6862
5	0.1458	0.7294
10	0.0839	0.8392
100	0.0098	0.9804
1000	9.98 10e-4	0.9980

Table 5.1: Values of k and Mk for different values of M.

An application of Lemma 5.2 to the bound (5.10) leads to another bounds of $a(w, w)$,

$$a(w, w) \geq k \ \ \min\{c, h_1, \ldots, h_M\} \int_\Omega (||\varepsilon(u)||^2 + ||p_1||^2 + \cdots + ||p_M||^2)\,\mathrm{d}x. \tag{5.16}$$

According to the *Korn's first inequality,*

$$\int_\Omega ||\varepsilon(u)||^2\,\mathrm{d}x \geq K||u||_{H^1_D(\Omega)} \qquad \text{for all } u \in H^1_D(\Omega),$$

where $K > 0$ depends only on the domain Ω we finally obtain

Proposition 5.2 (Ellipticity of the bilinear form $a(\cdot,\cdot)$). *A bilinear form $a(\cdot,\cdot)$ is $\mathcal{H}$-elliptic,*

$$a(w, w) \geq \Big(k \ \min\{c, h_1, \ldots, h_M\} \min\{1, K\}\Big)||w||^2_{\mathcal{H}}, \tag{5.17}$$

where k depends only on the number of multi-yields $k = k(M)$ in (5.15), K on the domain Ω and the dimension d, i.e., $K = K(\Omega, d)$.

Remark 5.1 (Meaning of the value Mk in Table 5.1). Let us assume the M-yield model generated from the single-yield model according to Remark 4.2. It means

$$h_1 = \cdots = h_M = Mh.$$

In the case of sufficiently *small hardening*, $h_1, \ldots, h_M \leq c$, the ellipticity constant from Proposition 5.2 reads

$$k\, \min\{c, h_1, \ldots, h_M\} \min\{1, K\} = Mk\, h \min\{1, K\},$$

where only the product Mk depends on number of multi-yields M. By comparing the values Mk in Table 5.1, it can be seen that replacing the single-yield model by the M-yield model (with arbitrary M) does not significantly affect the ellipticity of the bilinear form $a(\cdot, \cdot)$.

5.3 Non-negativity, positive homogeneity, and Lipschitz continuity of $\psi(z)$

Since $\mathcal{D}_i(q_i) = \sigma_i^y ||q_i||$ for all $i = 1, \ldots, M$ is a convex, nonnegative and positively homogeneous function,

$$\psi(z) = \int_\Omega \Big(\mathcal{D}_1(q_1) + \mathcal{D}_2(q_2) + \cdots + \mathcal{D}_M(q_M) \Big)\, \mathrm{d}x$$

is a convex, nonnegative and positively homogeneous functional. We show the Lipschitz continuity of $\psi(z)$, i.e. the existence of a constant $L \geq 0$ such that

$$|\psi(z^1) - \psi(z^2)| \leq L ||z^1 - z^2||_{\mathcal{H}} \quad \text{for all } z^1, z^2 \in \mathcal{H}.$$

Let us define $z^1 = (v^1, q_1^1, \ldots, q_M^1)$, $z^2 = (v^2, q_1^2, \ldots, q_M^2)$. Then

$$\begin{aligned}
&|\psi(z^1) - \psi(z^2)| = \\
=&\Big| \int_\Omega \Big((\mathcal{D}_1(q_1^1) - \mathcal{D}_1(q_1^2)) + \cdots + (\mathcal{D}_M(q_M^1) - \mathcal{D}_M(q_M^2)) \Big)\, \mathrm{d}x \Big| \\
=&\Big| \int_\Omega \Big(\sigma_1^y (||q_1^1|| - ||q_1^2||) + \cdots + \sigma_M^y (||q_M^1|| - ||q_M^2||) \Big)\, \mathrm{d}x \Big| \\
\leq& \max\{\sigma_1^y, \sigma_2^y, \ldots, \sigma_M^y\} \Big| \int_\Omega \Big((||q_1^1|| - ||q_1^2||) + \cdots + (||q_M^1|| - ||q_M^2||) \Big)\, \mathrm{d}x \Big|.
\end{aligned} \tag{5.18}$$

Since $(||a|| - ||b||) \leq \big| ||a|| - |b|| \big| \leq ||a - b||$ for all $a, b \in \mathcal{H}$, than it further holds

$$|\psi(z^1) - \psi(z^2)| \leq \max\{\sigma_1^y, \sigma_2^y, \ldots, \sigma_M^y\} \int_\Omega \Big(||q_1^1 - q_1^2|| + \cdots + ||q_M^1 - q_M^2|| \Big)\, \mathrm{d}x. \tag{5.19}$$

With the help of the Cauchy-Schwartz inequality in $L^2(\Omega)$,

$$\int_\Omega ||q_i^1 - q_i^2|| 1\, \mathrm{d}x \leq \Big(\int_\Omega ||q_i^1 - q_i^2||\, \mathrm{d}x \Big)^{\frac{1}{2}} \Big(\int_\Omega 1\, \mathrm{d}x \Big)^{\frac{1}{2}}$$

for all $i = 1, \dots, M$, it is possible to estimate

$$\begin{aligned}
&|\psi(z^1) - \psi(z^2)| \leq \\
&\leq \max\{\sigma_1^y, \dots, \sigma_M^y\} \, \text{meas}(\Omega)^{\frac{1}{2}} \Big((\int_\Omega ||q_1^1 - q_1^2||^2 \, \mathrm{d}x)^{\frac{1}{2}} + \dots + (\int_\Omega ||q_M^1 - q_M^2||^2 \, \mathrm{d}x)^{\frac{1}{2}} \Big) \\
&= \max\{\sigma_1^y, \dots, \sigma_M^y\} \, \text{meas}(\Omega)^{\frac{1}{2}} \, (||q_1^1 - q_1^2||_{Q_0} + \dots + ||q_M^1 - q_M^2||_{Q_0}).
\end{aligned} \tag{5.20}$$

The Cauchy-Schwartz inequality for vectors

$$h_1 + h_2 + \ldots + h_M \leq (h_1^2 + h_2^2 + \ldots + h_M^2)^{\frac{1}{2}} \;\; M^{\frac{1}{2}} \text{ for all } h_1, \dots, h_M \in \mathbb{R}$$

yields further

$$\begin{aligned}
|\psi(z^1) - \psi(z^2)| &\leq \max\{\sigma_1^y, \dots, \sigma_M^y\} \text{meas}(\Omega)^{\frac{1}{2}} M^{\frac{1}{2}} (||q_1^1 - q_1^2||_{Q_0}^2 + \dots + ||q_M^1 - q_M^2||_{Q_0}^2)^{\frac{1}{2}} \\
&\leq \max\{\sigma_1^y, \sigma_2^y, \dots, \sigma_M^y\} \text{meas}(\Omega)^{\frac{1}{2}} M^{\frac{1}{2}} ||z^1 - z^2||_{\mathcal{H}},
\end{aligned} \tag{5.21}$$

which ends the proof of the Lipschitz continuity. We proved the following proposition:

Proposition 5.3 (Lipschitz continuity of the functional $\psi(\cdot)$). *The functional $\psi(\cdot)$ is a Lipschitz continuous functional in the space $\mathcal{H}$ with a Lipschitz constant*

$$L = \max\{\sigma_1^y, \sigma_2^y, \dots, \sigma_M^y\} \textit{meas}(\Omega)^{\frac{1}{2}} M^{\frac{1}{2}}. \tag{5.22}$$

5.4 Existence and uniqueness

In order to formulate an existence and uniqueness result for the Problem 4.1 we use the analogy with more general problem **(ABS)** [HR99].

Problem 5.1 (ABS). *Find $w : [0, T] \to \mathcal{H}, w(0) = 0$, such that for almost all $t \in (0, T), \dot{w}(t) \in Z$ and*

$$\langle \ell(t), z - \dot{w}(t) \rangle \leq a(w(t), z - \dot{w}(t)) + \psi(z) - \psi(\dot{w}(t)) \qquad \textit{for all } z \in Z$$

The following existence result is proved in [HR99].

Theorem 5.1 ([HR99]). *Let $\mathcal{H}$ be a Hilbert space, $Z \subset \mathcal{H}$ be a nonempty, closed, convex cone; $a : \mathcal{H} \times \mathcal{H} \to \mathbb{R}$ be a bilinear form that is symmetric, bounded, and $\mathcal{H}$-elliptic; $l \in H^1(0, T; \mathcal{H}^*)$ with $\ell(0) = 0$; and $\psi : Z \to \mathbb{R}$ nonnegative, convex, positively homogeneous, and Lipschitz continuous. Then there exists a unique solution w of Problem ABS satisfying $w \in H^1(0, T; \mathcal{H})$. Furthermore, $w : [0, T] \to \mathcal{H}$ is the solution to Problem ABS if and only if there is a function $w^*(t) : [0, T] \to \mathcal{H}^*$ such that for almost all $t \in (0, T)$*

$$\begin{aligned}
a(w(t), z) + \langle w^*(t), z \rangle = \langle \ell(t), z \rangle \quad &\textit{for all } z \in \mathcal{H}, \\
w^*(t) \in \partial\psi(\dot{w}(t)).&
\end{aligned}$$

All assumptions in Theorem 5.1 are satisfied for Problem 4.1. Symmetry of the bilinear form $a(\cdot,\cdot)$ is a consequence of symmetry properties of $\mathbb{C}, \mathbb{H}_i$ (5.8). Therefore the choice $Z = \mathcal{H}$ reduces Problem **(ABS)** to Problem 4.1 and Theorem 5.1 infers the existence and the uniqueness result for Problem 4.1.

Theorem 5.2. *Let $l \in H^1(0,T;\mathcal{H}^*)$ with $\ell(0) = 0$. Then there exists a unique solution $w = (u, p_1, \ldots, p_M)(t)$ of Problem 4.1 in the space $H^1(0,T;\mathcal{H})$.*

5.5 Extension to Measure Problem

Application of the same technique as for Problem 4.1 can also be generalized for Problem 4.2. In Problem 4.2, we search for a solution $w = (u, p_r) \in \mathcal{H}, r \in I$ satisfying the variational inequality (3.32). The Hilbert space $\mathcal{H}$ is defined as the Cartesian product

$$\mathcal{H} = V \times L^2_\mu(I; Q_0), \tag{5.23}$$

where

$$L^2_\mu(I;Q_0) := \{x \in I \times Q_0 : \int_{r\in I} ||x_r||^2_{Q_0} \,\mathrm{d}\mu(r) < \infty\}.$$

A scalar product $(\cdot,\cdot)_{\mathcal{H}}$ and an induced norm $||\cdot||_{\mathcal{H}}$ in the space $\mathcal{H}$ are

$$\begin{aligned} (w,z)_{\mathcal{H}} &:= (u,v)_V + \int_\Omega \int_I p_r : q_r \,\mathrm{d}\mu(r)\,\mathrm{d}x, \\ ||w||^2_{\mathcal{H}} &:= (u,u)_V + \int_\Omega \int_I p_r : p_r \,\mathrm{d}\mu(r)\,\mathrm{d}x, \\ ||z||^2_{\mathcal{H}} &:= (v,v)_V + \int_\Omega \int_I q_r : q_r \,\mathrm{d}\mu(r)\,\mathrm{d}x. \end{aligned}$$

The sum $\sum_{r=1}^{M}$ in the forms of $a(\cdot,\cdot)$ and $\psi(\cdot)$ is formally replaced by $\int_I \mathrm{d}\mu(r)$, i.e.,

$$\begin{aligned} a(w,z) &= \int_\Omega \Big(\mathbb{C}(\varepsilon(u) - \int_I p_r \,\mathrm{d}\mu(r)\Big) : \Big(\varepsilon(v) - \int_I q_r \mu(r)\Big)\,\mathrm{d}x + \\ &\quad + \int_\Omega \int_I \mathbb{H}_r p_r : q_r \,\mathrm{d}\mu(r)\,\mathrm{d}x, \\ \psi(z) &= \int_\Omega \int_I \mathcal{D}_r(q_r)\,\mathrm{d}\mu(r)\,\mathrm{d}x. \end{aligned} \tag{5.24}$$

We repeat the same steps as for the boundedness of $a(w,z)$ in the case of the standard Prandtl-Ishlinskii model of play type. Note that

$$\Big|\Big|\varepsilon(u) - \int_I p_r \,\mathrm{d}\mu(r)\Big|\Big|^2 \le 2\Big(||\varepsilon(u)||^2 + \mu(I)\cdot \int_I ||p_r||^2 \,\mathrm{d}\mu(r)\Big), \tag{5.25}$$

which infers

$$\int_\Omega \Big|\Big|\varepsilon(u) - \int_I p_r \,\mathrm{d}\mu(r)\Big|\Big|^2 \mathrm{d}x \le 2\max\Big\{1, \mu(I)\Big\}\, ||w||^2_{\mathcal{H}}.$$

For the same reason we get

$$\int_\Omega \Big|\Big|\varepsilon(v) - \int_I q_r \,\mathrm{d}\mu(r)\Big|\Big|^2 \,\mathrm{d}x \le 2\max\Big\{1, \mu(I)\Big\}\, ||z||^2_{\mathcal{H}}.$$

We bound the term $|\int_\Omega \int_I \mathbb{H}_r p_r : q_r \,\mathrm{d}\mu(r)\,\mathrm{d}x|$ as

$$\begin{aligned}
&\Big|\int_\Omega \int_I \mathbb{H}_r p_r : q_r \,\mathrm{d}\mu(r)\,\mathrm{d}x\Big| \le \int_\Omega \int_I |\mathbb{H}_r p_r : q_r| \,\mathrm{d}\mu(r)\,\mathrm{d}x \\
&\le \sup_{i\in I} ||\mathbb{H}_i|| \int_\Omega \int_I ||p_r|| \cdot ||q_r|| \,\mathrm{d}\mu(r)\,\mathrm{d}x \\
&\le \sup_{i\in I} ||\mathbb{H}_i|| \int_\Omega \Big(\int_I ||p_r||^2 \,\mathrm{d}\mu(r)\Big)^{1/2} \Big(\int_I ||q_r||^2 \,\mathrm{d}\mu(r)\Big)^{1/2} \mathrm{d}x \\
&\le \sup_{i\in I} ||\mathbb{H}_i|| \Big(\int_\Omega \int_I ||p_r||^2 \,\mathrm{d}\mu(r)\,\mathrm{d}x\Big)^{1/2} \Big(\int_\Omega \int_I ||q_r||^2 \,\mathrm{d}\mu(r)\,\mathrm{d}x\Big)^{1/2} \\
&= \sup_{i\in I} ||\mathbb{H}_i|| ||w||_{\mathcal{H}} ||z||_{\mathcal{H}}
\end{aligned} \tag{5.26}$$

and obtain the following proposition:

Proposition 5.4 (Boundedness of the bilinear form $a(\cdot,\cdot)$, measure case). *A bilinear form $a(\cdot,\cdot)$ is continuous bounded in the space $\mathcal{H}$*

$$a(w,z) \le \Big(2\max\big\{1, \mu(I)\big\} ||\mathbb{C}|| + \sup_{r\in I} ||\mathbb{H}_r||\Big) ||w||_{\mathcal{H}} ||z||_{\mathcal{H}}, \tag{5.27}$$

Ellipticity of the bilinear form $a(\cdot,\cdot)$ can be proved in the similar manner as for the standard model. Symmetry and positive definiteness assumptions on $\mathbb{C}$ and $\mathbb{H}_i$ yield analogically to (5.10)

$$\begin{aligned}
&\mathbb{C}\Big(\varepsilon(u) - \int_I p_r \,\mathrm{d}\mu(r)\Big) : \Big(\varepsilon(u) - \int_I p_r \,\mathrm{d}\mu(r)\Big) + \int_I \mathbb{H}_r p_r : p_r \,\mathrm{d}\mu(r) \\
&\qquad \ge \min\{c, \inf_{i\in I} h_i\} \Big(\Big|\Big|\varepsilon(u) - \int_I p_r \,\mathrm{d}\mu(r)\Big|\Big|^2 + \int_I ||p_r||^2 \,\mathrm{d}\mu(r)\Big).
\end{aligned} \tag{5.28}$$

A slightly modified version of Lemma 5.2 leads to the ellipticity of $a(\cdot,\cdot)$.

Lemma 5.3. *There exists $k = k(\mu(I)) > 0$ such that for all $x_0, x_r \in \mathbb{R}, r \in I, \int_I x_r^2 \, d\mu(r) < \infty$ it holds*

$$(x_0 - \int_I x_r \, d\mu(r))^2 + \int_I x_r^2 \, d\mu(r) \ge k(x_0^2 + \int_I x_r^2 \, d\mu(r)). \tag{5.29}$$

Proof. We show this result directly by rewriting:

$$\begin{aligned}
&\Big(x_0 - \int_I x_r \,\mathrm{d}\mu(r)\Big)^2 + \int_I (x_r)^2 \,\mathrm{d}\mu(r) \\
\le& (x_0)^2 + \Big(\int_I x_r \,\mathrm{d}\mu(r)\Big)^2 - 2(x_0)\Big(\int_I x_r \,\mathrm{d}\mu(r)\Big) + \int_I (x_r)^2 \,\mathrm{d}\mu(r) \\
\le& (x_0)^2 + \Big(\int_I x_r \,\mathrm{d}\mu(r)\Big)^2 - d(x_0)^2 - \frac{1}{d}\Big(\int_I x_r \,\mathrm{d}\mu(r)\Big)^2 + \int_I (x_r)^2 \,\mathrm{d}\mu(r) \\
\le& (1-d)(x_0)^2 + \Big[(1 - \frac{1}{d})\mu(I) + 1\Big] \int_I (x_r)^2 \,\mathrm{d}\mu(r),
\end{aligned} \tag{5.30}$$

where we have used a well known inequality $2ab \leq da^2 + \frac{1}{d}b^2$ for all $a, b \in \mathbb{R}, d \in (0, \infty)$ and the Cauchy-Schwarz inequality

$$\Big(\int_I x_r \,\mathrm{d}\mu(r)\Big)^2 \leq \int_I 1 \,\mathrm{d}\mu(r) \cdot \int_I (x_r)^2 \,\mathrm{d}\mu(r) = \mu(I) \int_I (x_r)^2 \,\mathrm{d}\mu(r).$$

We choose $d \in (0,1)$, such that $\min\{1-d, 1-\mu(I)\frac{1-d}{d}\} = k > 0$. It is satisfied for all $d \in (\frac{\mu(I)}{1+\mu(I)}, 1)$. $\square$

Remarks 5.2. (i) The technique involved in this proof was previously used by Han and Reddy in [HR99].
(ii) A matrix version of inequality (5.29) in Lemma 5.3 reads

$$||x_0 - \int_I x_r \,\mathrm{d}\mu(r)||^2 + \int_I ||x_r||^2 \,\mathrm{d}\mu(r) \geq k(||x_0||^2 + \int_I ||x_r||^2 \,\mathrm{d}\mu(r)). \tag{5.31}$$

(iii) The greatest value of k according to the proof is

$$k = \max_{d \in (\frac{\mu(I)}{1+\mu(I)}, 1)} \min\{1-d, 1-\mu(I)\frac{1-d}{d}\}.$$

The first Korn's inequality with the constant K together with Lemma 5.3 infer

Proposition 5.5 (Ellipticity of the bilinear form $a(\cdot,\cdot)$, measure case). *A bilinear form $a(\cdot,\cdot)$ is $\mathcal{H}$-elliptic with*

$$a(w,w) \geq \Big(k \,\min\{c, \inf_{r \in I}\{h_r\}\} \min\{1, K\}\Big) ||w||^2_{\mathcal{H}}, \tag{5.32}$$

where k depends only on the measure of the index set I, $k = k(\mu(I))$, K on the domain Ω and the dimension d, $K = K(\Omega, d)$.

The Lipschitz continuity for $\psi(z) = \int_\Omega \int_I \mathcal{D}_r(q_r) \,\mathrm{d}\mu(r) \,\mathrm{d}x$ follows from the estimate

$$\begin{aligned}
|\psi(z^1) - \psi(z^2)| &\leq \int_\Omega \int_I |\mathcal{D}_r(q_r^1) - \mathcal{D}_r(q_r^2)| \,\mathrm{d}\mu(r) \,\mathrm{d}x \\
&= \int_\Omega \int_I \sigma_r^y(||q_r^1|| - ||q_r^2||) \,\mathrm{d}\mu(r) \,\mathrm{d}x \leq \int_\Omega \int_I \sigma_r^y ||q_r^1 - q_r^2|| \,\mathrm{d}\mu(r) \,\mathrm{d}x \\
&\leq \sup_{r \in I}\{\sigma_r^y\} \int_\Omega (\int_I 1 \,\mathrm{d}\mu(r))^{1/2} (\int_I ||q_r^1 - q_r^2||^2 \,\mathrm{d}\mu(r))^{1/2} \,\mathrm{d}x \\
&\leq \sup_{r \in I}\{\sigma_r^y\} \mu(I)^{1/2} \int_\Omega (\int_I ||q_r^1 - q_r^2||^2 \,\mathrm{d}\mu(r))^{1/2} \,\mathrm{d}x \\
&\leq \sup_{r \in I}\{\sigma_r^y\} \mu(I)^{1/2} \mathrm{meas}(\Omega)^{1/2} \int_\Omega \int_I ||q_r^1 - q_r^2||^2 \,\mathrm{d}\mu(r) \,\mathrm{d}x \\
&\leq \sup_{r \in I}\{\sigma_r^y\} \mu(I)^{1/2} \mathrm{meas}(\Omega)^{1/2} ||z^1 - z^2||_{\mathcal{H}},
\end{aligned} \tag{5.33}$$

and it is formulated in the following proposition.

Proposition 5.6 (Lipschitz continuity of the functional $\psi(\cdot)$, measure case). *The functional $\psi(\cdot)$ is a Lipschitz continuous functional in the space $\mathcal{H}$ with a Lipschitz constant*

$$L = \sup_{r\in I}\{\sigma_r^y\}\mu(I)^{1/2}\textit{meas}(\Omega)^{1/2}. \tag{5.34}$$

For the same reason as for the standard model is $\psi(z)$ a nonnegative and positive homogeneous functional. All assumptions of Lemma 5.1 are also satisfied for Problem 4.2, and therefore the choice $Z = \mathcal{H}$ reduces Problem **(ABS)** to Problem 4.2 and Theorem 5.1 infers the existence and the uniqueness result for Problem 4.2.

Theorem 5.3. *Let $l \in H^1(0,T;\mathcal{H}^*)$ with $\ell(0) = 0$. Then there exists a unique solution $w = (u,p_r)(t), r \in I$ of Problem 4.2 in the space $H^1(0,T;\mathcal{H})$.*

Chapter 6

Numerical Modeling

This chapter is devoted to the discretization of the variational inequality (3.32) with the implicit Euler method in time and with the finite element method in space. We use capital letters for discrete variables. For instance, $X = (U, P)$ denotes a discrete approximation of $x = (u, p)$. The discretization of Problem 4.2 consists in our approach of measure, time and space discretizations.

Measure discretization: We replace a measurable function p by the vector P of M elements (the continuous model is approximated by the discrete problem with M multi-yields) with state variables

$$X = (U, P), \text{ where } P = (P_1, \ldots, P_M),$$

$$Y = (V, Q), \text{ where } Q = (Q_1, \ldots, Q_M)$$

and approximate the integral $\int_I P \,\mathrm{d}\mu(r)$ as

$$\int_I p_r \,\mathrm{d}\mu(r) \approx \sum_{i=1}^{M} \alpha_i P_i, \tag{6.1}$$

where constants α_i are related to some integration rule, for instance the weights of the *Newton-Cotes* formulae. Similarly, we derive discrete forms for the terms of the variational inequality. (3.32), i.e.,

$$\begin{aligned} a(X, Y) = &\int_\Omega \mathbb{C}(\epsilon(U) - \sum_{i=1}^{M} \alpha_i P_i) : (\epsilon(V) - \sum_{i=1}^{M} \alpha_i Q_i) \;\; \mathrm{d}x, \\ &+ \int_\Omega \sum_{i=1}^{M} \alpha_i \mathbb{H}_i P_i : Q_i \,\mathrm{d}x, \\ \psi(Y) = &\int_\Omega \sum_{i=1}^{M} \alpha_i \mathcal{D}_i(Q_i) \,\mathrm{d}x, \\ \mathcal{D}_i(Q_i) = &\sigma_i^y ||Q_i|| \quad \text{for all } i = 1, \ldots, M. \end{aligned} \tag{6.2}$$

Note that for the choice $\alpha_i = 1$ for all $i = 1, \dots, M$, we have the same form of terms $a(\cdot, \cdot), \psi(\cdot)$ as in Problem 4.2. In the following we consider only this case for the simplicity of notation.

Time discretization: We replace the continuous time interval $(0, T)$ by the sequence of discrete times $t_0, \dots, t_N$ with

$$0 = t_0 < \tau_1 \leq t_1 < \tau_2 \leq t_2 < \cdots \leq t_{N-1} < \tau_N \leq t_N = T,$$

with a time step $k_j = t_j - t_{j-1}, j = 1, \dots, N$. Knowing the values of $X(t)$ at times $t_0, \dots, t_N$ one can interpolate

$$X(\tau_j) = \frac{\tau_j - t_{j-1}}{k_j} X(t_j) + \frac{t_j - \tau_j}{k_j} X(t_{j-1}) \quad \text{for } j = 1, \dots, N. \tag{6.3}$$

The time derivative is consequently approximated by

$$\dot{X}(\tau_j) = \frac{X(t_j) - X(t_{j-1})}{k_j} \quad \text{for } j = 1, \dots, N. \tag{6.4}$$

Spatial discretization: We divide a polygonal domain $\Omega \in \mathbb{R}^2$ by a *regular triangulation* $\mathcal{T}$ (it means no hanging nodes, domain is matched exactly) into triangles and define the set of $\mathcal{T}$*-piecewise constant* functions by

$$\mathcal{S}^0(\mathcal{T}) := \{a \in L^2(\Omega) : \text{ for all } T \in \mathcal{T}, a|_T \in \mathbb{R}\} \tag{6.5}$$

and the set of $\mathcal{T}$*-piecewise affine* functions that are zero on Γ_D by

$$\mathcal{S}^1_D(\mathcal{T}) := \{v \in H^1_D(\Omega) : \text{ for all } T \in \mathcal{T}, v|_T \in \mathcal{P}_1(T)^d\}. \tag{6.6}$$

($\mathcal{P}_1(T)$ denotes the affine functions on T.) We can replace

$$\mathcal{H} = V \times \underbrace{Q_0 \times \cdots \times Q_0}_{M \text{ times}}$$

by its *finite element* subspace S (therefore we speak of *conforming finite elements*)

$$S = \mathcal{S}^1_D(\mathcal{T}) \times \underbrace{\operatorname{dev} \mathcal{S}^0(\mathcal{T})^{d\times d}_{sym} \times \cdots \times \operatorname{dev} \mathcal{S}^0(\mathcal{T})^{d\times d}_{sym}}_{M \text{ times}}.$$

The discrete problem is then posed in the space

$$\begin{aligned} \mathcal{S} :=\{X \in C(0,T;S) : X(0) = X^0 \text{ and} \\ X(t) = \frac{t - t_j}{k_j} X(t_j) + \frac{t_j - t}{k_j} X(t_{j-1}) \\ \text{for } t_{j-1} \leq t \leq t_j, j = 1, \dots, N\}. \end{aligned} \tag{6.7}$$

Problem 6.1 (S). *Seek $X \in \mathcal{S}$ that satisfies, for all $j = 1, \dots, N$,*

$$\ell(\tau_j)(Y - \dot{X}(\tau_j)) \leq a(X(\tau_j), Y - \dot{X}(\tau_j)) + \psi(Q) - \psi(\dot{P}(\tau_j)) \quad \textit{for all } Y \in S. \tag{6.8}$$

We define for $i = 0, \ldots, N$,

$$X^i := (U^i, P^i) = X(t_i),$$

substitute $\dot{X}^1 = \frac{X^1 - X^0}{k_1}$ into (3.32) and deduce the inequality in the first discrete time t_1,

$$\ell(t_1)(Y - \frac{X^1 - X^0}{k_1}) \leq a(X^1, Y - \frac{X^1 - X^0}{k_1}) + \psi(Q) - \psi(\frac{P^1 - P^0}{k_1}) \quad \text{for all } Y \in S. \tag{6.9}$$

We define an *incremental* variable $X = (U, P) := X^1 - X^0, l := \ell(t_1)$, the linear operator

$$L(Y) = \ell(Y) - a(X^0, Y) \tag{6.10}$$

and obtain a problem:

Problem 6.2 (S_2). *Seek $X = (U, P) \in S$ that satisfies*

$$L(Y - X) \leq a(X, Y - X) + \psi(Q) - \psi(P) \quad \textit{for all } Y = (V, Q) \in S. \tag{6.11}$$

Problem 6.2 is further equivalent to the minimization problem:

Problem 6.3 (M_2). *For $f(Y) = \frac{1}{2}a(Y, Y) + \psi(Q) - L(Y)$ seek $X = (U, P) \in S$ with*

$$f(X) = \min_{Y \in S} f(Y). \tag{6.12}$$

Lemma 6.1 (Equivalence of problems (S_2) and (M_2)).

X is a solution of Problem (S_2) if and only if X is a solution of Problem (M_2).

Proof. $(M_2) \Rightarrow (S_2)$: (M_2) implies, for all $Y, \theta \in (0, 1)$,

$$f(X + \theta(Y - X)) \geq f(X).$$

Hence

$$\theta a(X, Y - X) + \frac{1}{2}\theta^2 a(Y - X, Y - X) + \psi(X + \theta(Y - X)) - \psi(X) - \theta L(Y - X) \geq 0.$$

The convexity of $\psi(\cdot) : \psi(X + \theta(Y - X) - \psi(X) \leq \theta(\psi(X) - \psi(Y))$ yields

$$a(X, Y - X) - L(Y - X) + \frac{1}{2}\theta a(Y - X, Y - X) \geq \theta(\psi(X) - \psi(Y)).$$

Dividing the last inequality by θ and taking the limit $\theta \downarrow 0$, we end up with the inequality (6.9) in Problem (S_2).

$(S_2) \Rightarrow (M_2)$: for all Y holds

$$\begin{aligned} f(Y) =& f(X + (Y - X)) = \\ =& \frac{1}{2}a(X, X) + a(X, Y - X) + \frac{1}{2}a(Y - X, Y - X) \\ & + \psi(P) + \psi(Q) - \psi(P) - L(X) - L(Y - X) = \\ =& f(X) + \frac{1}{2}\underbrace{a(Y - X, Y - X)}_{\geq 0} + \underbrace{a(X, Y - X) + \psi(Q) - \psi(P) - L(Y - X)}_{\geq 0 \quad (M_2)} \\ \geq& f(X). \end{aligned} \tag{6.13}$$

□

The Problem (S_2) can also be written as a problem with more inequalities.

Problem 6.4 (S_2-more equations). *Seek $X = (U, P) \in S$ with $P = (P_1, \dots, P_M)$ that satisfies*

$$\begin{aligned} L(Y - X) &= a(X, Y - X) \quad \textit{for all} \quad Y = (V, P) \in S, && (6.14)\\ L(Y_i - X) &\leq a(X, Y_i - X) + \psi(Y_i) - \psi(X) \quad \textit{for all} \quad Y_i \in S, i = 1, \dots, M, && (6.15) \end{aligned}$$

where $Y_i = (U, Q), Q = (P_1, \dots, P_{i-1}, Q_i, P_{i+1}, \dots, P_M)$.

The detailed form of (6.14) and (6.15) reads for all $V \in \mathcal{S}^1_D(\mathcal{T}), Q_i \in \operatorname{dev} S^0(\mathcal{T}), i = 1, \dots, M$

$$\int_\Omega f(t)(V - U)\,\mathrm{d}x + \int_{\Gamma_N} g(t)(V - U)\,\mathrm{d}s = \int_\Omega \mathbb{C}(\epsilon(U) - \sum_{i=1}^{M} P_i) : \epsilon(V - U)\,\mathrm{d}x, \quad (6.16)$$

$$\begin{aligned} &\int_\Omega (\mathbb{C}(\epsilon(U^0) - \sum_{i=1}^{M} P_i^0) - \mathbb{H}_i P_i^0) : (Q_i - P_i)\,\mathrm{d}x \\ \leq -&\int_\Omega (\mathbb{C}(\epsilon(U) - \sum_{i=1}^{M} P_i) - \mathbb{H}_i P_i) : (Q_i - P_i)\,\mathrm{d}x + \int_\Omega (\mathcal{D}(Q_i) - \mathcal{D}(P_i))\,\mathrm{d}x. \end{aligned} \quad (6.17)$$

We sum all inequalities (6.15) over $i = 1, \dots, M$, noticing that

$$\sum_{i=1}^{M} (Y_i - X) = \sum_{i=1}^{M} (0, 0, \dots, 0, Q_i - P_i, 0, \dots, 0) = (0, Q - P) = (Y - X),$$

$$\sum_{i=1}^{M} (\psi(Y_i) - \psi(X)) = \psi(Y) - \psi(X),$$

and conclude

$$L(Y - X) \leq a(X, Y - X) + \psi(Y) - \psi(X),$$

where $Y = \sum_{i=1}^{M} Y_i = (U, Q_1, \dots, Q_M) = (0, Q)$. It gives rise to another equivalent formulation of Problem 6.4.

Problem 6.5 (S_2-two equations). *Seek $X = (U, P) \in S$ with $P = (P_1, \dots, P_M)$ that satisfies*

$$\begin{aligned} L(V - U, 0) &= a(X, Y - X) \quad \textit{for all } Y = (V, P) \in S, && (6.18)\\ L(Y - X) &\leq a(X, Y - X) + \psi(Y) - \psi(X) \quad \textit{for all } Y = (U, Q) \in S. && (6.19) \end{aligned}$$

The equivalence of defined problems can be written schematically:

$$(S_2) \Leftrightarrow (M_2) \Leftrightarrow (S_2 - \text{more equations}) \Leftrightarrow (S_2 - \text{two equations})$$

The form of $a(\cdot,\cdot), L(\cdot), \psi(\cdot)$ in (6.19), for the two-yield model with $M = 2$ (generalization to the case $M > 2$ follows immediately), have the form

$$\begin{aligned} a(X, Y-X) &= \int_\Omega \Big(\mathbb{C}(\epsilon(U) - P_1 - P_2) : (-Q_1 + P_1 - Q_2 + P_2) + \mathbb{H}_1 P_1 : (Q_1 - P_1) \\ &\qquad + \mathbb{H}_2 P_2 : (Q_2 - P_2) \Big) \, \mathrm{d}x \\ &= -\int_\Omega \Big[\begin{pmatrix} \mathbb{C}\epsilon(U) \\ \mathbb{C}\epsilon(U) \end{pmatrix} - \Big(\begin{pmatrix} \mathbb{C} & \mathbb{C} \\ \mathbb{C} & \mathbb{C} \end{pmatrix} + \begin{pmatrix} \mathbb{H}_1 & 0 \\ 0 & \mathbb{H}_2 \end{pmatrix} \Big) \begin{pmatrix} P_1 \\ P_2 \end{pmatrix} \Big] : \begin{pmatrix} Q_1 - P_1 \\ Q_2 - P_2 \end{pmatrix} \, \mathrm{d}x, \\ L(Y - X) &= -a(X^0, Y - X) \\ &= \int_\Omega \Big[\begin{pmatrix} \mathbb{C}\epsilon(U^0) \\ \mathbb{C}\epsilon(U^0) \end{pmatrix} - \Big(\begin{pmatrix} \mathbb{C} & \mathbb{C} \\ \mathbb{C} & \mathbb{C} \end{pmatrix} + \begin{pmatrix} \mathbb{H}_1 & 0 \\ 0 & \mathbb{H}_2 \end{pmatrix} \Big) \begin{pmatrix} P_1^0 \\ P_2^0 \end{pmatrix} \Big] : \begin{pmatrix} Q_1 - P_1 \\ Q_2 - P_1 \end{pmatrix} \, \mathrm{d}x, \\ \psi(Y) &= \int_\Omega \left(\sigma_1^y ||Q_1|| + \sigma_2^y ||Q_2|| \right) \mathrm{d}x = \int_\Omega || \begin{pmatrix} Q_1 \\ Q_2 \end{pmatrix} ||_{\sigma^y} \, \mathrm{d}x, \end{aligned}$$

where $||(P_1, P_2)^T||_{\sigma^y} := \sigma_1^y ||P_1|| + \sigma_2^y ||P_2||$ defines a matrix norm (since $\sigma_1^y, \sigma_2^y > 0$). With the help of substitutions

$$\begin{aligned} &\hat{\mathbb{C}} := \begin{pmatrix} \mathbb{C} & \mathbb{C} \\ \mathbb{C} & \mathbb{C} \end{pmatrix} \quad \text{and} \quad \hat{\mathbb{H}} := \begin{pmatrix} \mathbb{H}_1 & 0 \\ 0 & \mathbb{H}_2 \end{pmatrix}, \\ &P := \begin{pmatrix} P_1 \\ P_2 \end{pmatrix} \quad \text{and} \quad P^0 := \begin{pmatrix} P_1^0 \\ P_2^0 \end{pmatrix} \quad \text{and} \quad Q := \begin{pmatrix} Q_1 \\ Q_2 \end{pmatrix}, \\ &\hat{A} := \begin{pmatrix} \mathbb{C}\epsilon(U) \\ \mathbb{C}\epsilon(U) \end{pmatrix} + \begin{pmatrix} \mathbb{C}\epsilon(U^0) \\ \mathbb{C}\epsilon(U^0) \end{pmatrix} - (\hat{\mathbb{C}} + \hat{\mathbb{H}}) P^0, \end{aligned} \tag{6.20}$$

we rewrite the inequality (6.19) as the inequality for all $Q \in \operatorname{dev} \mathcal{S}^0(\mathcal{T})^{d\times d}_{sym} \times \operatorname{dev} \mathcal{S}^0(\mathcal{T})^{d\times d}_{sym}$

$$\int_\Omega (\hat{A} - (\hat{\mathbb{C}} + \hat{\mathbb{H}})P) : (Q - P) \, \mathrm{d}x \le \int_\Omega (||Q||_{\sigma^y} - ||P||_{\sigma^y}) \, \mathrm{d}x. \tag{6.21}$$

Owing to our space discretization, P and $\hat{A}$ are constant matrices on every triangle T of our triangulation $\mathcal{T}$. It enables to decompose the inequality (6.21) elementwise. Given $\hat{A}, \hat{\mathbb{C}}, \hat{\mathbb{H}} \in \mathbb{R}^{d\times d}$, we seek $P = (P_1, P_2)^T, P_1, P_2 \in \mathbb{R}^{d\times d}_{sym}, \operatorname{tr} P_1 = \operatorname{tr} P_2 = 0$ such that for all $Q = (Q_1, Q_2)^T, Q_1, Q_2 \in \mathbb{R}^{d\times d}_{sym}, \operatorname{tr} Q_1 = \operatorname{tr} Q_2 = 0$ holds

$$(\hat{A} - (\hat{\mathbb{C}} + \hat{\mathbb{H}})P) : (Q - P) \le ||Q||_{\sigma^y} - ||P||_{\sigma^y}. \tag{6.22}$$

The next two sections are addressed to the question, whether inequality (6.22) has a unique solution, separately for the single-yield and the two-yield models.

6.1 Single-yield model, $M = 1$

The single-yield model is specified by one plastic strain P and $\mathbb{C} = \hat{\mathbb{C}}$ with $\mathbb{C}P = 2\mu P$ and $\mathbb{H} = \hat{\mathbb{H}}$ with $\mathbb{H}P = hP$, the matrix norm $||P||_{\sigma^y} = \sigma^y ||P||$ and $A = \hat{A} = \mathbb{C}\varepsilon(U) + \mathbb{C}\varepsilon(U^0) - (\mathbb{C} + \mathbb{H})P^0$. The existence of the unique solution P of the inequality (6.22) on every element T is then guaranteed by the following lemma.

Lemma 6.2 ([ACZ99]). *Given* $A \in \mathbb{R}^{d\times d}_{sym}$ *and* $\sigma^y > 0$ *there exists exactly one* $P \in \mathbb{R}^{d\times d}_{sym}$ *with* $\operatorname{tr} P = 0$ *that satisfies*

$$\{A - (\mathbb{C} + \mathbb{H})P\} : (Q - P) \leq \sigma^y\{||Q|| - ||P||\} \tag{6.23}$$

for all $Q \in \mathbb{R}^{d\times d}_{sym}$ *with* $\operatorname{tr} Q$*=0. This is characterized as the minimizer of*

$$\frac{1}{2}(\mathbb{C} + \mathbb{H})P : P - P : A + \sigma^y||P|| \tag{6.24}$$

(amongst trace-free symmetric $d \times d$*-matrices) and equals*

$$\frac{(||\text{dev}\, A|| - \sigma^y)_+}{2\mu + h}\frac{\text{dev}\, A}{||\text{dev}\, A||}, \tag{6.25}$$

where $(\cdot)_+ := \max\{0, \cdot\}$ *denotes the non-negative part. The minimal value of (6.24) (attained for* P *as in (6.25)) is*

$$-\frac{1}{2}(||\text{dev}\, A|| - \sigma^y)^2_+/(2\mu + h). \tag{6.26}$$

Proof. Although the proof is given in [ACZ99], we recall it here again, since it is useful for understanding of cases with two- and more yield models. In the convex analysis, the inequality 6.23 states that

$$A - (\mathbb{C} + \mathbb{H})P \in \sigma^y \partial|| \cdot ||(P), \tag{6.27}$$

where $\partial|| \cdot || =$sign denotes the sub-gradient of the norm, and only trace-free arguments are under consideration. The function $|| \cdot ||$ is convex and so is (6.24). Identity (6.23) is equivalent to 0 belonging to the sub-gradient of (6.24). If $P = 0$ the inequality (6.23) states

$$A : Q \leq \sigma^y||Q|| \tag{6.28}$$

for all $Q \in \mathbb{R}^{d\times d}_{sym}$ with $\operatorname{tr} Q = 0$. Hence, $||\text{dev}\, A|| \leq \sigma^y$. If $||\text{dev}\, A|| > \sigma^y$ we conclude $P \neq 0$ and obtain $\partial|| \cdot ||(P) = \{P/||P||\}$. Hence (6.23) yields

$$\text{dev}\, A - (\mathbb{C} + \mathbb{H})P = \sigma^y P/||P||. \tag{6.29}$$

Notice that $\operatorname{tr} \mathbb{C}P = 0$ as $\operatorname{tr} P = 0$, and only trace-free arguments are under consideration. Since $\mathbb{C}P = 2\mu P$ we obtain

$$\text{dev}\, A = (\sigma^y + (2\mu + h)||P||)P/||P|| \tag{6.30}$$

and so $||\text{dev}\, A|| = \sigma^y + (2\mu + h)||P||$, whence

$$||P|| = (||\text{dev}\, A|| - \sigma^y)/(2\mu + h).$$

Using this in (6.30) we deduce

$$P = \frac{(||\text{dev}\, A|| - \sigma^y)_+}{2\mu + h}\frac{\text{dev}\, A}{||\text{dev}\, A||}. \tag{6.31}$$

Formula (6.31) holds also for P=0. Taking (6.31) in (6.24) we calculate the minimal value (6.26). □

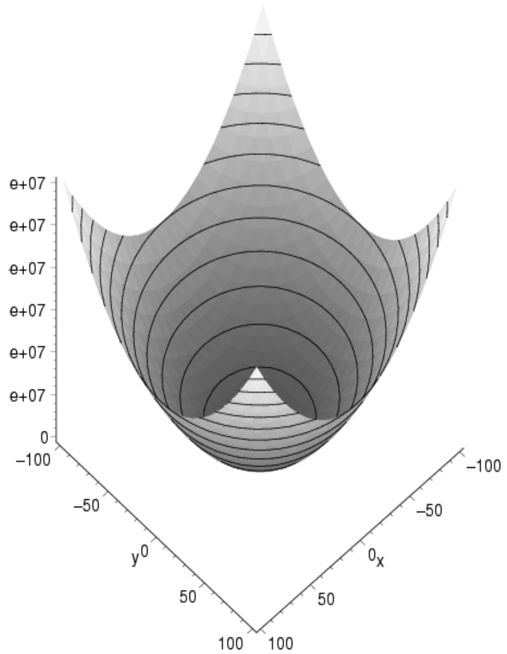

Figure 6.1: Values of quadratic functional $\frac{1}{2}(\mathbb{C} + \mathbb{H})P : P$ as a function of x and y for argument $P = (x, y; y, -x)$.

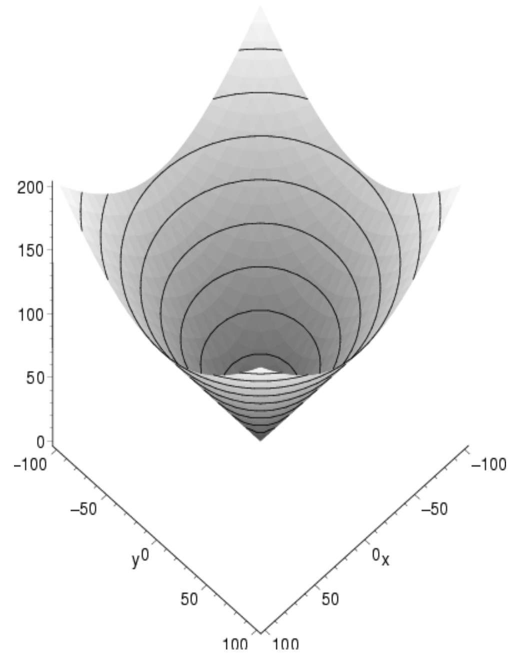

Figure 6.3: Values of the functional with the norm $\sigma^y||P||$ as a function of x and y for argument $P = (x, y; y, -x)$.

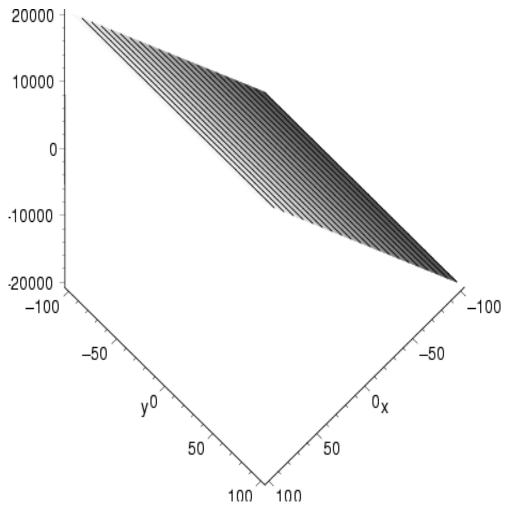

Figure 6.2: Values of the linear functional $P : A$ as a function of x and y for argument $P = (x, y; y, -x)$.

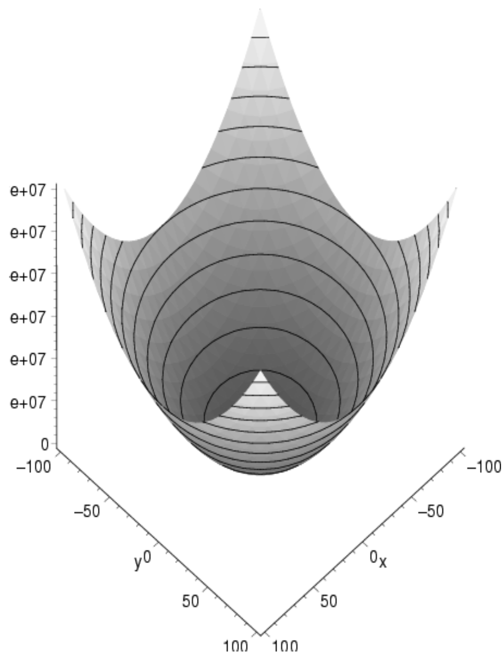

Figure 6.4: Values of the functional $\frac{1}{2}(\mathbb{C}+\mathbb{H})P : P - P : A + \sigma^y||P||$ as a function of x and y for argument $P = (x, y; y, -x)$.

Remark 6.1. The minimizing functional (6.24) consist of the quadratic term $\frac{1}{2}(\mathbb{C}+\mathbb{H})P : P$, the linear term dev $A : P$ and the term with the norm $\sigma^y||P||$. Since $2\mu + h > 0$ and $\sigma^y > 0$ represent the quadratic term and the term with the norm strictly convex functionals. As the result of it is (6.24) also a strictly convex functional. Figures 6.1, 6.2, 6.3, 6.4 display a possible form of the quadratic, the linear, the term with the norm and the functional (6.25), assuming symmetric and trace free matrix argument P in the form

$$P = \begin{pmatrix} x & y \\ y & -x \end{pmatrix}.$$

6.2 Two-yield model, $M = 2$

The two-yield model is specified by two plastic strains P_1, P_2 that can be coupled in a plastic strain $P = (P_1, P_2)^T$. Further $\hat{\mathbb{C}}P = \begin{pmatrix} 2\mu(P_1+P_2) \\ 2\mu(P_1+P_2) \end{pmatrix}$, $\hat{\mathbb{H}}P = \begin{pmatrix} h_1P_1 \\ h_2P_2 \end{pmatrix}$, $||P||_{\sigma^y} = \sigma_1^y||P_1|| + \sigma_2^y||P_2||$ and $\hat{A} = \begin{pmatrix} A_1 \\ A_2 \end{pmatrix} = \begin{pmatrix} \mathbb{C}\epsilon(U) \\ \mathbb{C}\epsilon(U) \end{pmatrix} + \begin{pmatrix} \mathbb{C}\epsilon(U^0) \\ \mathbb{C}\epsilon(U^0) \end{pmatrix} - (\hat{\mathbb{C}} + \hat{\mathbb{H}})P^0$.

Similarly as for the single-yield model we can show the existence and uniqueness of the plastic strain $P = (P_1, P_2)^T$ on every element $T \in \mathcal{T}$.

Lemma 6.3. *Given $\hat{A} = (A_1, A_2)^T, A_1, A_2 \in \mathbb{R}^{d\times d}_{sym}$ there exists exactly one $P = (P_1, P_2)^T, P_1, P_2 \in \mathbb{R}^{d\times d}_{sym}$ with* tr P_1 = tr $P_2 = O$ *that satisfies*

$$(\hat{A} - (\hat{\mathbb{C}} + \hat{\mathbb{H}})P) : (Q - P) \le ||Q||_{\sigma^y} - ||P||_{\sigma^y} \tag{6.32}$$

for all $Q = (Q_1, Q_2)^T, Q_1, Q_2 \in \mathbb{R}^{d\times d}_{sym}$ with tr Q_1 = tr $Q_2 = O$. *This P is characterized as the minimizer of*

$$f(P) = \frac{1}{2}(\hat{\mathbb{C}} + \hat{\mathbb{H}})P : P - P : \hat{A} + ||P||_{\sigma^y} \tag{6.33}$$

(amongst trace-free symmetric $d \times d$ matrices P_1, P_2).

Proof. The equivalence of $f(P) = \min_Q f(Q)$ and (6.32) is obvious. The function $f(P)$ is strictly convex, continuous in the space of all trace-free symmetric d×d matrices P_1, P_2, $\lim_{||Q||\to\infty} f(Q) = +\infty$ so it attains exactly one minimum. □

If $\hat{\mathbb{C}}$ was in some block diagonalizable form $\hat{\mathbb{C}} = \begin{pmatrix} \mathbb{C} & 0 \\ 0 & \mathbb{C} \end{pmatrix}$, it would be possible to separate the variational inequality (6.22) into two M variational inequalities of type (6.23), use Lemma 6.2 and express the exact minimizer of (6.33) as a linear combination of them. In the next subsection, we focus on an analytical approach for minimizing (6.33).

6.2.1 Analytical approach

Lemma 6.4. *Let B be a unit ball at the point 0,$B := \{Q \in \mathbb{R}^{d\times d}_{sym} : ||Q|| \leq 1\}$. Then*

$$\partial || \cdot ||_{\sigma^y}(P_1, P_2) = \begin{cases} \{\sigma_1^y B, \sigma_2^y B\} & \textit{if} \quad P_1 = P_2 = 0, \\ \{\sigma_1^y \frac{P_1}{||P_1||}, \sigma_2^y B\} & \textit{if} \quad P_1 \neq 0, P_2 = 0, \\ \{\sigma_1^y B, \sigma_2^y \frac{P_2}{||P_2||}\} & \textit{if} \quad P_1 = 0, P_2 \neq 0, \\ \{\sigma_1^y \frac{P_1}{||P_1||}, \sigma_2^y \frac{P_2}{||P_2||}\} & \textit{if} \quad P_1 \neq 0, P_2 \neq 0. \end{cases} \tag{6.34}$$

Proof. By the definition, the convex function $||P||_{\sigma^y}$ is decomposed as two convex functions $\sigma_1^y||P_1||$ and $\sigma_2^y||P_2||$. Both functions have subdifferentials, namely

$$\partial(\sigma_1^y||P_1||)(P_1, P_2) = \begin{cases} \{\sigma_2^y B, 0\} & \text{if} \quad P_1 = 0, \\ \{\sigma_2^y \frac{P_2}{||P_2||}, 0\} & \text{if} \quad P_1 \neq 0 \end{cases} \tag{6.35}$$

and

$$\partial(\sigma_2^y||P_2||)(P_1, P_2) = \begin{cases} \{0, \sigma_1^y B\} & \text{if} \quad P_2 = 0, \\ \{0, \sigma_2^y \frac{P_2}{||P_2||}\} & \text{if} \quad P_2 \neq 0. \end{cases} \tag{6.36}$$

Both convex functions $\sigma_1^y||P_1||$ and $\sigma_2^y||P_2||$, considered as functions of two variables P_1, P_2, are continuous at the point $P_1 = P_2 = 0$ in Banach space $\mathbb{R}^{d\times d}_{sym} \times \mathbb{R}^{d\times d}_{sym}$. According to the convex analysis (for instance Theorem 7.11 in [Bro97]), we can write

$$\partial(||(P_1, P_2)||_{\sigma^y}) = \partial(\sigma_1^y||P_1||) + \partial(\sigma_2^y||P_2||),$$

which concludes the proof. □

The last lemma divides the problem of minimizing $f(P)$ into four cases, depending of the values of P_1 and P_2.
Case 1: $P_1 = P_2 = 0$ with the following equivalences

$$\begin{aligned} P_1 = P_2 = 0 \quad &\Leftrightarrow \quad \hat{A} : Q \leq ||Q||_{\sigma^y} \quad \text{for all } Q = (Q_1, Q_2)^T, \text{ tr}\, Q_1 = \text{tr}\, Q_2 = 0 \\ &\Leftrightarrow \quad \text{dev}\, A_i : Q_i \leq ||Q_i||_{\sigma_i^y} \quad \text{for all } Q_i, \text{ tr}\, Q_i = 0, i = 1, 2 \\ &\Leftrightarrow \quad ||\text{dev}\, A_i|| \leq \sigma_i^y, i = 1, 2. \end{aligned} \tag{6.37}$$

Case 2: $P_1 = 0, P_2 \neq 0$, which means

$$\begin{pmatrix} \text{dev}\, A_1 \\ \text{dev}\, A_2 \end{pmatrix} - \begin{pmatrix} (2\mu + h_1)\mathbb{I} & 2\mu\mathbb{I} \\ 2\mu\mathbb{I} & (2\mu + h_2)\mathbb{I} \end{pmatrix} \begin{pmatrix} 0 \\ P_2 \end{pmatrix} \in \begin{pmatrix} \sigma_1^y B \\ \{\sigma_2^y \frac{P_2}{||P_2||}\} \end{pmatrix}. \tag{6.38}$$

We may write equivalently

$$\text{dev}\, A_1 - 2\mu P_2 \in \sigma_1^y B, \tag{6.39}$$

$$\text{dev}\, A_2 - (2\mu + h_2)P_2 = \sigma_2^y \frac{P_2}{||P_2||}. \tag{6.40}$$

Elimination of P_2 from (6.40) yields

$$P_2 = \frac{||\text{dev}\, A_1|| - \sigma_2^y}{2\mu + h_2} \frac{\text{dev}\, A_2}{||\text{dev}\, A_2||}$$

and the substitution of this into (6.39) gives finally the condition

$$\text{dev}\,A_1 - 2\mu\Big(\frac{||\text{dev}\,A_1|| - \sigma_2^y}{2\mu + h_2}\frac{\text{dev}\,A_2}{||\text{dev}\,A_2||}\Big) \in \sigma_1^y B. \tag{6.41}$$

Case 3: $P_1 \neq 0, P_2 = 0$. The same technique as in Case 2., only with the reversed indices 1 and 2, gives

$$P_1 = \frac{||\text{dev}\,A_2|| - \sigma_1^y}{2\mu + h_1}\frac{\text{dev}\,A_1}{||\text{dev}\,A_1||},$$

$$\text{dev}\,A_2 - 2\mu\Big(\frac{||\text{dev}\,A_2|| - \sigma_1^y}{2\mu + h_1}\frac{\text{dev}\,A_1}{||\text{dev}\,A_1||}\Big) \in \sigma_2^y B. \tag{6.42}$$

Case 4: $P_1 \neq 0, P_2 \neq 0$ implies

$$\begin{pmatrix}\text{dev}\,A_1\\ \text{dev}\,A_2\end{pmatrix} - \begin{pmatrix}(2\mu + h_1)\mathbb{I} & 2\mu\mathbb{I}\\ 2\mu\mathbb{I} & (2\mu + h_2)\mathbb{I}\end{pmatrix}\begin{pmatrix}P_1\\ P_2\end{pmatrix} = \begin{pmatrix}\sigma_1^y\frac{P_1}{||P_1||}\\ \sigma_2^y\frac{P_2}{||P_2||}\end{pmatrix}. \tag{6.43}$$

Applying substitutions $P_i = \xi_i X_i$, where $||X_i|| = 1, i = 1, 2$, (6.43) becomes the system of nonlinear equations with positive parameters $\xi_1 = ||P_1||, \xi_2 = ||P_2||$,

$$\begin{pmatrix}\text{dev}\,A_1\\ \text{dev}\,A_2\end{pmatrix} = \begin{pmatrix}(\sigma_1^y + (2\mu + h_1)\xi_1)\mathbb{I} & 2\mu\xi_2\mathbb{I}\\ 2\mu\xi_1\mathbb{I} & (\sigma_2^y + (2\mu + h_2)\xi_2)\mathbb{I}\end{pmatrix}\begin{pmatrix}X_1\\ X_2\end{pmatrix}. \tag{6.44}$$

Another substitutions $\eta_1 := \sigma_1^y + (2\mu + h_1)\xi_1, \eta_2 := \sigma_2^y + (2\mu + h_2)\xi_2, \nu_1 := 2\mu\xi_1, \nu_2 := 2\mu\xi_2$ and the fact that

$$\begin{pmatrix}\eta_1\mathbb{I} & \nu_2\mathbb{I}\\ \nu_1\mathbb{I} & \eta_2\mathbb{I}\end{pmatrix}^{-1} = \frac{1}{\eta_1\eta_2 - \nu_1\nu_2}\begin{pmatrix}\eta_2\mathbb{I} & -\nu_2\mathbb{I}\\ -\nu_1\mathbb{I} & \eta_1\mathbb{I}\end{pmatrix}$$

yield

$$\begin{aligned}\eta_2\text{dev}\,A_1 - \nu_2\text{dev}\,A_2 &= (\eta_1\eta_2 - \nu_1\nu_2)X_1,\\ -\nu_1\text{dev}\,A_1 + \eta_1\text{dev}\,A_2 &= (\eta_1\eta_2 - \nu_1\nu_2)X_2.\end{aligned} \tag{6.45}$$

Normalization of (6.45) and the application of substitutions for $\eta_1, \eta_2, \nu_1, \nu_2$ give the system of nonlinear equations for positive ξ_1, ξ_2

$$\begin{aligned}||l_1(\xi_1)|| - |r(\xi_1, \xi_2)| &= 0,\\ ||l_2(\xi_2)|| - |r(\xi_1, \xi_2)| &= 0,\end{aligned} \tag{6.46}$$

where

$$\begin{aligned}l_1(\xi_1) &= (\sigma_1^y + (2\mu + h_1)\xi_1)\text{dev}\,A_2 - 2\mu\xi_1\text{dev}\,A_1,\\ l_2(\xi_2) &= (\sigma_2^y + (2\mu + h_2)\xi_2)\text{dev}\,A_1 - 2\mu\xi_2\text{dev}\,A_2,\\ r(\xi_1, \xi_2) &= (\sigma_1^y + (2\mu + h_2)\xi_1)(\sigma_2^y + (2\mu + h_2)\xi_2) - 4\mu^2\xi_1\xi_2.\end{aligned} \tag{6.47}$$

Instead of the solving (6.46) we prefer to solve the equivalent system of nonlinear equations

$$\begin{aligned}\Phi_1(\xi_1, \xi_2) &= ||l_1(\xi_1)||^2 - (r(\xi_1, \xi_2))^2 = 0,\\ \Phi_2(\xi_1, \xi_2) &= ||l_2(\xi_2)||^2 - (r(\xi_1, \xi_2))^2 = 0.\end{aligned} \tag{6.48}$$

Remark 6.2. There is a geometrical interpretation of (6.48). For fixed $\alpha > 0$, curves $||l_1(\xi_1)||^2 = \alpha$ and $||l_2(\xi_2)||^2 = \alpha$ represent two pairs of parallel lines in the $\xi_1 - \xi_2$ coordinate system, that are perpendicular to each other and $||r(\xi_1, \xi_2)||^2 = \alpha$ is a hyperbole. The solution of (6.48) is then the intersection point of two pairs of lines and the hyperbole, cf. Figure 6.5.

Is is possible to solve (6.48) exactly? This question can partly be answered by the following lemma.

Lemma 6.5. *Given* $\sigma_1^y, \sigma_2^y, h_1, h_2, \mu, \mathrm{dev}\, A_1, \mathrm{dev}\, A_2$. *Then the solution* ξ_2 *of the nonlinear system (6.48) is a root of the 8-th degree polynomial of the form*

$$
\begin{aligned}
&\Big(J^4F^2\Big)\xi_2^8+\Big(2\%4J^2F\Big)\xi_2^7+\Big(2\%3J^2F+\%4^2\Big)\xi_2^6+\Big(2\%2J^2F+2\%3\%4\Big)\xi_2^5\\
+&\Big(2\%1J^2F+2\%2\%4+\%3^2-F(BJ+2IC)^2\Big)\xi_2^4\\
+&\Big(-E(BJ+2IC)^2-2F(2CG+BH)(BJ+2IC)+2\%1\%4+2\%2\%3\Big)\xi_2^3\\
+&\Big(-\mathrm{D}(BJ+2IC)^2-2E(2CG+BH)(BJ+2IC)-F(2CG+BH)^2\\
&+2\%1\%3+\%2^2\Big)\xi_2^2\\
+&\Big(-2\mathrm{D}(2CG+BH)(BJ+2IC)-E(2CG+BH)^2+2\%1\%2\Big)\xi_2\\
+&\Big(\%1^2-\mathrm{D}(2CG+BH)^2\Big)=0,
\end{aligned}
\tag{6.49}
$$

where

$$
\begin{aligned}
&\%1 := H^2\,\mathrm{D} - C\,G^2 - A\,H^2 - B\,G\,H - C\,\mathrm{D},\\
&\%2 := -B\,G\,J - 2\,H\,J\,A - C\,E - 2\,I\,C\,G + H^2\,E - I\,B\,H + 2\,H\,J\,\mathrm{D},\\
&\%3 := -C\,F - J^2\,A + 2\,H\,J\,E - I\,B\,J + C + J^2\,\mathrm{D} + H^2\,F,\\
&\%4 := 2\,H\,J\,F + J^2\,E
\end{aligned}
\tag{6.50}
$$

and the coefficients $A, B, C, D, E, F, G, H, I, J$ *are specified in the proof.*

Proof. We can rewrite

$$
\begin{aligned}
||l_1(\xi_1)||^2 &= ||((2\mu + h_1)\mathrm{dev}\, A_2 - 2\mu\mathrm{dev}\, A_1)\xi_1 + \sigma_1^y\mathrm{dev}\, A_2||^2 =\\
&= \underbrace{||\sigma_1^y\mathrm{dev}\, A_2||^2}_{A} + \underbrace{2(\sigma_1^y\mathrm{dev}\, A_2) : ((2\mu + h_1)\mathrm{dev}\, A_2 - 2\mu\mathrm{dev}\, A_1)}_{B}\,\xi_1\\
&\quad + \underbrace{||(2\mu + h_1)\mathrm{dev}\, A_2 - 2\mu\mathrm{dev}\, A_1||^2}_{C}\,\xi_1^2 = A + B\xi_1 + C\xi_1^2,
\end{aligned}
$$

$$\begin{aligned}
||l_2(\xi_2)||^2 &= ||((2\mu + h_2)\text{dev}\, A_1 - 2\mu\text{dev}\, A_2)\xi_2 + \sigma_2^y\text{dev}\, A_1||^2 = \\
&= \underbrace{||\sigma_2^y\text{dev}\, A_1||^2}_{D} + \underbrace{2(\sigma_2^y\text{dev}\, A_1) : ((2\mu + h_2)\text{dev}\, A_1 - 2\mu\text{dev}\, A_2)}_{E}\,\xi_2 \\
&\quad + \underbrace{||((2\mu + h_2)\text{dev}\, A_1 - 2\mu\text{dev}\, A_2)||^2}_{F}\,\xi_2^2 = D + E\xi_2 + F\xi_2^2, \\
r(\xi_1,\xi_2)^2 &= (\underbrace{\sigma_1^y\sigma_2^y}_{G} + \underbrace{(2\mu + h_1)\sigma_2^y}_{H}\,\xi_1 + \underbrace{(2\mu + h_2)\sigma_1^y}_{I}\,\xi_2 + \underbrace{(2\mu(h_1 + h_2) + h_1h_2)}_{J}\,\xi_1\xi_2)^2 \\
&= (G + H\xi_1 + I\xi_2 + J\xi_1\xi_2)^2
\end{aligned}$$

Then Φ_1, Φ_2 are polynomials of the second degree in two variables ξ_1, ξ_2.

$$\Phi_1(\xi_1,\xi_2) = A + B\xi_1 + C\xi_1^2 - (G + H\xi_1 + I\xi_2 + J\xi_1\xi_2)^2 = 0 \tag{6.51}$$
$$\Phi_2(\xi_1,\xi_2) = D + E\xi_2 + F\xi_2^2 - (G + H\xi_1 + I\xi_2 + J\xi_1\xi_2)^2 = 0 \tag{6.52}$$

Expressing ξ_1 from (6.52),

$$\xi_1 = \frac{-I\,\xi_2 - G \pm \sqrt{\mathrm{D} + E\,\xi_2 + F\,\xi_2^2}}{H + J\,\xi_2}, \tag{6.53}$$

the substitution of (6.53) into (6.51), infers after some transformations (MAPLE 6) the polynomial (6.49). □

Finding roots ξ_2 of the eight degree polynomial (6.49), one can substitute ξ_2 into (6.53) and determinate values of ξ_1. Since ξ_2 generally attains 8 values, the solution (ξ_1, ξ_2) can even attain 16 different values.

Remark 6.3. Lemma 6.5 states that if $P_1 \neq 0$ and $P_2 \neq 0$ then $\xi_2 = ||P_2||$ is a root of the 8-th degree polynomial (6.49). In some special cases the 8-th degree polynomial can be replaced by some lower degree polynomial. This is demonstrated in the next example.

Example 6.1. Let $\mu = 1, \sigma_1^y = 1, \sigma_2^y = 2, h_1 = 1, h_2 = 1$ and

$$A_1 = A_2 = \begin{pmatrix} 20 & 0 \\ 0 & 0 \end{pmatrix}.$$

The direct calculation shows

$$\begin{aligned}
l_1 &= \begin{pmatrix} 10 + 10\xi_1 & 0 \\ 0 & -10 - 10\xi_1 \end{pmatrix}, \\
l_2 &= \begin{pmatrix} 20 - 10\xi_2 & 0 \\ 0 & -20 - 10\xi_2 \end{pmatrix}, \\
r &= 5\,\xi_1\,\xi_2 + 6\,\xi_1 + 3\,\xi_2 + 2
\end{aligned}$$

and the nonlinear system of equations (6.48) reads

$$\Phi_1 \quad = 200 + 400\,\xi_1 + 200\,\xi_1^2 - (2 + 3\,\xi_2 + 6\,\xi_1 + 5\,\xi_1\,\xi_2)^2 = 0, \tag{6.54}$$
$$\Phi_2 \quad = 800 + 800\,\xi_2 + 200\,\xi_2^2 - (2 + 3\,\xi_2 + 6\,\xi_1 + 5\,\xi_1\,\xi_2)^2 = 0. \tag{6.55}$$

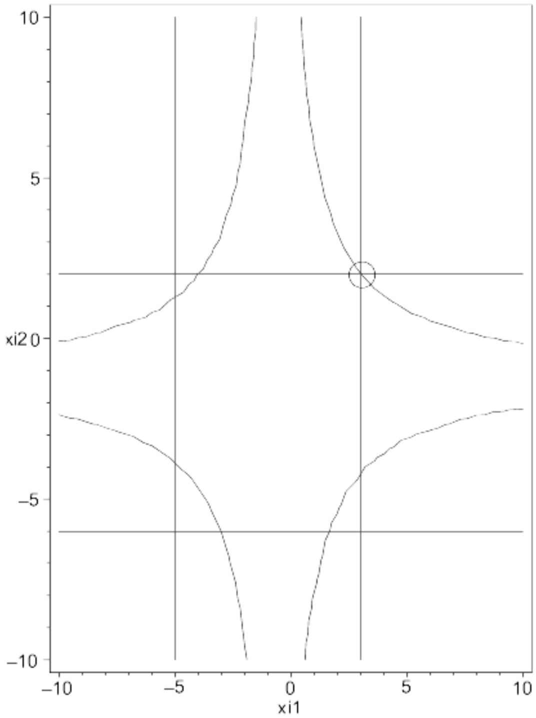

Figure 6.5: Geometrical interpretation of the solution (ξ_1, ξ_2) of the nonlinear system (6.48): (ξ_1, ξ_2) is the intersection point of two perpendicular lines and a hyperbole. In Example 6.1, $\xi_1 = 3.02, \xi_2 = 2.02$ and parameter $\alpha = 3244$.

Graph of the nonlinear system (6.54), (6.55) is displayed in Figure 6.10. ξ_1 is solved from (6.55) with

$$\xi_1 = -\frac{1}{2}\frac{24 + 56\xi_2 + 30\xi_2^2 \pm 20\sqrt{2}\,(12 + 16\xi_2 + 5\xi_2^2)}{(6 + 5\,\xi_2)^2}$$

and the substitution of it (only the $-$ term, the $+$ term leads to different signs of ξ_1 and ξ_2) into (6.54) implies the equation

$$200\frac{-25\xi_2^4 - 160\xi_2^3 + (40\sqrt{2} - 172)\xi_2^2 + (432 + 160\sqrt{2})\xi_2 + 672 + 160\sqrt{2}}{(6 + 5\,\xi_2)^2} = 0.$$

Since $(6 + 5\,\xi_2) > 0$ it is sufficient to solve ξ_2 from the 4-th degree polynomial

$$25\xi_2^4 + 160\xi_2^3 - (40\sqrt{2} - 172)\xi_2^2 - (432 + 160\sqrt{2})\xi_2 - 672 - 160\sqrt{2} = 0.$$

Without this condition ξ_2 could be calculated as the root of the 8-th degree polynomial (6.49). The exact calculation shows that

$$\xi_2 = \{-4.428427124, 2.028427124, -2, -2\}$$

and only the positive solution $\xi_2 = 2.028427124$ is admissible. Figures 6.6, 6.7, 6.8, 6.9 display the form of the quadratic, the linear, the term with the norm and the functional (6.33), assuming

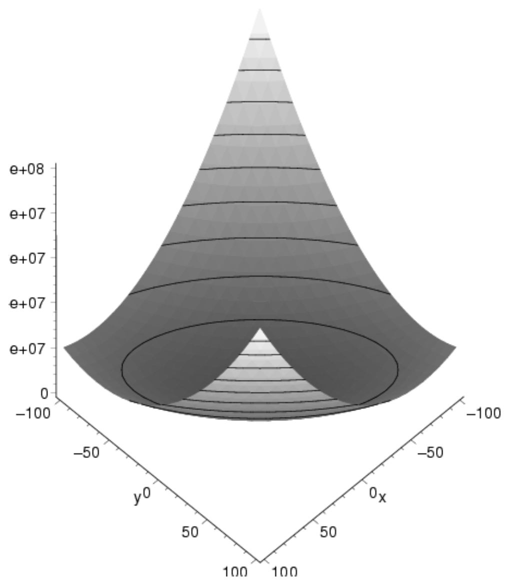

Figure 6.6: Values of the quadratic functional $\frac{1}{2}(\hat{\mathbb{C}} + \hat{\mathbb{H}})P : P$ as a function of x and y, where $P = (P_1, P_2)^T, P_1 = (x, 0; 0, -x), P_2 = (y, 0; 0, -y)$.

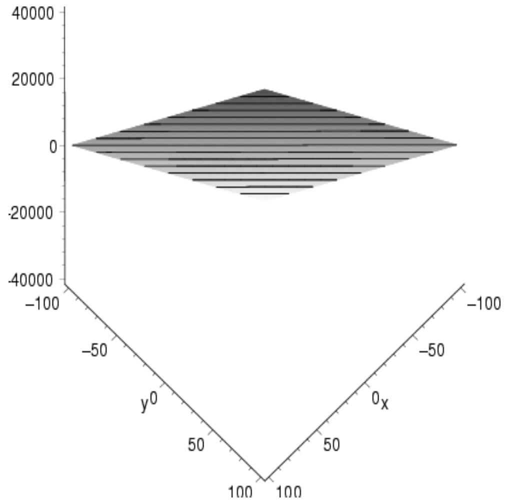

Figure 6.7: Values of the linear functional $P : A$ as a function of x and y, where $P = (P_1, P_2)^T, P_1 = (x, 0; 0, -x), P_2 = (y, 0; 0, -y)$.

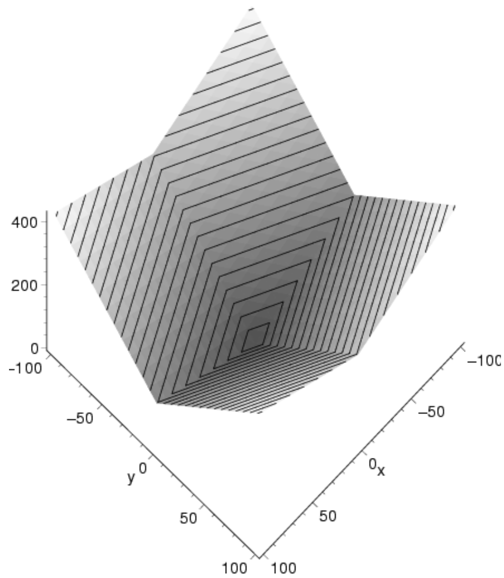

Figure 6.8: Values of the functional with the norm $||P||_{\sigma_y}$ as a function of x and y, where $P = (P_1, P_2)^T, P_1 = (x, 0; 0, -x), P_2 = (y, 0; 0, -y)$.

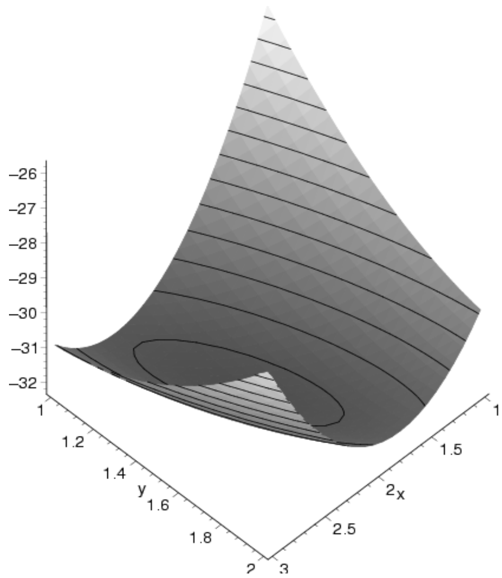

Figure 6.9: Values of the functional $\frac{1}{2}(\hat{\mathbb{C}} + \hat{\mathbb{H}})P : P - P : A + ||P||_{\sigma_y}$ as a function of x and y, where $P = (P_1, P_2)^T, P_1 = (x, 0; 0, -x), P_2 = (y, 0; 0, -y)$.

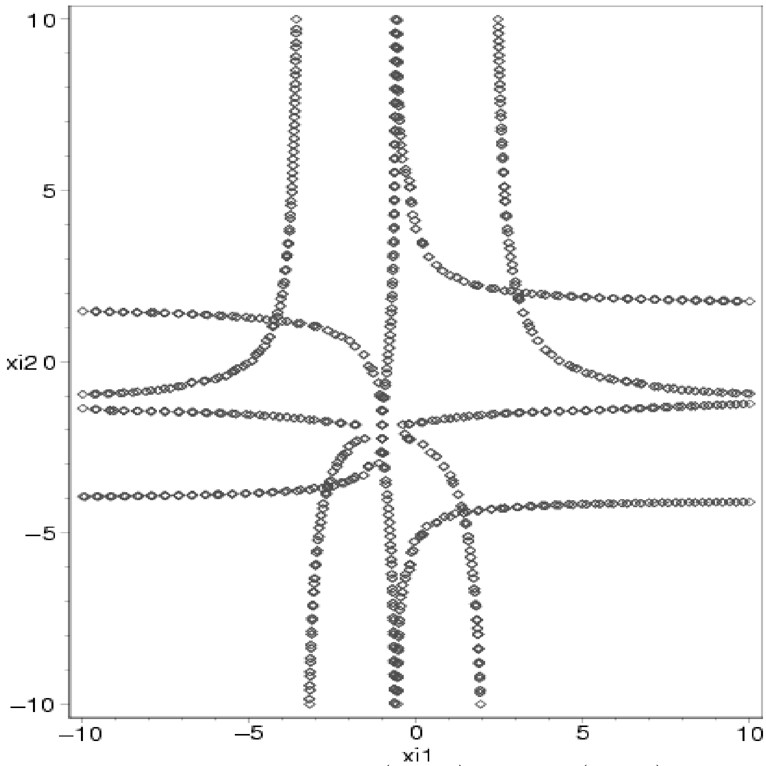

Figure 6.10: Graph of the nonlinear system $\Phi_1(\xi_1, \xi_2) = 0, \Phi_2(\xi_1, \xi_2) = 0$ in Example 6.1. The intersection points (ξ_1, ξ_2) of the displayed branches are the solutions of the nonlinear system.

symmetric and trace free matrices P_1, P_2 in the form

$$P_1 = \begin{pmatrix} x & 0 \\ 0 & -x \end{pmatrix} \quad \text{and} \quad P_2 = \begin{pmatrix} y & 0 \\ 0 & -y \end{pmatrix}.$$

All figures in this example were produced by a Maple program $maple.ms$ listed in Appendix was used.

We end up with the algorithm for the calculation of P_1, P_2.

Algorithm 1 (Polynomial approach for calculation of P_1, P_2). Given $\mu, h_1, h_2, \sigma_1^y, \sigma_2^y$ and dev A_1, dev A_2.
(a) If $||\text{dev}\, A_1|| \le \sigma_1^y$ and $||\text{dev}\, A_2|| \le \sigma_2^y$ then set

$$P_1 := 0 \quad \text{and} \quad P_2 := 0$$

and output (P_1, P_2).
(b) If $||\text{dev}\, A_1 - 2\mu(\frac{||\text{dev}\, A_2|| - \sigma_2^y}{2\mu + h_2} \frac{\text{dev}\, A_2}{||\text{dev}\, A_2||})|| \le \sigma_1^y B$ then set

$$P_1^{(case2)} := 0 \quad \text{and} \quad P_2^{(case2)} := \frac{||\text{dev}\, A_2|| - \sigma_2^y}{2\mu + h_2} \frac{\text{dev}\, A_2}{||\text{dev}\, A_2||}.$$

(c) If $||\text{dev}\, A_2 - 2\mu(\frac{||\text{dev}\, A_1|| - \sigma_1^y}{2\mu + h_1} \frac{\text{dev}\, A_1}{||\text{dev}\, A_1||})|| \leq \sigma_2^y$ then set

$$P_1^{(case3)} := \frac{||\text{dev}\, A_1|| - \sigma_1^y}{2\mu + h_1} \frac{\text{dev}\, A_1}{||\text{dev}\, A_1||} \quad \text{and} \quad P_2^{(case3)} := 0.$$

(d) Find all $\xi_1^i > 0, \xi_2^i > 0$ (either no solution or from 1 to 16 solutions) satisfying (6.51) and (6.52), then for all i

$$P_1^{(case4)_i} := \xi_1^i X_1^i \quad \text{and} \quad P_2^{(case4)_i} := \xi_2^i X_1^i,$$

where X_1^i and X_2^i solve the linear system (6.44) with parameters ξ_1^i, ξ_2^i.
(e) Determine (P_1, P_2) from

$$f(P_1, P_2) = \min\{f(P_1^{(case2)}, P_2^{(case2)}), f(P_1^{(case3)}, P_1^{(case3)}), \min_i\{f(P_1^{(case4)_i}, P_2^{(case4)_i})\}$$

and output (P_1, P_2).

Remark 6.4. If the conditions in steps (b) or (c) of Algorithm 1 are not satisfied, P_1^{case2}, P_2^{case2} or P_1^{case3}, P_2^{case3} are not defined and therefore their values are not considered in step (e).

6.2.2 Iterative approach

In order to avoid the solving of a polynomial of the eight degree in step (d) of Algorithm 1 we introduce a numerical algorithm solving the minimization problem (6.33) iteratively.

Algorithm 2 (Iterative approach for calculation of P_1, P_2). Given $\mu, h_1, h_2, \sigma_1^y, \sigma_2^y$, dev A_1, dev A_2 and $tolerance \geq 0$.
(a) Choose an initial approximation $(P_1^0, P_2^0) \in \text{dev}\, \mathbb{R}^{d\times d}_{sym} \times \text{dev}\, \mathbb{R}^{d\times d}_{sym}$, set $i := 0$.
(b) Find $P_2^{i+1} \in \text{dev}\, \mathbb{R}^{d\times d}_{sym}$ such that

$$f(P_1^i, P_2^{i+1}) = \min_{Q_2 \in \text{dev}\, \mathbb{R}^{d\times d}_{sym}} f(P_1^i, Q_2).$$

(c) Find $P_1^{i+1} \in \text{dev}\, \mathbb{R}^{d\times d}_{sym}$ such that

$$f(P_1^{i+1}, P_2^{i+1}) = \min_{Q_1 \in \text{dev}\, \mathbb{R}^{d\times d}_{sym}} f(Q_1, P_2^{i+1}).$$

(d) If $\frac{||P_1^{i+1} - P_1^i|| + ||P_2^{i+1} - P_2^i||}{||P_1^{i+1}|| + ||P_1^i|| + ||P_2^{i+1}|| + ||P_2^i||} > tolerance$ set $i := i + 1$ and goto (b), otherwise output (P_1^{i+1}, P_2^{i+1}).

Remarks 6.1. (i) Algorithm 2 belongs to the class of *alternating direction* algorithms. The minimization problems in steps (b) and (c) can be solved explicitly as

$$P_2^{i+1} = \frac{(||\text{dev}\, A_2 - 2\mu P_1^i|| - \sigma_2^y)_+}{2\mu + h_2} \frac{\text{dev}\, A_2 - 2\mu P_1^i}{||\text{dev}\, A_2 - 2\mu P_1^i||}, \tag{6.56}$$

$$P_1^{i+1} = \frac{(||\text{dev}\, A_1 - 2\mu P_2^{i+1}|| - \sigma_1^y)_+}{2\mu + h_1} \frac{\text{dev}\, A_1 - 2\mu P_2^{i+1}}{||\text{dev}\, A_1 - 2\mu P_2^{i+1}||}. \tag{6.57}$$

(ii) The choice of the parameter $tolerance$ has significant effect of the computational complexity of Algorithm 2. Theoretically, for $tolerance = 0$ the upgrade in steps (b) and (c) needs to be performed infinitely many times. Rounding errors can cause this for $tolerance > 0$ as well. If the rounding errors are neglected, one can show that Algorithm 2 converge to the minimizer (P_1, P_2).

Lemma 6.6 (Uniform ellipticity and Lipschitz continuity). *The functionals*

$$\Phi : \text{dev}\,(\mathbb{R}^{d\times d}_{sym}) \times \text{dev}\,(\mathbb{R}^{d\times d}_{sym}) \to \mathbb{R}, \quad \Phi(P) = \frac{1}{2}(\hat{\mathbb{H}} + \hat{\mathbb{C}})P : P - A : P \tag{6.58}$$

is Fréchet-differentiable and $D\Phi$ is uniformly elliptic and Lipschitz continuous with constants

$$\alpha = \frac{1}{2}\lambda_{min}(\hat{\mathbb{C}} + \hat{\mathbb{H}}) \quad \textit{and} \quad L = ||\hat{\mathbb{C}} + \hat{\mathbb{H}}||, \tag{6.59}$$

where $\lambda_{min}(\hat{\mathbb{C}} + \hat{\mathbb{H}})$ denotes the minimal eigenvalue of the matrix $(\hat{\mathbb{C}} + \hat{\mathbb{H}})$.

Proof. The direct calculation shows that for the symmetric matrix $\hat{\mathbb{C}} + \hat{\mathbb{H}}$, the functional f is Fréchet-differentiable,

$$D\Phi(P) = (\hat{\mathbb{C}} + \hat{\mathbb{H}})P - A. \tag{6.60}$$

By the definition of uniformly ellipticity of $D\Phi$, there exists a constant $\alpha > 0$ such that for all $P, Q \in \text{dev}\,(\mathbb{R}^{d\times d}_{sym}) \times \text{dev}\,(\mathbb{R}^{d\times d}_{sym})$,

$$\alpha||P - Q||^2 + D\Phi(P; Q - P) \leq \Phi(Q) - \Phi(P) \tag{6.61}$$

The substitution of (6.60) into (6.61) and an orthonormal transformation $Q = TQ', P = TP'$ such that $T^T(\hat{\mathbb{C}} + \hat{\mathbb{H}})T = \text{diag}\,(\lambda_i)$ imply

$$\alpha||P' - Q'||^2 + \text{diag}\,(\lambda_i)P' : (Q' - P') \leq \frac{1}{2}\text{diag}\,(\lambda_i)P' : P' - \frac{1}{2}\text{diag}\,(\lambda_i)Q' : Q', \tag{6.62}$$

for all $P', Q' \in \text{dev}\,(\mathbb{R}^{d\times d}_{sym}) \times \text{dev}\,(\mathbb{R}^{d\times d}_{sym})$. Further we decompose the inequality (6.62) as the sum of inequalities

$$\alpha_{ij}(P'_{ij} - Q'_{ij})^2 + \lambda_i P'_{ij} : (Q'_{ij} - P'_{ij}) \leq \frac{1}{2}\lambda_i P'_{ij} : P'_{ij} - \frac{1}{2}\lambda_i Q'_{ij} : Q'_{ij}, \tag{6.63}$$

over all $i, j = 1, \ldots 2d$. Since for all $x, y, \lambda \in \mathbb{R}, \lambda > 0$,

$$\alpha(y - x)^2 + \lambda x(y - x) \leq \frac{1}{2}\lambda x^2 - \frac{1}{2}\lambda y^2, \tag{6.64}$$

for positive $\alpha \leq \frac{1}{2}\lambda$, we estimate for all $i, j = 1 \ldots 2d$,

$$\alpha_{ij} \leq \frac{1}{2}\lambda_i \tag{6.65}$$

Therefore, the choice $\alpha_{ij} = \alpha = \min_i\{\lambda_i\}$ finishes the part of the proof concerning the uniform ellipticity. Lipschitz continuity of $D\Phi$ with a constant $L = ||\hat{\mathbb{C}} + \hat{\mathbb{H}}||$ follows immediately from the multiplicativity of the Frobenius norm $||\cdot||$,

$$||(\hat{\mathbb{C}} + \hat{\mathbb{H}})P - (\hat{\mathbb{C}} + \hat{\mathbb{H}})Q|| \leq ||(\hat{\mathbb{C}} + \hat{\mathbb{H}})|| \cdot ||P - Q||, \tag{6.66}$$

for all $P, Q \in \text{dev}\,(\mathbb{R}^{d\times d}_{sym}) \times \text{dev}\,(\mathbb{R}^{d\times d}_{sym})$. $\square$

Proposition 6.1 (Convergence of Algorithm 2). *Let (P_1, P_2) be the minimizer of f and let the sequence $(P_1^i, P_2^i)_{i=0}^{\infty}$ be generated by Algorithm 2. Define $q := \gamma/(1+\gamma), \gamma := L^2 \cdot \alpha^{-2}, C_0 := 2(1+\gamma)\cdot\alpha^{-1}\cdot(f(P_1^0, P_2^0) - f(P_1, P_2))$, where α and L are given in Lemma 6.6. Then, for any $i \geq 1$ there holds*

$$||P_1^i - P_1||^2 + ||P_2^i - P_2||^2 \leq C_0 \cdot q^i. \tag{6.67}$$

Proof. Let us decompose the space of $X := \text{dev}\,(\mathbb{R}^{d\times d}_{sym}) \times \text{dev}\,(\mathbb{R}^{d\times d}_{sym})$ as $X = X_1 + X_2$, where

$$X_1 := \{(P_1, 0) : P_1 \in \text{dev}\,(\mathbb{R}^{d\times d}_{sym})\} \quad \text{and} \quad X_2 := \{(0, P_2) : P_2 \in \text{dev}\,(\mathbb{R}^{d\times d}_{sym})\}.$$

Let $M_1 : X \to X_1$ and $M_2 : X \to X_2$ be linear mappings defined as

$$M_1(P_1, P_2) := (P_1, 0) \quad \text{and} \quad M_2(P_1, P_2) := (0, P_2).$$

Then we can show that for all subsets $\Lambda \subseteq \{1, 2\}$ and all $P = (P_1, P_2) \in X$ there holds

$$||\sum_{\lambda\in\Lambda} M_\lambda(P_1, P_2)|| \leq 1 \cdot ||(P_1, P_2)||.$$

We decompose the functional f as the sum of functionals Φ and ψ, where

$$\Phi(P) := \frac{1}{2}(\hat{\mathbb{H}} + \hat{\mathbb{C}})P : P - A : P \quad \text{and} \quad \psi(P) := ||P||_{\sigma^y} = \sigma_1^y||P_1|| + \sigma_2^y||P_2||.$$

From Lemma 6.6 we know that the functional Φ is Fréchet-differentiable and $D\Phi$ is uniformly elliptic Lipschitz continuous. The convex, lower-semicontinuous functional ψ is additive and independent with respect to the partition $X = X_1 + X_2$, i.e. in the sense that, for all $(x_1, x_2) \in X_1 \times X_2$,

$$\psi(\sum_{j=1}^{2} x_j) = \sum_{j=1}^{2} \psi(x_j).$$

and, for all $j \in \{1, 2\}$, for all $x_j \in X_j$ and for all $y_j \in \sum_{k=1,k\neq j}^{2} X_k$, there holds

$$\psi(x_j + M_j y_j) = \psi(x_j).$$

Finally, the estimate (6.67) is the consequence of the Theorem 2.1 in [Car97]. □

Remark 6.5. Proposition 6.1 states that Algorithm 2 converges with the convergence rate $1/2$.

The next example demonstrates the behavior of Algorithm 2.

Example 6.2. We consider parameters of Example 6.1, $tolerance = 10^{-12}$ and the initial approximation

$$P_2^0 = \frac{||\text{dev}\,A_2|| - \sigma_2^y}{2\mu + h_2}\frac{\text{dev}\,A_2}{||\text{dev}\,A_2||} \quad \text{and} \quad P_1^0 = \frac{||\text{dev}\,A_1 - 2\mu P_2^0|| - \sigma_1^y}{2\mu + h_1}\frac{\text{dev}\,A_1 - 2\mu P_2^0}{||\text{dev}\,A_1 - 2\mu P_2^0||}.$$

Algorithm 2 generates approximations $P_1^i, P_2^i, i = 1, 2, \ldots$ in the form

$$P_1^i = \begin{pmatrix} x^i & 0 \\ 0 & -x^i \end{pmatrix} \quad \text{and} \quad P_2^i = \begin{pmatrix} y^i & 0 \\ 0 & -y^i \end{pmatrix},$$

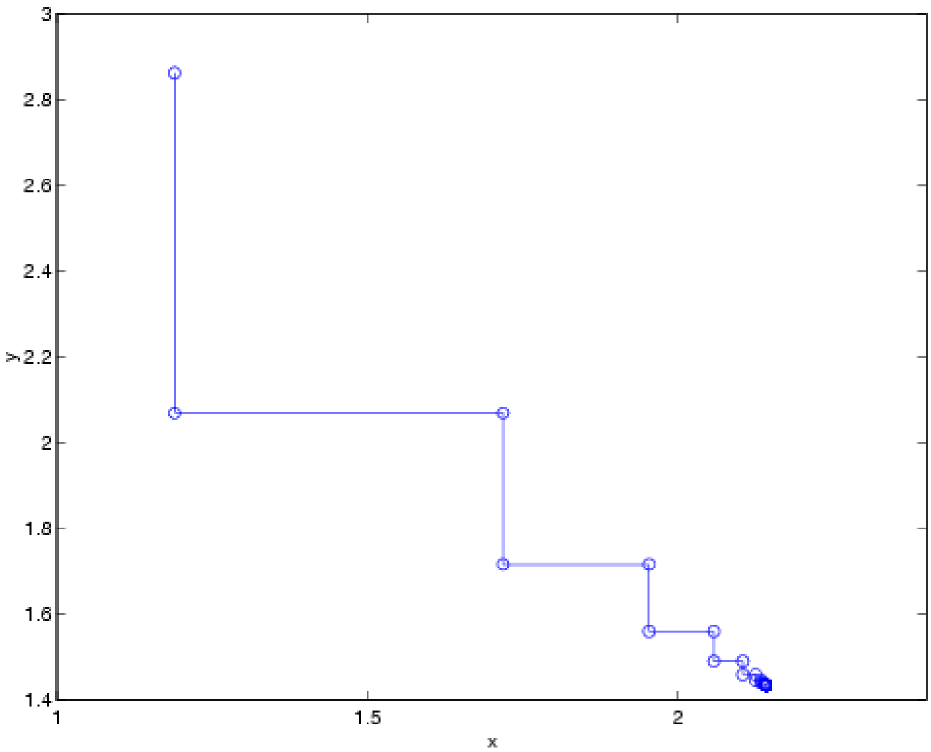

Figure 6.11: Example 6.2: The approximations $P_1^i = (x^i, 0; 0, -x^i), P_2^i = (y^i, 0; 0, -y^i), i = 0, 1, \ldots$ of Algorithm 2 displayed as the points (x^i, y^i) in the $x - y$ coordinate system.

where $x, y \in \mathbb{R}$ and terminates after 34 approximations at the final approximation

$$P_1^{34} = \begin{pmatrix} 2.14142 & 0 \\ 0 & -2.14142 \end{pmatrix} \quad \text{and} \quad P_2^{34} = \begin{pmatrix} 1.43431 & 0 \\ 0 & -1.4343 \end{pmatrix}.$$

Note that the value $||P_2^{34}|| = 2.02842712474404$ is coincident with the value of ξ_2 calculated by Algorithm 1 in Example 6.1. Figure 6.11 displays the approximations $(P_1^i, P_2^i), i = 0, 1, 2, \ldots$ as the points (x^i, y^i) in the $x - y$ coordinate system.

Chapter 7

Convergence analysis

This chapter is devoted to the analysis of the space and time discretization errors for Problem (S). The arguments of the proof are partly based on the paper [AC00]. The first section concentrates on the derivation of the discretization error, the second section specifies results for the problem with one discrete time step and introduces a *residual* refinement indicator as a tool for the space discretization error control. Throughout this chapter, $x = (u, p_1, \ldots, p_M)$ solves Problem 4.1 and $X = (U, P_1, \ldots, P_M)$ solves Problem (S).

7.1 Convergence of the discrete problem

Let the discretization error be

$$e_j := x(t_j) - X(t_j)$$

and let a piecewise affine function $\tilde{x}(t) \in \mathcal{C}(0, T; H)$ be defined by

$$\tilde{x}(t) := \frac{t - t_{j-1}}{k_j} x(t_j) + \frac{t_j - t}{k_j} x(t_{j-1}), \tag{7.1}$$

where $I_j := (t_{j-1}, t_j), k_j := t_j - t_{j-1}$. Set $\tilde{e} := \tilde{x} - X \in \mathcal{C}(0, T; H)$. Let $t_{j-1/2} := (t_j + t_{j-1})/2$ and recall $t_{j-1/2} \le t \le t_j$. Through a symmetric and positive definite bilinear form $a(\cdot, \cdot)$ we can define the energy norm

$$|| \cdot || := a(\cdot, \cdot)^{1/2}.$$

Proposition 7.1. *For all $Y_1, \ldots, Y_N \in S, t_{j-1/2} \le \tau_j \le t_j$ there exists $n \in \{0, 1, \ldots, N\}$ such that*

$$\begin{aligned} 1/2 \max_{l=0,\ldots,N} ||e_l||^2 \le & ||e_0||^2 + 19/2 ||k\ddot{x}||^2_{L^1(0,t_n)} \\ & + \sum_{j=1}^{n} 2k_j \{ a(X(\tau_j), Y_j - \dot{x}(\tau_j)) - l(\tau_j)(Y_j - \dot{x}(\tau_j)) \} \\ & + \sum_{j=1}^{n} 2k_j \{ \psi(Y_j) - \psi(\dot{x}(\tau_j)) \}, \end{aligned} \tag{7.2}$$

where $k \in L^\infty(0,T)$ is defined by $k(t) = k_j$ if $t_{j-1} \leq \tau_{j-1} \leq t_j$, and

$$\begin{aligned}\sum_{j=1}^{n}(\theta_j - 1/2)||e_j - e_{j-1}||^2 \leq ||e_0||^2 + 1/2 \max_{l=0,\ldots,N} ||e_l||^2 + 19/2||k\ddot{x}||^2_{L^1(0,T)} \\ + \sum_{j=1}^{n} 2k_j\{a(X(\tau_j), Y_j - \dot{x}(\tau_j)) - l(\tau_j)(Y_j - \dot{x}(\tau_j)) + \psi(Y_j) - \psi(\dot{x}(\tau_j))\}\end{aligned} \tag{7.3}$$

In case that $k = k_j = T/N$ and $\tau_j = t_{j-1/2}$ for all $j = 1, \ldots, N$, we have some $n \in \{0, 1, \ldots, N\}$ such that

$$\begin{aligned}&1/2 \max_{l=0,\ldots,N} ||e_l||^2 \\ &\leq ||e_0||^2 + k^4/2(||\dddot{x}||^2_{L^1(0,t_n)} + 7/8||\ddot{x}||^2_{L^\infty(0,t_n)}) \\ &\quad + \sum_{j=1}^{n} 2k_j\{a(X(t_{j-1/2}), Y_j - \dot{x}(t_{j-1/2})) - l(t_{j-1/2})(Y_j - \dot{x}(t_{j-1/2}))\} \\ &\quad + \sum_{j=1}^{n} 2k\{\psi(Y_j) - \psi(\dot{x}(t_{j-1/2}))\},\end{aligned} \tag{7.4}$$

Proof. [AC00], Proposition 5.1. □

Definition 7.1 (Choosing Y_j). Suppose $x = (u, p_1, \ldots, p_M)$ solves Problem 4.1 and $X = (U, P_1, \ldots, P_M)$ solves Problem (S). Then let $W_j \in \mathcal{S}^1_D(\mathcal{T})$ be a fixed approximation to $\dot{u}(t)$ and let

$$Q_j = (\mathcal{M}\dot{p}_1(\tau_j), \ldots, \mathcal{M}\dot{p}_M(\tau_j)), \tag{7.5}$$

where $\mathcal{M} : L^1(\Omega) \to \mathcal{S}^0(\mathcal{T})$ denotes a mean operator defined by

$$(\mathcal{M}\sigma)|_T := \int_T \sigma \,\mathrm{d}x/\mathrm{meas}(T) \qquad (T \in \mathcal{T}) \tag{7.6}$$

and, for all $j = 1, \ldots, N$, set

$$Y_j := (W_j, Q_j) \in S. \tag{7.7}$$

For a special choice of $Y_j, j = 1, \ldots, N$ from the Definition 7.1 we can prove the following lemma.

Lemma 7.1. *For all $j = 1, \ldots, N$ we have*

$$\psi(Y_j) \leq \psi(\dot{x}(\tau_j)). \tag{7.8}$$

Proof. By a definition of $\psi(\cdot)$,

$$\psi(Y_j) = \int_\Omega \Big(\mathcal{D}_1(\mathcal{M}\dot{p}_1(\tau_j)) + \cdots + \mathcal{D}_M(\mathcal{M}\dot{p}_M(\tau_j))\Big)\,\mathrm{d}x$$

and

$$\psi(\dot{x}(\tau_j)) = \int_\Omega \Big(\mathcal{D}_1(\dot{p}_1(\tau_j, x)) + \cdots + \mathcal{D}_M(\dot{p}_M(\tau_j, x))\Big)\,\mathrm{d}x.$$

The *Jensen inequality* for convex functions $\mathcal{D}_i(\cdot) = \sigma_i^y||\cdot||, i = 1, \ldots, M$ yields for every triangle $T \in \mathcal{T}$ the inequality

$$\mathcal{D}_i(\mathcal{M}\dot{p}_i(\tau_j)) = \mathcal{D}_i\Big(\int_T \dot{p}_i(\tau_j, x)\,\mathrm{d}x/\mathrm{meas}(T)\Big) \leq \int_T \mathcal{D}_i(\dot{p}_i(\tau_j, x))\,\mathrm{d}x/\mathrm{meas}(T)$$

and after the integration of this over T it holds for all $i = 1, \ldots M$ that

$$\int_T \mathcal{D}_i(\mathcal{M}\dot{p}_i(\tau_j))\,\mathrm{d}x \leq \int_T \mathcal{D}_i(\dot{p}_i(\tau_j, x))\,\mathrm{d}x \tag{7.9}$$

We sum inequalities (7.9) over $i = 1, \ldots, M$ and all elements $T \in \mathcal{T}$ and deduce the inequality (7.8). $\square$

Lemma 7.2. *For all $j = 1, \ldots, N$ we have*

$$a(X(\tau_j), Y_j - \dot{x}(\tau_j)) - l(\tau_j)(Y_j - \dot{x}(\tau_j)) = \int_\Omega (\sigma(\tau_j) - \Sigma(\tau_j)) : \varepsilon(\dot{u}(\tau_j) - W_j)\,dx. \tag{7.10}$$

Proof. [AC00], Lemma 5.5. $\square$

Now we are in the position to prove

Theorem 7.1. *a) If $t_{j-1/2} \leq \tau_j \leq t_j$ for all $j = 1, \ldots, N$, we have for all $W_j \in \mathcal{S}_D^1(\mathcal{T})$*

$$\begin{aligned}
&\max_{l=0,\ldots,N}\{1/4||\mathbb{C}^{-1/2}(\sigma - \Sigma)(t_l)||^2_{L^2(\Omega)} + 1/2\sum_{i=1}^M ||\mathbb{H}_i^{1/2}(p_i - P_i)(t_l)||^2_{L^2(\Omega)}\} \\
&\leq ||\mathbb{C}^{-1/2}(\sigma - \Sigma)(0)||^2_{L^2(\Omega)} + \sum_{i=1}^M ||\mathbb{H}_i^{1/2}(p_i - P_i)(0)||^2_{L^2(\Omega)} \\
&\quad + 19/2||k(\mathbb{C}^{-1/2}\ddot{\sigma}, \mathbb{H}_1^{1/2}\ddot{p}_1, \ldots, \mathbb{H}_M^{1/2}\ddot{p}_M)||^2_{L^1(0,T;L^2(\Omega))} \\
&+ 1/2||k^2\mathbb{C}^{-1/2}\ddot{\sigma}||^2_{L^2(0,T;L^2(\Omega))} + (1/2 + 4T)\sum_{j=1}^N k_j||\mathbb{C}^{1/2}\varepsilon(\dot{u}(\tau_j) - W_j)||^2_{L^2(\Omega)}
\end{aligned} \tag{7.11}$$

and, with $\theta_j := (\tau_j - t_{j-1})/k_j$,

$$\begin{aligned}
&\sum_{j=1}^N (\theta_j - 1/2)\Big\{||\mathbb{C}^{-1/2}\{(\sigma - \Sigma)(t_j) - (\sigma - \Sigma)(t_{j-1})\}||^2_{L^2(\Omega)} \\
&\qquad + \sum_{i=1}^M ||\mathbb{H}_i^{1/2}\{(p_i - P_i)(t_j) - (p_i - P_i)(t_{j-1})\}||^2_{L^2(\Omega)}\Big\} \\
&\leq 3||\mathbb{C}^{-1/2}\{(\sigma - \Sigma)(0)\}||^2_{L^2(\Omega)} + 3\sum_{i=1}^M ||\mathbb{H}_i^{1/2}(p_i - P_i)(0)||^2_{L^2(\Omega)} \\
&\quad + 57/2||k(\mathbb{C}^{-1/2}\ddot{\sigma}, \mathbb{H}_1^{1/2}\ddot{p}_1, \ldots, \mathbb{H}_M^{1/2}\ddot{p}_M)||^2_{L^1(0,T;L^2(\Omega))} + 3/2||k^2\mathbb{C}^{-1/2}\ddot{\sigma}||^2_{L^2(0,T;L^2(\Omega))} \\
&\quad + (3/2 + 12T)\sum_{j=1}^N k_j||\mathbb{C}^{1/2}\varepsilon(\dot{u}(\tau_j) - W_j)||^2_{L^2(\Omega)}.
\end{aligned} \tag{7.12}$$

b) If $k = k_j = T/N$ and $\tau_j = t_{j-1/2}$ for all $j = 1, \ldots, N$, we have for all $W_j \in \mathcal{S}^1_D(\mathcal{T})$

$$\begin{aligned}
&\max_{l=0,\ldots,N}\{1/4||\mathbb{C}^{-1/2}(\sigma-\Sigma)(t_l)||^2_{L^2(\Omega)} + 1/2\sum_{i=1}^{M}||\mathbb{H}_i^{1/2}(p_i-P_i)(t_l)||^2_{L^2(\Omega)}\}\\
&\leq ||\mathbb{C}^{-1/2}(\sigma-\Sigma)(0)||^2_{L^2(\Omega)} + \sum_{i=1}^{M}||\mathbb{H}_i^{1/2}(p_i-P_i)(0)||^2_{L^2(\Omega)}\\
&\quad + 1/2(||k^2(\mathbb{C}^{-1/2}\ddot{\sigma}, \mathbb{H}_1^{1/2}\ddot{p}_1, \ldots, \mathbb{H}_M^{1/2}\ddot{p}_M)||^2_{L^\infty(0,T;L^2(\Omega))}\\
&\qquad\quad + 7/8||k^2(\mathbb{C}^{-1/2}\dddot{\sigma}, \mathbb{H}_1^{1/2}\dddot{p}_1, \ldots, \mathbb{H}_M^{1/2}\dddot{p}_M)||^2_{L^1(0,T;L^2(\Omega))})\\
&\quad + 1/2||k^2\mathbb{C}^{-1/2}\ddot{\sigma}||^2_{L^2(0,T;L^2(\Omega))} + (1/2+4T)\sum_{j=1}^{N}k_j||\mathbb{C}^{1/2}\varepsilon(\dot{u}(\tau_j)-W_j)||^2_{L^2(\Omega)}.
\end{aligned} \tag{7.13}$$

Proof. According to the definition of a, we have

$$||e||^2 = a(x-X, x-X) = ||\mathbb{C}^{-1/2}(\sigma-\Sigma)||_{L^2(\Omega)} + \sum_{j=1}^{M}||H_j^{1/2}(p_j-P_j)||^2_{L^2(\Omega)}. \tag{7.14}$$

Hence, with Lemma 7.1 and 7.2, the estimate (7.2) implies

$$\begin{aligned}
&1/2\max_{l=0,\ldots,N}\left(||\mathbb{C}^{-1/2}(\sigma-\Sigma)(t_l)||^2_{L^2(\Omega)} + \sum_{i=1}^{M}||\mathbb{H}_i^{1/2}(p_i-P_i)(t_l)||^2_{L^2(\Omega)}\right)\\
\leq&||\mathbb{C}^{-1/2}(\sigma-\Sigma)(t_0)||^2_{L^2(\Omega)} + \sum_{i=1}^{M}||\mathbb{H}_i^{1/2}(p_i-P_i)(t_0)||^2_{L^2(\Omega)}\\
&+ 19/2||k(\mathbb{C}^{-1/2}\ddot{\sigma}, \mathbb{H}_1^{1/2}\ddot{p}_1, \ldots, \ddot{\mathbb{H}}_M^{1/2}\ddot{p}_M)||^2_{L^1(0,t_n)}\\
&+ 2\sum_{j=1}^{n}k_j\int_\Omega(\sigma-\Sigma)(\tau_j) : \varepsilon(\dot{u}(\tau_j)-W_j)\,\mathrm{d}x.
\end{aligned} \tag{7.15}$$

Define the continuous, piecewise affine function $\tilde{\sigma}$ by the nodal interpolation, for $t_{j-1} \leq t \leq t_j, j = 1, \ldots, N$

$$\tilde{\sigma}(t) := \frac{(t_j - t)}{k_j}\sigma(t_j) + \frac{(t-t_j)}{k_j}\sigma(t_{j-1}). \tag{7.16}$$

A simple one dimensional interpolation error estimate [AC00] yields

$$\begin{aligned}
||\mathbb{C}^{-1/2}(\sigma-\tilde{\sigma})(\tau_j)||_{L^\Omega} \leq &\int_{\tau_j}^{t_j}||\mathbb{C}^{-1/}(\dot{\sigma}-\tilde{\sigma})||_{L^2(\Omega)}\,\mathrm{d}t\\
\leq&k_j/2||\mathbb{C}^{-1/2}\ddot{\sigma}||_{L^1(t_{j-1},t_j;L^2(\Omega))}.
\end{aligned} \tag{7.17}$$

The last term in (7.15) is then bounded

$$\begin{aligned}
&2\sum_{j=1}^{n} k_j \int_\Omega ((\sigma-\Sigma)(\tau_j)) : \varepsilon(\dot u(\tau_j) - W_j)\,\mathrm{d}x \\
\leq &2\sum_{j=1}^{N} k_j ||\mathbb{C}^{-1/2}(\sigma-\Sigma)(\tau_j)||_{L^2(\Omega)} ||\mathbb{C}^{1/2}\varepsilon(\dot u(\tau_j)-W_j)||_{L^2(\Omega)} \\
\leq &2\sum_{j=1}^{N} \Big(k_j^{1/2} ||\mathbb{C}^{-1/2}(\sigma-\tilde\sigma)(\tau_j)||_{L^2(\Omega)}\Big)\Big(k_j^{1/2}||\mathbb{C}^{1/2}\varepsilon(\dot u(\tau_j)-W_j)||_{L^2(\Omega)}\Big) \\
&+ 2\sum_{j=1}^{N} \Big(||\mathbb{C}^{-1/2}(\tilde\sigma-\Sigma)(\tau_j)||_{L^2(\Omega)}\Big)\Big(k_j||\mathbb{C}^{1/2}\varepsilon(\dot u(\tau_j)-W_j)||^2_{L^2(\Omega)}\Big) \\
\leq &2\sum_{j=1}^{N} k_j ||\mathbb{C}^{-1/2}(\sigma-\tilde\sigma)(\tau_j)||^2_{L^2(\Omega)} + 1/2\sum_{j=1}^{N} k_j ||\mathbb{C}^{1/2}\varepsilon(\dot u(\tau_j)-W_j)||^2_{L^2(\Omega)} \\
&+ 1/4\sum_{j=1}^{N} ||\mathbb{C}^{-1/2}(\tilde\sigma-\Sigma)(\tau_j)||^2_{L^2(\Omega)} + 4\sum_{j=1}^{N} k_j^2 ||\mathbb{C}^{1/2}\varepsilon(\dot u(\tau_j)-W_j)||^2_{L^2(\Omega)}. \\
\leq &1/2\sum_{j=1}^{n} k_j^3 ||\mathbb{C}^{-1/2}\ddot\sigma||^2_{L^1(t_{j-1},t_j;L^2(\Omega))} + 1/4||\mathbb{C}^{-1/2}(\tilde\sigma-\Sigma)(\tau_j)||_{L^2(\Omega)} \\
&+ (1/2+4T)\sum_{j=1}^{N} k_j ||\mathbb{C}^{1/2}\varepsilon(\dot u(\tau_j)-W_j)||^2_{L^2(\Omega)} \\
\leq &1/2||k^2\mathbb{C}^{-1/2}\ddot\sigma||^2_{L^2(0,T;L^2(\Omega))} + 1/4||\mathbb{C}^{-1/2}(\tilde\sigma-\Sigma)(\tau_j)||_{L^2(\Omega)} \\
&+ (1/2+4T)\sum_{j=1}^{N} k_j ||\mathbb{C}^{1/2}\varepsilon(\dot u(\tau_j)-W_j)||^2_{L^2(\Omega)}.
\end{aligned} \tag{7.18}$$

Substitution of (7.18) into (7.15) and the absorption of $||\mathbb{C}^{-1/2}(\tilde\sigma-\Sigma)(t_j)||_{L^2(\Omega)}$ together with the estimate

$$||\mathbb{C}^{-1/2}(\tilde\sigma-\Sigma)(\tau_j)||_{L^2(\Omega)} \leq \max_{l=0,\dots,N} ||\mathbb{C}^{-1/2}(\sigma-\Sigma)(t_l)||_{L^2(\Omega)}, \tag{7.19}$$

infer the estimate (7.11).

Similarly, an assertion (7.3) due to (7.1) and (7.2) implies

$$\begin{aligned}
\sum_{j=1}^{n}(\theta_j-1/2)||e_j-e_{j-1}||^2 \leq &||e_0||^2 + 1/2\max_{l=0,\dots,N}||e_l||^2 + 19/2||k\ddot x||^2_{L^1(0,T)} \\
&+ 2\sum_{j=1}^{n} k_j\int_\Omega ((\sigma-\Sigma)(\tau_j)) : \varepsilon(\dot u(\tau_j)-W_j)\,\mathrm{d}x.
\end{aligned} \tag{7.20}$$

Here, we can bound the term $2\sum_{j=1}^{n} k_j \int_\Omega ((\sigma-\Sigma)(\tau_j)) : \varepsilon(\dot{u}(\tau_j) - W_j)\,\mathrm{d}x$ by the inequality (7.18). Besides

$$1/2 \max_{l=0,\dots,N} ||e_l||^2 \leq 2 \max_{l=0,\dots,N} \{1/4||\mathbb{C}^{-1/2}(\sigma-\Sigma)(t_l)||^2_{L^2(\Omega)} + 1/2 \sum_{i=1}^{M} ||\mathbb{H}_i^{1/2}(p_i - P_i)(t_l)||^2_{L^2(\Omega)}\},$$
$$\leq 2\{\text{right-hand side of } (7.11)\}, \tag{7.21}$$

which infers an assertion (7.12).

The same arguments as for (7.2) yield for (7.4) the claimed higher convergence estimate in time (7.13). □

7.2 One time step convergence

Let us analyze one discrete time step only, i.e., $N = 1$. We recall the error e_i is defined as

$$e_i = (u - U, p_1 - P_1, \dots, p_M - P_M)(t_i),$$

for $i = 0, 1$. (7.15) reads for the (energy) norm of e_1

$$1/2\,||e_1||^2 \leq ||e_0||^2 + 19/2||k_1(\mathbb{C}^{-1/2}\ddot{\sigma}, \mathbb{H}_1^{1/2}\ddot{p}_1, \dots, \ddot{\mathbb{H}}_M^{1/2}\ddot{p}_M)||^2_{L^1(0,t_1)}$$
$$+2k_1 \int_\Omega (\sigma - \Sigma)(\tau_1) : \varepsilon(\dot{u}(\tau_1) - W_1)\,\mathrm{d}x. \tag{7.22}$$

With the choice $W_1 = \dot{U}(\tau_1) - \mathcal{J}(\dot{e}(\tau_1))$, where $e(\tau_1)$ represents the displacement error $e(\tau_1) := u(\tau_1) - U(\tau_1)$ and $\mathcal{J}$ is an approximation operator defined in [CB00], one obtains the estimate

$$\int_\Omega (\sigma(\tau_1) - \Sigma(\tau_1)) : \varepsilon(\dot{u}(\tau_1) - W_1)\,\mathrm{d}x \leq \int_\Omega (\sigma(\tau_1) - \Sigma(\tau_1)) : \varepsilon(\dot{e}(\tau_1) - \mathcal{J}\dot{e}(\tau_1))\,\mathrm{d}x. \tag{7.23}$$

We omit the time argument τ_1 for simplicity of notation. Since $\sigma - \Sigma$ is a symmetric matrix, we have

$$(\sigma - \Sigma) : \varepsilon(\dot{u} - W_1) = (\sigma - \Sigma) : \nabla(\dot{u} - W_1)$$

and an elementwise integration by parts shows

$$\int_\Omega (\sigma - \Sigma) : \varepsilon(\dot{e} - \mathcal{J}\dot{e})\,\mathrm{d}x = \int_\Omega (f + \mathrm{div}_\mathcal{T}\Sigma) : (\dot{e} - \mathcal{J}\dot{e})\,\mathrm{d}x - \int_{\cup\mathcal{E}} [\Sigma\cdot n] : (\dot{e} - \mathcal{J}\dot{e})\,\mathrm{d}x, \tag{7.24}$$

where $\cup\mathcal{E}$ is the skeleton of all edges in $\mathcal{T}$, $\mathrm{div}_\mathcal{T}$ is the elementwise divergence and $[\Sigma\cdot n] \in L^2(\cup\mathcal{E})$ denotes a *jump* of Σ defined on every edge $E \in \mathcal{E}$ by

$$[\Sigma\cdot n]_E = \begin{cases} (\Sigma|_{T_1} - \Sigma|_{T_2})\cdot n & \text{if } E = T_1 \cap T_2, T_1, T_2 \in \mathcal{T}, n \text{ points out of } T_1, \\ 0 & \text{if } E \in \overline{\Gamma_D}, \\ g|_E - \Sigma|_T \cdot n & \text{if } E \in \overline{\Gamma_N} \cap \partial T, n \text{ points out of } T. \end{cases} \tag{7.25}$$

Since Σ is elementwise constant matrix, $\mathrm{div}_T(\Sigma) = 0$. Introducing the local mesh-size and the edge-size denoted by $h_\mathcal{T}$ and $h_\mathcal{E}$, the Cauchy-Schwartz inequality yields

$$\int_\Omega f(\tau_1) : (\dot{e} - \mathcal{J}\dot{e})\,\mathrm{d}x \;\leq\; ||h_\mathcal{T} f||_{L^2(\Omega)} ||h_\mathcal{T}^{-1}(\dot{e} - \mathcal{J}\dot{e})||_{L^2(\Omega)}, \tag{7.26}$$

$$\int_{\cup\mathcal{E}} [\Sigma \cdot n] : (\dot{e} - \mathcal{J}\dot{e})\,\mathrm{d}x \;\leq\; ||h_\mathcal{E}^{1/2}[\Sigma \cdot n]||_{L^2(\cup\mathcal{E})} ||h_\mathcal{E}^{-1/2}(\dot{e} - \mathcal{J}\dot{e})||_{L^2(\cup\mathcal{E})}. \tag{7.27}$$

We notice that $\dot{e} = (e(t_1) - e(t_0))/k_1$ and apply Theorem 2.1 in [CB00] concerning approximation properties of functions on finite element spaces,

$$\begin{aligned} ||h_\mathcal{T}^{-1}(\dot{e} - \mathcal{J}\dot{e})||_{L^2(\Omega)} &\leq (C_4/k_1)||\nabla(e(t_1) - e(t_0))||_{L^2(\Omega)}, \\ ||h_\mathcal{E}^{-1/2}(\dot{e} - \mathcal{J}\dot{e})||_{L^2(\cup\mathcal{E})} &\leq (C_5/k_1)||\nabla(e(t_1) - e(t_0))||_{L^2(\Omega)}, \end{aligned} \tag{7.28}$$

where $(h_\mathcal{T}, h_\mathcal{E})$-independent constants $C_4, C_5 > 0$ only depend on $\Omega, \Gamma_N, \Gamma_D$ and the shape of the elements $T \in \mathcal{T}$ and patches (not on their size). Ellipticity of the bilinear form $a(\cdot,\cdot)$, formulated in Proposition 5.2, implies for $i = 0, 1$,

$$||\nabla e(t_i)||_{L^2(\Omega)} \leq C_6 ||e_i||,$$

where the constant $C_6 > 0$ depends on the number of plastic strains M, elastoplastic material parameters $\mathbb{C}, \mathbb{H}_1, \ldots, \mathbb{H}_M$ and the domain Ω. Taking $C_7 := C_6 \max\{C_4, C_5\}$, we obtain

$$2k_1 \int_\Omega (\sigma - \Sigma) : \varepsilon(\dot{e} - \mathcal{J}\dot{e})\,\mathrm{d}x \leq C_7(||e_0|| + ||e_1||)\underbrace{(||h_\mathcal{T} f||_{L^2(\Omega)} + ||h_\mathcal{E}^{1/2}[\Sigma \cdot n]||_{L^2(\cup\mathcal{E})})}_{=:\eta_R}, \tag{7.29}$$

where η_R represents a *residual* refinement indicator, established in [JH92]. The substitution of well-known inequalities for all $\alpha > 0$,

$$||e_0||\eta_R \leq \frac{1}{2C_7\alpha}||e_0|| + \frac{C_7\alpha}{2}\eta_R^2,$$

$$||e_1||\eta_R \leq \frac{1}{2C_7\alpha}||e_1|| + \frac{C_7\alpha}{2}\eta_R^2$$

into (7.29) and into (7.22) deduces

$$\frac{\alpha - 1}{2\alpha}||e_1||^2 \leq (1 + \frac{1}{2\alpha})||e_0||^2 + \alpha C_7^2\,\eta_R^2 + 19/2||k_1(\mathbb{C}^{-1/2}\ddot{\sigma}, \mathbb{H}_1^{1/2}\ddot{p}_1, \ldots, \ddot{\mathbb{H}}_M^{1/2}\ddot{p}_M)||^2_{L^1(t_0,t_1)}.$$

Taking $\alpha = 2$ and $C_8^2 := 8C_7^2$, we have proved the following proposition.

Proposition 7.2 (One time step discrete error). *Let e_0 be the discretization error in the initial discrete time t_0. That the discretization error in the first discrete time t_1 satisfies*

$$||e_1||^2 \leq 5||e_0||^2 + C_8^2\,\eta_R^2 + 38||k_1(\mathbb{C}^{-1/2}\ddot{\sigma}, \mathbb{H}_1^{1/2}\ddot{p}_1, \ldots, \ddot{\mathbb{H}}_M^{1/2}\ddot{p}_M)||^2_{L^1(t_0,t_1)}. \tag{7.30}$$

Chapter 8

Numerical Algorithms

8.1 FEM

Let $\mathcal{T}$ be a regular triangulation in triangles of Ω in $\mathbb{R}^2$ and let $\mathcal{N}$ be the set of all nodes in $\mathcal{T}, N = \text{card}(\mathcal{N})$. For $i = 1, \ldots, N$, let $\hat{\varphi}_i$ be a hat function on the i-th node [Car00c]. As it has been show in Chapter 6, the discrete problem (S_2-two equations) involves the nonlinear equality coupled with the minimization problems posed on every element T of the triangulation $\mathcal{T}$.

Problem 8.1 (FEM problem). *Given $U^0 \in \mathcal{S}^1_D(\mathcal{T}), P^0_1, P^0_2 \in \operatorname{dev} \mathcal{S}^0(\mathcal{T})^{d\times d}_{sym}$, seek $U^1 \in \mathcal{S}^1_D(\mathcal{T})$ satisfying, for all $V \in S^1_D(\mathcal{T})$,*

$$\int_\Omega \mathbb{C}(\epsilon(U^1) - P^1_1 - P^1_2) : \epsilon(V)\, dx - \int_\Omega f(t) V\, dx - \int_{\Gamma_N} gV\, dx = 0, \tag{8.1}$$

where $P = (P_1, P_2)^T = (P^1_1, P^1_2)^T - (P^0_1, P^0_2)^T$ minimizes on every element $T \in \mathcal{T}$ the functional

$$\min_Q \frac{1}{2}(\hat{\mathbb{C}} + \hat{\mathbb{H}})Q : Q - \hat{A} : Q + ||Q||_{\sigma^y}, \tag{8.2}$$

among all $Q = (Q_1, Q_2)^T, Q_1, Q_2 \in \mathbb{R}^{d\times d}_{sym}, \operatorname{tr} Q_1 = \operatorname{tr} Q_2 = 0$. Matrices $\hat{\mathbb{C}}, \hat{\mathbb{H}}, \hat{A}$ are defined as

$$\begin{aligned} \hat{\mathbb{C}} &:= \begin{pmatrix} \mathbb{C} & \mathbb{C} \\ \mathbb{C} & \mathbb{C} \end{pmatrix} \quad \textit{and} \quad \hat{\mathbb{H}} := \begin{pmatrix} \mathbb{H}_1 & 0 \\ 0 & \mathbb{H}_2 \end{pmatrix}, \\ \hat{A} &:= \begin{pmatrix} \mathbb{C}\epsilon(U) \\ \mathbb{C}\epsilon(U) \end{pmatrix} + \begin{pmatrix} \mathbb{C}\epsilon(U^0) \\ \mathbb{C}\epsilon(U^0) \end{pmatrix} - (\hat{\mathbb{C}} + \hat{\mathbb{H}}) \begin{pmatrix} P^0_1 \\ P^0_2 \end{pmatrix}. \end{aligned} \tag{8.3}$$

and the norm $||\cdot||_{\sigma^y}$, $||Q||_{\sigma^y} := \sigma^y_1 ||Q_1||_1 + \sigma^y_2 ||Q_2||$.

Let us denote the left size of (8.1) as $F(U^1, V)$ and reformulate (8.1) as a nonlinear problem in U^1.

Problem 8.2 (abstract FEM problem). *Find $U^1 \in \mathcal{S}^1_D(\mathcal{T})$ satisfying*

$$F(U^1, V) = 0 \quad \textit{for all } V \in \mathcal{S}^1_D(\mathcal{T}). \tag{8.4}$$

Note that $F(\cdot, V)$ is a nonlinear functional, that is generally *non-smooth*. Finite element basis φ_i for $i = 1, \ldots, 2N$ in $\mathcal{S}^1_D(\mathcal{T})$ is generated as

$$\varphi_i := \begin{cases} (\hat{\varphi}_{\frac{i+1}{2}}, 0) & \text{if } i \text{ odd} \\ (0, \hat{\varphi}_{\frac{i}{2}}) & \text{if } i \text{ even.} \end{cases} \tag{8.5}$$

We look for U^1 in the form of the linear combination of finite element basis

$$U^1 = \sum_{i=1}^{2N} U^1_i \varphi_i$$

and assembly coefficients of the linear combination in a vector

$$\mathbf{U^1} = (U^1_1, \ldots, U^1_{2N})^T. \tag{8.6}$$

Further, by substituting $v = \varphi_i$ for $i = 1, \ldots, 2N$ to (8.4), we obtain the vector form of the nonlinear problem

$$\mathbf{F}_i(U^1) := F(U^1, \varphi_i) = 0 \quad \text{for all} \quad i = 1, \ldots, 2N,$$

which can be reformulated as a nonlinear system of equations for $2N$ unknowns in U^1_i,

$$\mathbf{F}_i(\mathbf{U^1}) = 0 \quad \text{for all} \quad i = 1, \ldots, 2N. \tag{8.7}$$

The nonlinear system (8.7) is solved iteratively. Starting with the initial approximation vector $\mathbf{U^1_0}$ of the solution $\mathbf{U^1}$ we generate the k-th approximation $\mathbf{U^1_k}$ from the $k-1$-th approximation $\mathbf{U^1_{k-1}}$ by the *Newton-Raphson* method

$$\mathbf{U^1_k} = \mathbf{U^1_{k-1}} + \triangle\mathbf{U^1_k}, \tag{8.8}$$

where the increment $\triangle\mathbf{U^1_k}$ solves a linear system of $2N$ equations

$$\begin{pmatrix} D\mathbf{F}(\mathbf{U^1_{k-1}}) & B^T \\ B & 0 \end{pmatrix} \begin{pmatrix} \triangle\mathbf{U^1_k} \\ \lambda \end{pmatrix} = \begin{pmatrix} -\mathbf{F}(\mathbf{U^1_{k-1}}) \\ \mathbf{0} \end{pmatrix}. \tag{8.9}$$

A matrix B and the vector of *Lagrange parameters* λ are related to the incooperation of the Dirichlet boundary conditions [CK01]. A matrix $D\mathbf{F}(\mathbf{U^1_k}) \in \mathbb{R}^{2N \times 2N}$ represents a sparse *tangential stiffness matrix*

$$(D\mathbf{F}(\mathbf{U}))_{ij} = \frac{\partial(\mathbf{F}(\mathbf{U}))_i}{\partial U_j}.$$

Since we can not determine $\mathbf{F}(\mathbf{U})$ exactly, but only iteratively, the tangential matrix $D\mathbf{F}(\mathbf{U})$ is approximated by a *central difference scheme*

$$(D\mathbf{F}(\mathbf{U}))_{ij} \approx \frac{(\mathbf{F}(U_1, \ldots, U_j + \epsilon_j, \ldots, U_{2N}) - \mathbf{F}(U_1, \ldots, U_j - \epsilon_j, \ldots, U_{2N}))_i}{2\epsilon_j}, \tag{8.10}$$

with small difference parameters $\epsilon_j > 0, j = 1 \ldots N$. Typically we can choose for all $j = 1, \ldots, 2N$

$$\epsilon_j := \sqrt{\epsilon_M} \max(1, |U_j|),$$

where ϵ_M represents a computer relative accuracy of a number representation [Luk90].

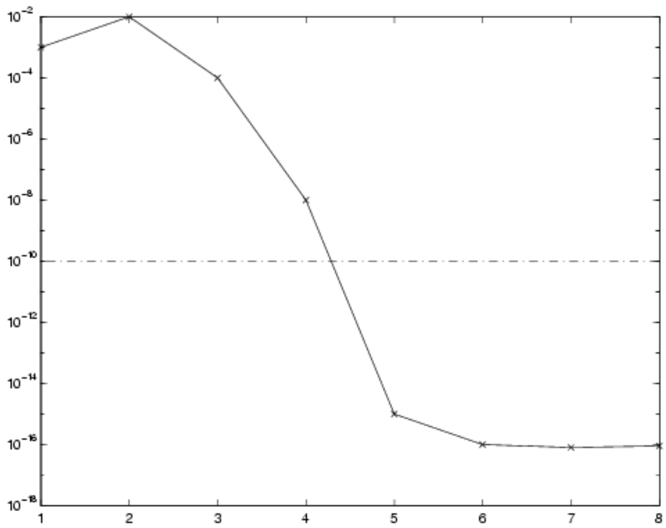

Figure 8.1: Example of the convergence behavior of Algorithm 3, displayed is residual versus number of Newton iterations. The required $tolerance = 1e-10$ is reached already in the 5-th iteration, the algorithm terminates in the 8-the step when residual grows $r_{\mathbf{8}} > r_{\mathbf{7}}$.

Remark 8.1. Another kind of methods for solving (8.4) would be for instance the *Quasi-Newton methods* that approximate $D\mathbf{F}(\mathbf{U})$ by *least change secant methods* such as the *Broyden method, DFP, BFGS* methods or some of their implementations for sparse matrices [Kos93].

The following algorithms is used for solving the nonlinear system (8.4).

Algorithm 3 (Newton-Raphson solver with three stages convergence control). Given initial $\mathbf{U_0^1} \in \mathbb{R}^{2N}$ satisfying Dirichlet boundary condition, an integer $maxstep$, a $tolerance > 0$, set $r_0 = ||\mathbf{F}(\mathbf{U_0^1})||$ the initial residual, $\mathbf{k} = 0, close = 0$.
(a) Set $\mathbf{k} = \mathbf{k} + 1$.
(b) If $\mathbf{k} = maxstep$ then set $convergence = 0$ and stop.
(c) Set $\mathbf{U_k^1} := \mathbf{U_{k-1}^1} + \triangle\mathbf{U_k^1}$, where $\triangle\mathbf{U_k^1}$ solves the linear system

$$\begin{pmatrix} D\mathbf{F}(\mathbf{U_{k-1}^1}) & B^T \\ B & 0 \end{pmatrix} \begin{pmatrix} \triangle\mathbf{U_k^1} \\ \lambda \end{pmatrix} = \begin{pmatrix} -\mathbf{F}(\mathbf{U_{k-1}^1}) \\ \mathbf{0} \end{pmatrix}.$$

(d) Set $r_{\mathbf{k}} = ||\mathbf{F}(\mathbf{U_k^1}) - B^T\lambda||, rel = \frac{||\mathbf{U_k^1} - \mathbf{U_{k-1}^1}||}{||\mathbf{U_k^1}|| + ||\mathbf{U_{k-1}^1}||}$ (or $rel = 0$, if $||\mathbf{U_{k-1}^1}|| + ||\mathbf{U_k^1}|| = 0$).
(e) If $close = 1$ and $r_{\mathbf{k}} \geq r_{\mathbf{k-1}}$ then set $convergence = 1$, output $\mathbf{U_k^1}$ and stop.
(f) If $rel < tolerance$ then set $close = 1$.
(g) Goto (a).

Algorithm 3 works in the following way. Due to the upgrade in the step (c), we generate approximations $\mathbf{U_k^1}, \mathbf{k} = 1, 2, \ldots$ of the exact solution $\mathbf{U^1}$ iteratively. The iterative process becomes stable, if

$$\frac{||\mathbf{U_k^1} - \mathbf{U_{k-1}^1}||}{||\mathbf{U_k^1}|| + ||\mathbf{U_{k-1}^1}||} < tolerance \quad \text{or} \quad ||\mathbf{U_k^1}|| + ||\mathbf{U_{k-1}^1}|| = 0.$$

We carry on iterating with the residual decreasing theoretically down to 0. Due to the rounding errors, the residual $r_{\mathbf{k}}$ does not attain the zero value, however stops at certain value related to the machine precision. For this reason we terminate the iterative process if the next residual is smaller than the previous residual $r_{\mathbf{k}} \geq r_{\mathbf{k-1}}$. The condition (b) controls the maximal number of iterations. If $\mathbf{k} = maxstep$ the iteration process fails to give a good approximation of the solution within given number of iterations $maxstep$.

Remark 8.2 (Choice of $maxstep$ and damping). For the purely elastic problem is the system of equations (8.7) linear and the one Newton step (8.9) is sufficient for reaching the zero residual (apart from rounding effects). For plasticity problems (with present hardening), one needs to apply more Newton steps (8.9) for reaching the residual under the given parameter $tolerance$. Roughly speaking, the smaller the hardening is, the more Newton steps are required and consequently the higher $maxstep$ has to be given. In general, the Newton-Raphson method does not convergence globally [Neč83]. In order to improve the convergence one introduces the *damped* Newton-Raphson method with the upgrade

$$\mathbf{U^1_{k+1}} = \mathbf{U^1_k} + \rho_{k+1} \triangle \mathbf{U^1_{k+1}}, \tag{8.11}$$

where ρ_{k+1} is a (small) damping parameter > 0. The question of the proper choice of ρ_{k+1} is not studied here, and only *non-damped Newton-Raphson method* with $\rho_{k+1} = 1$ for $k = 1, 2, \dots$ is applied in the numerical solver.

Algorithm 4 (Newton-Raphson solver with prescribed number of steps). Given initial $\mathbf{U^1_0} \in \mathbb{R}^{2N}$ satisfying Dirichlet boundary condition, an integer $steps$, set $r_0 = ||\mathbf{F}(\mathbf{U^1_0})||$ the initial residual, $\mathbf{k} = 0$.
(a) Set $\mathbf{k} = \mathbf{k} + 1$.
(b) Set $\mathbf{U^1_k} := \mathbf{U^1_{k-1}} + \triangle \mathbf{U^1_k}$, where $\triangle \mathbf{U^1_k}$ solves the linear system

$$\begin{pmatrix} D\mathbf{F}(\mathbf{U^1_{k-1}}) & B^T \\ B & 0 \end{pmatrix} \begin{pmatrix} \triangle \mathbf{U^1_k} \\ \lambda \end{pmatrix} = \begin{pmatrix} -\mathbf{F}(\mathbf{U^1_{k-1}}) \\ \mathbf{0} \end{pmatrix}.$$

(c) Set $r_{\mathbf{k}} = ||\mathbf{F}(\mathbf{U^1_k}) - B^T \lambda||$.
(d) If k=steps then end else goto (a).

Remark 8.3. There is no control over the residual r_k calculated in step (c) and therefore no guaranteed convergence. However, in our numerical experiments (Chapter 9), it turns out sufficient to apply Algorithm 4 even with a small number of $steps$, e.g., $steps = 1$.

8.2 Adaptive Mesh-Refining

Let $X = (U, P_1, \dots, P_M)$ be the approximation of the (unknown) solution $x = (u, p_1, \dots, p_M)$ calculated on the triangulation $\mathcal{T}$. With the help of (exact) stress σ and the discrete stress Σ,

$$\sigma = \mathbb{C}(\varepsilon(u) - p_1 - \dots - p_M) \quad \text{and} \quad \Sigma = \mathbb{C}(\varepsilon(U) - P_1 - \dots - P_M),$$

the energy norm of the error $e = x - X$ can be expressed as

$$e^2 = a(x - X, x - X) = ||\mathbb{C}^{-1/2}(\sigma - \Sigma)||^2_{L^2(\Omega)} + \sum_{i=1}^{M} ||\mathbb{H}_i(p_i - P_i) : (p_i - P_i)||^2_{L^2(\Omega)}. \quad (8.12)$$

Our numerical experiments focus on the *ZZ-error estimator* [CF00]. Since Σ is a piecewise constant, we compute a continuous piecewise affine function $\Sigma^* \in \mathcal{S}^1(\mathcal{T})^{d\times d}$ such that

$$||\Sigma - \Sigma^*||_{L^2(\Omega)} = \min_{\Sigma' \in \mathcal{S}^1(\mathcal{T})^{d\times d}} ||\Sigma - \Sigma'||_{L^2(\Omega)}. \quad (8.13)$$

It is naturally required that the proper averaging function Σ^* of $\mathcal{S}^1(\mathcal{T})^{d\times d}$ has to approximate the Neumann boundary conditions. To make this possible, it is required that the averaging function $\Sigma^* \in \mathcal{S}^1(\mathcal{T})^{d\times d}$ may be non-symmetric and that g satisfies some compatibility conditions. Let $\mathcal{E}$ denote the set of edges, $\mathcal{N}$ the set of nodes of the triangulation $\mathcal{T}$ and $\mathcal{E}_N := \{E \in \mathcal{E} : E \in \overline{\Gamma_N}\}$ the set of edges at the Neumann boundary. For each $E \in \mathcal{E}_N$, let n_E denote the (constant) outer unit normal along the flat surface piece E. To enable a nodal interpolation

$$\Sigma^*(z) \cdot n_E = g(z) \quad \text{for all } z \in \mathcal{N} \text{ with } E \in \mathcal{E}_N \quad (8.14)$$

we require some continuity on g, cf. [CF00] for details. We can define

$$\mathcal{Q}(\mathcal{T}, g) := \{\Sigma^* \in \mathcal{S}^1(\mathcal{T})^{d\times d} : \Sigma^*_h \text{ satisfies } (8.14)\}$$

and can calculate the global averaging function Σ^* from

$$||\Sigma - \Sigma^*||_{L^2(\Omega)} = \min_{\Sigma' \in \mathcal{Q}(\mathcal{T},g)} ||\Sigma - \Sigma'||_{L^2(\Omega)}. \quad (8.15)$$

With the assumption of 'a small plastic error', $\sum_{i=1}^{M} ||p_i - P_i||_{L^2(\Omega)} \approx 0$ can one construct the error estimator η^2 of e^2 as

$$\eta^2 := ||\mathbb{C}^{-1/2}(\Sigma - \Sigma^*)||^2_{L^2(\Omega)}.$$

Since the calculation of Σ^* from (8.15) is expensive we construct instead the upper bound

$$||\Sigma - \mathcal{A}\Sigma||_{L^2(\Omega)} \geq \min_{\Sigma' \in \mathcal{Q}(\mathcal{T},g)} ||\Sigma - \Sigma'||_{L^2(\Omega)}, \quad (8.16)$$

with an *averaging* operator $\mathcal{A}$ and $\mathcal{A}\Sigma$ satisfying (8.14), see [CF00] for more information. Finally, we construct the *ZZ-error estimator*

$$\eta_Z := ||\mathbb{C}^{-1/2}(\Sigma - \mathcal{A}\Sigma)||_{L^2(\Omega)}$$

and the elementwise *ZZ-refinement indicator* $\eta_{T,Z}$,

$$\eta_{T,Z} := ||\mathbb{C}^{-1/2}(\Sigma - \mathcal{A}\Sigma)||_{L^2(T)}.$$

Remark 8.4 (residual error estimator). Another kind of the error indicator is *residual* error indicator $\eta_{T,R}$ defined by

$$\eta_{T,R}^2 = h_T^2 \int_T ||f||^2 \, \mathrm{d}x + \int_{\partial T} h_E [\Sigma \cdot n]^2 \, \mathrm{d}x,$$

with the residual error estimator η_R already introduced in Chapter 7.

Theorem 8.1 (Equivalence of η_Z and η_R). *Let $f = 0$ in $\mathcal{T}$. Then there exist λ and μ and the smallest angle (in the triangulation)-depending constants $C' \geq C \geq 0$ such that*

$$C\eta_R \leq \eta_Z \leq C'\eta_R. \tag{8.17}$$

Proof. The multiplicativity of the (Frobenius) matrix norm $||\cdot||$ yields

$$\frac{1}{||\mathbb{C}^{+1/2}||} ||(\Sigma - \mathcal{A}\Sigma)||_{L^2(T)} \leq ||\mathbb{C}^{-1/2}(\Sigma - \mathcal{A}\Sigma)||_{L^2(T)} \leq ||\mathbb{C}^{-1/2}|| \, ||(\Sigma - \mathcal{A}\Sigma)||_{L^2(T)}.$$

Moreover, Proposition 1.21. in [Ver96] states the existence of constants $C_1 \geq C_2 \geq 0$, that depend on the smallest angle in the triangulation $\mathcal{T}$, such that

$$C_1\eta_R \leq ||(\Sigma - \mathcal{A}\Sigma)||_{L^2(T)} \leq C_2\eta_R.$$

Combining both estimates and defining $C := \frac{C_1}{||\mathbb{C}^{+1/2}||}$ and $C' := ||\mathbb{C}^{-1/2}||C_2$, the proof is finished. $\square$

8.3 Nested Iteration Technique

The Newton-Raphson solver with three stages convergence control (Algorithm 3) performs well on coarse meshes. Then the generation of the small system of linear equations (8.9) and its solution is not very time consuming. For finer triangulations, we obtain a large system of linear equations and every iteration step (c) in Algorithm 3 requires additional number of floating point operations. In order to save the computational costs, one can implement a *nested iteration technique*, a technique of solving a nonlinear system of more meshes (triangulations). The idea of this approach is the following: Assume we have a set of $F+1$ nested triangulations $\{\mathcal{T}_0, \mathcal{T}_1, \ldots, \mathcal{T}_F\}$ satisfying

$$\mathcal{T}_0 \subseteq \mathcal{T}_1 \subseteq \cdots \subseteq \mathcal{T}_F.$$

We solve a nonlinear system (8.9) using a (small) fixed number of iterations k on a very coarse initial mesh $\mathcal{T}_0$. We prolongate the obtained approximation of the solution onto a finer mesh $\mathcal{T}_1$ and use it as an initial approximation for an iterative solver on $\mathcal{T}_1$ and perform again k iterations. This can be repeated on further meshes $\mathcal{T}_2, \ldots$ until we end up at solving k iterations on the finest triangulation $\mathcal{T}_F$.

Nested triangulation $\mathcal{T}_1, \ldots, T_F$ can be generated by using *adaptive mesh-refinement* techniques. To the approximation $\mathbf{U_k^1}$ of the solution $\mathbf{U^1}$ on the mesh $\mathcal{T}_i$ we can calculate for every triangle $T \in \mathcal{T}_i$ an *error indicator* η_T. For given $0 \leq \theta \leq 1$, we mark the element T for *red-*refinement (it means the element T of lengths l_1, l_2, l_3 will be split into four elements of lengths $l_1/2, l_2/2, l_3/2$) if

$$\eta_T \geq \theta \max_{T' \in \mathcal{T}_i} \eta_{T'}.$$

In order to avoid hanging nodes a *red-green-blue* refinement is performed [Car00c]. In this way is the next mesh $\mathcal{T}_{i+1}$ from the mesh $\mathcal{T}_i$ generated. As the initial approximation $\mathbf{U_0^1}$ on the new triangulation $\mathcal{T}_{i+1}$, we take the approximation $\mathbf{U_k^1}$ defined on the triangulation $\mathcal{T}_i$ prolongated to the triangulation $\mathcal{T}_{i+1}$. More details about the nested iteration technique can be found in [Hac85].

Algorithm 5 (Nested iteration technique with adaptivity).
(a) Start with coarse mesh $\mathcal{T}_0$ and a 'good' initial approximation $\mathbf{U_0^1}$ defined on $\mathcal{T}_0$, set $i := 0$.
(b) Compute the approximation $\mathbf{U_k^1}$ applying $\mathbf{k}$ Newton iterations with respect to $\mathcal{T}_i$.
(c) Compute η_T for all $T \in \mathcal{T}_i$.
(d) Compute error bound $\left(\sum_{T\in\mathcal{T}_i} \eta_T^2\right)^{1/2}$ and terminate or goto (e).
(e) Mark element T red if $\eta_T \geq \theta \max\limits_{T' \in \mathcal{T}_i} \eta_{T'}$.
(f) Perform red-green-blue refinement to avoid hanging nodes, update mesh to $\mathcal{T}_{i+1}$.
(g) Generate $\mathbf{U_0^1}$ as the prolongation of $\mathbf{U_k^1}$ to $\mathcal{T}_{i+1}$, set $i := i + 1$ and goto (b).

Remark 8.5. The choice $\theta = 0$ leads to the refinement of every element $T \in T$, to the *uniform mesh-refinement*. The closer θ is to 1 the less number of elements will be refined (possibly only one element for $\theta = 1$). Typical choice of θ is then $\theta = 1/2$.

8.4 Time-stepping

Let $\{t_0, \ldots, t_N\}$ be a (ordered) set of discrete times, with a time step $k_i = t_i - k_{i-1}$ for $i = 1, \ldots, N$. Let $T \in \mathcal{T}$ be a (prescribed) triangulation of Ω. Our objective is to solve the discrete problem on triangulation T for all (prescribed) discrete times $t_i, i = 1, \ldots, N$ with the least possible computer complexity. Suppose for instance, Algorithm 3 is applied at every discrete time t_i with S_i iteration steps needed for reaching the required convergence. It seems logical to assume that the total number of iteration steps $\sum_{i=1}^N S_i$ reflects the complexity of the calculation. From Proposition 7.2 we conclude that the smaller the time step k_i, the smaller is the discrete error and, consequently, the smaller is the number of iteration steps S_i in i-th discrete time. This suggests an idea of solving the problem on a (ordered) larger set of discrete times

$$\{t'_0, \ldots, t'_{N'}\} \supseteq \{t_0, \ldots, t_N\},$$

with $t_0 = t'_0, t_N = t'_{N'}, N' \geq N$. The proposed algorithm calculates the discrete problem on the original set $\{t_0, \ldots, t_N\}$ than is being adaptively 'enlarged' in dependence of number of iterations S_i.

Algorithm 6 (Adaptive time-stepping). Given $\{t_0, \ldots, t_N\}$ and two integers
$0 \leq S_{min} \leq S_{max} \leq \infty$. Set $i := 0, time\_step = t_1 - t_0$.
(a) Solve the discrete problem with Algorithm 3. Output number of needed iterations S_i.

(b) If $S_i < S_{min}$ set $time\_step := time\_step/2$ and goto (d).
(c) If $S_i > S_{max}$ set $time\_step := 2\ time\_step$.
(d) If $(i < N)$ and $(t_i + time\_step < t_{i+1})$ then insert $t_i + time\_step$ between t_i and t_{i+1}, set $N := N + 1$
(e) If $i = N$ end, otherwise set $i := i + 1$ and goto (a).

Remarks 8.1. (i) Integers S_{min}, S_{max} determinate size of 'the next' time step. If the number of needed iterations S_i is sufficiently small respectively large (condition (b) respectively condition (c) of Algorithm 6 the time step is divided by 2 respectively doubled.)

(ii) The choice $S_{min} = 0, S_{max} = \infty$ leads to the 'uniform' time discretization. If the initial set of discrete times is $\{t_0, t_0 + \Delta t, t_0 + N\Delta t\}$. Algorithm 6 performs calculations for the discrete times $\{t_0, t_0 + \Delta t, t_0 + 2\Delta t, \ldots, t_0 + N\Delta t\}$.

Chapter 9

Numerical Experiments

Presented numerical experiments report on simulations in MATLAB 5.3 run on an Ultra SPARC - II processor with 14 GB RAM and 250 MHz CPU speed. The implemented MATLAB solver runs calculations for either elastic, single-yield or two-yield material models, involves the nested iteration technique combined with adaptive or uniform mesh-refinement and adaptive time-stepping. The numerical experiments demonstrate:

1. Two-yield plastic effects that arise in addition to single-yield plastic effects, such as different hysteresis curves and the evolution of elastoplastic zones.

2. Properties of the nested iteration technique such as experimental convergence rates for adaptive (ZZ-refinement indicator) and uniform mesh-refinements, an influence of the number of used Newton steps on the convergence.

3. The different computational complexity for elastic, single-yield and two-yield material models.

Remark 9.1 (Meaning of colors in figures). In pictures, at those we would like to stress out different elastoplastic zones of the deformed material, the following colors are used:

- black - denotes the material zones in purely elastic phase (plastic strains $P_1 = 0, P_2 = 0$),

- dark gray (brown in the color scale) - denotes the material zones in the first plastic phase (plastic strains $P_1 \neq 0, P_2 = 0$),

- light gray (light yellow in the color scale) - denotes the material zones in the second plastic phase (plastic strains $P_1 \neq 0, P_2 \neq 0$).

Remark 9.2 (Approximation of error). Since there is no example in two-yield plasticity with known exact solution available, the error of the discrete approximation can not be computed exactly. However, we calculate a reference solution $(U^{ref}, P_1^{ref}, P_2^{ref})$ on a sufficiently fine reference triangulation $\mathcal{T}_{ref}$. Let $\mathcal{T}_0 \subset \mathcal{T}_1 \subset \cdots \subset T_F$ denote the nested triangulations in the nested iteration technique. The reference triangulation $\mathcal{T}_{ref}$ is chosen for all numerical experiments as the two times uniformly refined triangulation $\mathcal{T}_F$ (see Figure 9.1 for comparison

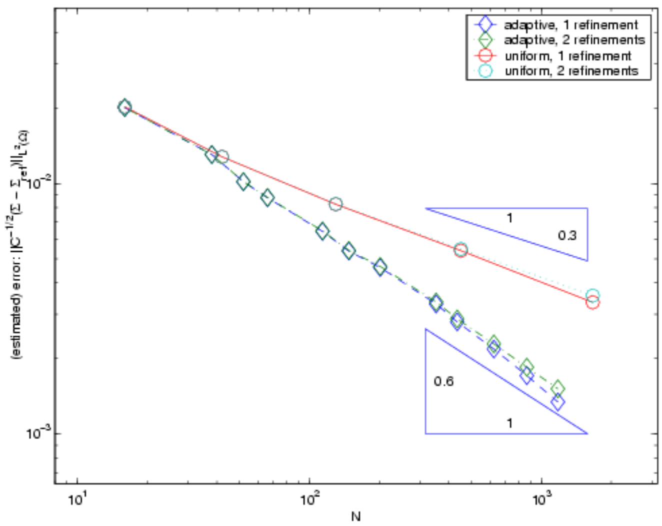

Figure 9.1: Estimated error is displayed versus the degrees of freedom N for the uniform and adaptive mesh-refining, then the reference solution is calculated on once (curves with '1 refinement' legend) or two times (curves with '2 refinements' legend) uniformly refined triangulation T_F. The difference of the convergence rates is more obvious for the adaptive refinements (the expected convergence rate is 0.5): 'two refinements' give more realistic convergence rate than 'one refinement'.

with 'one uniform refinement' strategy). If Σ and Σ^{ref} denote the stresses of the discrete and the reference solutions, i.e., Σ^{ref} is the solution on $\mathcal{T}_{ref}$, then

$$||\mathbb{C}^{-1/2}(\Sigma - \Sigma^{ref})||_{L^2(\mathcal{T}_{ref})},$$

estimates the error in the energy norm.

9.1 Beam with 1D effects

The problem of a beam to show one dimensional effects is displayed in Figure 9.2. We consider the unit square shape $\Omega = (0,1)^2$ in a $x - y$ coordinate system. The edge 1 is a Dirichlet edge with fixed y coordinate. The intersection point $(0,0)$ of edges 1 and 2 remains fixed in both coordinates x and y, i.e.,

$$\begin{aligned} u(0,y) &= (0,u_2) \quad \text{for } 0 < y < 1, \\ u(0,0) &= (0,0). \end{aligned} \tag{9.1}$$

The edges 2 and 3 represent the Neumann edges with zero Neumann condition (tension free surfaces)

$$g(x,0) = g(x,1) = (0,0) \quad \text{for } 0 < x < 1 \tag{9.2}$$

and the edge 4 is also a Neumann edge with a nonzero Neumann condition representing the constant surface force that deforms the beam in x coordinate

$$g(1,y) = (g_x, 0) \quad \text{for } 0 < y < 1. \tag{9.3}$$

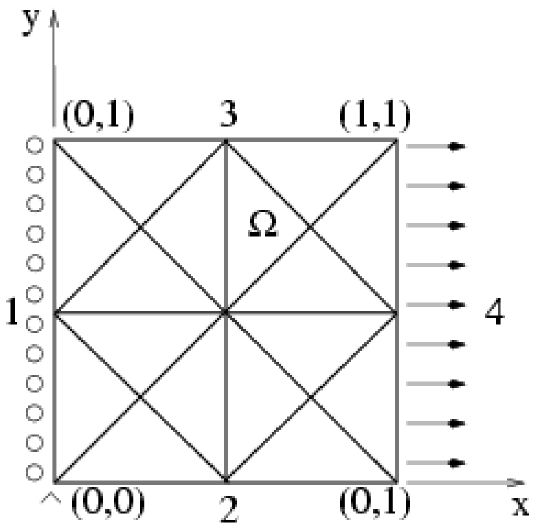

Figure 9.2: Geometry and coarse mesh $\mathcal{T}_0$ of a beam problem with 1D effects.

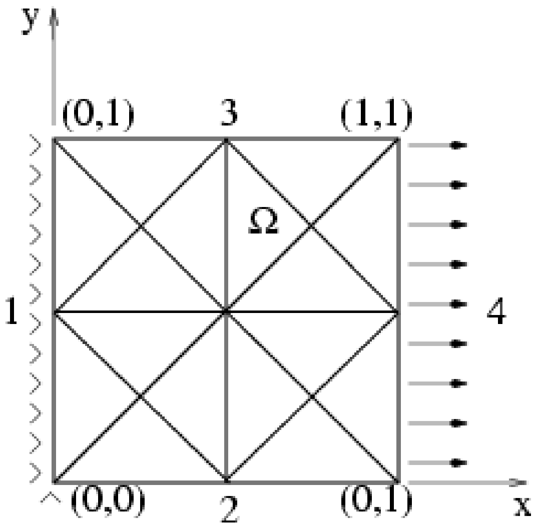

Figure 9.3: Geometry and coarse mesh $\mathcal{T}_0$ of a beam with 2D effects.

The deformation of the beam is expected in the form

$$u(x,y) = (u_1,u_2)(x,y) = (x \cdot u_1(1,0), y \cdot u_2(0,1)) \quad \text{for } (x,y) \in \Omega, \tag{9.4}$$

which implies for the strain tensor

$$\varepsilon(u) = \begin{pmatrix} u_1(1,0) & 0 \\ 0 & u_2(0,1) \end{pmatrix} \quad \text{in } \Omega. \tag{9.5}$$

Besides that, the Neumann boundary conditions admit the stress tensor

$$\sigma = \begin{pmatrix} g_x & 0 \\ 0 & 0 \end{pmatrix} \quad \text{in } \Omega. \tag{9.6}$$

There holds the Hook's law in the purely elasticity phase (no plasticity), $\sigma = 2\mu\varepsilon + \lambda(\operatorname{tr}\varepsilon)\mathbb{I}$, i.e.,

$$\begin{pmatrix} g_x \\ 0 \\ 0 \end{pmatrix} = \begin{pmatrix} 2\mu+\lambda & \lambda & 0 \\ \lambda & 2\mu+\lambda & 0 \\ 0 & 0 & 2\mu \end{pmatrix} \begin{pmatrix} u_1(1,0) \\ u_2(0,1) \\ 0 \end{pmatrix}. \tag{9.7}$$

Simple inverse rule

$$\begin{pmatrix} 2\mu+\lambda & \lambda & 0 \\ \lambda & 2\mu+\lambda & 0 \\ 0 & 0 & 2\mu \end{pmatrix}^{-1} = \begin{pmatrix} \frac{2\mu+\lambda}{4\mu(\mu+\lambda)} & -\frac{\lambda}{4\mu(\mu+\lambda)} & 0 \\ -\frac{\lambda}{4\mu(\mu+\lambda)} & \frac{2\mu+\lambda}{4\mu(\mu+\lambda)} & 0 \\ 0 & 0 & \frac{1}{2\mu} \end{pmatrix}$$

implies that the deformation of the beam can be expressed as

$$u(x,y)(t) = (x \cdot \frac{2\mu+\lambda}{4\mu(\mu+\lambda)}, -y \cdot \frac{\lambda}{4\mu(\mu+\lambda)}) \cdot g_x(t). \tag{9.8}$$

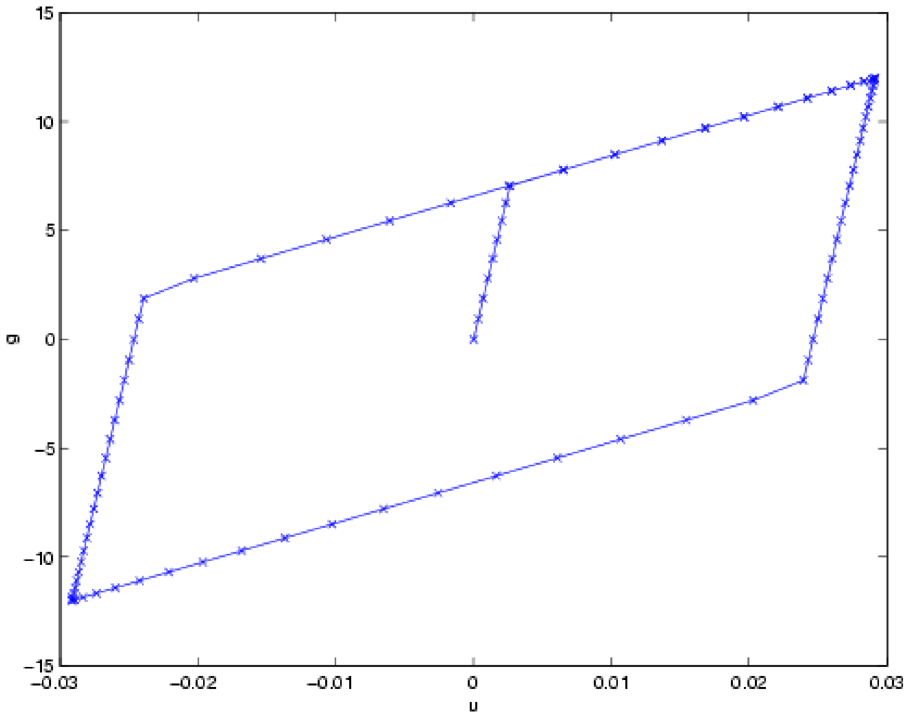

Figure 9.4: Displayed loading-deformation relation in terms of the uniform surface loading $g_x(t)$ versus the x-displacement of the point $(0, 1)$ for problem of the single-yield beam with 1D effects.

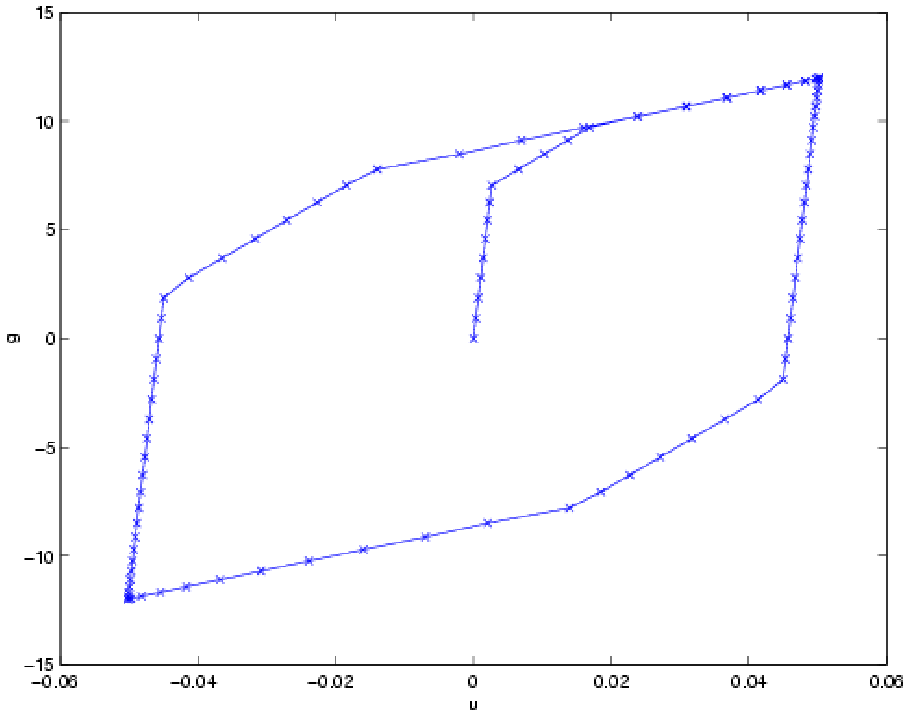

Figure 9.5: Displayed loading-deformation relation in terms of the uniform surface loading $g_x(t)$ versus the x-displacement of the point $(0, 1)$ for problem of the two-yield beam with 1D effects.

material model	CPU time (in sec)	total number of Newton steps	CPU time spent on Algorithm 2 (in %)
single-yield	347	492	13.8
two-yield	1603	588	77.4

Table 9.1: Performance of MATLAB solver for the problem of beam with 1D effects. The calculation was run for the discrete times $t = \{0, 0.5, 1, \ldots, 50\}$, and uniform mesh $\mathcal{T}_0$ with 16 Elements.

material model	CPU time (in sec)	total number of Newton steps	CPU time spent on Algorithm 2 (in %)
single-yield	430	589	14.8
two-yield	1647	677	74.2

Table 9.2: Performance of MATLAB solver for the first numerical experiment for the problem of beam with 2D effects. The calculation was run for the discrete times $t = \{0, 0.5, 1, \ldots, 50\}$, and uniform mesh $\mathcal{T}_0$ with 16 Elements.

Remark 9.3 (Limitation of our model). For the critical value $g_x = \frac{4\mu(\mu+\lambda)}{\lambda}$ is obviously $u_2(0,1) = -1$ and the shifted edge 3 originally located above the edge 2 coincides with the edge 2. It would mean that the original volume 1 of the elastic beam becomes 0, which is not mechanically allowed. The reason for it is that we have considered the linear elastic tensor ε, which only gives realistic description of an elastic medium for small deformations.

The elasticity phase lasts till $||\mathrm{dev}\,\sigma|| \leq \sigma_1^y$ or equivalently till it holds

$$\sqrt{2} g_x \leq \sigma_1^y,$$

the plasticity phase occurs for $g_x > \frac{\sigma_1^y}{\sqrt{2}}$.

The numerical experiment for the hysteresis behavior demonstration was the calculation on the coarse mesh $\mathcal{T}_0$ with 16 elements, discrete times {0, 0.5, 1,…, 50}, in case of the uniform cyclic surface loading

$$g_x = 12\sin(t\pi/20).$$

MATLAB solver was specified by these properties: no time-stepping, no nested iteration technique, Newton-Raphson solver with three stages convergence control (Algorithm 3). In order to compare two different material models, we firstly considered the two-yield material specified by parameters

$$\mu = 1000, \lambda = 1000, \sigma_1^y = 5, h_1 = 100, \sigma_2^y = 7, h_2 = 50$$

and secondly the single-yield material specified by parameters

$$\mu = 1000, \lambda = 1000, \sigma^y = 5, h = 100.$$

Figures 9.4 and 9.5 show *hysteresis curves* in terms of the dependence of $g_x(t)$ on the x-displacement $u_x(t)$ of the point $(x = 1, y = 0)$ for the single and two-yield material models.

According to theoretical prediction, the calculated hysteresis curve for the two-yield material consists of the two plastic parts, whereas there is only one plastic part for the single-yield material.

9.2 Beam with 2D effects

In order to take two dimensional effect into account, we study another beam problem. Its geometry is identical to the problem of beam with 1D effects, and the only difference being modified is the Dirichlet boundary condition, see Figure 9.3. We prescribe the Dirichlet boundary Γ_D in both directions (i.e, the beam is fixed in both directions at Γ_D), i.e.,

$$u(0,y) = (0,0) \quad \text{for } 0 < y < 1. \tag{9.9}$$

It is expected that there is no known analytical solution of this problem.

The first numerical experiment demonstrates two-dimensional hysteresis effects. Material and time parameters, the shape of the mesh and the solver properties are identical to the numerical experiment for the problem of the beam with 1D effects. Figures 9.6 and 9.7 show the *hysteresis curves* for the single and the two-yield material. A comparison of Figures 9.6 and 9.7 with Figures 9.4 and 9.5 indicates that two-dimensional deformation effects smooth out the elasto-plastic transition. Besides of that, the beam with 2D effects is less deformed than the beam with 1D effects.

The second numerical experiment describes an elasto-plastic transition during the deformation process. The calculation was performed at discrete times $\{0, 0.5, 1, ..., 10\}$, applying the uniform surface loading

$$g_x = t$$

and the same materials as in the first experiment. MATLAB solver was specified by these properties: no time-stepping, nested iteration technique (Algorithm 5) with uniformly refined meshes $\mathcal{T}_0 \subset \mathcal{T}_1 \subset \mathcal{T}_2 \subset \mathcal{T}_3 \subset \mathcal{T}_4 \subset \mathcal{T}_5$ (with $16, 64, 256$, 1024, 4096 and 16384 elements), Newton-Raphson solver with one step (Algorithm 4). Figures 9.8 and 9.9 display the evolution of elastoplastic zones at chosen discrete times in the deformed configuration. As the deformation process starts (at discrete times $t = \{0, 0.5, \ldots, 4.5\}$), material behaves purely elastically. At discrete time $t = 5.0$ there appear the first plastic zones in corners (where the material is fixed) and also in the right part of the domain Ω (where external forces g act). For the two-yield model there appear the second plastic zones after the discrete time $t = 5.5$, and they develop in the same way as the first plastic zones at the time $t = 5$. For the final discrete time $t = 10$, both material models are in entirely plastic phases.

The third numerical experiment indicates properties of the nested iteration technique. We consider one discrete time-step problem with $t_0 = 0$ and $t_1 = 8.5$, the material with same properties as in the second numerical experiment. MATLAB solver was specified by these properties: no time-stepping, nested iteration technique (Algorithm 5) with uniformly ($\mathcal{T}_0 \subset$

material model	CPU time (in hours)	total number of Newton steps	CPU time spent on Algorithm 2 (in %)
single-yield	15.59	126	3.5
two-yield	29.57	126	49.6

Table 9.3: Performance of MATLAB solver in the second numerical experiment for the problem of beam with 2D effects. The calculation was run for the discrete times $t = \{0, 0.5, 1, \ldots, 10\}$, and uniform mesh $\mathcal{T}_5$ with 16384 elements.

$\mathcal{T}_1 \subset \mathcal{T}_2 \subset \mathcal{T}_3 \subset \mathcal{T}_4 \subset \mathcal{T}_5$ with $16, 64, 256, 1024, 4096$ and 16384 elements) or adaptively refined meshed, Newton-Raphson solver with 1, 2, or 3 steps (Algorithm 4). Figures 9.10 and 9.11 display uniform and adaptive mesh-refinements. Figures 9.12 display the (estimated) error and the ZZ-error estimator versus degrees of freedom in each nested iteration for $1, 2$ or 3 Newton steps. The experimental convergence rate is 0.2 in case of the uniform mesh-refinement, while the adaptive mesh-refinement strategy improves the experimental convergence rate to 0.5. Note that the convergence rate 0.5 is optimal and it indicates the linear convergence (then error $e \sim O(N^{-1/2})$ for two dimensional problems). There is one practically important aspect of the nested iteration technique evident in this numerical experiment. The application of more $(2, 3, \ldots)$ Newton steps within every nested iteration does not improve the experimental convergence rate in comparison to one Newton step. Since every extra Newton step requires more computational effort, it is therefore recommendable to apply just one Newton step for every nested iteration.

9.3 Rotationally symmetric ring

The model of a rotationally symmetric ring is shown in Figure 9.13 which represents a two dimensional section of a tube of inner radius of $r = 1$ and an outer radius of $r = 2$. We assume no volume forces $f = 0$ but radially applied surface forces defined with the help of the vector $e_r = (\cos\phi, \sin\phi)$ in polar coordinates system $r - \phi$ via

$$g(r, \phi, t) = \begin{cases} te_r & \text{for } r = 1, \\ -t/4e_r & \text{for } r = 2. \end{cases} \tag{9.10}$$

Due to the radial symmetry of the geometry and the applied surface forces, one expects a rotationally symmetric solution $u(r, \phi, t) = u(r, t), p_1(r, \phi, t) = p_1(r, t), p_2(r, \phi, t) = p_2(r, t)$ for all r, ϕ, t. Indeed, an analytical calculation [Alb01] admits in the single-yield case (i.e., $p = p_1, p_2 = 0$) the solution

$$\begin{aligned} u(r, \phi, t) &= u_r(r, t) \cdot e_r, \\ p(r, \phi, t) &= P_r(r, t) \cdot (e_r \otimes e_r - e_\phi \otimes e_\phi), \end{aligned} \tag{9.11}$$

$e_\phi = (-\sin\phi, \cos\phi)$ and the exact formulae for $u_r(r, t)$ and $P_r(r, t)$ given in [Alb01]. Possible generalization to the two-yield case is however not known to the author. For reason of the symmetrical solution property, we discretize one quarter of the ring only; see Figure 9.14, which

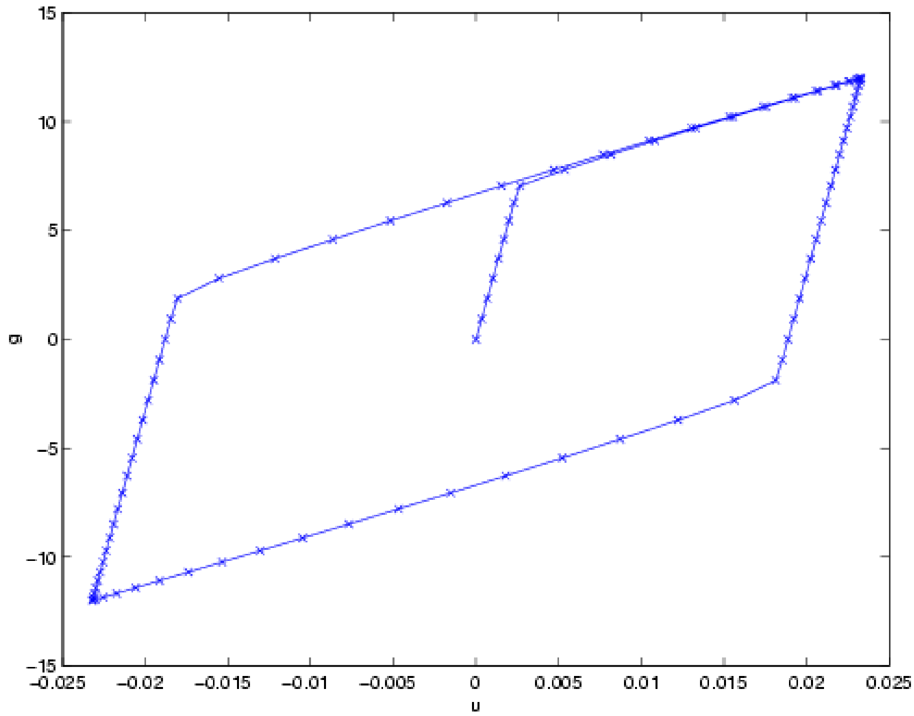

Figure 9.6: Displayed loading-deformation relation in terms of the uniform surface loading $g_x(t)$ versus the x-displacement of the point $(0, 1)$ in the first numerical experiment for the problem of the single-yield beam with 2D effects.

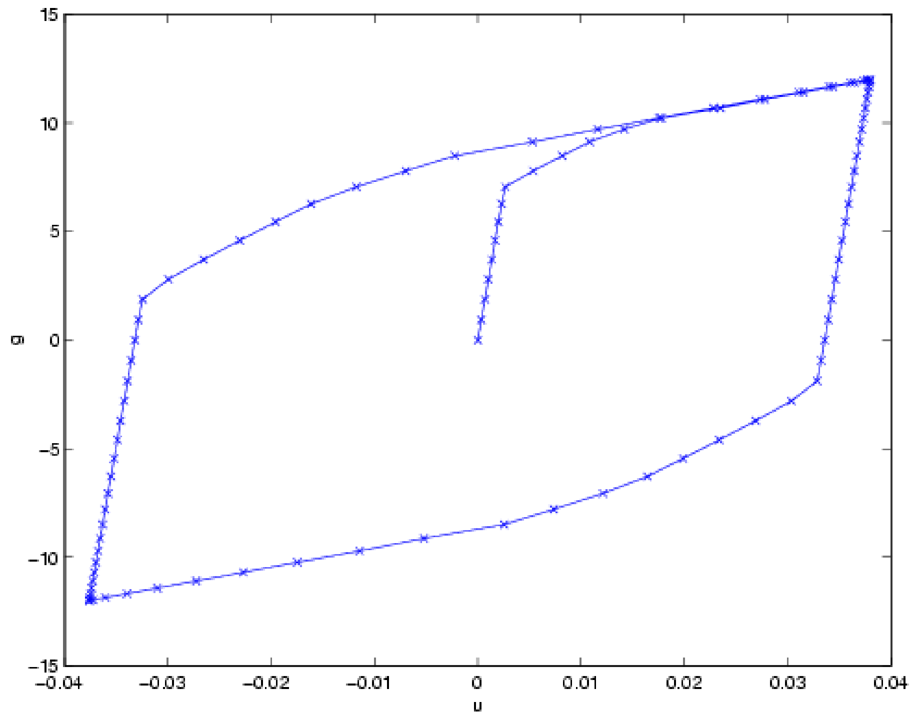

Figure 9.7: Displayed loading-deformation relation in terms of the uniform surface loading $g_x(t)$ versus the x-displacement of the point $(0, 1)$ in the first numerical experiment for the problem of the two-yield beam with 2D effects.

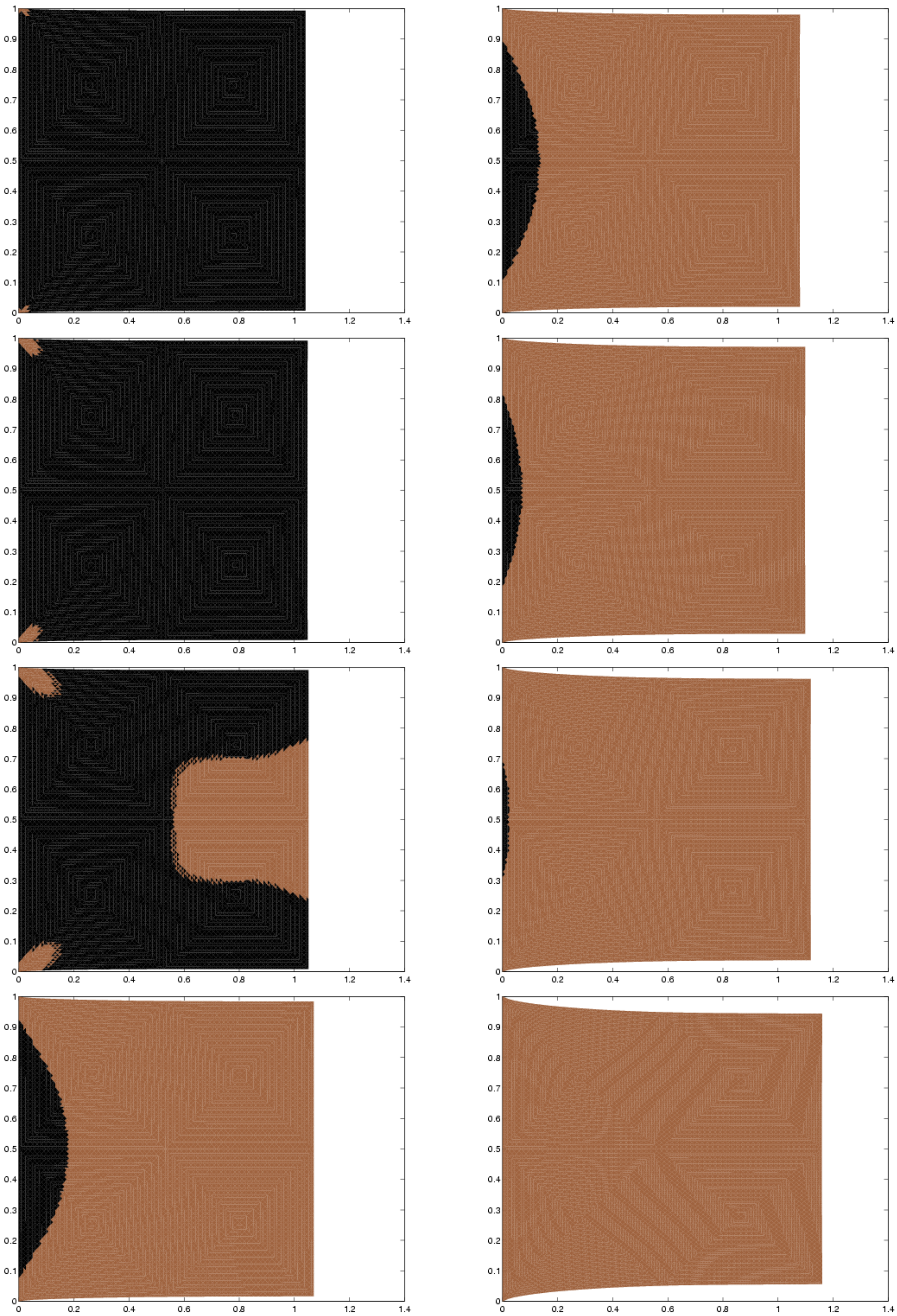

Figure 9.8: Evolution of elastoplastic zones at discrete times $t = 4.5, 5, 5.5, 6, 6.5, 7, 8, 9$ in the second numerical experiment with problem of the single-yield beam with 2D effects. The black color shows elastic zones, darker gray color zones in the plastic phase. The displayed meshes consists of 16334 elements, CPU time $= 15.59$ hours.

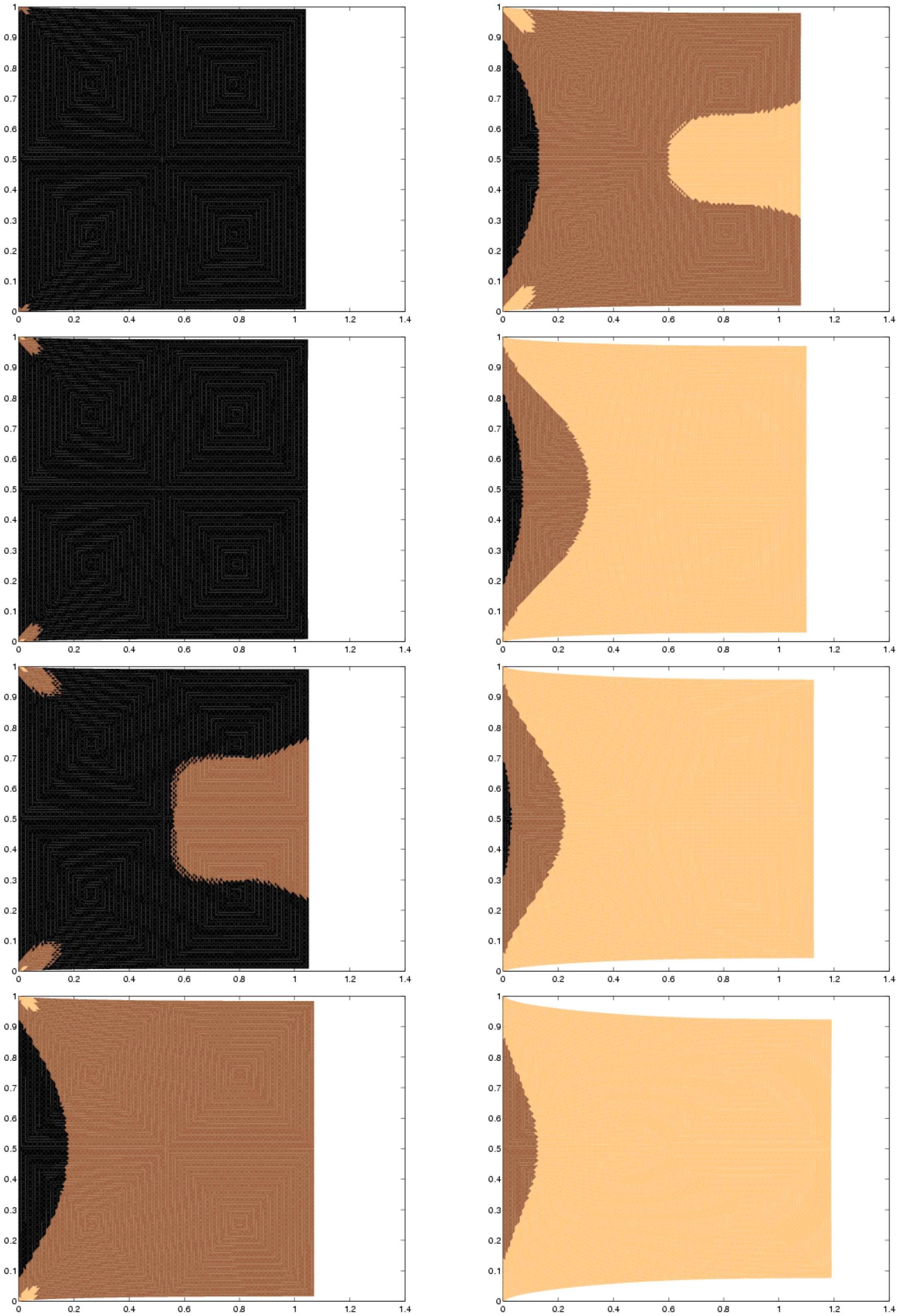

Figure 9.9: Evolution of elastoplastic zones at discrete times $t = 4.5, 5, 5.5, 6, 6.5, 7, 8, 9$ in the second numerical experiment with problem of the two-yield beam with 2D effects. The black color shows elastic zones, darker and lighter gray color zones in the first and second plastic phase. The displayed meshes consist of 16334 elements, CPU time $= 25.17$ hours.

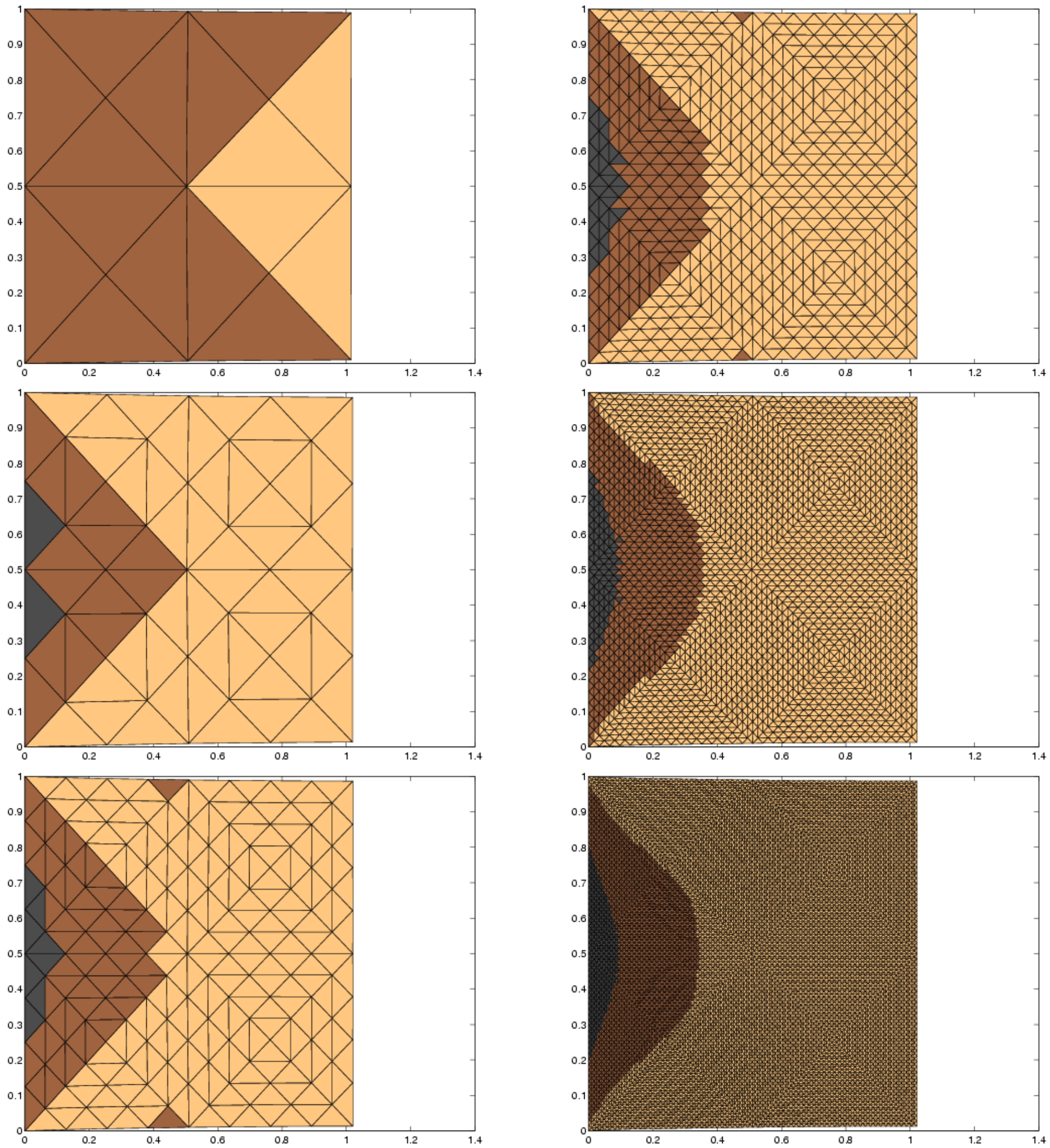

Figure 9.10: Uniformly refined meshes $\mathcal{T}_0, \mathcal{T}_1, \mathcal{T}_2, \mathcal{T}_3, \mathcal{T}_4, \mathcal{T}_5$ (with 16, 64, 256, 1024, 4096, 16384 elements) and elastoplastic zones for the one time-step with $t_0 = 0$ and $t_1 = 8.5$ in the third numerical experiment for the problem of the two-yield beam with 2D effects.

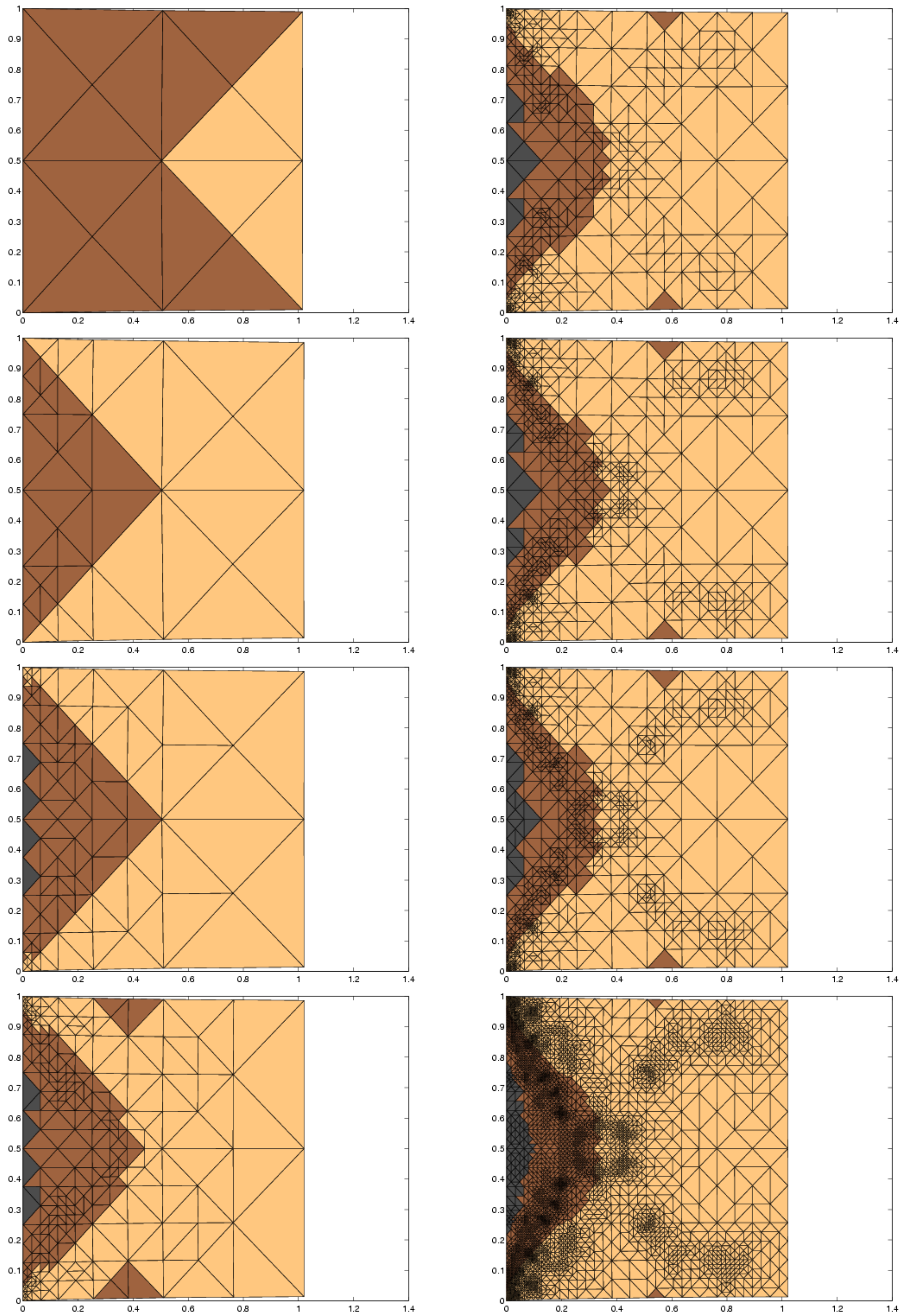

Figure 9.11: Adaptively refined meshes $\mathcal{T}_0, \mathcal{T}_2, \mathcal{T}_4, \mathcal{T}_6, \mathcal{T}_8, \mathcal{T}_{10}, \mathcal{T}_{12}, \mathcal{T}_{14}$ (with 16, 46, 136, 420, 712, 1432, 1752, 9952 elements) and elastoplastic zones for the one time-step with $t_0 = 0$ and $t_1 = 8.5$ in the third numerical experiment for the problem of the two-yield beam with 2D effects.

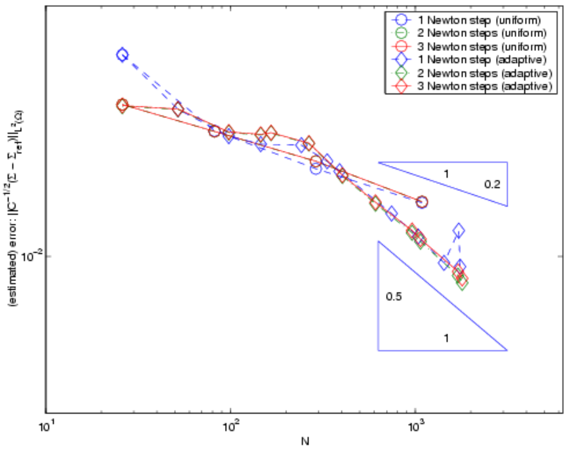

(Estimated) error for 1, 2 and 3 Newton steps.

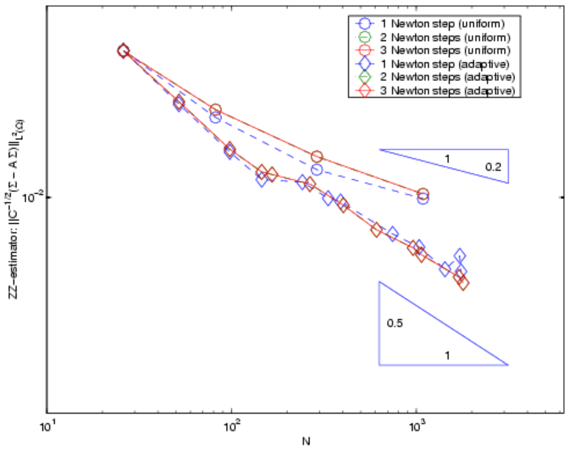

ZZ-error estimator for 1, 2 and 3 Newton step.

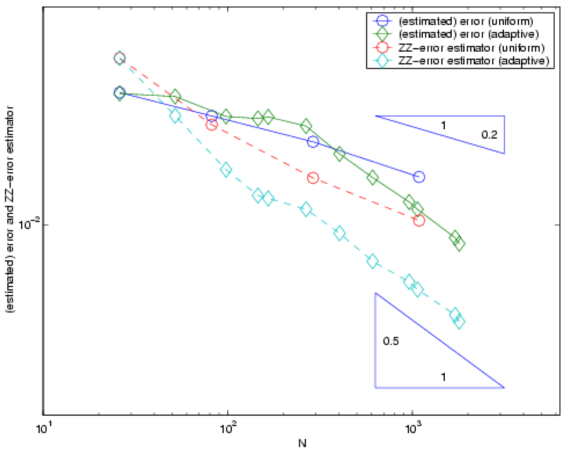

(Estimated) error and ZZ-error estimator for 3 Newton steps.

Figure 9.12: The third numerical experiment for the problem of the two-yield beam with 2D effects, one time-step with $t_0 = 0, t_1 = 9$. (Estimated) error and ZZ-error estimator are displayed versus the degrees of freedom N.

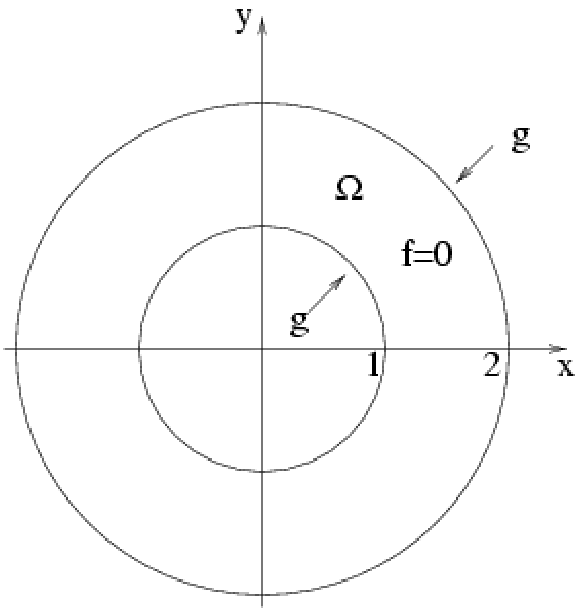

Figure 9.13: Ring problem.

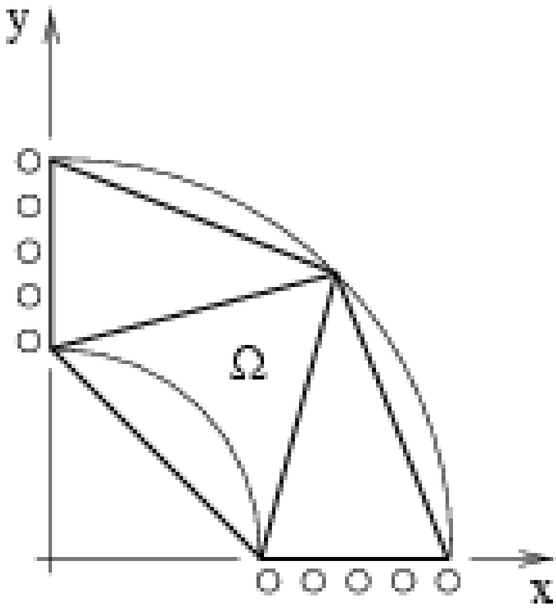

Figure 9.14: Geometry and coarse mesh $\mathcal{T}_0$ of Ring problem.

also shows the coarse mesh $\mathcal{T}_0$.

The first numerical experiment describes an elasto-plastic transition during the deformation process. The calculation was performed at discrete times $\{0, 10, 20, \ldots, 430\}$ on a finest mesh generated by 6 uniform refinements of the mesh $\mathcal{T}_0$ with 12288 elements smoothing the non-polygonal boundary. For the two-yield material model, we choose material parameters

$$E = 70000, \nu = 0.33, \sigma_1^y = 243\sqrt{2/3}, h_1 = 1, \sigma_2^y = 250\sqrt{2/3}, h_2 = 1.$$

MATLAB solver was specified by these properties: no time-stepping, nested iteration technique (Algorithm 5) with uniformly refined meshes $\mathcal{T}_0 \subset \mathcal{T}_1 \subset \mathcal{T}_2 \subset \mathcal{T}_3 \subset \mathcal{T}_4 \subset \mathcal{T}_5 \subset \mathcal{T}_6$ (with 3, 12,48, $192, 768, 3072$ and 12288 elements), Newton-Raphson solver with one step (Algorithm 4). Figure 9.15 displays the evolution of elastoplastic zones at chosen discrete times. For the initial discrete times, the whole ring is in the elastic phase only. As the time increases, we observe first plastic and later second plastic phase zones moving radically the original boundary $r = 1$ towards the boundary $r = 2$. In the last discrete time the whole ring is completely in the second plastic phase.

The second numerical experiment indicates properties of the nested iteration technique. We consider one discrete time-step problem with $t_0 = 0$ and $t_1 = 200$ and the single-yield material with

$$E = 70000, \nu = 0.33, \sigma^y = 220\sqrt{2/3}, h = 1.$$

MATLAB solver was specified by these properties: no time-stepping, nested iteration technique (Algorithm 5 with uniformly ($\mathcal{T}_0, \mathcal{T}_1, \mathcal{T}_2, \mathcal{T}_3, \mathcal{T}_4, \mathcal{T}_5, \mathcal{T}_6$ with $3, 12, 48, 192, 768, 3072$ and 12288

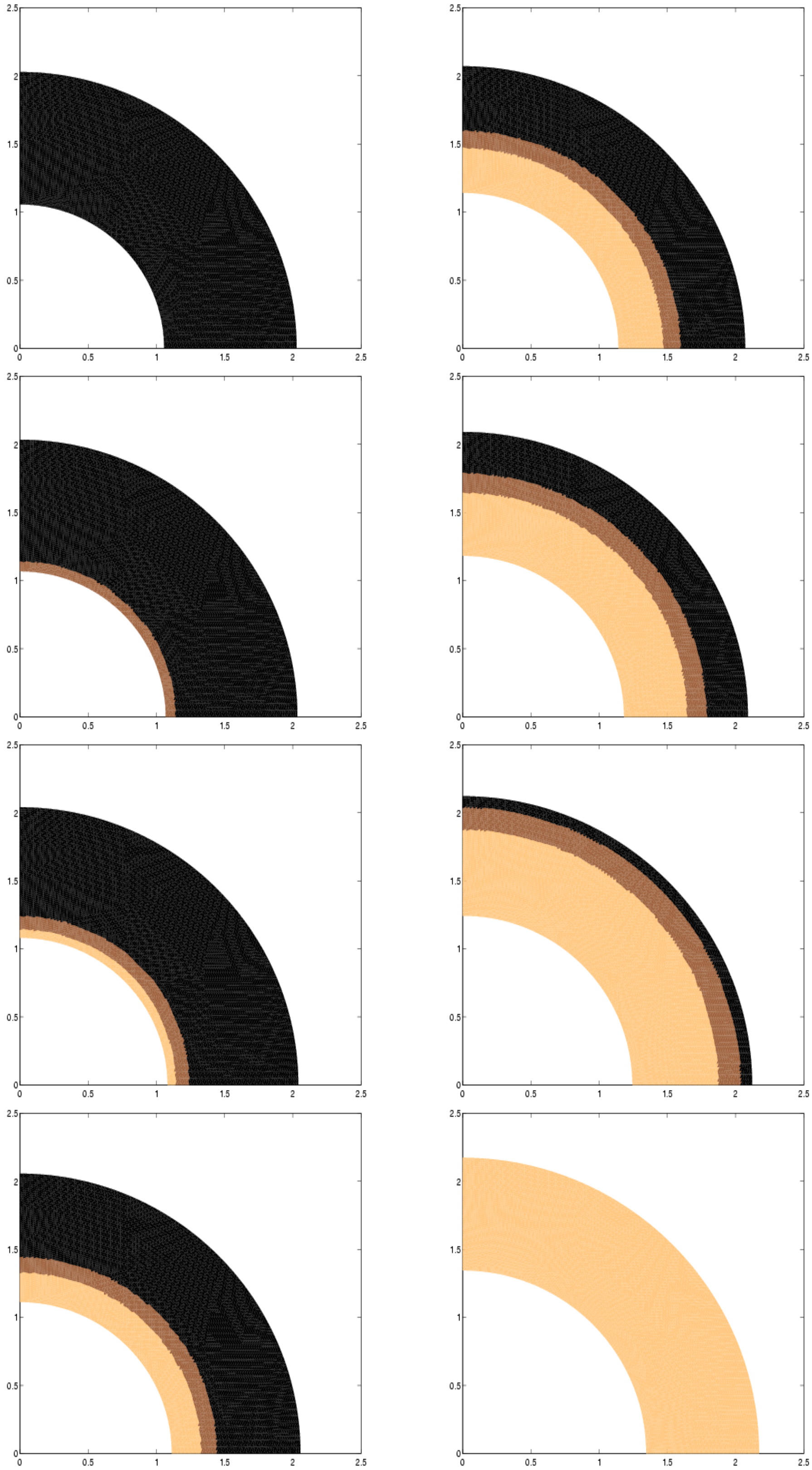

Figure 9.15: Evolution of elastoplastic zones at discrete times $t = 150, 180, 210, 260, 290, 320, 350, 380$ in the first numerical experiment with problem of the two-yield ring. The black color shows elastic zones, darker and lighter gray color zones in the first and second plastic phase. The displayed meshes consist of 12288 elements, CPU time $= 21.9$ hours.

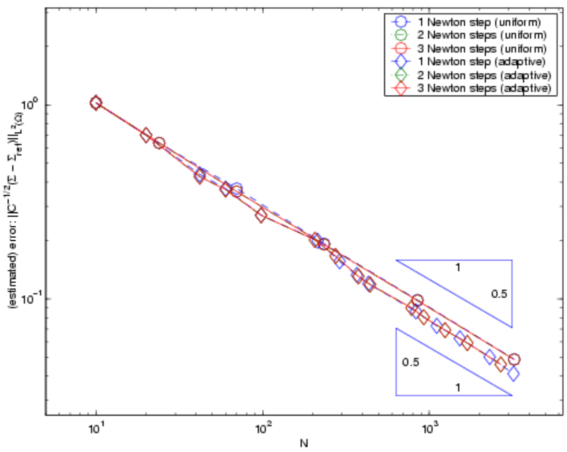

(Estimated) error for 1, 2 and 3 Newton steps.

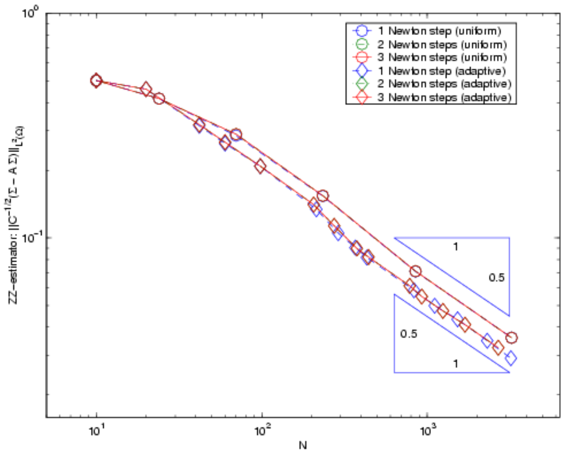

ZZ-error estimator for 1, 2 and 3 Newton steps.

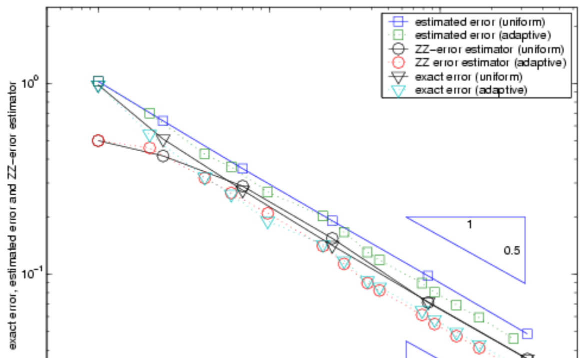

(Estimated) error and ZZ-error estimator for 3 Newton steps.

Figure 9.16: The second numerical experiment for the single-yield ring, one time-step with $t_0 = 0$ and $t_1 = 200$. Exact error, estimated error and ZZ-error estimator are displayed versus the degrees of freedom N.

material model	CPU time (in hours)	total number of Newton steps	CPU time spent on Algorithm 2 (in %)
single-yield	18.08	264	3.3
two-yield	25.17	264	21.9

Table 9.4: Performance of MATLAB solver for the first numerical experiment with the symmetric ring problem. The calculation was run at discrete times $t = \{0, 12, 20, \ldots, 430\}$, and uniform mesh $\mathcal{T}_6$ with 12288 elements.

elements) or adaptively refined meshes, Newton-Raphson solver with 1, 2, or 3 steps (Algorithm 4). Figure 9.16 displays the exact error, the estimated error and the ZZ-error estimator versus degrees of freedom in each nested iteration for $1, 2$ or 3 Newton steps. The ZZ-error estimator shows for both uniform and adaptive mesh-refinements the optimal experimental convergence rate 0.5. After some minor preasymptotic differences, the exact error and the ZZ-error estimator are practically identical (cf. [AC00]).

9.4 L Shape

The model of an L shape body is shown in Figure 9.17. As the result of surface forces (vanishing volume forces f are assumed) L-shaped body is deformed. The final deformation at the time $t_1 = 1$ is expressed by a non-homogeneous boundary condition $u = u_D$ on the Dirichlet boundary Γ_D. u_D is defined in the polar coordinate system $r \in [0, \infty), \theta \in [-\pi, \pi]$ by

$$\begin{aligned} u_r(r,\theta) &= \tfrac{1}{2\mu} r^\alpha [-(\alpha+1)\cos\big((\alpha+1)\theta\big) + \big(C_2 - (\alpha+1)\big) C_1 \cos\big((\alpha-1)\theta\big)], \\ u_\theta(r,\theta) &= \tfrac{1}{2\mu} r^\alpha [(\alpha+1)\sin\big((\alpha+1)\theta\big) + \big(C_2 + \alpha - 1\big) C_1 \sin\big((\alpha-1)\theta\big)]. \end{aligned}$$

The constants α, C_1, C_2 have the values

$$\alpha = 0.544483737, \quad C_1 = \frac{\cos\big((\alpha+1)\frac{3}{4}\pi\big)}{\cos\big((\alpha-1)\frac{3}{4}\pi\big)}, \quad C_2 = \frac{2(\lambda+2\mu)}{\lambda+\mu}.$$

The first numerical experiment indicates properties of the nested iteration technique. We consider one discrete time-step problem with $t_0 = 0$ and $t_1 = 1$. Calculations are performed for the two-yield material specified by parameters

$$E = 100000, \nu = 0.3, \sigma_1^y = 1, h_1 = 1, \sigma_2^y = 1.41, h_2 = 0.02.$$

MATLAB solver was specified by these properties: no time-stepping, nested iteration technique (Algorithm 5) with uniformly ($\mathcal{T}_0 \subset \mathcal{T}_1 \subset \mathcal{T}_2 \subset \mathcal{T}_3 \subset \mathcal{T}_4 \subset \mathcal{T}_5 \subset \mathcal{T}_5$ with $6, 24, 96, 384, 1536$ and 6144 elements) or adaptively refined meshes, Newton-Raphson solver with with 1, 2 or 3 steps (Algorithm 4). Figure 9.19 displays adaptive mesh-refinements, Figure 9.20 (estimated) error and the ZZ-error estimator versus degrees of freedom in nested iterations step for 1, 2 or 3 Newton steps. The ZZ-error estimator shows the experimental convergence rate 0.3 for the uniform mesh-refinements and the rate 0.6 for the adaptive mesh-refinements. For adaptive

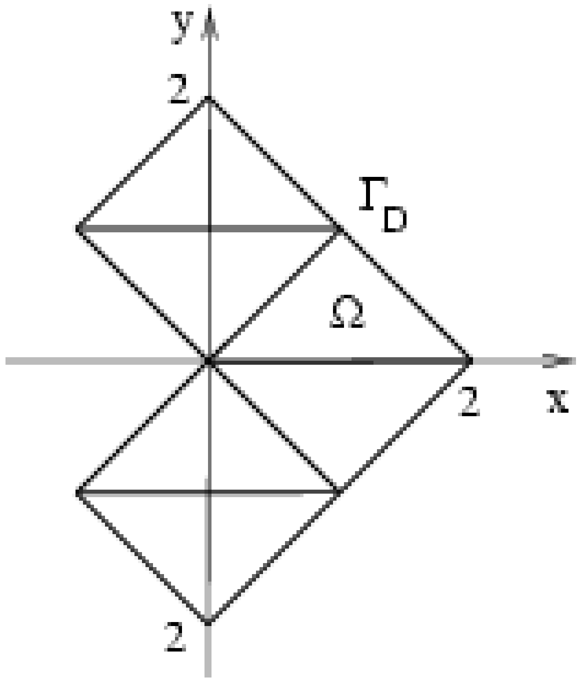

Figure 9.17: Geometry of the L shape problem and coarse mesh $\mathcal{T}_0$.

mesh-refinements the conditional number of the global matrix in the Newton upgrade (8.9) becomes for higher number of refinements (more than 10^3 degrees of freedom) very large (Figure 9.18). We do not observe the same effect for the calculation with the purely elastic material. A possible explanation is that the global convergence of the Newton-Raphson method is not guaranteed without damping.

The second numerical experiment compares the computational complexity of the nested iteration technique and the direct calculation. The problem is specified as in the first experiment, four techniques for the computation of the discrete solution on $\mathcal{T}_i$ for $i = 1, \ldots, 6$ are analyzed:

- The nested iteration technique (Algorithm 5) with Newton-Raphson solver with 1, 2 or 3 steps (Algorithm 4)
- The nested iteration technique (Algorithm 5) with Newton-Raphson solver with three stages convergence control (Algorithm 3)
- The direct calculation on $\mathcal{T}_i$ with Newton-Raphson solver with 1, 2 or 3 steps (Algorithm 4)
- The direct calculation on $\mathcal{T}_i$ with with Newton-Raphson solver with three stages convergence control (Algorithm 3)

CPU times and the (ZZ-) error estimators for are given in Table 9.5. The nested iteration technique with the three stages convergence control always converged on every triangulation

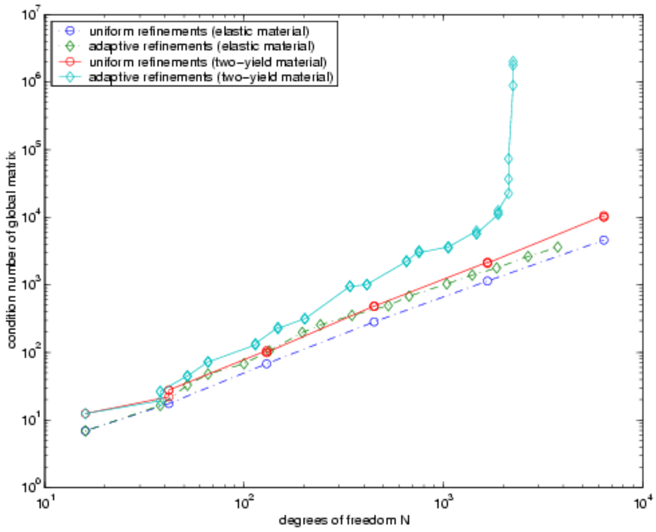

Figure 9.18: Condition number of the global stiffness matrix versus the degrees of freedom in the first numerical experiment for the L shape problem.

$\mathcal{T}_1, \ldots, \mathcal{T}_6$ for the zero initial approximation $U|_{\mathcal{T}_0} = 0$. The direct calculation on $\mathcal{T}_i$ converged for the zero initial approximation $U|_{\mathcal{T}_i} = 0$ on the triangulations $\mathcal{T}_0, \mathcal{T}_1, \mathcal{T}_2, \mathcal{T}_3$, however we observe the divergence on $\mathcal{T}_4$ and $\mathcal{T}_5$. The possible reason is that the considered initial approximation for the Newton-Raphson

method was not close enough to the discrete solution. If convergence is obtained, then the nested iteration technique performs faster then the direct calculation (with exception of the triangulation $\mathcal{T}_1$), and it is therefore more efficient. The direct calculation with 1, 2, or 3 steps requires smaller computation costs than the nested iteration technique (with the same number of steps) coarser meshes $\mathcal{T}_0, \ldots, \mathcal{T}_{i-1}$. Corresponding error estimates (the column error est. η_Z in Table 9.5) indicate that the direct calculation would require more steps (than considered 1, 2, or 3) for reaching the convergence. The nested iteration technique provides ’sufficiently’ good approximation, even after 1 step. It is therefore recommendable to apply the nested iteration technique with Newton-Raphson solver with one step (Algorithm 4).

9.5 Cook’s membrane

Cook’s membrane with a coarse mesh $\mathcal{T}_0$ is visualized in Figure 9.21, where a panel is clamped at one end and subjected to a shear load $g = (0, g_y)$ along the opposite end (and vanishing volume force $f = 0$).

The first numerical experiment demonstrates two-dimensional hysteresis effects. Material, time parameters and the solver properties are identical to the model of the beam with 1D effects. The coarse mesh $\mathcal{T}_0$ consists of 6 elements. The uniform cyclic load is acting in the y-coordinate and is of the form

$$g_y = 12\sin(t\pi/20).$$

SOLVER TYPE	6 elements		24 elements		96 elements	
	CPU time (sec)	error est. η_Z	CPU time (sec)	error est. η_Z	CPU time (sec)	error est. η_Z
DIRECT (1 New. step)	0.35	1.10 e-2	1.55	7.79 e-3	5.20	6.90 e-3
NESTED (1 New. step)	0.35	$-\|\|-$	1.33	7.91 e-3	5.71	5.06 e-3
DIRECT (2 New. steps)	0.47	$-\|\|-$	2.14	7.97 e-3	8.84	5.47 e-3
NESTED (2 New. steps)	0.47	$-\|\|-$	2.07	7.93 e-3	9.18	5.10 e-3
DIRECT (3 New. steps)	0.67	$-\|\|-$	2.88	7.93 e-3	11.38	5.09 e-3
NESTED (3 New. steps)	0.67	$-\|\|-$	2.71	7.93 e-3	13.07	5.10 e-3
DIRECT (three stages)	0.17	$-\|\|-$	4.67	7.93 e-3	49.98	5.10 e-3
NESTED (three stages)	0.17	$-\|\|-$	4.78	7.93 e-3	46.66	5.10 e-3

SOLVER TYPE	384 elements		1536 elements		6114 elements	
	CPU time (sec)	error est. η_Z	CPU time (sec)	error est. η_Z	CPU time (sec)	error est. η_Z
DIRECT (1 New. step)	15.79	5.39 e-3	61.53	3.98 e-3	433.76	2.88 e-3
NESTED (1 New. step)	24.07	3.32 e-3	107.87	2.21 e-3	623.72	1.58 e-3
DIRECT (2 New. steps)	31.11	5.39 e-3	123.57	5.60 e-3	765.47	4.82 e-3
NESTED (2 New. steps)	40.18	3.31 e-3	174.31	2.20 e-3	930.23	1.47 e-3
DIRECT (3 New. steps)	44.82	4.17 e-3	200.57	1.65 e-3	1147.55	2.85 e-2
NESTED (3 New. steps)	57.88	3.31 e-3	243.10	2.20 e-3	1194.75	1.52 e-3
DIRECT (three stages)	344.14	3.31 e-3	divergence		divergence	
NESTED (three stages)	300.19	3.31 e-3	1227.48	2.20 e-3	7136.45	1.46 e-3

Table 9.5: Comparison: direct calculation versus the nested iteration technique in the second numerical experiment for the L shape problem. Considered is one time-step with $t_0 = 0$ and $t_1 = 1$ and six uniform triangulations with $6, 24, 94, 384, 1536$ and 6114 elements.

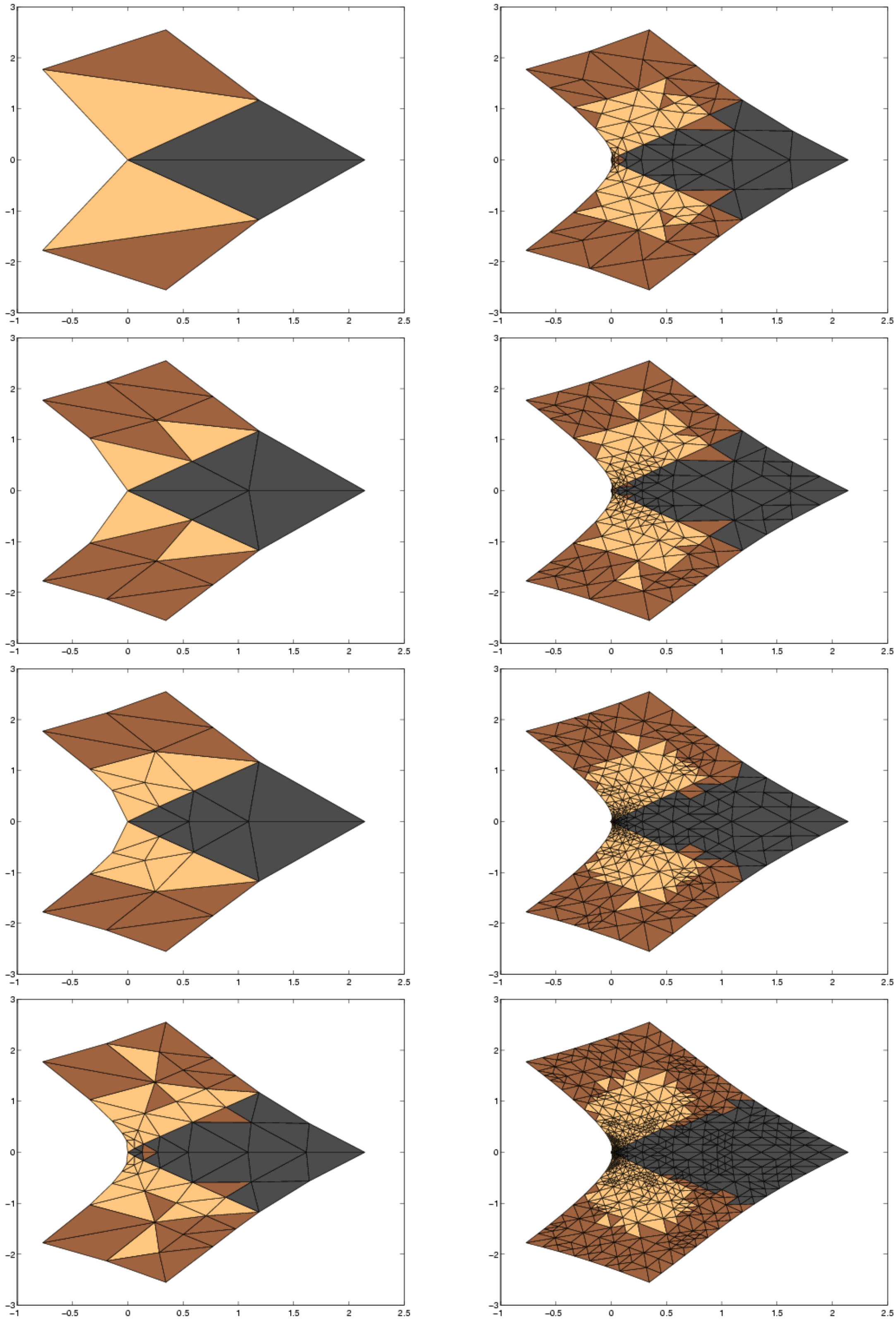

Figure 9.19: Adaptively refined meshes $\mathcal{T}_0, \mathcal{T}_1, \mathcal{T}_2, \mathcal{T}_4, \mathcal{T}_6, \mathcal{T}_8, \mathcal{T}_{10}, \mathcal{T}_{12}$ (with 6, 22, 34, 88, 170, 366, 694, 1372 elements) and elastoplastic zones for the one time-step with $t_0 = 0$ and $t_1 = 1$ in the first numerical experiment for the problem of the two-yield L shape. Displacement factor=10000.

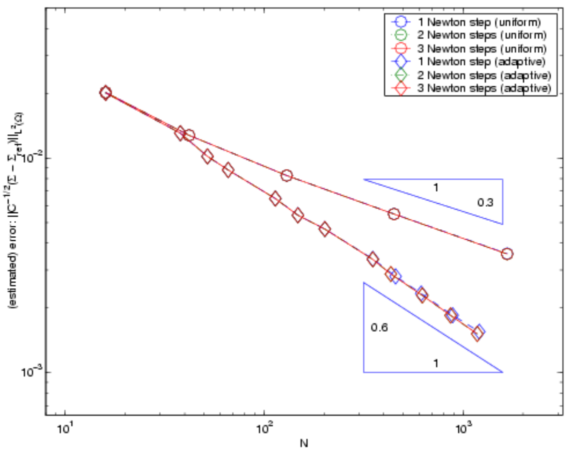

(Estimated) error for 1, 2 and 3 Newton steps.

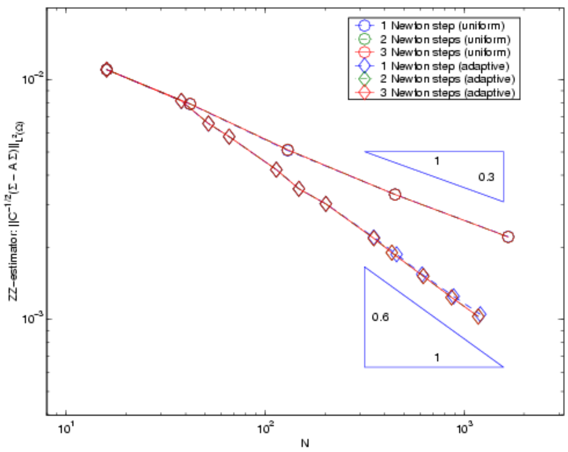

ZZ-error estimator for 1, 2 and 3 Newton steps.

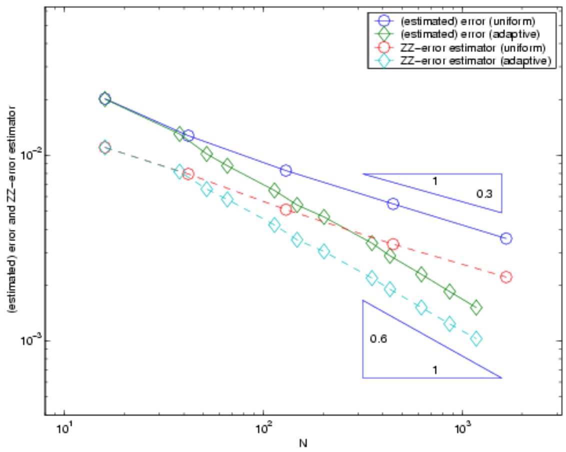

(Estimated) error and ZZ-error estimator for 3 Newton steps.

Figure 9.20: The first numerical experiment for the two-yield the L shape problem, one time-step with $t_0 = 0, t_1 = 1$. (Estimated) error and ZZ-error estimator are displayed versus the degrees of freedom N.

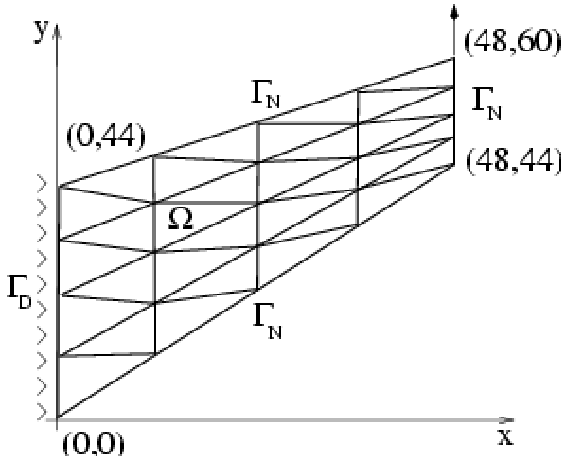

Figure 9.21: Geometry and coarse mesh $\mathcal{T}_0$ of a Cook's membrane problem.

material model	CPU time (in sec)	total number of Newton steps	CPU time spent on Algorithm 2 (in %)
single-yield	430	589	14.8
two-yield	1647	677	74.2

Table 9.6: Performance of MATLAB solver in the first numerical experiment with the Cook's membrane problem effects. The calculation was run at discrete times $t = \{0, 0.5, 1, \ldots, 50\}$, and uniform mesh $\mathcal{T}_0$ with 6 elements.

Figures 9.22 and 9.23 show the *hysteresis curves* in terms of the dependence of $g_y(t)$ on the y-displacement $u_y(t)$ of the point $(46, 60)$ for single and two-yield models. In both curves we observe strong two-dimensional effects causing the smoothing of the elasto-plastic transition.

The second numerical experiment indicates properties of the nested iteration technique. We consider one discrete time-step problem with $t_0 = 0$ and $t_1 = 1.7$, the material with same properties as in the first numerical experiment. MATLAB solver was specified by these properties: no time-stepping, nested iteration technique (Algorithm 5 with uniformly or adaptively refined meshes), Newton-Raphson solver with 1, 2 or 3 steps (Algorithm 4). Figure 9.25 displays the (estimated) error and the ZZ-error estimator versus degrees of freedom in nested iteration step for $1, 2$ or 3 Newton steps. The ZZ-error estimator shows the experimental convergence rate 0.4 for the uniform and the experimental convergence rate 0.5 for the adaptive mesh-refinements.

9.6 Plate with a hole

A two dimensional squared plate with a hole is under the time-dependent tension as shown in Figure 9.26. Due to the symmetry reasons, only the quarter of the square, depicted in Figure 9.27, is discretized. For a calculation we consider the single-yield material with

$$E = 206900, \nu = 29, \sigma^y = 450\sqrt{2/3}, h = 1$$

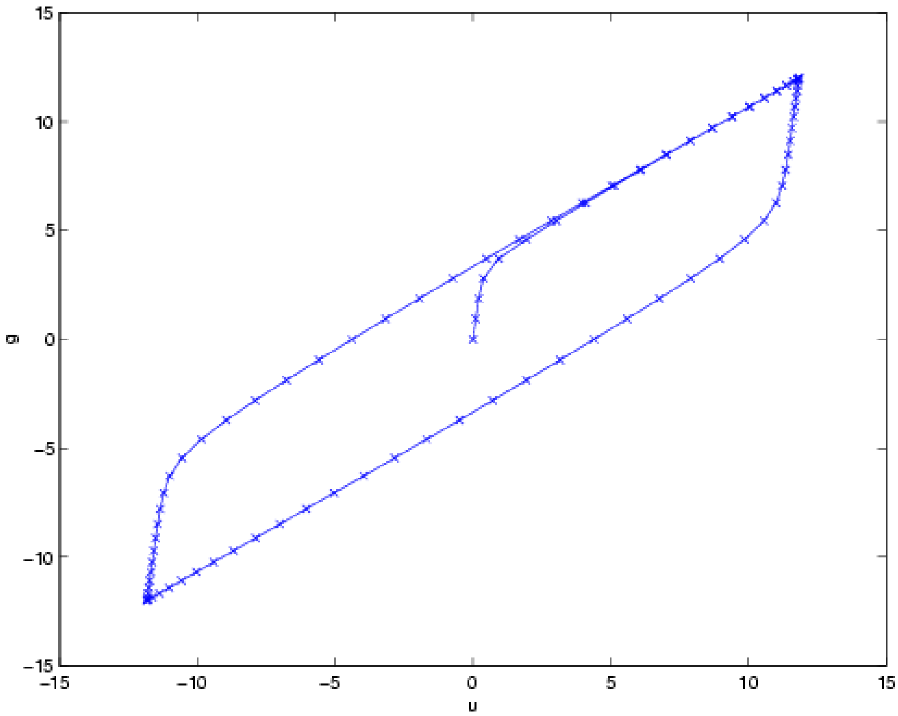

Figure 9.22: Displayed loading-deformation relation in terms of the uniform surface loading $g_y(t)$ versus the y-displacement of the point $(0, 1)$ in the first numerical experiment for the problem of the single-yield Cook's membrane.

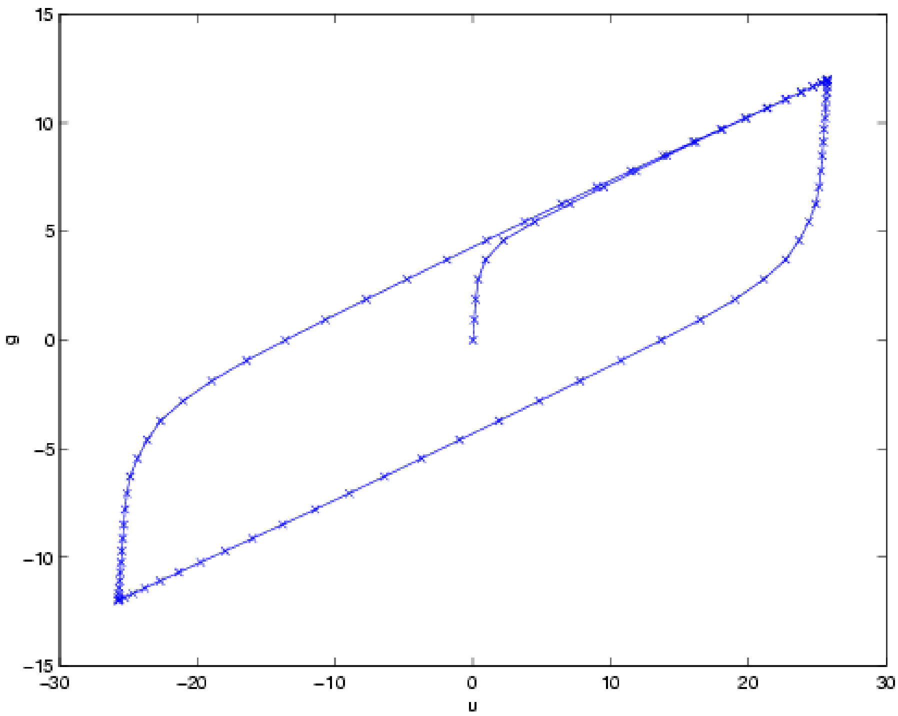

Figure 9.23: Displayed loading-deformation relation in terms of the uniform surface loading $g_y(t)$ versus the y-displacement of the point $(0, 1)$ in the first numerical experiment for the problem of the two-yield Cook's membrane.

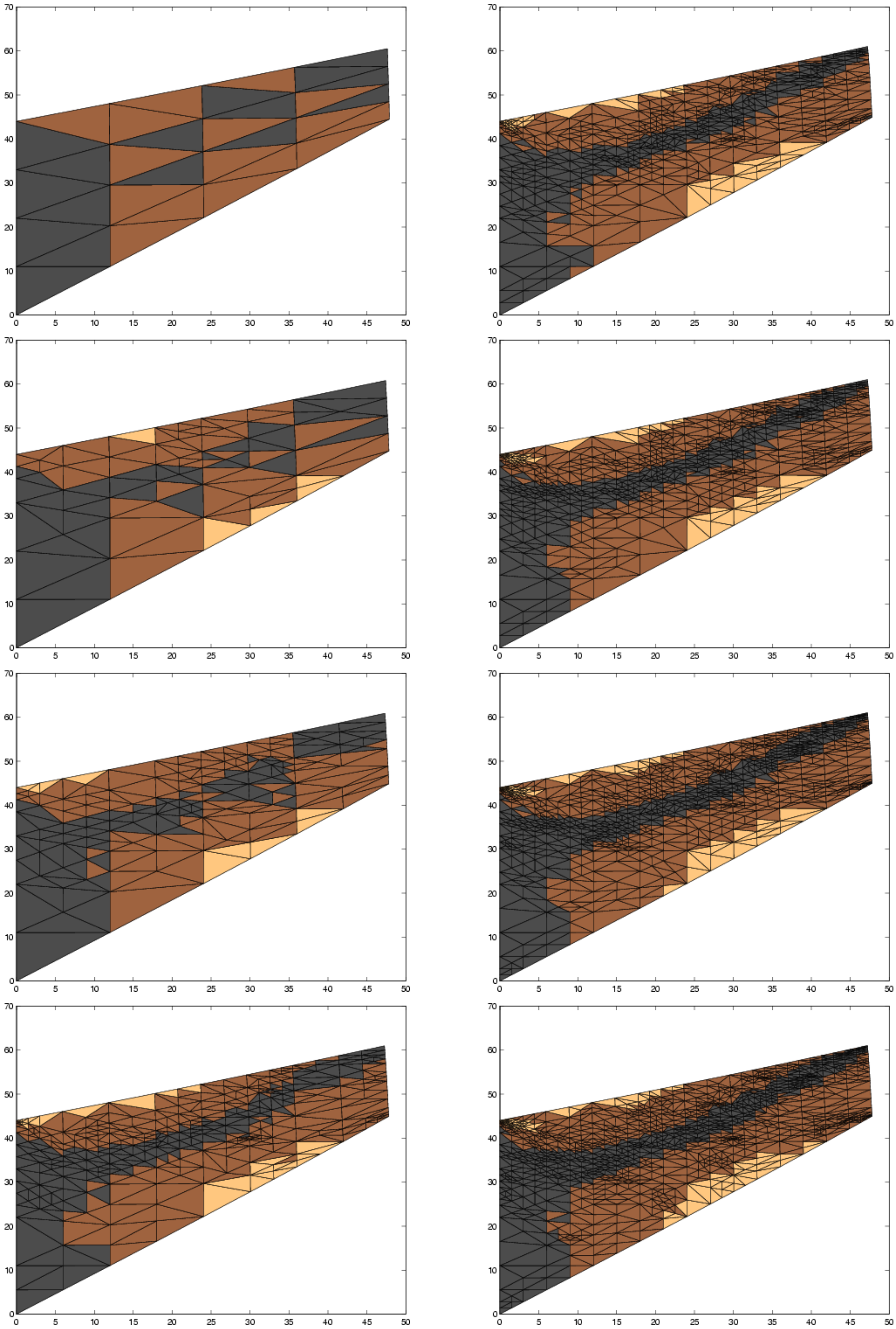

Figure 9.24: Adaptively refined meshes $\mathcal{T}_0, \mathcal{T}_2, \mathcal{T}_4, \mathcal{T}_6, \mathcal{T}_8, \mathcal{T}_9, \mathcal{T}_{10}, \mathcal{T}_{11}$ (with 32, 104, 259, 584, 1088, 1329, 1645, 2021 elements) and elastoplastic zones for the one time step problem with $t_0 = 1$ and $t_1 = 0.7$ in the second numerical experiment for the problem of the two-yield Cook's membrane.

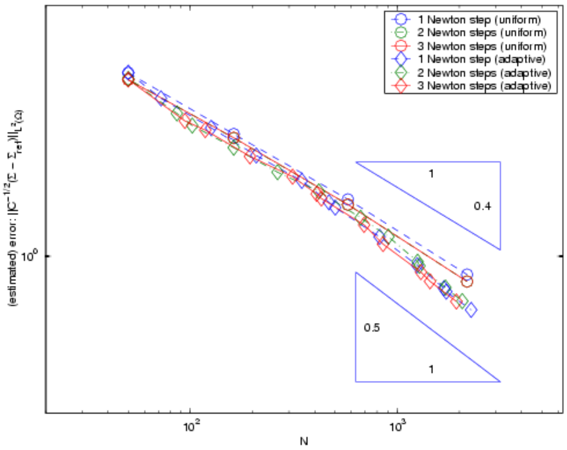

(Estimated) error for 1, 2 and 3 Newton steps.

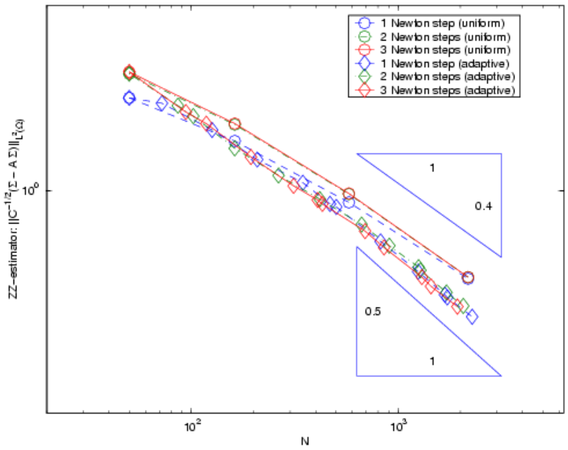

ZZ-error estimator for 1, 2 and 3 Newton steps.

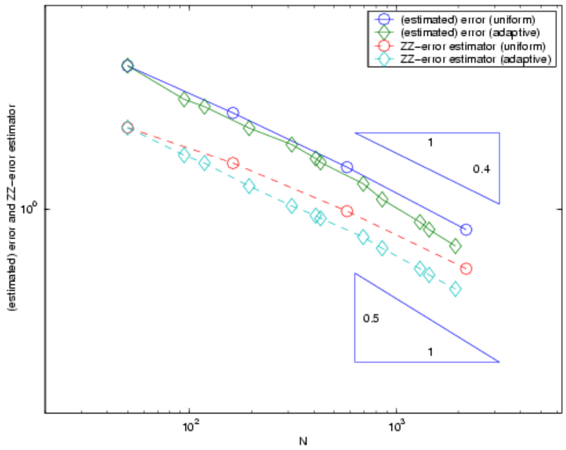

(Estimated) error and ZZ-error estimator for 3 Newton steps.

Figure 9.25: The second numerical experiment for the two-yield Cook's membrane problem, one time-step with $t_0 = 0, t_1 = 1.7$. (Estimated) error and ZZ-error estimator are displayed versus the degrees of freedom N.

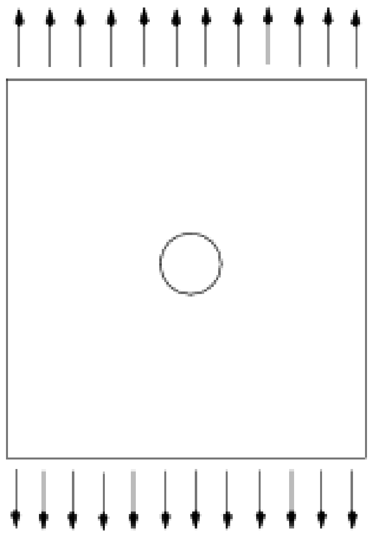

Figure 9.26: Problem of the plate with a hole.

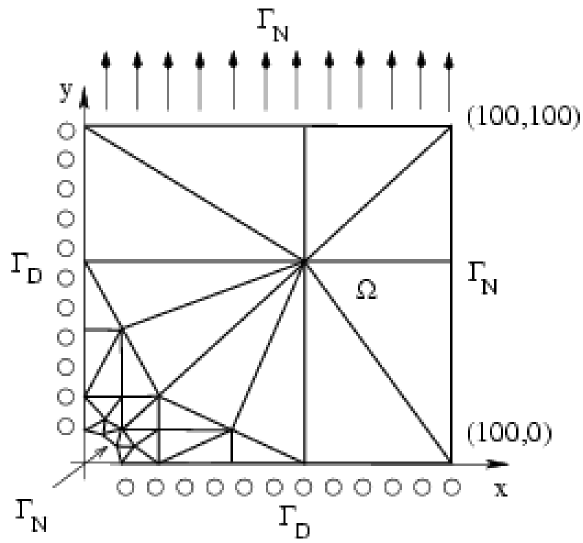

Figure 9.27: Geometry of the plate with a hole and coarse mesh $\mathcal{T}_0$.

or the two-yield material with

$$E = 206900, \nu = 29, \sigma_1^y = 450\sqrt{2/3}, h = 1, \sigma_2^y = 500\sqrt{2/3}, h_2 = 1$$

subjected to the time-dependent surface tension $g = (0, 600t)$.

The first numerical experiment indicates properties of the nested iteration technique. We consider one discrete time-step problem with $t_0 = 0$ and $t_1 = 0.7$ and the two-yield material with material parameters given above. MATLAB solver was specified by these properties: nested iteration technique (Algorithm 5 with uniformly or adaptively refined meshes, Newton-Raphson solver with 1, 2, or 3 steps (Algorithm 4). Figure 9.28 displays the exact error, the estimated error and the ZZ-error estimator versus degrees of freedom in each nested iteration for $1, 2$ or 3 Newton steps. The ZZ-error estimator shows the (experimental) convergence rate 0.3 for uniform mesh-refinements and the (experimental) convergence rate 0.5 for adaptive mesh-refinements .

The second numerical experiment demonstrates the adaptive time-stepping strategy described in Section 8.4. For time and space discretization, we set $t = \{0.4, 0.5, 0.6, 0.7\}$ and $\mathcal{T}_0$. For solving of the discrete problem, the adaptive time-stepping algorithm (Algorithm 6) with the following parameters is used:

- $S_{min} = 0, S_{max} = \infty$. This choice leads to no (uniform) time-stepping, i.e., the initial set of the discrete times remains unchanged.
- $S_{min} = 0, S_{max} = 3$. This means the adaptive time-stepping, i.e., if the number of Newton step in the time t_i is smaller than S_{max}, the time step $\Delta t_i = t_i - t_{i-1}$ will be divided by 2.

material model	CPU time (in sec)	total number of Newton steps	CPU time spent on Algorithm 2 (in %)
elastic	129	115	0
single-yield	384	255	8.7
two-yield	472	248	18.9

Table 9.7: Performance of MATLAB solver for the elastic, the single-yield and the two-yield plate with with a hole. The calculation was run for the times $\{0.4, 0.41, 0.42, \ldots, 0.8\}$ and the mesh $\mathcal{T}_1$ (generated by one uniform refinement of $\mathcal{T}_0$) with 124 elements.

The calculation shows that the number of Newton steps increases from 1 at time $t = 0.4$ to 5 at time $t = 0.8$ for the uniform time-stepping algorithm (Figure 9.29). The adaptive time-stepping algorithm attempts to reduce the original time step $\Delta t_1 = 0.1$ so that the number of Newton steps is 3 or less. As the result of it, the time step Δt at the time $t = 0.8$ equals 0.0001. The total calculation time is 11.8 seconds for the case of uniform (no) time-stepping and 497 seconds for the case of the adaptive time-stepping. We can observe that Algorithm 6 is sensitive to the choice of parameters S_{min}, S_{max}. (The choice $S_{max} = 4$ would enforce the uniform time-time stepping in this experiment).

9.7 Comments concerning numerical performance

The developed MATLAB solver enables the calculations of simple two-dimensional problems. It has been tested for meshes with up to 50.000 elements. Solving problems with higher number elements is very time consuming, from a couple of hours to days. What concerns the choice of the material model, computations based on the two-yield material are more expensive if compared to the single-yield model and the purely elastic model. The main reason for this is the expensive calculation of plastic dependencies (Algorithm 2) and a different number of Newton steps necessary for reaching convergence. This is illustrated by the second numerical experiment for the plate with a hole. The Newton-Raphson solver with the three stages control (Algorithm 3) is applied to the mesh $\mathcal{T}_1$ with 124 elements (generated by one uniform refinement of $\mathcal{T}_0$) at discrete times $\{0.4, 0.41, 0.42, \ldots, 0.8\}$. A comparison of the calculation complexity for the single-yield and the two-yield model for other numerical experiments are provided in Tables 9.1, 9.2, 9.3, 9.4, 9.6.

For the elastic material model, both plastic components P_1 and P_2 are zero and therefore the Algorithm 2 need not be applied. Besides, the system (8.1) is linear and its solution is found within only one Newton step (in fact, more steps are needed with respect to the termination property of the three stage algorithm, see Figure 8.1). Solving the (indeed nonlinear) system (8.4) in case of the single and two-yield models requires more Newton steps. Longer time, that Algorithm 2 needs for the two-yield material calculation compare to the single-yield material calculation is the consequence of the principal difference of both material models: for the single-yield material the plastic dependence can be calculated analytically, or equivalently, one iteration of Algorithm 2 yields the solution, however for the two-yield material more Newton steps are required.

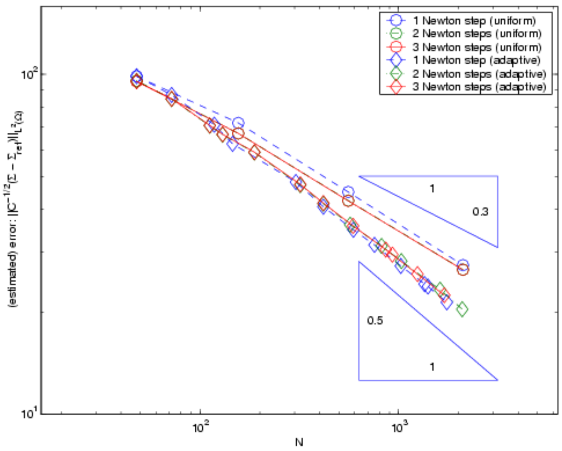

(Estimated) error for 1, 2 and 3 Newton steps.

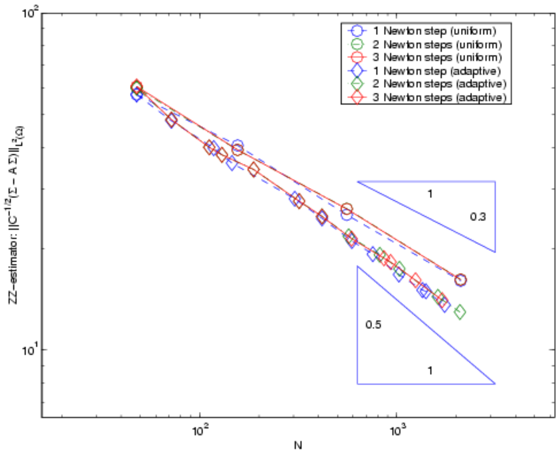

ZZ-error estimator for 1, 2 and 3 Newton steps.

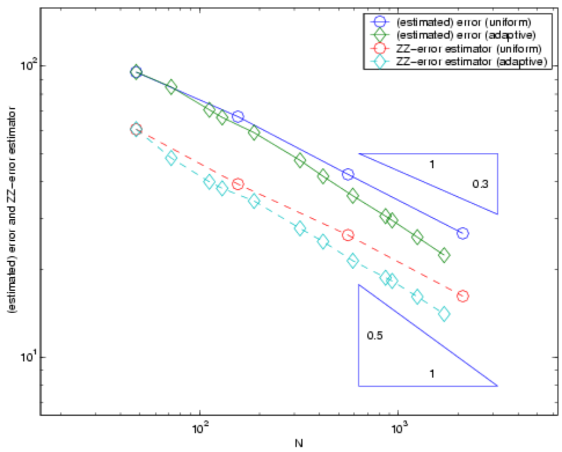

(Estimated) error and ZZ-error estimator for 3 Newton steps.

Figure 9.28: The first numerical experiment for the two-yield plate with a hole, one time-step with $t_0 = 0, t_1 = 0.7$. (Estimated) error and ZZ-error estimator are displayed versus the degrees of freedom N.

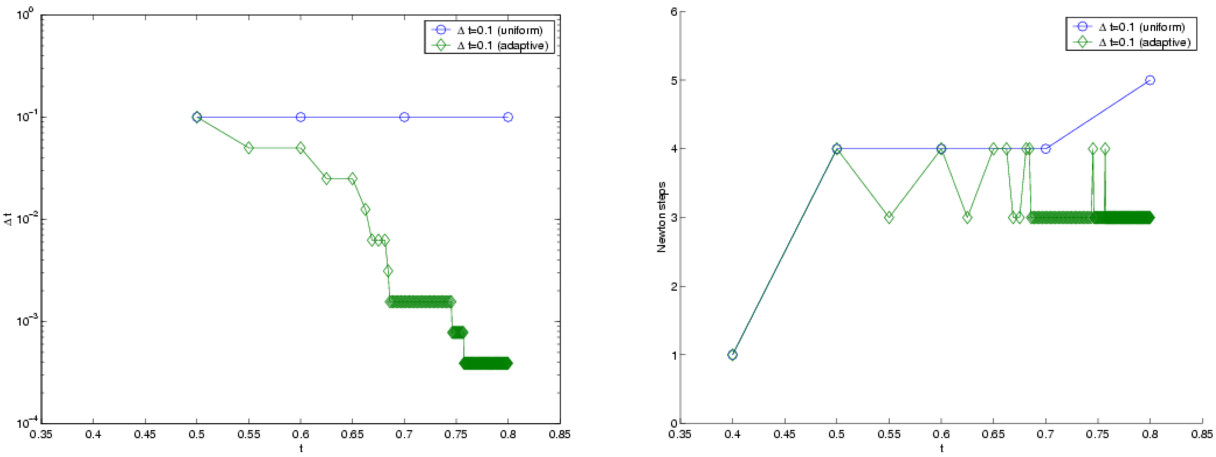

Time-steps Δt versus time t. Newton steps versus time t.

Figure 9.29: The second numerical experiment for the problem of the two-yield plate with a hole. Time-step Δt and the number of Newton step are displayed versus the time t for the uniform and adaptive time-stepping.

Adaptive mesh-refining strategies led in all numerical examples (with exception of L shape model) to optimal converge rates.

Chapter 10

Conclusions and open questions

We summarize the main results we have obtained in this thesis.

- Similarly to the linear kinematic hardening model, the weak form of Prandtl-Ishlinskii model of play type can be rewritten as a variational inequality on a Hilbert space $\mathcal{H}$ which involves a bilinear form $a(\cdot,\cdot)$, a linear functional $\ell(\cdot)$ and a nonlinear functional $\psi(\cdot)$.

- The bilinear form $a(\cdot,\cdot)$, the linear functional $\ell(\cdot)$ and the nonlinear functional $\psi(\cdot)$ satisfy sufficient conditions (i.e., ellipticity of $a(\cdot,\cdot)$, Lipschitz continuity of $\psi(\cdot)$ and others) that guarantee the existence and uniqueness of the variational inequality solution in a Hilbert space $\mathcal{H}$.

- For the one time-step discrete problem, the vector of incremental plastic strains $P = (P_1,\ldots,P_M)^T$ depends on every element T of the triangulation $\mathcal{T}$ on the displacement U only. In contrast to the linear kinematic hardening model, this dependency can not be expressed analytically, but has to be calculated by a numerical algorithm.

- Numerical examples indicate the priority of adaptive mesh-refinements over uniform mesh-refinements. Besides, one Newton iteration in the nested iteration technique is sufficient, more iterations only increase computational costs without large improvements with respect to accuracy.

The following questions stay so-far unanswered and their study might become a part of a future research.

- The Prandtl-Ishlinskii model of play type generalizes the model of linear kinematic hardening only. It would be chalenging to extend the Prandtl-Ishlinskii model of play type in order to respect isotropic hardening effects as well.

- Is there any example in two-yield plasticity with a known analytical solution?

- Is it possible to prove sufficient regularity of the solutions and clarify superiority of adaptive refinement techniques theoretically?

Notation

(a, b)	open interval
$[a, b]$	closed interval
$\mathbb{N}$	natural numbers (without 0)
$\mathbb{R}^d$	Euclidian space of (column-) vectors in d components
$\mathbb{R}^{m\times d}$	space of $m \times d$-matrices with real entries
$\mathbb{R}^{d\times d}_{sym}$	space of symmetric $d \times d$-matrices with real entries
dev $\mathbb{R}^{d\times d}_{sym}$	space of deviatoric symmetric $d \times d$-matrices with real entries
M^T	transposed matrix to $M \in \mathbb{R}^{m\times d}$
x^T	transposed vector to $x \in \mathbb{R}^d$
$\|\|X\|\|_F$ or $\|\|X\|\|$	Frobenius norm of matrix $X \in \mathbb{R}^{d\times d}$
$X : Y$ or $\langle X, Y\rangle$	(Euclidian) scalar product of matrices $X, Y \in \mathbb{R}^{d\times d}$
$x \otimes y$	dyadic product of x, y
det	determinant of a square matrix
diag$(\alpha_1, \ldots, \alpha_n)$	diagonal matrix with entries $\alpha_1, \ldots, \alpha_n$
∇	gradient (as row-vector)
div	divergence
∂A	boundary of set A
$\overline{A}$	closure of set A
Ω	bounded Lipschitz domain in $\mathbb{R}^d$
$\Gamma\ (= \partial\Omega)$	boundary of domain Ω

Γ_D	Dirichlet boundary of domain Ω
Γ_N	Neumann boundary of domain Ω
n	(outer) unit normal vector on $\Gamma = \partial\Omega$
$f\|_A$	restriction of $f : X \to Y$ to $A \subseteq X$
X^*	dual space of normed space X
$\mathcal{C}^m(\Omega)$	space of continuous functions on Ω with continuous (partial) derivatives up to order m
$L^p(\Omega)$	Lebesque space of Lebesque measurable functions on Ω, that are in p-th order integrable, $1 \leq p \leq \infty$
$W^{1,p}(\Omega)$	Sobolev space of functions in $L^p(\Omega)$, with weak derivatives in $L^p(\Omega)^d$
$H^1(\Omega)$	$= W^{1,2}(\Omega)$
$H^1_D(\Omega)$	space of functions in $H^1(\Omega)$ that vanish on Dirichlet boundary Γ_D
$W^{m,p}(\Omega)$	Sobolev space of m-th order, i.e., all partial derivatives up to m-th order exist in weak sence and belong to $L^p(\Omega)$
$H^m(\Omega)$	$= W^{m,2}(\Omega)$
$\\|\cdot\\|_X$	norm on the normed space X, e.g. $\\|\cdot\\|_{\ell_p}$, $\\|\cdot\\|_{L^p(\Omega)}$, $\\|\cdot\\|_{W^{1,p}(\Omega)}$
$\\|\cdot\\|_{p,\Omega}$, $\\|\cdot\\|_p$	norm on Lebesgue space $L^p(\Omega)$
$\\|\cdot\\|_{m,p,\Omega}$, $\\|\cdot\\|_{m,p}$	norm on Sobolev space $W^{m,p}(\Omega)$
$(x_n) \to x$	sequence (x_n) converges strongly to x
B	open ball at 0 with radius $r = 1$
$\mathcal{T}$	triangulation of domain Ω
T	element (triangle) of triangulation $\mathcal{T}$
$\mathcal{N}$	set of nodes (vertices)
$\mathcal{E}$	set of edges
$\mathcal{E}_\mathcal{N}$	set of edges on Γ_N
$\mathcal{S}^1(\mathcal{T})$	lowest order finite element space on $\mathcal{T}$ (elementwise affine)
$\mathcal{S}^1_D(\mathcal{T})$	finite element functions from $\mathcal{S}^1(\mathcal{T})$ which vanish on Γ_D
$\mathcal{S}^0(\mathcal{T})$	piecewise constant functions on $\mathcal{T}$
h_E	diameter of an edge
h_T	diameter of an element
$[\lambda_h \cdot n_E]$	jump of the normal component of λ_h across E
div_T	elementwise application of div

η_T, η	local error-indicator and error estimator
u or U	displacement
σ or Σ	Cauchy stress tensor
ε	Green strain tensor
p or P	plastic strain
$\mathbb{C}, \lambda, \mu$	elastic tensor and Lamé coefficients
$\mathbb{H}$	(kinematic) hardening tensor
$\mathcal{D}$	dissipation function

MAPLE programs

Program ’maple.ms’ displays the functional $f(P) = \frac{1}{2}(\hat{\mathbb{C}} + \hat{\mathbb{H}})P : P - P : A + ||P||_{\sigma_y}$ and its parts $\frac{1}{2}(\hat{\mathbb{C}} + \hat{\mathbb{H}})P : P, P : A, ||P||_{\sigma_y}$ in $x - y$ coordinate system. Two components plastic strain $P = (P_1, P_2)^T$ for modeling of two-yield plasticity assumes P_1 and P_2 in the form $P_1 = (x, 0; 0, -x), P_2 = (y, 0; 0, -y)$. It also displays the nonlinear system (6.48) for $\xi_1 = ||P_1||, \xi_2 = ||P_2||$ in coordinate system $\xi_1 - \xi_2$. For a different elastoplastic material parameters $\mu, \sigma_1^y, \sigma_2^y, h_1, h_2$ and values of $A_1, A_2 \in \mathbb{R}^{2\times 2}_{sym}$ can be changed in lines 2 and 3.

maple.ms

```
1  > with(linalg):n:=2;
2  > mu:=1;sigma1:=1; sigma2:=2;h1:=1;h2:=1;
3  > A1:=10*array([[2,0],[0,0]]); A2:=10*array([[2,0],[0,0]]);
4  > Identity:=evalm(array(identity, 1..n,1..n)):
5    devA1:=evalm(A1-(1/n)*trace(A1)*Identity);
6    devA2:=evalm(A2-(1/n)*trace(A2)*Identity);
7  > l1:=evalm((sigma1+(2*mu+h1)*xi1)*devA2-2*mu*xi1*devA1);
8    l2:=evalm((sigma2+(2*mu+h2)*xi2)*devA1-2*mu*xi2*devA2); r:=
9    simplify(((2*mu+h1)*xi1+sigma1)*((2*mu+h2)*xi2+sigma2)-4*mu^2*xi1*xi2);
10 > Phi1:=expand(trace(multiply(transpose(l1),l1)))-r^2;
11   Phi2:=expand(trace(multiply(transpose(l2),l2)))-r^2;
12 > implicitplot({Phi1=0,Phi2=0}, xi1=-10..10,xi2=-10..10,grid=[50,50]);
13 > with(linalg):P1:=array(1..2,1..2,[[x,0],[0,-x]]);
14   P2:=array(1..2,1..2,[[y,0],[0,-y]]);
15 > f1:=1/2*(((2*mu+h1)*norm(P1,’frobenius’)^2)+
16   2*(2*mu*trace(multiply(P1,P2)))+((2*mu+h2)*norm(P2,’frobenius’)^2));
17 > f2:=trace(multiply(P1,devA1))+trace(multiply(P2,devA2));
18 > f3:=sigma1*norm(P1,’frobenius’)+sigma2*norm(P2,’frobenius’);
19 > f:=f1+f3-f2;f_scaled:=subs({x=x/sqrt(2),y=y/sqrt(2)},f);
20 > plot3d(f1,x=-100..100,y=-100..100,axes=FRAME,style=PATCHCONTOUR,
21   shading=ZGREYSCALE);
22 > plot3d(f2,x=-100..100,y=-100..100,axes=FRAME,style=PATCHCONTOUR,
23   shading=ZGREYSCALE);
24 > plot3d(f3,x=-100..100,y=-100..100,axes=FRAME,style=PATCHCONTOUR,
25   shading=ZGREYSCALE);
26 > plot3d(f,x=1..3,y=1..2,axes=FRAME,style=PATCHCONTOUR,
27   shading=ZGREYSCALE);
```

MATLAB programs

MATLAB programs for the calculation of two-yield plasticity are partly listed below. The complete listing can be obtained via http://www.numerik.uni-kiel.de/$\sim$ jva. The nested iteration solver with adaptivity (ZZ-estimator) is run by calling the program 'start.m'. Lines $4 - 13$ can be modified:

- $Newtonsteps$ means the number (given as a string) of Newton-Raphson iterations (Algorithm 4) on every mesh, typically $'1',' 2',' 3'$, the choice $'three\_stages'$ leads to the Newton-Raphson solver with the three stages solver (Algorithm 3).
- $theta$ is the (adaptive) mesh-refinement parameter with the value between 0 and 1, typical choices are $theta = 0.5$ (adaptive mesh-refinement) or $theta = 1$ (uniform mesh-refinement).
- $step\_min, step\_max$ - the time-stepping parameters; the choice $step\_min = 0$, $step\_max = \infty$ leads to no (uniform) time stepping.
- $refinements$ denote the number of mesh-refinements for every time step.
- $tolerance$ specifies the stopping criterion for the calculation of the plastic dependence in Algorithm 2.
- $tolerance\_Newton$ - determines the parameter $tolerance$ for the Newton-Raphson solver with the three stages convergence control (Algorithm 3).
- $maximum\_Newton\_step$ - specifies the maximal number of Newton-Raphson steps for reaching convergence in case of the Newton-Raphson solver with the three stages convergence control (Algorithm 3).
- $yield\_type$ determines the type of material behavior, i.e., $'multi'$, $'single'$ or $'elastic'$ for the two-yield, single-yield or elastic material behavior.
- $problem$ specifies the example for calculation: $'beam2D'$, $'beam1D'$, $'ring'$ or $'Lshape'$ or $'platehole'$ are available.

For the observation of convergence behavior, a function $'test\_adaptive'$ can be used. The function is called together with two parameters $refinements$ and $maxNewtonsteps$. The function runs the program 'start.m' and it generates a coarse solution of according to the solver setup. Then, the nested iteration technique with $refinements$ refinements (uniform of adaptive, how it is set up in 'start.m') is applied. It is performed in the cycle for the fixed number of Newton steps $1, \ldots, maxNewtonsteps$. The reference solution is calculated on the mesh $\mathcal{T}_{refinements}$ according to Remark 9.2. The (estimated) error in the energy norm and the value of the error estimator (ZZ-estimator) for approximations on coarser meshes $1, \ldots, refinements - 2$ are evaluated.

start.m

```
declaration_of_variables % specifies global variables

%%%%%%%%%%%%%%%%%%%%%%%%%%%%%%%%%%%%%%%%%%%%%%%%%%%%%%%%%%%%
Newtonsteps='3'; %number of Newtonsteps (as a string)
%or 'three_stages' or 'fixed_residual'
theta=0; %0.5 adaptive, 0 uniform
maximum_Newton_step=100;
step_min=0; step_max=100; %time adaptivity
refinements=0;
tolerance=1e-4; %for the plastic-dependence scheme
tolerance_Newton=10e-6;
maximum_Newton_step=100;
yield_type='multi'; % 'multi' or 'single' or 'elastic';
problem='beam2D'; %'beam2D' or 'beam1D' or 'ring' or 'Lshape'
                  %or 'cook'or 'platehole';
%%%%%%%%%%%%%%%%%%%%%%%%%%%%%%%%%%%%%%%%%%%%%%%%%%%%%%%%%%%%%
last_uniform_refinements=1;  %minimal value=1, for the generation of the
                             %reference solution

material;
mu_times_2=mu*2;
C=mu*[2 0 0;0 2 0;0 0 1] + lambda*[1 1 0;1 1 0;0 0 0];

%Generation of the coarse mesh
while size(Elemente,1)<10
  [Koordinaten,Elemente,Dirichlet,Neumann]=Rotverfeinerung(Koordinaten,...
      Elemente,Dirichlet,Neumann);
end

Koordinaten_coarse=Koordinaten;
Elemente_coarse=Elemente;
Dirichlet_coarse=Dirichlet;
Neumann_coarse=Neumann;

%initial conditions
Uprev=zeros(size(Koordinaten,1),2); %defined on every node
P1prev=zeros(size(Elemente,1),2); %defined on every element - constant
P2prev=zeros(size(Elemente,1),2); %defined on every element - constant

%set up
condestA=[]; N=[]; hysteresis_u=[]; hysteresis_g=[];
state=[]; %0 -elastic, 1-first plastic, 2-second plastic
counter=1;
numberoftimes=size(t,2);
further=1;
```

```
%cycle over all discrete times
while further
   %switching to coarse mesh
   Koordinaten=Koordinaten_coarse;
   Elemente=Elemente_coarse;
   Dirichlet=Dirichlet_coarse;
   Neumann=Neumann_coarse;

   %testing the convergence on the coarse mesh for the time adaptivity
   %disp('Running FEM + Newton method on the coarse mesh');
   %[U,U_coarse,P1,P1_coarse,P2,P2_coarse,iterations_coarse]=...
   %nested_iteration_refinements(P1prev,...
   %   P2prev,Uprev,t(counter),'fixed_residual',0);

   %improving the space error - mesh-refining
   [U,U_coarse,P1,P1_coarse,P2,P2_coarse,iterations_fine]=...
      nested_iteration_refinements(P1prev,...
      P2prev,Uprev,t(counter),Newtonsteps,refinements);

   iterations(:,counter)=iterations_fine;
   iterations_coarse=iterations_fine(1);

   Uprev=U_coarse;
   P1prev=P1_coarse;
   P2prev=P2_coarse;

   %which state - elastic, single-yield or two-yield?
   if (norm(P1)+norm(P2)==0)
         disp('elasticity'); state=[state 0];
   else
      if (norm(P2)>0)
         disp('two-yield plasticity'); state=[state 2];
      else disp('single-yield plasticity'); state=[state 1];
      end
   end

   %generating figures
   cd MATRICES
   save(strcat('zones_',problem,'_',yield_type,'_',num2str(counter)),...
      'Elemente','Koordinaten','U','P1','P2','lambda','mu');
   cd ..
   generate_zones(strcat('zones_',problem,'_',yield_type,'_',...
      num2str(counter)));

   %output for hysteresis behavior
   %generate_hysteresis;
   %figure(30);
   %plot(hysteresis_u,hysteresis_g,'x-');
   %M(counter)=getframe;

   %adaptive time-stepping
   if (counter==numberoftimes)
      further=0;
```

```
   else
      if iterations_coarse>step_max
         t=adaptive_time(t,counter+1,0.5);
      else
         if iterations_coarse<step_min
            t=adaptive_time(t,counter+1,2);
         else
            t=adaptive_time(t,counter+1,1);
         end
      end

      numberoftimes=size(t,2);
      counter=counter+1;
   end
save time_adaptivity
end

save
%animation
%movie(M);
%movie2avi(M,'plasticity.avi','FPS',2);
```

nested_iteration_refinement.m

```
function [U,U_coarse,P1,P1_coarse,P2,P2_coarse,iterations]=...
nested_iteration_refinements(P1prev,P2prev,U,time,Newtonsteps,refinements)
global Koordinaten Elemente Neumann Dirichlet %mesh invariants
global problem
iterations=[];

disp('Number of elements');
disp(size(Elemente,1));

mesh_preparation; %gets mesh ready - STEMAelastic + maske and others
incorporate_Dirichlet;
if strcmp(problem,'Lshape')
   for j=1:size(Dirichlet,1)
      U(Dirichlet(j,1),:)=Lshape_Dirichlet(Koordinaten(Dirichlet(j,1),:));
      U(Dirichlet(j,2),:)=Lshape_Dirichlet(Koordinaten(Dirichlet(j,2),:));
   end
end
evaluate_fv(time);
evaluate_gv(time);

[U,P1,P2,iterations_Newton]=FEM_Newton(P1prev,P2prev,U,Newtonsteps);
iterations=[iterations;iterations_Newton];

if ~isempty(Neumann)
      NKV = Koordinaten(Neumann(:,2),:)- Koordinaten(Neumann(:,1),:);
      NKV = NKV./[sqrt(sum(NKV.*NKV,2)),sqrt(sum(NKV.*NKV,2))];
      % Neumann-Kanten % Vektoren, normiert
      NNV = [NKV(:,2),-NKV(:,1)]; % Neumann-Kanten Normalenvektoren
else NKV=[]; NNV=[];
end
```

```
[Kantennr,Elemente]=GeneriereKantennr(Elemente,Koordinaten);
Sigma=evaluate_sigma(U,P1,P2);
[eta,eta_s]=ZZ_Estimate(Elemente, Koordinaten, Dirichlet, ...
   Neumann, NKV, NNV, Sigma,time);
disp('ZZ-error estimator');
disp(norm(eta));

%cd MATRICES
%save(strcat('eta_',num2str(0)),'eta');
%cd ..

VK=AAlg1(eta',Elemente,Koordinaten,Kantennr);
VK = BlauGruen(Elemente,Koordinaten,Kantennr,VK);

U_coarse=U;
P1_coarse=P1;
P2_coarse=P2;

for i=1:refinements
  % generate mesh refinement
  triangles=howmanytriangles(Elemente,Kantennr,VK);
  [Koordinaten,Elemente,Dirichlet,Neumann]=Verfeinerung(Koordinaten,...
                              Elemente,Dirichlet,Neumann,Kantennr,VK);
  if strcmp(problem,'ring')
       Koordinaten=correct_ring_coordinates(Koordinaten,Neumann);
  end

  Prolongation_linear = GeneriereProlongation(Kantennr,VK);
  %generate Prolongation_constant matrix
  Prolongation_constant=sparse(size(P1prev,1),size(triangles,2));
  index=0;
  for j=1:size(triangles,2)
     Prolongation_constant(index+1:index+triangles(j),j)=1;
     index=index+triangles(j);
  end

  disp('Number of elements');
  disp(size(Elemente,1));

  %Prolongation
  U=Prolongation_linear*U;
  P1prev=Prolongation_constant*P1prev;
  P2prev=Prolongation_constant*P2prev;

  mesh_preparation; %gets mesh ready - STEMAelastic + maske and others
  incorporate_Dirichlet;
  if strcmp(problem,'Lshape')
    for j=1:size(Dirichlet,1)
      U(Dirichlet(j,1),:)=Lshape_Dirichlet(Koordinaten(Dirichlet(j,1),:));
      U(Dirichlet(j,2),:)=Lshape_Dirichlet(Koordinaten(Dirichlet(j,2),:));
    end
  end
```

```
  evaluate_fv(time);
  evaluate_gv(time);

  [U,P1,P2,iterations_Newton]=FEM_Newton(P1prev,P2prev,U,Newtonsteps);
  iterations=[iterations;iterations_Newton];

  if ~isempty(Neumann)
      NKV = Koordinaten(Neumann(:,2),:)- Koordinaten(Neumann(:,1),:);
      NKV = NKV./[sqrt(sum(NKV.*NKV,2)),sqrt(sum(NKV.*NKV,2))];
      % Neumann-Kanten % Vektoren, normiert
      NNV = [NKV(:,2),-NKV(:,1)]; % Neumann-Kanten Normalenvektoren
  else NKV=[]; NNV=[];
  end

  [Kantennr,Elemente]=GeneriereKantennr(Elemente,Koordinaten);
  Sigma=evaluate_sigma(U,P1,P2);
  [eta,eta_s]=ZZ_Estimate(Elemente, Koordinaten, Dirichlet, ...
     Neumann, NKV, NNV, Sigma,time);

  disp('ZZ-error estimator');
  disp(norm(eta));

  %cd MATRICES
  %save(strcat('eta_',num2str(i)),'eta');
  %cd ..

  VK=AAlg1(eta',Elemente,Koordinaten,Kantennr);
  VK = BlauGruen(Elemente,Koordinaten,Kantennr,VK);

  %figure(i+1);
  %show_zones(U,P1,P2);
  %cd FIGURES
  %print(gcf,'-depsc',strcat('zones',num2str(i+1)));
  %cd ..
end
```

FEM_Newton.m

```
function [U,P1,P2,iterations]=FEM_Newton(P1prev,P2prev,U,Newtonsteps)
switch Newtonsteps
 case {'three_stages'}
   [U,P1,P2,iterations]=FEM_Newton_three_stages(P1prev,P2prev,U);
   disp('Newton step needed for convergence');
   disp(iterations);
 case {'fixed_residual'}
   [U,P1,P2,iterations]=FEM_Newton_fixed_residual(P1prev,P2prev,U);
   disp('Newton step needed for convergence');
   disp(iterations);
 otherwise
   [U,P1,P2]=FEM_Newton_fixed_steps(P1prev,P2prev,U,str2num(Newtonsteps));
   iterations=Newtonsteps;
end
```

FEM_Newton_fixed_steps.m

```
function [U,P1,P2]=FEM_Newton_fixed_steps(P1prev,P2prev,U,number_of_steps)
global STEMAelastic B W
global condestA N
[help,feste2DKnoten]=find(B);

disp('Evaluating Phi');
[Phi,plasticelements,P1,P2]=evaluate_Phi(U,P1prev,P2prev);

residualvector=Phi; residualvector(feste2DKnoten)=[];
residual=sqrt(residualvector'*(residualvector));
disp('residual = ');
disp(residual);

for i=1:number_of_steps
   if isempty(find(plasticelements))        %elasticity only
      disp('Substituting elastic DPhi');
      %global matrix - set up
      stabilization=max(max(STEMAelastic));
      A=[STEMAelastic, stabilization*B';stabilization*B,...
                  sparse(size(B,1),size(B,1))];
   else %plasticity!!
      disp('Evaluating plastic DPHi');
      DPhi=evaluate_DPhi_plastic(U,P1prev,P2prev,plasticelements);
      %global matrix - set up
      stabilization=max(max(DPhi));
      %stabilization=1;
      A=[DPhi,stabilization*B';stabilization*B,sparse(size(B,1),...
                  size(B,1))];
   end
   %condestA=[condestA condest(A)];
   %N=[N size(STEMAelastic,2)];
   b=[Phi; stabilization*W];
   % one Newton iteration
   solution=A\b;
   lambda=solution(size(STEMAelastic,1)+1:end);
   Udeltavector=solution(1:size(STEMAelastic,1));
   Udelta=matrix2form(Udeltavector);
   U=U-Udelta;
   [Phi,plasticelements,P1,P2]=evaluate_Phi(U,P1prev,P2prev);
   %residualvector=Phi;residualvector(feste2DKnoten)=[];
   %residual=sqrt(residualvector'*(residualvector));
   residual=norm(stabilization*B'*lambda-Phi);
   disp('residual = ');
   disp(residual);
end
```

FEM_Newton_three_stages.m

```
function [U,P1,P2,step]=FEM_Newton_three_stages(P1prev,P2prev,U)
global STEMAelastic B W
global tolerance maximum_Newton_step;
global condestA N
```

```
[help,feste2DKnoten]=find(B);

disp('Evaluating Phi');
[Phi,plasticelements,P1,P2]=evaluate_Phi(U,P1prev,P2prev);

residualvector=Phi; residualvector(feste2DKnoten)=[];
residual=sqrt(residualvector'*(residualvector));
disp('residual = ');
disp(residual);


if residual==0
   further=0;
else
   further=1;
end

tolerance_reached=0;
step=0;
residualold=residual;

while (further==1) & (step<=maximum_Newton_step)
   if isempty(find(plasticelements))        %elasticity only
      disp('Substituting elastic DPhi');
      %global matrix - set up
      stabilization=max(max(STEMAelastic));
      A=[STEMAelastic, stabilization*B';stabilization*B,...
                   sparse(size(B,1),size(B,1))];
   else %plasticity!!
      disp('Evaluating plastic DPHi');
      DPhi=evaluate_DPhi_plastic(U,P1prev,P2prev,plasticelements);
      %global matrix - set up
      stabilization=max(max(DPhi));
      A=[DPhi,stabilization*B';stabilization*B,sparse(size(B,1),...
                   size(B,1))];
   end

   %condestA=[condestA condest(A)];
   %N=[N size(STEMAelastic,2)];
   b=[Phi; stabilization*W];
   % one Newton iteration
   solution=A\b;
   lambda=solution(size(STEMAelastic,1)+1:end);
   Udeltavector=solution(1:size(STEMAelastic,1));
   Udelta=matrix2form(Udeltavector);
   U=U-Udelta;
   disp('Evaluating Phi');
   [Phi,plasticelements,P1,P2]=evaluate_Phi(U,P1prev,P2prev);
   %residualvector=Phi; residualvector(feste2DKnoten)=[];
   %residual=sqrt(residualvector'*(residualvector));
   residual=norm(stabilization*B'*lambda-Phi);
   %fprintf('residual =%10.8f \n',residual);
   disp('residual = ');
```

```
   disp(residual);

   if residual<=tolerance
      tolerance_reached=1;
   end
   if (tolerance_reached==1) & (residual>residualold)
      further=0;
   end
   residualold=residual;
   step=step+1;
end

if step==maximum_Newton_step
   display('Maximum number of Newton steps exceeded!!!');
   pause
end
```

evaluate_Phi.m

```
function [Phi,plasticelements,P1,P2]=evaluatePhi(U,P1prev,P2prev)
global fv gv STEMAelastic Rglobal Areaglobal Elemente

%calculating Phi - right side for the Newton matrix - elementwise
%plasticelements=[];
Phi=zeros(1,2*size(U,1));
%Calculation C\epsilon(U):\epsilon(V), V=V_i ==> vector
Phi=(vectorform(U)'*STEMAelastic);
%-int_\Omega fv dx
Phi=Phi-fv-gv;

[P1,P2,plasticelements]=evaluate_P_global(U,P1prev,P2prev);
for j=1: size(Elemente,1);
      %assignment of real indices
      I=2*Elemente(j,[1 1 2 2 3 3])-[1,0,1,0,1,0];

      P1local=P1(j,:);
      P2local=P2(j,:);
      if plasticelements(j)~=0
         Rlocal=Rglobal(:,:,j);
         Arealocal=Areaglobal(j);
         %Calculating CP0:\epsilon(V), V=V_i ==> vector
         STEMA3Plasticlocal=integral_plastic(Rlocal,Arealocal,...
            P1local+P2local);
         Phi(I)=Phi(I)-STEMA3Plasticlocal;
      end
end
Phi=Phi';
```

evaluate_DPhi_plastic.m

```
function DPhi=evaluate_DPhi_plastic(U,P1prev,P2prev,plasticelements)
global STEMAelastic Koordinaten Elemente Rglobal Areaglobal

DPhi=STEMAelastic;
```

```
for j=1:size(Elemente,1);
   if plasticelements(j)>0
      %assignment of real indices
      I=2*Elemente(j,[1 1 2 2 3 3])-[1,0,1,0,1,0];
      P1prevlocal=P1prev(j,:);
      P2prevlocal=P2prev(j,:);
           Koordinatenlocal=Koordinaten(Elemente(j,:),:);
      Ulocal=U(Elemente(j,:),:);
      Rlocal=Rglobal(:,:,j);
      Arealocal=Areaglobal(j);

      for i=1:6
         Uvectorlocal=vectorform(Ulocal);
         %setting up the increment for the approximation of DPhi
         epsilon=sqrt(eps)*max(1,abs(Uvectorlocal(i)));
         Upluslocal=Uvectorlocal;
         Uminuslocal=Uvectorlocal;
         Upluslocal(i)=Upluslocal(i)+epsilon;
         Uminuslocal(i)=Uminuslocal(i)-epsilon;
         Upluslocal=matrix2form(Upluslocal);
         Uminuslocal=matrix2form(Uminuslocal);

         [P1pluslocal,P2pluslocal]=evaluate_P_on_element(Rlocal,...
                                 Upluslocal,P1prevlocal,P2prevlocal);
         [P1minuslocal,P2minuslocal]=evaluate_P_on_element(Rlocal,...
                                 Uminuslocal,P1prevlocal,P2prevlocal);

         %approximation of the derivation by the difference
         STEMA3Plastic(i,:)=integral_plastic(Rlocal,Arealocal,...
         (P1pluslocal+P2pluslocal-P1minuslocal-P2minuslocal)/2/epsilon);
      end
      DPhi(I,I)=DPhi(I,I)-STEMA3Plastic';
   end
end
```

STEMA3.m

```
function STEMA3=STEMA3(Knoten)
%calculates \int_elemet C epsilon_i:\epsilon_j,
%i,j=1..6 for tracefree and symmetic Plasticstrain
global C
Rlocal=R(Knoten);
STEMA3=det([1 1 1;Knoten'])/2*Rlocal'*C*Rlocal;
```

integral_plastic.m

```
function integral=integral_plastic(Rlocal,Arealocal,Plasticstrain)
%calculates \int_element CPlasticstrainn:\epsilon_i, i=1..6
%for trace-free and symmetric Plasticstrain
global mu
Plasticvector=[Plasticstrain(1) -Plasticstrain(1) Plasticstrain(2)];
integral=mu*Arealocal*(Plasticvector*Rlocal); %Area/2 * R'*2*mu*Plastic
```

evaluate_P_on_element.m

```
function [P1local,P2local]=evaluate_P_on_element(Rlocal,Ulocal,...
   P1prevlocal,P2prevlocal)
global C h1 h2 mu

P1prevlocalmatrix=[P1prevlocal;P1prevlocal(2) -P1prevlocal(1)];
P2prevlocalmatrix=[P2prevlocal;P2prevlocal(2) -P2prevlocal(1)];
Ulocalvector([1 3 5])=Ulocal(:,1);
Ulocalvector([2 4 6])=Ulocal(:,2);

%gamma (epsilon11,epsilon22,epsilon12) on the element
gamma=Rlocal*Ulocalvector';
CepsU=matrixform(C*gamma);

%A=C epsilon(U)-(C+H)Pprev
A1=CepsU-((2*mu+h1)*P1prevlocalmatrix+2*mu*P2prevlocalmatrix);
A2=CepsU-(2*mu*P1prevlocalmatrix+(2*mu+h2)*P2prevlocalmatrix);
devA1=dev(A1);
devA2=dev(A2);

[deltaP1localmatrix,deltaP2localmatrix]=dependence(devA1,devA2);

P1local=deltaP1localmatrix(1,:)+P1prevlocal;
P2local=deltaP2localmatrix(1,:)+P2prevlocal;
```

dependence.m

```
function [P1,P2]=dependence(devA1,devA2)
global yield_type
switch yield_type
   case 'elastic'
      P1=zeros(2);
      P2=P1;
   case 'single'
      global sigmay1 mu_times_2 h1
      P1=dependence_single_general(devA1,mu_times_2,sigmay1,h1);
      P2=zeros(2);
   case 'multi'
      global sigmay1 sigmay2 mu_times_2 h1 h2 tolerance
      %estimation of the solution
      P2=dependence_single_general(devA2,...
         mu_times_2,sigmay2,h2);
      P1=dependence_single_general(devA1-mu_times_2*P2,...
         mu_times_2,sigmay1,h1);
      %x=[P1(1,1)]; y=[P2(1,1)];
      normold=norm(P1,'fro')+norm(P2,'fro');

      while 1
         P2=dependence_single_general(devA2-mu_times_2*P1,...
            mu_times_2,sigmay2,h2);

         P1=dependence_single_general(devA1-mu_times_2*P2,...
            mu_times_2,sigmay1,h1);
```

```
        normnew=norm(P1,'fro')+norm(P2,'fro');
        difference=abs(normnew-normold);
        if difference>0
           difference=difference/(normnew+normold);
        end

        if difference<tolerance
           break
        end
        normold=normnew;
    end
end
```

dependence_single_general.m

```
function P=dependence_single_general(devA,mu_times_2,sigmay,h)
normdevA=norm(devA,'fro');
if normdevA<sigmay
   P=zeros(2);
else
   P=devA*(normdevA-sigmay)/normdevA/(mu_times_2+h);
end
```

mesh_preparation.m

```
function mesh_preparation
global Koordinaten Elemente Dirichlet
global STEMAelastic  maske Areaglobal maske DirichletKnoten Rglobal
%global SCALINGmatrix

Areaglobal=[];
Rglobal=[];
STEMAelastic=sparse(2*size(Koordinaten,1),2*size(Koordinaten,1));
%SCALINGmatrix=STEMAelastic;
%node_in_element=sparse(size(Koordinaten,1),size(Elemente,1));
for j=1: size(Elemente,1);
   I=2*Elemente(j,[1 1 2 2 3 3])-[1,0,1,0,1,0];
   Elementelocal=Elemente(j,:);
   Koordinatenlocal=Koordinaten(Elementelocal,:);
   Rglobal(:,:,j)=R(Koordinatenlocal);
   Areaglobal(j)=det([1 1 1;Koordinatenlocal']);
   %CepsUlocal(:,:,j)=matrixform(C*gamma);
   STEMAelastic(I,I)=STEMAelastic(I,I)+STEMA3(Koordinatenlocal);
   %SCALINGmatrix(I,I)=SCALINGmatrix(I,I)+STEMAH1(Koordinatenlocal);
end
%SCALINGmatrix=STEMAelastic;

%Preparation - extracting Dirichlet nodes
maske=zeros(size(Koordinaten,1),1);
maske(Dirichlet)=ones(size(Dirichlet));
DirichletKnoten=find(maske);
freieKnoten=find(~maske);
```

R.m

```
function R=R(Knoten)
PhiGrad=[1 1 1;Knoten']\[zeros(1,2);eye(2)];
R([1,3],[1,3,5])=PhiGrad';
R([3,2],[2,4,6])=PhiGrad';
```

material.m

```
switch problem
case 'beam1D',
   t=[0 0.5 10*5]; %first experiment - hysteresis
   mu=1000;lambda=1000;
   sigmay1=5; h1=100; sigmay2=7; h2=50;
   [Koordinaten,Elemente,Dirichlet,Neumann]=beam_1D_symetric_mesh(0);
case 'beam2D',
   t=[0 0.5 10*5]; %first experiment - hysteresis
   t=[3:0.5:10];   %second experiment - evolution
   t=8.5;           %third experiment - one time step adaptivity
   mu=1000;lambda=1000;
   sigmay1=5; h1=100; sigmay2=7; h2=50;
   [Koordinaten,Elemente,Dirichlet,Neumann]=beam_2D_symetric_mesh(0);
case 'ring',
   t=[0 10 430]; %evolution
   t=200;        % one time step adaptivity
   E=70000; nu=0.33; lambda=E*nu/((1+nu)*(1-2*nu)); mu=E/(2+2*nu); %glass
   sigmay1=243*sqrt(2/3); h1=1; sigmay2=250*sqrt(2/3); h2=1;  %only for
                                                             %comparison with JA
   [Koordinaten,Elemente,Dirichlet,Neumann]=ring_mesh(0);
case 'Lshape'
   t=1; %one time step adaptivity
   E=100000; nu=0.3; lambda=E*nu/((1+nu)*(1-2*nu)); mu=E/(2+2*nu); %glass
   sigmay1=1; h1=2; sigmay2=1.41; h2=0.02;
   h1=1;
   [Koordinaten,Elemente,Dirichlet,Neumann]=Lshape_mesh(0);
case 'cook'
   t=[0 0.5 10*5]; %hysteresis
   t=1.7; %one time step adaptivity
   mu=1000; lambda=1000;
   sigmay1=5; h1=100; sigmay2=7; h2=50; % - hysteresis
   sigmay2=6;  % - one time step
   [Koordinaten,Elemente,Dirichlet,Neumann]=cook_mesh(0);
case 'platehole'
   t=[0.4 0.41 0.8];
   %t=[0.7]; %one time step adaptivity
   E=206900; nu=0.29; lambda=E*nu/((1+nu)*(1-2*nu)); mu=E/(2+2*nu); %glass
   mu=1000; lambda=1000;
   sigmay1=450*sqrt(2/3); h1=1; sigmay2=500*sqrt(2/3); h2=1;
   [Koordinaten,Elemente,Dirichlet,Neumann]=platehole_mesh(0);
end
```

dev.m

```
function A=dev(B)
tr_over_2=(B(1,1)+B(2,2))/2;
A=B-[tr_over_2 0; 0 tr_over_2];
```

test_adaptive.m

```
function [norm_error,norm_eta]=test_adaptive(number_of_refinements,...
   maxNewtonsteps)
global problem yield_type
global last_uniform_refinements;

evaluate_U_coarse
close all

for j=1:maxNewtonsteps
   evaluate_U_exact(number_of_refinements,j);
   cd MATRICES
   load exact_solution;
   cd ..

   for k=0:(number_of_refinements-last_uniform_refinements)
      cd MATRICES
      load(strcat('U_',num2str(k)));
      load(strcat('P1_',num2str(k)));
      load(strcat('P2_',num2str(k)));
      load(strcat('eta_',num2str(k)));
      cd ..

      number_of_flops(j,k+1)=flops;
      number_of_unknowns(j,k+1)=size(U,1)*2;
      number_of_elements(j,k+1)=size(P1,1);

      for l=k:(number_of_refinements-1)
         cd MATRICES
         load(strcat('Prolongation_linear_',num2str(l)));
         load(strcat('Prolongation_constant_',num2str(l)));
         cd ..

         U=Prolongation_linear*U;
         P1=Prolongation_constant*P1;
         P2=Prolongation_constant*P2;
      end

      error_U=U-U_exact;
      error_P1=P1-P1_exact;
      error_P2=P2-P2_exact;

      norm_eta(j,k+1)=norm(eta);
      %mesh_preparation
      norm_error(j,k+1)=NormEnergy(error_U,error_P1,error_P2,...
         Elemente_exact,Koordinaten_exact,...
         Areaglobal_exact,Rglobal_exact);

      %normaL2(j,k+1)=NormL2(U,Elemente_exact,Koordinaten_exact);
   end
end

%exact solution for the single-yield ring
```

```
if strcmp(yield_type,'single') & strcmp(problem,'ring')
   for k=0:(number_of_refinements-last_uniform_refinements)
      cd MATRICES
      load(strcat('mesh_',num2str(k)));
       cd ..
       Koordinaten=[zeros(size(Koordinaten,1),1) Koordinaten];
       Elemente=[zeros(size(Elemente,1),1) Elemente];
       Dirichlet=[zeros(size(Dirichlet,1),1) Dirichlet];
       Neumann=[zeros(size(Neumann,1),1) Neumann];
       od=cd;
       cd ../JOCHEN_SOLVER
       save Koordinaten Koordinaten
       save Elemente Elemente
       save Dirichlet Dirichlet
       save Neumann Neumann
       [relTmSpcError,ZZ_Est,Res_Est,SpcError,dof]=...
           fem_plast([0 200],1,10,1e-12,1,1,0,[0])
       cd(od)
       norm_error_exact(k+1)=SpcError;
    end
end

%clear Rglobal_exact Prolongation_constant Prolongation_linear
%clear U P1 P2 error_U error_P1 error_P2

if strcmp(yield_type,'single') & strcmp(problem,'ring')
   save matlab norm_eta norm_error norm_error_exact number_of_unknowns
else
   save matlab norm_eta norm_error number_of_unknowns
end

x1=number_of_unknowns(1,:);
y1=norm_error(1,:);
z1=norm_eta(1,:);
x2=number_of_unknowns(2,:);
y2=norm_error(2,:);
z2=norm_eta(2,:);
x3=number_of_unknowns(3,:);
y3=norm_error(3,:);
z3=norm_eta(3,:);
loglog(x1,y1,'-o',x2,y2,'-.o',x3,y3,'--o');
hold on
loglog(x1,z1,'-o',x2,z2,'-.o',x3,z3,'--o');
if strcmp(yield_type,'single') & strcmp(problem,'ring')
   loglog(x3,norm_error_exact,'-d');
end

xlabel('N');
ylabel('\eta_{Z} and error');
```

evaluate_U_coarse.m

```
function evaluate_U_coarse
start
```

```
clear Newtonsteps number_of_refinements U Elemente Koordinaten ...
Dirichlet Neumann
cd MATRICES
save coarse_solution
cd ..
```

evaluate_U_exact.m

```
function evaluate_U_exact(number_of_refinements,Newtonsteps)
global last_uniform_refinements;  %minimal value=1

declaration_of_variables
cd MATRICES
load coarse_solution;  %only structure, not solution
cd ..

Elemente=Elemente_coarse;
Koordinaten=Koordinaten_coarse;
Dirichlet=Dirichlet_coarse;
Neumann=Neumann_coarse;

time=t(counter);

Uprev=zeros(size(Koordinaten,1),2); %defined on every node
P1prev=zeros(size(Elemente,1),2); %defined on every element - constant
P2prev=zeros(size(Elemente,1),2); %defined on every element - constant

U=Uprev;   %initial approximation for Newton method

for i=0:(number_of_refinements-1)
  mesh_preparation; %gets mesh ready - STEMAelastic + maske and others
  incorporate_Dirichlet;
  evaluate_fv(time);
  evaluate_gv(time);

  if strcmp(problem,'Lshape')
    for j=1:size(Dirichlet,1)
      U(Dirichlet(j,1),:)=Lshape_Dirichlet(Koordinaten(Dirichlet(j,1),:));
      U(Dirichlet(j,2),:)=Lshape_Dirichlet(Koordinaten(Dirichlet(j,2),:));
    end
  end

  disp('Number of elements');
  disp(size(Elemente,1));

  if i>=(number_of_refinements-last_uniform_refinements+1)
        global theta
      thetaold=theta;
      theta=0;
      [U,P1,P2]=FEM_Newton_fixed_steps(P1prev,P2prev,U,1);
      theta=thetaold;
  else
       [U,P1,P2]=FEM_Newton_fixed_steps(P1prev,P2prev,U,Newtonsteps);
  end
```

```
cd MATRICES
    save(strcat('U_',num2str(i)),'U');
    save(strcat('P1_',num2str(i)),'P1');
    save(strcat('P2_',num2str(i)),'P2');
    global Elemente Koordinaten Dirichlet Neumann
    save(strcat('mesh_',num2str(i)),'Elemente','Koordinaten',...
                'Neumann','Dirichlet');
cd ..

if ~isempty(Neumann)
    NKV = Koordinaten(Neumann(:,2),:)- Koordinaten(Neumann(:,1),:);
    NKV = NKV./[sqrt(sum(NKV.*NKV,2)),sqrt(sum(NKV.*NKV,2))];
    % Neumann-Kanten % Vektoren, normiert
    NNV = [NKV(:,2),-NKV(:,1)];  % Neumann-Kanten Normalenvektoren
else
    NKV=[]; NNV=[];
end
[Kantennr,Elemente]=GeneriereKantennr(Elemente,Koordinaten);
Sigma=evaluate_sigma(U,P1,P2);
[eta,eta_s]=ZZ_Estimate(Elemente, Koordinaten, Dirichlet, ...
   Neumann, NKV, NNV, Sigma,time);

cd MATRICES
save(strcat('eta_',num2str(i)),'eta');
cd ..

if i>=(number_of_refinements-last_uniform_refinements)
   global theta
   thetaold=theta;
   theta=0;
   VK=AAlg1(eta',Elemente,Koordinaten,Kantennr);
   theta=thetaold;
else
   VK=AAlg1(eta',Elemente,Koordinaten,Kantennr);
end
VK = BlauGruen(Elemente,Koordinaten,Kantennr,VK);

% Generiere neue Triangulierung
trianglesdistribution=howmanytriangles(Elemente,Kantennr,VK);
[Koordinaten,Elemente,Dirichlet,Neumann]=Verfeinerung(Koordinaten,...
      Elemente,Dirichlet,Neumann,Kantennr,VK);

if strcmp(problem,'ring')
     Koordinaten=correct_ring_coordinates(Koordinaten,Neumann);
end
Prolongation_linear = GeneriereProlongation(Kantennr,VK);

Prolongation_constant=sparse(size(P1prev,1),...
                             size(trianglesdistribution,2));
index=0;
for j=1:size(trianglesdistribution,2)
   Prolongation_constant(index+1:index+trianglesdistribution(j),j)=1;
```

```
      index=index+trianglesdistribution(j);
    end

    cd MATRICES
    save(strcat('Prolongation_linear_',num2str(i)),'Prolongation_linear');
    save(strcat('Prolongation_constant_',num2str(i)),...
                'Prolongation_constant');
    cd ..

    U=Prolongation_linear*U;
    P1prev=Prolongation_constant*P1prev;
    P2prev=Prolongation_constant*P2prev;
  end

mesh_preparation; %gets mesh ready - STEMAelastic + maske and others
incorporate_Dirichlet;
evaluate_fv(time);
evaluate_gv(time);

if strcmp(problem,'Lshape')
    for j=1:size(Dirichlet,1)
      U(Dirichlet(j,1),:)=Lshape_Dirichlet(Koordinaten(Dirichlet(j,1),:));
      U(Dirichlet(j,2),:)=Lshape_Dirichlet(Koordinaten(Dirichlet(j,2),:));
    end
end

disp('Number of elements');
disp(size(Elemente,1));

%enforced uniform refinement
thetaold=theta;
theta=0;
[U_exact,P1_exact,P2_exact]=FEM_Newton_fixed_steps(P1prev,P2prev,U,1);
theta=thetaold;

Koordinaten_exact=Koordinaten;
Elemente_exact=Elemente;

global STEMAelastic Areaglobal
STEMAelastic_exact=STEMAelastic;
Areaglobal_exact=Areaglobal;
number_of_refinements_exact=number_of_refinements;
Rglobal_exact=Rglobal;

cd MATRICES
save exact_solution U_exact Koordinaten_exact Elemente_exact P1_exact ...
      P2_exact Areaglobal_exact Rglobal_exact number_of_refinements_exact
cd ..
```

Bibliography

[AC00] J. Alberty and C. Carstensen. Numerical analysis of time-depending primal elastoplasticity with hardening. *SIAM J. Numer. Anal.*, 37(4):1271–1294, 2000.

[ACF99] J. Alberty, C. Carstensen, and S. A. Funken. Remarks around 50 lines of matlab: short finite element implementation. *Numerical Algorithms*, (20):117–137, 1999.

[ACFK00] J. Alberty, C. Carstensen, S. A. Funken, and R. Klose. Matlab implementation of the finite element method in elasticity. Technical report, Christian-Albrechts-Universität zu Kiel, 2000.

[ACZ99] J. Alberty, C. Carstensen, and D. Zarabi. Adaptive numerical analysis in primal elastoplasticity with hardening. *Comput. Methods Appl. Mech. Eng.*, 171(3-4):175–204, 1999.

[ACZ00] J. Alberty, C. Carstensen, and D. Zarrabi. Numerical analysis in primal elastoplasticity with hardening. *ZAMM, Z. Angew. Math. Mech.*, (80), 2000.

[Alb01] J. Alberty. *Zeitdiskretisierungsverfahren für elastoplastische Probleme der Kontinuumsmechanik*. PhD thesis, Christian-Albrechts-Universität zu Kiel, 2001.

[ALRA90] J.C. Anderson, K.D. Leaver, R.D. Rawlings, and J.M. Alexander. *Materials Science*. Chapman & Hall, 1990.

[Axe94] O. Axelsson. *Iterative Solution Methods*. Cambridge University Press, 1994.

[BK98a] M. Brokate and Krejčí, P. On the wellposedness of the Chaboche model. *Birkhäser, Basel*, 1998.

[BK98b] M. Brokate and Krejčí, P. Wellposedness of kinematic hardening models in elastoplasticity. *Elsevier, Paris*, 32(2):177–209, 1998.

[Bla99] R. Blaheta. *Numerical methods in elasto-plasticity*. PERES publishers, 1999.

[Bro87] M. Brokate. *Optimale Steuerung von gewöhnlichen Differentialgleichungen mit Nichtlinearitäten vom Hysteresis-Typ*. Verlag Peter Lang, Frankfurt am Main, 1987.

[Bro97] M. Brokate. *Konvexe Analysis*. Christian-Albrechts-Universität zu Kiel, 1997. Vorlesungsskript, WS 1997/98, http://www.numerik.uni-kiel.de/mbr/.

[Bro98] M. Brokate. Elastoplastic constitutive laws of nonlinear kinematic hardening type. In *Functional analysis with current applications in science, technology and industry*, number 377 in Longman. Pitman Res. Notes Math. Ser., pages 238–272, Harlow, 1998. Longman.

[BS96] M. Brokate and J. Sprekels. *Hysteresis and Phase Transitions*. Springer-Verlag New York, 1996.

[CA00] C. Carstensen and J. Alberty. Averaging techniques for reliable a posteriori fe-error control in elastoplasticity with hardening? Technical report, Christian-Albrechts-Universität zu Kiel, 2000.

[Car96] C. Carstensen. Coupling of fem and bem for interface problems in viscoplasticity and plasticity with hardening. *SIAM J. Numer. Anal.*, 33(1):171–207, 1996.

[Car97] C. Carstensen. Domain decomposition for a non-smooth convex minimalization problems and its application to plasticity. *Numerical Linear Algebra with Applications*, 4(3):177–190, 1997.

[Car00a] C. Carstensen. Numerical analysis of of the primal elastoplasticity with hardening. *Numer. Math.*, (82):577–597, 2000.

[Car00b] C. Carstensen. *Wissenschaftliches Rechnen: Elastische Festkörper*. Christian-Albrechts-Universität zu Kiel, 2000.

[Car00c] C. Carstensen. *Wissenschaftliches Rechnen: Finite Elemente*. Christian-Albrechts-Universität zu Kiel, 2000.

[CB00] C. Carstensen and S. Bartels. Each averaging technique yields reliable a posteriori error control in fem on unstructured grids. Part I: Low order conforming, and mixed fem. Technical report, Christian-Albrechts-Universität zu Kiel, 2000.

[CDFH00] C. Carstensen, G. Dolzmann, S. A. Funken, and D. S. Helm. Locking-free adaptive mixed finite element methods in linear elasticity. *Comput. Methods Appl. Mech. Eng.*, 190(13-14):1701–1718, 2000.

[CF00] C. Carstensen and S. A. Funken. Averaging technique for fe-a posteriori error control in elasticity: Part II: $\lambda-$ independent estimates. Technical report, Christian-Albrechts-Universität zu Kiel, 2000. http://www.numerik.uni-kiel.de/reports/1999/99-14.html.

[CHM00] C. Carstensen, K. Hackl, and A. Mielke. Nonconvex potentials and microstructures in finite-strain plasticity. Technical report, Max-Planck-Institute for Mathematics in the Sciences, Leipzig, 2000. http://www.mis.mpg.de/preprints/2000/.

[Cia83] P. G. Ciarlet. *Lectures on Three-Dimensional Elasticity*. Tata institute of fundamental research, Bombay, 1983.

[Cia94] P. G. Ciarlet. *Mathematical Elasticity, Volume 1: Three dimensional elasticity*. Cambridge University Press, 1994.

[CK01] C. Carstensen and R. Klose. Matlab-implementation of the finite element method in visco-plasticity, 2001. In Preparation.

[DL76] G. Duvaut and Lions J. L. *Numerical analysis of Variational Inequalities*. Springer-Verlag Berlin Heidelberg, 1976.

[EEHJ95] K. Eriksson, D. Estep, P. Hansbo, and C. Johnson. Introduction to adaptive methods for differential equations. *Acta Numerica*, pages 105–158, 1995.

[ET99] I. Ekeland and R. Témam. *Convex Analysis and Variational Problems*. SIAM, 1999.

[GLR81] R. Glowinskii, Lions J. L., and Trémolières R. *Numerical analysis of Variational Inequalities*. North-Holland, Amsterdam, 1981.

[Hac85] W. Hackbush. *Multi-Grid Methods and Applications*. Springer-Verlag Berlin, Heidelberg, 1985.

[HHNL88] I. Hlaváček, J. Haslinger, J. Nečas, and J. Lovíšek. *Solutions of Variational Inequalities in Mechanics*. Springer-Verlag New York, 1988.

[Hig93] N. J. Higham. *Handbook of Writing for the Mathematical Sciences*. SIAM, 1993.

[HR95] W. Han and B.D. Reddy. Computational plasticity: the variational basis and numerical analysis. *Computer methods in applied mechanics and engineering*, pages 283–400, 1995.

[HR99] W. Han and B. Reddy. *Plasticity: Mathematical Theory and Numerical Analysis*. Springer-Verlag New York, 1999.

[Ish54] A. Ju. Ishlinskii. The general theory of plasticity with linear hardening (in russians). *Ukrainian mathematical journal*, 6(3), 1954.

[JH92] C. Johnson and P. Hansbo. Adaptive finite element methods in computational mechanics. *Comput. Methods Appl. Mech. Eng.*, 101(1-3):143–181, 1992.

[Joh76] C. Johnson. Existence theorems for plasticity problems. *J. math. pures et appl.*, 55:431–444, 1976.

[KL84] V. G. Korneev and U. Langer. *Approximate solution of plastic flow theory problems*, volume 69 of *Teubner-Texte zur Mathematik*. Teubner-Verlag, Leipzig, 1984.

[Kos91] P. Kosmol. *Optimierung und Approximation*. Walter de Gruyter, 1991.

[Kos93] P. Kosmol. *Methoden zur numerischen Behandlung nichtlinearer Gleichungen und Optimierungsaufgaben*. Teubner, 1993.

[Kre96] P. Krejčí. *Hysteresis, Convexity and Dissipation in Hyperbolic Equations*. GAKUTO International Series, Mathematical Sciences and Applications, 1996.

[Luk90] L. Lukšan. *Metody s proměnou metrikou*. Academia Praha, 1990.

[Neč83] J. Nečas. *Introduction to the theory of Nonlinear Elliptic Equations*. Teubner, 1983.

[Nef00] P. Neff. *Mathematische Analyse multiplikativer Viskoplastizität*. PhD thesis, Universität Darmstadt, 2000.

[OKZ99] J. Outrata, M. Kočvara, and J. Zowe. *Nonsmooth Approach to Optimization Problems with Equilibrium Constraints*. Kluwer Academic Publisher, Dordrecht, 1999.

[Roy68] H. L. Royden. *Real analysis*. The Maccmillan Company, 1968.

[SH98] J.C. Simo and T.J.R. Hughes. *Computational Inelasticity*. Springer-Verlag New York, 1998.

[Sut97] F.-T. Suttmeier. *Adaptive Finite Element Approximation of Problems in Elastoplasticity Theory*. PhD thesis, Universität Heidelberg, 1997.

[Val88] T. Valent. *Boundary Value Problems of Finite Elasticity*, volume 31. Springer Tracts in Natural Philosophy, 1988.

[Ver96] R. Verfürth. *A review of A Posteriori Error Estimation and Adaptive Mesh-Refinement Techniques*. Wiley and Teubner, 1996.

[Vis94] A. Visintin. *Differential models of hysteresis*. Springer, 1994.

[Wer84] J. Werner. *Optimization Theory and Applications*. Vieweg, Braunschweig-Wiesbaden, 1984.

[Wes99] M. J. Wester, editor. *Computer algebra systems - A practical guide*. John Willey & Sons, 1999.

[Zei78] E. Zeidler. *Vorlesungen über nichtlineare Funktionalanalysis III - Variationsmethoden und Optimierung*. Teubner, 1978.